UNIVERSITAT DE BARCELONA

Composició, origen i transport de matèria orgànica en marges continentals i conques de la mar Mediterrània

Composition, origin and transport of organic matter in continental margins and basins of the Mediterranean Sea

Rut Pedrosa Pàmies

Aquesta tesi doctoral està subjecta a la llicència ***Reconeixement- NoComercial – SenseObraDerivada 3.0. Espanya de Creative Commons***.

Esta tesis doctoral está sujeta a la licencia ***Reconocimiento - NoComercial – SinObraDerivada 3.0. España de Creative* Commons**.

This doctoral thesis is licensed under the ***Creative Commons Attribution-NonCommercial-NoDerivs 3.0. Spain License***.

Composició, origen i transport de matèria orgànica en marges continentals i conques de la mar Mediterrània

Rut Pedrosa Pàmies

Memòria de Tesi Doctoral
Programa de Doctorat en Ciències del Mar
Universitat de Barcelona
2016

Composició, origen i transport de matèria orgànica en marges continentals i conques de la mar Mediterrània

Composition, origin and transport of organic matter
in continental margins and basins of the Mediterranean Sea

Memòria de Tesi Doctoral presentada per

Rut Pedrosa Pàmies

sota la direcció de

la Dra. Anna Sànchez Vidal i del Dr. Antoni M. Calafat Frau

al Departament de Dinàmica de la Terra i de l'Oceà de la Universitat de Barcelona, dins del programa de doctorat de Ciències del Mar, per optar al grau de Doctora per la Universitat de Barcelona.

Barcelona, Juliol 2016

La Doctoranda	La Directora	El Director
Rut Pedrosa Pàmies	Dra. Anna Sànchez Vidal	Dr. Antoni M. Calafat Frau

Aquesta Tesi ha estat realitzada al Departament de Dinàmica de la Terra i de l'Oceà de la Universitat de Barcelona, dins el Grup de Recerca en Geociències Marines amb reconeixement de la Generalitat de Catalunya com a Grup de Recerca Consolidat (refs. 2009 SGR 1305 i 2014 SGR 1068). Durant el període d'elaboració de la Tesi la doctoranda ha gaudit d'una beca predoctoral de Formación de Profesorado Universitario (FPU) del Ministerio de Educación y Ciencia (ref. AP2010-1733). Les estades que la doctoranda realitzà a l'Hellenic Center of Marine Research (Atenes, Grècia) foren finançades per "Euromarine Mobility Fellowships Programme 2012" i la Fundació Montcelimar de la Universitat de Barcelona. Altres beques que la doctoranda ha rebut per assistir a congressos i cursos han estat concedides per la Facultat de Geologia de la Universitat de Barcelona a través del programa d'Ajuts a la Recerca de la Comissió de Recerca de la Facultat. A més dels projectes esmentats anteriorment, la recerca que es presenta en aquesta Tesi ha estat finançada pels projectes HERMIONE (ref. FP7-ENV-2008-1-226354), BIOFUN (ref. CTM2007-28739-E), PROMETEO (ref. CTM2007-66316-C02-01/MAR), ReDEco (ref. CTM2008-04973-E/MAR), DOS MARES (ref. CTM2010-21810-C03-01), PERSEUS (ref. GA 287600) i ARISTEUS (ref. PERG04-GA-2008-239175).

Il·lustració de la portada: Imatge de microscòpia electrònica de rastreig de partícules sedimentades a la conca profunda de Ierapetra l'abril de 2012. En aquesta s'hi observen diatomees (principalment del gènere *Chaetoceros*), coccolitoforis, cendres volcàniques, etc.

"When once [the deep ocean] has been seen, it will remain forever the most vivid memory in life, solely because of its cosmic chill and isolation, the eternal and absolute darkness and the indescribable beauty of its inhabitants."

Half Mile Down (William Beebe, 1934)

"Un cop s'ha vist [l'oceà profund], serà per sempre el record més vívid de la vida, pel sol fet de la seva fredor còsmica i aïllament, la foscor eterna i absoluta i la indescriptible bellesa dels seus hàbitats."

Mitja milla cap al fons (William Beebe, 1934)

A la meva iaia, als meus pares, a en Tino i la Teresa, i a en Joaquim

Agraïments/ Acknowledgements/ Ευχαριστίες

Ben entrada la matinada, al vaixell oceanogràfic Ángeles Alvariño, amb la mar una mica revoltada, amb els monitors de la multifeix davant meu i amb Blaumut sonant de fons, mentre escric aquestes quatre paraules penso què és el que m'ha portat fins aquí en aquest precís moment.

Tot va començar passejant per la facultat la primavera del 2009, la frase "Passa l'estiu al Parc!", referint-se al Parc Científic de Barcelona, em va cridar l'atenció quan estava a finals de tercer de carrera. Mai oblidaré aquesta frase, perquè és aquesta la que em va obrir la primera porta al món de la geologia marina, que, en aquell moment, m'era quasi del tot desconeguda. Alguna cosa a dins meu em deia que tenia ganes de conèixer més sobre aquest món i, efectivament, no em vaig equivocar.

Totes i cadascuna de les gotes que han fet possible l'existència del meu mar d'estudi han estat aportades per persones com tu, que ara mateix estàs llegint aquestes quatre paraules. Persones que m'han donat suport incondicional, que m'han nodrit amb tot el seu coneixement, que m'han acompanyat durant tot aquest camí, un camí que només ha fet que començar.

Primer de tot agrair als meus directors de Tesi, a l'Anna i en Toni, l'ànima dels tramperus del Grup de Recerca de Geociències Marines, GRCGM. Anna, Toni, us estic profundament agraïda per tot el suport que m'heu donat al llarg de tots aquests anys. La confiança que heu dipositat amb mi ha fet que no perdés en cap moment les ganes de seguir aprenent, investigant, i tingués capacitat d'autosuperació davant de qualsevol adversitat. Gràcies per la vostra orientació i correcció. Entrar al vostre despatx i discutir com seguir el següent pas sempre em donava molta força, crec de tot cor que sou un gran equip! Anna, "Endavant les atxes!" una frase que en els moments més intensos m'ha donat un plus d'energia immens! Moltes gràcies per la motivació que m'has transmès, per les hores de dedicació, per fer-me sentir part de l'equipàs dels tramperus. Toni, qualsevol dels teus consells val un imperi! Moltes gràcies Toni. No perdis mai aquest bon humor contagiós que tens, desprens tranquil·litat i paciència i, com sempre s'ha dit, la paciència és la mare de la ciència.

Miquel, encara recordo el primer dia quan m'estaves explicant quines línies de recerca seguia el GRCGM i em vas preguntar si coneixia què eren els canyons submarins i el cascading. Moltes gràcies per donar-me l'oportunitat d'haver pogut estar en aquest Grup de Recerca, i realitzar la Tesi Doctoral. Gràcies per haver-me donat l'oportunitat de créixer, tant professionalment com personalment. També et vull agrair de tot cor l'esforç del dia a dia que fas per a tots nosaltres, pel grup.

Aquests anys de doctorat han estat una cursa de fons, amb tot d'obstacles a superar durant el camí. Aprens coneixement, el comparteixes, el consolides, l'apliques, t'equivoques i aprens dels teus propis errors. Un camí que he compartit amb amics i companys, però sobretot amb vosaltres els tramperus becaris. Uri, Marc però molt especialment tu Aitor. Que sapigueu que ha estat un plaer immens tenir-vos al costat i compartir tots aquests anys. Aitor sense tu el meu estudi del mar profund segur que hagués estat d'un altre color, junts hem crescut com a científics. Gràcies

pels bons moments viscuts durant les campanyes, al laboratori, etc., durant tots aquests anys. Tanquem una etapa, la del doctorat (ara ja ho podem dir! Ara sí! Ja estem!), i se n'obren d'altres.

També vull agrair de tot cor a tots els de les sales 336 i 337 i voltants, que dia a dia hem compartit molts bons moments. Tot i estar cadascú al seu món concentrat, en els moments de kit-kat, discussió, guerra de pilotes, visites d'en Galde, hora de les carmanyoles o cafès, riures, etc., han fet que sempre hi hagi caliu. Anna Ayma, Xavi Rayo, Xavi Tubau, David, Jaime, Oli, Galde, Ruth, Patri, Judit, Albert, Mercè, Montse G., Ester, Leo, José Noel, Lluís, Isa, José Luís, Rubén, Pilar, Sergi, Aaron, Maria, etc., gràcies. Anna Ayma, Aitor, Xavi, Marc i Tubau, les converses amb vosaltres del matí o mitja tarda parlant de tot i de res no tenen preu! Paleoteam (o millor dit els xixos), els vostres "holeeeeees" matiners plens de dinamisme i vitalitat es contagien, sou genials! Galde, el teu grau d'exigència i detallisme ha fet que durant aquest temps m'hagi enriquit una visió encara més primmirada, gràcies. Xavi gràcies per la paciència que tens amb tots plegats quan et preguntem dubtes de l'Arcgis! David gràcies per transmetre'ns a tots la teva vitalitat, ganes de créixer i saber! *Aaron thank you very much to be there always and for all your help and corrections!* Leo gràcies per animar-me a volar, per la paciència que tens quan anem a veure a l'Anna a explicar-li o preguntar-li coses, i per compartir el teu coneixement i experiència viscuda.

També agrair a la Lucia Quirós, per la seva perseverança i bon fer. M'ha encantat treballar amb tu! Ets i seràs una gran científica.

Agrair també a totes aquelles persones que han ajudat amb l'execució de les anàlisis que formen part de la present Tesi Doctoral. Montse Guart moltes gràcies per ser com ets, per l'energia positiva que transmets a tots nosaltres! Sense tu el laboratori no tindria vida! Agrair al personal dels Centres Científics i Tecnològics de la Universitat de Barcelona i del Parc Científic de Barcelona, especialment a la Pilar Teixidor, a la Pili, a la Maite i a la Regina. Gràcies per la paciència quan us portava desenes i desenes de mostres per analitzar, per la vostra precisió i atenció.

Ah i no m'oblido pas de tu Sílvia. Gràcies per tot el que fas per nosaltres. El primer bon dia i somriure del departament sempre és el teu, fins i tot quan et trobes un escampall de closques de nou. Personal d'administració del departament, Maite, Teresa, Montses, Elisenda, Bernat, agrair el vostre esforç constant que feu per tots nosaltres. Sou una peça clau dins de tot l'entramat.

Als co-autors i revisors dels articles els hi agraeixo els temps que han dedicat a enriquir i millorar els treballs recollits en aquesta Tesi. Agrair també a tots els participants de les campanyes oceanogràfiques on s'han obtingut mostres per aquesta Tesi. Batis, Siscu, Ulla, Ariadna i tot el vostre grup de Recursos Marins Renovables, moltes gràcies per la bona harmonia que genereu i per ensenyar-me a diferenciar i mostrejar diferents espècies de peixos d'aigües profundes!.

Una part important d'aquesta Tesi s'ha realitzat a Grècia, a l'Hellenic Center for Marine Research, amb l'Alexandra Gogou, en Constanine Parinos, en Dimitris Velaoras, en Nikolaos Lampadariou i la Katherina Sevastou. Moltes gràcies per haver-me donat l'oportunitat de poder aprendre de vosaltres i per la vostra dedicació. *Δημήτρη, Νίκο, Κατερίνα, και κυρίως Αλέκα και Κώστα, θα σας είμαι πάντα ευγνώμων, για το κίνητρο, την επιστημονική βοήθεια, την αφοσίωση, καθώς και την*

υποστήριξη εντός και εκτός εργαστηρίου. Σας ευχαριστώ για όλα. Είσαστε ένα σημαντικό κομμάτι της παρούσας διατριβής.

A tots els amics de les terres Montserratines (però sobretot a la Gemma, la Mercè, la Laura, i la Núria!), de la bona colla d'Ambientals (especialment a la Marta A., però també a l'Ibor, la Pilar, en Carles, la Judit, en Pol, en Ricard, en Ximo, en Pablo, en Xus, etc.), a la Sílvia Aibar i a la Marta Bonet, agrair-vos de tot cor la vostra amistat. Tot i estar perduda per arreu constantment, vosaltres sempre hi sou. Les nostres trobades són úniques!

I sens dubte, agrair a tota la família, la que hi era, és i hi serà. Mama, papa, Pau, iaia, àvia, el petit Guiu, Tino i com no, a la Teresa, gràcies per ser-hi sempre, per tota la valentia que m'heu donat sempre durant tots aquests anys tot i no sempre saber què estava fent ben bé hehe.

I finalment, a en Joaquim, gràcies per compartir el teu camí amb el meu, per haver-me fet costat i animar-me en tot moment i perdó per les vacances i caps de setmana robats! Sempre amb tu!

A tots, gràcies! Thank you! *ευχαριστώ*!

Índex

Resum 1

Resumen 2

Abstract 3

Enfocament i objectius 5

Estructura de la Tesi 7

CAPÍTOL 1. Introducció 9

1.1. Origen i composició dels sediments marins 11
1.1.1. Components detrítics 11
1.1.2. Components biogènics 13

1.2. Processos i ambients sedimentaris 20
1.2.1. Processos sedimentaris 20
1.2.2. Ambients sedimentaris 22

1.3. Àrea d'estudi: marges continentals i conques de la mar Mediterrània 23
1.3.1. La plataforma continental de Barcelona i el canyó de Blanes 25
1.3.2. La mar Mediterrània oriental i la conca de Ierapetra 27

1.4. Material i mètodes 29
1.4.1. Tècniques de mostreig 30
1.4.1.1. Mostreig de sediment 30
1.4.1.2. Mostreig de partícules 31
1.4.2. Tècniques analítiques 33
1.4.2.1. Anàlisi granulomètrica 33
1.4.2.2. Mètode de fraccionament per mida de gra 35
1.4.2.3. Anàlisi de la composició elemental i isòtops estables del C 36
1.4.2.4. Anàlisi d'òpal 37
1.4.2.5. Anàlisi de biomarcadors lipídics 38
1.4.2.6. Anàlisi microestructural 39
1.4.3. Altres paràmetres i eines de suport 39

CAPÍTOL 2. Resultats 41

2.1. Distribution and sources of organic matter in size-fractionated nearshore and inner-shelf sediments of the NW Mediterranean 43
Abstract 43
2.1.1. Introduction 44

2.1.2. Study area 45
2.1.2.1. Geographic and geological setting 45
2.2.2.2. Oceanographic, meteorological and hydrological settings 46
2.1.3. Material and methods 47
2.1.3.1. Sample collection and analytical methods 47
2.2.3.2. External forcing parameters 48
2.1.4. Results 49
2.1.4.1. Forcing conditions 49
2.2.4.2. Grain-size 50
2.2.4.3. Organic matter content and stable isotope ratios 52
2.1.5. Discussion 55
2.1.5.1. Grain-size distribution and variability in surface sediments 55
2.2.5.2. Organic matter distribution and variability among the grain-size fractions 58
2.2.5.3. Organic matter sources from nearshore to lower slope 60
2.1.6. Conclusions 63
2.1.7. Acknowledgments 64
2.1.8. References 64

2.2. Impact of storm-induced remobilization on grain size distribution and organic carbon content in sediments from the Blanes Canyon area, NW Mediterranean Sea 73
Abstract 73
2.2.1. Introduction 74
2.2.2. Study area 75
2.2.2.1. Geographical and geological settings 75
2.2.2.2. Oceanographic setting 75
2.2.3. Material and methods 76
2.2.3.1 Sediment sample collection 76
2.2.3.2. Analytical methods 77
2.2.3.3. Meteorological, hydrological and oceanographic data 78
2.2.4. Results 79
2.2.4.1. Forcing conditions 79
2.2.4.2. Grain-size and calcium carbonate distribution 81
2.2.4.3. OC, TN/OC and $\delta^{13}C$ 85
2.2.5. Discussion 88
2.2.5.1. Storm impact on near-bottom currents, sediment transport and grain size distribution 88
2.2.5.2. Impact of the storm on OC transport and provenance 90
2.2.6. Conclusions 94
2.2.7. Acknowledgements 95
2.2.8. References 95

2.3. Composition and sources of sedimentary organic matter in the deep eastern Mediterranean Sea 103
Abstract 103
2.3.1. Introduction 104
2.3.2. Oceanographic setting 104
2.3.3. Material and methods 106
2.3.3.1. Sampling 106
2.3.3.2. Analytical procedures 107
2.3.4. Results 111
2.3.4.1. Grain size characteristics 111
2.3.4.2. Bulk geochemical sediment composition 114

2.3.4.3. Elemental and stable isotopic composition of sedimentary OM 115
2.3.4.4. Lipid biomarkers 116
2.3.4.5. Multivariate analysis of geochemical parameters 118
2.3.5. Discussion 120
2.3.5.1. Sources of sedimentary material in the deep Eastern Mediterranean Sea 120
2.3.5.2. Regional variability and oceanographic control on the geochemical composition of deep Eastern Mediterranean Sea surface sediments 124
2.3.6. Conclusions 129
2.3.7. Acknowledgments 130
2.3.8. References 130

2.4. Enhanced carbon export to the abyssal depths driven by atmosphere dynamics 143
Abstract 143
2.4.1. Introduction 144
2.4.2. Data and methods 144
2.4.3. Results 146
2.4.3.1. Air-sea exchanges and ocean response 146
2.4.3.2. Particle fluxes 147
2.4.4. Discussion 148
2.4.4.1. Atmospheric Forcing 148
2.4.4.2. Oceanographic and Biological Response 149
2.4.4.3. Impact on the Carbon Cycle 151
2.4.5. Acknowledgments 153
2.4.6. Supplementary table and figure 153
2.4.7. References 155

2.5. Resum de resultats 163

CAPÍTOL 3. Discussió 165

3.1. Caracterització de la matèria orgànica 167
3.1.1. Distribució i fonts de la matèria orgànica al marge continental nord-català 167
3.1.2. Distribució, fonts i preservació de la matèria orgànica a la Mediterrània oriental 169

3.2. Mecanismes de transferència de carboni orgànic 171
3.2.1. Temporals costaners 171
3.2.2. Convecció a mar obert 172

CAPÍTOL 4. Conclusions 177

CAPÍTOL 5. Bibliografia 181

Annex 197

Taules 199

Resum

Un dels grans reptes de la biogeoquímica marina és millorar el coneixement sobre la variabilitat temporal (estacional i interanual) i espacial (regional i global) de l'absorció de CO_2 per part dels oceans, així com també sobre els processos físics i biològics que la regulen.

En aquest context, l'estudi de les condicions ambientals que controlen la fixació, el transport, l'enfonsament, l'enterrament i, conseqüentment, el segrest de carboni orgànic (OC) és fonamental per entendre la interrelació entre les concentracions de CO_2 a l'atmosfera i als oceans, i com aquests tenen un paper clau en la regulació del clima global i el canvi climàtic. La caracterització d'aquestes condicions ambientals és d'especial importància en zones oligotròfiques, ja que aquestes cobreixen aproximadament el 75% de la superfície oceànica i contribueixen en més d'un 30% de la fixació global de carboni marí.

En aquesta Tesi s'han intentat resoldre qüestions fonamentals com 'Quins forçaments ambientals estan implicats en la fixació i enfonsament de l'OC en un ambient oligotròfic i semi-tancat, com és el cas de la mar Mediterrània?' i 'Com i on s'acumula l'OC, i com el seu origen afecta a la seva preservació i enterrament en els sediments profunds?'. L'anàlisi combinada de les característiques biogeoquímiques dels sediments superficials de plataforma continental, talussos i conques profundes de la mar Mediterrània, així com de fluxos de partícules, juntament amb l'avaluació dels paràmetres meteorològics, hidrològics i oceanogràfics de cada ambient, ha posat de manifest que els esdeveniments oceanogràfics forçats per processos atmosfèrics juguen un paper clau en el cicle del carboni a la mar Mediterrània. Les tempestes costaneres amb forts vents, els quals provoquen fort onatge i intensificació dels corrents de fons, han demostrat ser un mecanisme eficient en el transport d'OC des de zones someres a ambients més profunds, essent els canyons submarins els conductes preferencials de transport. Aquest transport cap a ambients sedimentaris profunds determina la classificació i deposició de les partícules en funció de la seva mida de gra, on les més fines i més riques en OC són aquelles que es transporten grans distàncies. D'altra banda, les tempestes a mar obert, amb forts vents de nord freds i secs, poden generar processos de convecció, que comporten moviments verticals de mescla de les masses d'aigua, aflorament de nutrients en superfície i augment de la productivitat primària, i exportació d'OC fins a profunditats batipelàgiques. A més, en aquests casos, l'arribada de nutrients addicional deguda a una deposició atmosfèrica extraordinària de cendres volcàniques pot provocar la intensificació de l'exportació de fitodetritus frescos.

Els resultats obtinguts en aquesta Tesi són de gran interès tan per a la comunitat científica que tracta de resoldre aspectes importants relacionats amb la bomba biològica (fixació, exportació, transport i enterrament del carboni), com aquella que investiga el funcionament dels ecosistemes profunds (entenent els fluxos de carboni com arribades de material nutritiu per la fauna bentònica).

Resumen

Uno de los grandes retos de la biogeoquímica marina es mejorar el conocimiento sobre la variabilidad temporal (estacional e interanual) y espacial (regional y global) de la absorción de CO_2 por parte de los océanos, así como también sobre los procesos físicos y biológicos que la regulan.

En este contexto, el estudio de las condiciones ambientales que controlan la fijación, el transporte, el hundimiento, el entierro y, consecuentemente, el secuestro de carbono orgánico (OC) es fundamental para entender la interrelación entre las concentraciones de CO_2 en la atmósfera y los océanos, y qué papel clave tienen éstos en la regulación del clima global y el cambio climático. La caracterización de estas condiciones ambientales es de especial importancia en zonas oligotróficas, ya que éstas cubren aproximadamente el 75% de la superficie oceánica y contribuyen en más de un 30% de la fijación global de carbono marino.

En esta Tesis se han estudiado varias cuestiones fundamentales como: ¿Qué forzamientos ambientales están implicados en la fijación y hundimiento del OC en un ambiente oligotrófico y semicerrado, como es el caso del mar Mediterráneo? y ¿Cómo y dónde se acumula el OC, y como su origen afecta a su preservación y entierro en los sedimentos profundos?". El análisis combinado de las características biogeoquímicas de los sedimentos superficiales de plataforma continental, taludes y cuencas profundas del mar Mediterráneo, tanto occidental como oriental, así como de flujos de partículas, junto con la evaluación de los parámetros meteorológicos, hidrológicos y oceanográficos de cada ambiente, ha puesto de manifiesto que los eventos oceanográficos forzados por procesos atmosféricos juegan un papel clave en el ciclo del carbono en el mar Mediterráneo. Los temporales costeros con fuertes vientos, los cuales provocan fuerte oleaje e intensificación de las corrientes de fondo, han demostrado ser un mecanismo eficiente en el transporte de OC de zonas someras a ambientes más profundos, siendo los cañones submarinos los conductos preferenciales de transporte. Este transporte hacia ambientes sedimentarios profundos determina la clasificación y deposición de las partículas en función de su tamaño de grano, siendo las más finas las más ricas en OC y aquellas que se transportan grandes distancias. Por otra parte, las tormentas en mar abierto, con fuertes vientos de norte, fríos y secos, pueden generar procesos de convección que conllevan movimientos verticales de mezcla de las masas de agua, afloramiento de nutrientes en superficie, junto a un aumento de la productividad primaria y exportación de OC hasta profundidades batipelágicas. Además, en estos casos, la llegada de nutrientes adicional mediante una deposición atmosférica extraordinaria de cenizas volcánicas puede provocar la intensificación de la exportación de fitodetritus frescos.

Los resultados obtenidos en esta Tesis son de gran interés tanto para la comunidad científica que trata de resolver aspectos importantes relacionados con la bomba biológica (fijación, exportación, transporte y entierro del carbono), como aquella que investiga el funcionamiento de los ecosistemas profundos (entendiendo los flujos de carbono como llegadas de material nutritivo para la fauna bentónica).

Abstract

One of the grand challenges in marine biogeochemistry is to improve our understanding on the temporal (seasonal and multi-annual) and spatial (regional and global) variability of ocean uptake of CO_2, and the physical and biological processes that regulate this process. In this context, the study of the environmental conditions that control organic carbon (OC) fixation, OC sinking, OC burial, and thus OC sequestration becomes critical to better understand feedbacks between the atmospheric CO_2 concentration and the oceans, and how they play a key role in climate regulation and climate change. This is of special importance in oligotrophic waters, which roughly cover 75% of the ocean's surface and contribute over 30% of the global marine carbon fixation.

In this PhD Thesis several fundamental questions have been studied such as 'Which environmental forcings are involved in OC fixation and sinking in an oligotrophic and semi-enclosed environment such as the Mediterranean Sea?', and 'How and where does OC accumulate, and how its origin affects its preservation and burial in the deep sediments?'. The combined analysis of continental shelf, slope, and deep basin surface sediments and particle fluxes, together with the study of the meteorological, hydrological and oceanographic settings at each environment, have revealed that atmosphere-driven oceanographic events play a major role in the carbon cycle in the Mediterranean Sea. Thus, coastal storms with strong winds, high waves and intensified currents have been proved to be efficient at transporting OC from shallow to deeper environments, with submarine canyons acting as a preferential conduit. This transport to deep sedimentary environments is mainly controlled by the hydrodynamic sorting and differential deposition of particles with different grain sizes, being the finer those with the highest loadings of OC and those that can be transported long distances. In addition, open sea storms with cold and dry northerly winds trigger convective mixing, nutrient uplifting and episodic events of increased carbon export to abyssal areas. Moreover, in these cases, the arrival of additional nutrients due to extraordinary atmospheric deposition of volcanic ash can cause the intensification of export of fresh phytodetritus.

The results obtained in this PhD Thesis are of great interest for the scientific community trying to resolve important aspects of the biological pump (fixation, export, transport and burial of carbon), and all those researchers that investigate the functioning of deep ecosystems (the carbon flux is an input of nutritive material for benthic fauna).

Enfocament i objectius

Els elements clau per entendre el funcionament dels ecosistemes marins rauen en la interrelació i dependència dels processos biogeoquímics (cicles dels nutrients essencials, origen, evolució i valor nutricional de la matèria orgànica), físics (característiques de les masses d'aigua, velocitat i direcció del corrent), i geològics (aportació de sediments, característiques del substrat) que tenen lloc al seu entorn.

Quin són els processos que propicien la formació de sediments, i un cop formats, com arriben aquests al fons del mar? Quin paper juguen els processos físics i biològics en l'origen, transport i deposició dels sediments? Com i on es transporta, dipositа i preserva la matèria orgànica al mar, i quines implicacions té per a l'escalfament global?.

La present Tesi aporta informació rellevant per poder respondre a aquestes preguntes clau, aportant una interpretació del cicle del transport de partícules (litogèniques i biogèniques) a través de la columna d'aigua, des de les potencials fonts fins al seu enterrament, contribuint d'aquesta manera al coneixement del paper de l'oceà en el cicle global del carboni i altres elements associats. Aquesta investigació s'ha dut a terme a la mar Mediterrània, una mar semi-enclosa amb unes característiques que la converteixen en una regió idònia per dur a terme estudis de processos físics i biogeoquímics que tenen lloc a escala global. Les seves característiques especials són: 1) una circulació termohalina, incloent la formació d'aigües profundes, 2) patrons de circulació de mesoescala que afecten a la distribució dels nutrients i carboni orgànic, 3) elevades taxes de ventilació i temps de residència de les aigües profundes (20-126 anys), 4) temperatura de les aigües profundes 10 ºC més elevada que les aigües de mar obert, 5) elevades taxes de respiració i mineralització del carboni orgànic, i 6) diversos patrons d'estratificació en zones situades molt pròximes entre elles. Estudis recents han demostrat que els ecosistemes de la mar Mediterrània són altament vulnerables a les pertorbacions ambientals, i que la biodiversitat es veu afectada per canvis bruscos en les condicions fisicoquímiques (p.ex., Company et al., 2008). No obstant això, gran part de les conseqüències d'aquests canvis en les condicions ambientals dels ecosistemes de la Mediterrània són, a data d'avui, desconegudes.

Aquesta Tesi s'emmarca en els projectes REDECO (*Regional Drivers of Ecosystem Change and its Influence on Deep-Sea populations in the Mediterranean*, ref. CTM2008-04.973-E), PROMETEO (Estudio integrado de Cañones Submarinos y Taludes profundos del Mediterráneo Occidental: Un hàbitat essencial, ref. CTM2007-66316-C02-01/MAR) i HERMIONE (*Hotspot Ecosystem Research and Man's Impact on European Seas*, ref. FP7-ENV-2008-1-226354), concebuts per generar avenços significatius en els coneixements actuals sobre el funcionament dels ecosistemes marins, tant de canyons submarins com de talussos i conques profundes.

La hipòtesi plantejada a través d'aquesta Tesi es basa en la possibilitat que existeixi una relació entre els paràmetres ambientals dels ecosistemes marins, determinats a darrera instància per forçaments de caràcter atmosfèric, i el seu funcionament.

Així doncs, l'objectiu general d'aquesta Tesi es centra en caracteritzar la variabilitat temporal i espacial dels sediments superficials i els fluxos de partícules a la mar Mediterrània, des de la

plataforma continental fins a profunditats batipelàgiques, i determinar com aquests es veuen afectats per l'ocurrència de processos energètics puntuals d'origen atmosfèric.

Els objectius concrets d'aquesta Tesi són:

1) Millorar el coneixement sobre els processos responsables del transport de sediments i carboni orgànic al marge continental nord-català a la Mediterrània occidental, i identificar com els forçaments externs (règim de vents, temperatura, pluviometria, aports fluvials, règim d'onatge i corrents) propicien aquest transport.

2) Investigar la distribució espacial, les principals fonts (terrestre, marina, antropogènica) i l'estat de preservació de la matèria orgànica als sediments superficials de les conques més profundes de la Mediterrània oriental.

3) Quantificar l'exportació de carboni orgànic des de la superfície fins a profunditats batipelàgiques en una zona concreta de la Mediterrània oriental, la conca de Ierapetra, i identificar els forçaments externs vinculats a aquesta exportació.

Estructura de la Tesi

Aquesta Tesi es presenta com a compendi de publicacions, i s'estructura seguint la normativa de la Universitat de Barcelona i la normativa específica del Programa de Doctorat de Ciències del Mar. La Tesi s'estructura en 5 capítols.

En el primer capítol (Capítol 1) s'hi presenta el context científic que justifica el treball realitzat. S'inicia amb una introducció general explicant l'origen i composició dels sediments marins, amb especial èmfasi al material particulat biogènic, així com també els possibles processos de transferència de material particulat al mar. A més, s'hi inclou una descripció de l'àrea d'estudi, de les mostres treballades, i de les tecnologies i metodologies emprades.

El següent capítol (Capítol 2), correspon als articles científics realitzats per la doctoranda. Són una còpia completa i fidedigne dels articles publicats o en fase de revisió en revistes indexades en el *Science Citation Index* del *ISI Web of Knowledge*. A cada publicació s'hi ha afegit la referència completa de la revista al qual ha estat publicada o enviada, així com també el nom i afiliacions dels diferents coautors. A part dels 4 subcapítols relacionats amb cada article, al final hi ha un subcapítol de resum de resultats.

En el subcapítol 2.1 es presenta l'article *Distribution and sources of organic matter in size-fractionated nearshore sediments off the Barcelona city (NW Mediterranean)*, enviat a la revista Estuarine, Coastal and Shelf Science. En aquest article es combina informació meteorològica, hidrològica i oceanogràfica amb l'anàlisi biogeoquímica (composició elemental i relació isotòpica) i sedimentològica (mida de gra) de sediments superficials obtinguts a la plataforma continental interna de Barcelona durant l'estiu-tardor 2012 per a de determinar els mecanismes de dispersió de sediments.

El subcapítol 2.2, que és el segon article d'aquesta Tesi, porta per títol *Impact of storm-induced remobilization on grain size distribution and organic carbon content in sediments from the Blanes Canyon area, NW Mediterranean Sea,* publicat a la revista Progress in Oceanography l'any 2013. En aquest article s'utilitzen les mateixes tècniques analítiques i anàlisi de variables meteorològiques, hidrològiques i oceanogràfiques que en el súbcapítol 2.1, per a determinar els mecanismes de dispersió de sediments al canyó de Blanes i a la plataforma continental de Barcelona i talús adjacent durant el període entre setembre del 2008 i maig del 2009.

En el subcapítol 2.3 es presenta l'últim article de la Tesi Doctoral. Aquest porta per títol *Composition and sources of sedimentary organic matter in the deep Eastern Mediterranean Sea* i va ser publicat a la revista Biogeosciences l'any 2015. En aquest subcapítol es presenten els resultats de l'anàlisi de la mida de gra, la composició elemental, la relació isotòpica i el contingut en biomarcadors lipídics de sediments superficials recollits a les mars Jònica, Egea i de Llevant a profunditats de 1000 a 4000 m.

El subcapítol 2.4, titulat *Enhanced carbon export to the abyssal depths driven by atmosphere dynamics*, enviat a la revista Geophysical Research Letters el passat maig de 2016. En aquest subcapítol es presenta una sèrie temporal de 3 anys (de 2010 a 2013) de fluxos de carboni orgànic i sílice biogènica a 4285 m de profunditat a la conca de Ierapetra (Mediterrània oriental).

Al Capítol 3 es duu a terme una síntesi i discussió integradora de tots els resultats obtinguts durant el transcurs de la Tesi, incloent els articles esmentats anteriorment.

El capítol 4, conté les principals conclusions obtingudes en aquesta Tesi Doctoral. Així mateix, s'inclou una ressenya sobre les implicacions i possibles línies de recerca futures sorgides arran d'aquesta Tesi.

Finalment, a part de la presentada dins dels subcapítols dels articles (Capítol 2), el capítol 5 recull la bibliografia emprada a la resta de capítols de la Tesi.

Capítol 1

Introducció

1.1. Origen i composició dels sediments marins

> *"When I think of the floor of the deep sea, the single, overwhelming fact that possesses my imagination is the accumulation of sediments. I see always the steady, unremitting, downward drift of materials from above, flake upon flake, layer upon layer – a drift that has continued for hundreds of millions of years, that will go on as long as there are seas and continents... For the sediments are the materials of most stupendous snowfall the Earth has ever seen..."*
> ***Rachael Carson, The Sea Around Us***

El concepte sediment, el qual deriva del mot llatí *sedimentum,* es defineix com a matèria que un líquid portava en suspensió i s'ha dipositat al fons. Els sediments dipositats a l'oceà són un arxiu d'informació històrica sobre la Terra i proporcionen informació sobre els cicles biogeoquímics globals.

Els sediments marins són heterogenis en quant a la seva composició (Figura 1.1). Tenint en compte l'origen i la formació de les seves partícules, en els sediments marins es poden distingir tres tipus bàsics de material (Goldberg, 1954): detrític (o litogènic), biogènic i autigènics (o hidrogènic). Mentre que els materials detrítics s'originen per la fracturació, la desintegració i l'esmicolament d'una roca preexistent coherent, els biogènics són produïts per l'acció d'organismes vius. Els materials autigènics (precipitats o diagènetics) són aquells que es formen *in situ* a la columna d'aigua, a la superfície dels sediments, o en els sediments a través de processos inorgànics (Kastner, 1999). Els components predominants en els sediments marins són generalment els materials detrítics i biogènics. Els components autigènics tot i ser quantitativament menys importants, poden jugar un paper important en els cicles geoquímics de certs elements com és el cas del Fe, Mn, P, i S (Burdige, 2006).

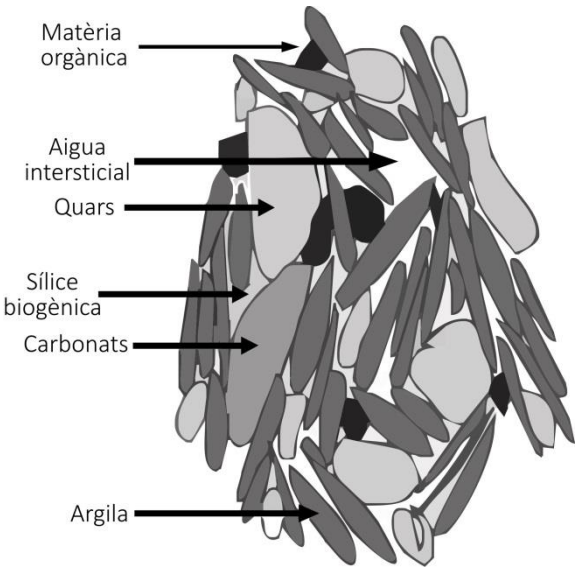

Figura 1.1. Esquema d'una mescla heterogènia típica de sediments marins composta d'aigua intersticial i diversos tipus de partícules sòlides: argila i quars (fracció litogènica) i carbonats, sílice i matèria orgànica (fracció biogènica). Modificada de Boudreau (1997).

1.1.1. Components detrítics

La principal font de partícules litogèniques són les roques continentals, les quals han estat trencades, disgregades i dissoltes per meteorització física, química i biològica. La naturalesa de la roca mare i les condicions climàtiques prevalents determinen la intensitat a la qual es duu a terme

l'erosió i, conseqüentment, la composició dels sediments detrítics. Quantitativament, els minerals derivats de la terra més importants en els sediments són els minerals d'argila i quars, juntament amb petites quantitats d'altres minerals com els feldspats. Els minerals argilosos, formats per silicats d'alumini hidratats, són d'especial importància ja que constitueixen la major proporció de sediments de gra fi i a més tenen la capacitat d'absorbir ions dins la seva estructura cristal·lina, unir-se entre ells superficialment a través d'adsorció reversible, o absorbir grans quantitats d'aigua.

La major aportació de sediments detrítics a l'oceà s'efectua a través de la descàrrega fluvial (84%), seguit per la deposició atmosfèrica (>7%) i pel transport glacial (<7%) (Lisitzin, 1996; Weaver, 1990).

Els rius canalitzen tant material litogènic dissolt com material en suspensió (i.e., material particulat sòlid). Tot i que depèn de la intensitat del flux de descàrrega i de la càrrega en suspensió, les partícules transportades pels rius normalment tenen una mida de gra inferior al llim groller (<30 μm). Es calcula que la quantitat total de partícules descarregades pels rius als oceans anualment a escala mundial és d'aproximadament $20 \cdot 10^9$ tones (Milliman i Syvitski, 1992). La quantitat i concentració de partícules en suspensió varia essencialment per la superfície i el relleu de la conca hidrogràfica, i secundàriament depèn del clima, de la massa d'aigua dels rius, de les condicions geològiques i de l'activitat humana de l'entorn (Walling i Fang, 2003; Walling, 2009). La majoria dels sediments transportats pels rius es dipositen a zones costaneres d'escassa energia, a estuaris, i a plataformes continentals. Només una petita part d'aquests sediments, generalment la fracció més fina, poden arribar a ser dispersats més enllà del límit de plataforma i arribar a zones profundes dels oceans.

A través del transport eòlic, els materials litogènics poden arribar a recórrer distàncies de centenars a milers de quilòmetres des dels continents fins als oceans en forma de pols mineral (aerosols) o cendres volcàniques. La mida de gra màxima aproximada que s'assumeix que el vent és capaç de transportar és 80 μm. Mentre que les partícules més grolleres, com són les sorres fines típiques dels sòls continentals, generalment es dipositen a zones costaneres, les més fines ho fan a zones molt més allunyades. El transport eòlic de pols mineral es concentra en regions específiques del planeta atès que les principals fonts són les regions àrides i semiàrides. El desert del Sàhara representa la font de pols més important del planeta (58%) (Jickells i Moore, 2015; Tanaka i Chiba, 2006) (Figura 1.2). La mar Mediterrània, objecte d'estudi d'aquest treball, és la mar més influenciada per deposició atmosfèrica del planeta. La quantitat de pols mineral que s'introdueix a l'oceà anualment és d'aproximadament $0.45 \cdot 10^9$ tones (Jickells et al., 2005), la qual correspon al 60-91% del total introduït a l'atmosfera (Prospero, 1996). La taxa de deposició de fragments piroclàstics transportats pel vent és molt menor. Tot i així, l'abast de distribució de cendres volcàniques pot arribar a ser tant a nivell local com a nivell mundial quan hi ha gran erupcions volcàniques (Segschneider et al., 2013). La presència de dipòsits de cendres als sediments marins proporcionen informació sobre els períodes d'activitat volcànica i faciliten la cronologia dels sediments.

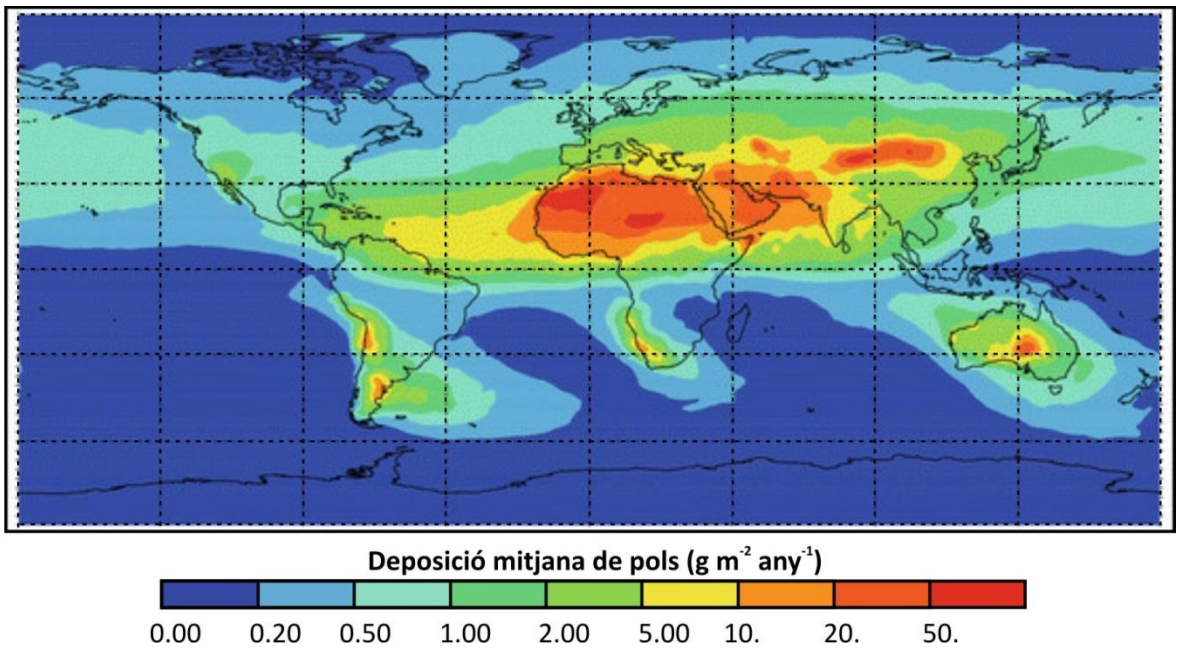

Figura 1.2. Deposició global de pols atmosfèrica (Jickells et al., 2005).

En algunes regions, fora de l'àrea d'estudi d'aquest treball, el transport glacial (glaceres i icebergs) juga un paper fonamental en els processos de distribució dels materials detrítics. Això és especialment cert a l'Oceà Àrtic, on durant la formació del gel de les àrees costaneres poc profundes aquest incorpora sediment que posteriorment és incorporat a la columna d'aigua i dipositat al fons marí.

1.1.2. Components biogènics

En sentit ampli, els sediments biogènics es defineixen com tot material sòlid format a la biosfera, incloent tant les partícules inorgàniques (restes i fragments de closques d'organismes) com les orgàniques (matèria orgànica) (Goldberg, 1954).

Els carbonats i la sílice biogènica són els **biominerals** predominants als sediments marins. Els carbonats poden presentar-se en forma de calcita o d'aragonita, sent la primera molt més abundant a causa de l'alta solubilitat de l'aragonita. Ambdues formes tenen la mateixa fórmula química ($CaCO_3$) però difereixen en la seva estructura cristal·lina. Gairebé tots els carbonats dipositats als oceans es formen exclusivament a través de processos biològics. Els organismes productors de calcita més importants són els coccolitoforis (algues planctòniques amb coberta de plaques calcàries, els coccòlits), i els foraminífers planctònics (protozous) (Milliman, 1993), mentre que els pteròpodes (mol·luscs pelàgics) són els capaços de produir closques d'aragonita. La forma predominant de sílice biogènica als sediments marins és la sílice hidratada amorfa ($SiO_2 \cdot nH_2O$) o òpal. Les diatomees (algues unicel·lulars) i els radiolaris (zooplàncton d'aigües superficials i profundes) són els organismes que produeixen la majoria d'òpal que es troba als sediments marins (Tréguer i De La Rocha, 2013)

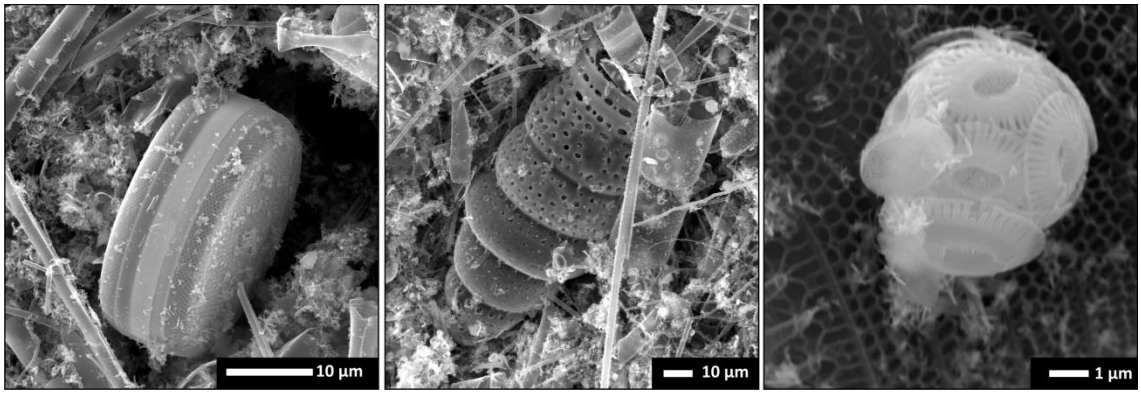

Figura 1.3. Fotografies de microscòpia electrònica de rastreig d'organismes planctònics rellevants per la formació de sediments biogènics. *A l'esquerra*: diatomees silíciques cèntriques. *Al mig*: Radiolaris silícics. *A baix*: coccolitoforis calcaris .

S'estima que les taxes de producció total anual de carbonat calci i sílice són de $5.3 \cdot 10^{15}$ g i $0.2\text{-}0.3 \cdot 10^{15}$ g Si, respectivament (Iglesias-Rodríguez et al., 2002; Milliman, 1993; Ragueneau et al., 2000). Tot i que les regions d'alta producció de carbonat i de sílice sovint són similars, la distribució de dipòsits d'aquests elements són molt diferents. Al contrari que el carbonat calci, el silici pot ser un nutrient limitant ja que es troba generalment a concentracions baixes a les aigües oceàniques superficials. Només una petita part de l'òpal produït a les aigües superficials dels oceans arriba a ser enterrat en els sediments marins. Això és degut a que la majoria de l'òpal es dissol a la columna d'aigua durant l'enfonsament de les partícules (Nelson et al., 1995). Per tant, els patrons de distribució de sílice en els sediments superficials es modulen per les entrades de silici a la superfície de l'oceà. A certes zones on hi ha un gran ascens d'aigües profundes riques en sílice (ex., Antàrtida o el Pacífic equatorial), la producció de sílice és suficientment gran com perquè el flux d'exportació sigui superior al de dissolució, permetent així l'acumulació als sediments.

La **matèria orgànica** marina que trobem a la columna d'aigua o als sediments marins pot tenir dos orígens: aquella que prové d'una font externa al medi marí (al·lòctona) i aquella originada al mateix medi marí (autòctona). La matèria orgànica al·lòctona arriba als oceans a través de les descàrregues fluvials i la deposició atmosfèrica, essent les principals fonts la vegetació, els sòls i biomassa fresca o cremada, o aquelles derivades d'activitats antropogèniques. Per contra, la matèria orgànica autòctona és aquella que es genera mitjançant la producció primària marina, controlada essencialment per la fotosíntesi del fitoplàncton, algues microscòpiques flotants (generalment <10 micres), o per algues bentòniques en zones costaneres poc profundes. A través de la respiració de la comunitat planctònica, principalment bacteris heteròtrofs i fitoplàncton, gran part de la matèria orgànica produïda és remineralitzada. A més, mitjançant la biosíntesi, els productes derivats de la fotosíntesi, és a dir sucres, proteïnes, lípids, etc., s'utilitzen com a font d'energia per a altres organismes i també per generar altres compostos bioquímics. Les reaccions reversibles que participen en la fotosíntesi i respiració de la matèria orgànica queden descrites a la Figura 1.4 mitjançant una equació conceptual (Anderson, 1995; Paulmier et al., 2009).

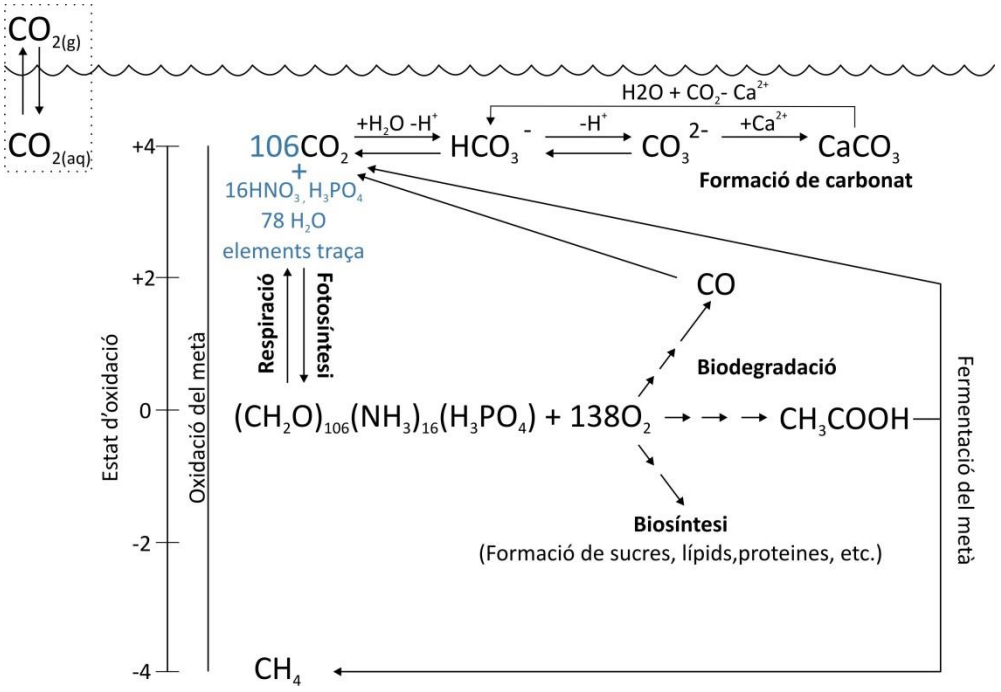

Figura 1.4. Representació esquemàtica de les principals rutes biogeoquímiques del cicle del carboni. Modificada de Liu et al. (2010).

Els factors més importants per la producció i remineralització de la matèria orgànica són la disponibilitat de llum i nutrients, el contingut d'oxigen i l'acidesa de l'aigua. Mentre que la fotosíntesi està limitada a la zona fòtica dels oceans, la profunditat de la qual varia en funció de la quantitat de material particulat, situant-se a l'oceà obert al voltant dels 200 m de profunditat, la respiració es pot dur a terme al llarg de tota la columna d'aigua. Els elements que poden limitar la fotosíntesi es coneixen com a nutrients. Els macronutrients (N, P i Si) i micronutrients (elements traça com el Fe) tenen una concentració mitjana de mmol m^{-3} i µmol m^{-3}, respectivament. Les ràtios estequiomètriques, constants en els organismes, de C:N:P de 106:16:1 s'anomenen les ràtios de Redfield (Redfield, 1934; Redfield et al., 1963).

El cicle del carboni als oceans. El diòxid de carboni (CO_2) té un paper clau en la modulació del clima del planeta, sent el principal responsable del conegut efecte hivernacle. Des de la Revolució Industrial, iniciada a finals del segle XVIII, a escala global, el CO_2 atmosfèric augmenta perquè hi ha una manca de balanç entre les emissions de CO_2 a l'atmosfera i l'absorció per part dels diferents reservoris de CO_2 (Figura 1.5) (Ciais et al., 2014).

Els oceans juguen un paper molt important en el cicle global del carboni ja que són un embornal amb flux net continu de CO_2, absorbint més carboni del que emeten (Watson i Orr, 2003). Durant l'última dècada l'oceà ha absorbit gairebé el 30% del CO_2 antropogènic emès. El CO_2 atmosfèric s'intercanvia amb la superfície de l'oceà a través de l'intercanvi de gasós. Part d'aquest CO_2 roman com a gas dissolt, però gran part es transforma en diferents especies químiques en equilibri (Figura 1.4) (Karl et al., 2003). El reservori de C oceànic està distribuït de manera irregular entre els constituents dissolts i particulats, amb diferents estats redox. Aquestes fonts inclouen el carboni inorgànic i orgànic particulat (PIC i POC, partícules >0.45µm) i el dissolt (DIC i DOC). El PIC està format essencialment per carbonat de calci ($CaCO_3$), provinent d'organismes amb exo i endoesquelets calcaris, i el POC, que inclou tant organismes vius com el detritus (organismes

morts, material fecal i agregats orgànics de diferents tipus). El DOC exportat contribueix només un 10-20%, a escala global, a les taxes de remineralització a l'oceà profund (Arístegui et al., 2002). Aquest fet sosté la idea que la vida microbiana de l'oceà profund està principalment impulsada pel POC (Arístegui et al., 2009; Honjo, 1996).

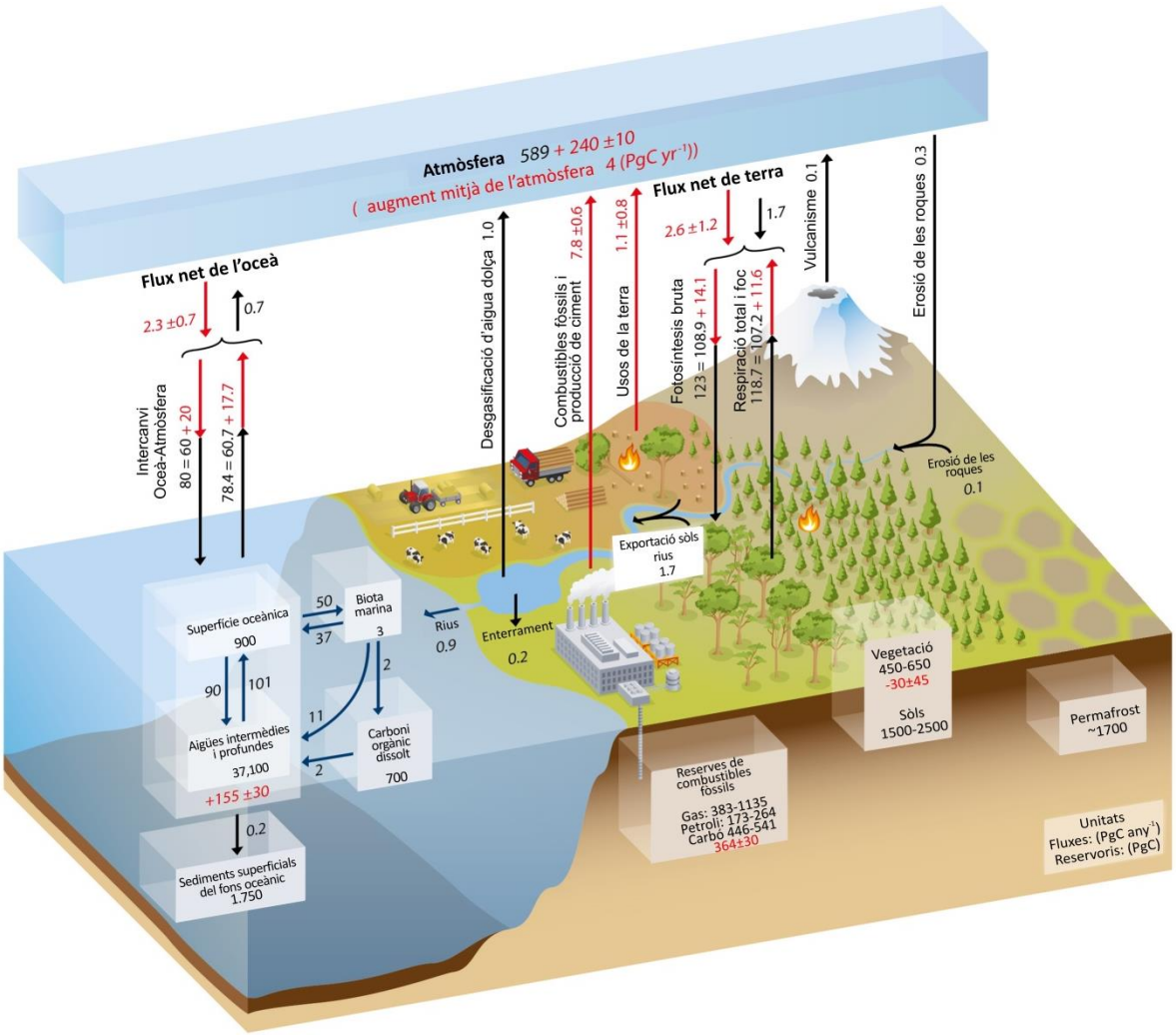

Figura 1.5. Representació esquemàtica del cicle del Carboni. Els números representen els reservoris de carboni amb Petagrams de carboni (PgC; 10^{15}gC) i els fluxos anuals entre reservoris amb PgC any^{-1}. Els números i fletxes de color negre mostren els reservoris i fluxos ja existent durant l'època pre-Industrial. Els números i fletxes vermelles mostren els fluxos addicionals induïts per l'ésser humà (mitjana del període 2000-2009). Part del carboni antropogènic generat és absorbit per la terra i el mar (aproximadament 5 PgC any^{-1}) mentre que la resta roman a l'atmosfera (4 PgC any^{-1}), provocant l'augment de les concentracions atmosfèriques de CO_2. Els números vermells als reservoris mostren els canvis acumulatius de carboni antropogènic de l'any 1750 fins al 2011; un canvi positiu indica que el dipòsit ha guanyat carboni. Modificada de Ciais et al. (2014).

La distribució i transport del carboni i nutrients des de la superfície fins a l'oceà profund es controla tant per processos físics ("bomba de solubilitat o bomba física") com biològics ("bomba biològica") (Figura 1.6). La **bomba física** és induïda per diferència de pressió parcial de CO_2 entre l'aire i el mar, la velocitat del vent i el sistema de circulació termohalina dels oceans. El refredament de les aigües de superfície a latituds altes afavoreix la seva capacitat de dissoldre el CO_2 atmosfèric (augment de la solubilitat del gas), així com l'augment de la seva densitat.

Aquestes aigües superficials fredes, denses i riques en CO_2 s'enfonsen a grans profunditats, propiciant l'exportació de CO_2. L'oceà Atlàntic nord i les mars que envolten al continent Antàrtic són les principals regions de formació d'aigua profunda. El C dissolt és retornat a l'atmosfera diversos centenars o fins i tot milers anys després, quan es completa el circuit oceànic global. La **bomba biològica** és el segrest de carboni des de la capa fòtica cap a l'interior de l'oceà impulsat per processos biològics: fotosíntesi, predació del zooplàncton, enfonsament de partícules orgàniques i carbonatades (bomba de carbonat), migració activa de la biomassa, remineralització de la matèria orgànica a carboni inorgànic en profunditat i precipitació biogènica dels carbonats, i enterrament del carboni orgànic. Cada any la bomba biològica exporta ~10% de la producció primària oceànica global anual (Karl et al., 1996; Laws et al., 2000). Encara que només una petita fracció (~0.2 PgC any^{-1}) del carboni exportat per processos biològics de la superfície arriba al fons de la mar, el fet que aquesta fracció pot ser emmagatzemada en els sediments de centenars a milions d'anys (Ciais et al., 2014 i referències allà citades), converteix a la bomba biològica en el mecanisme biològic més important de la Terra per segrestar CO_2 del cicle del carboni.

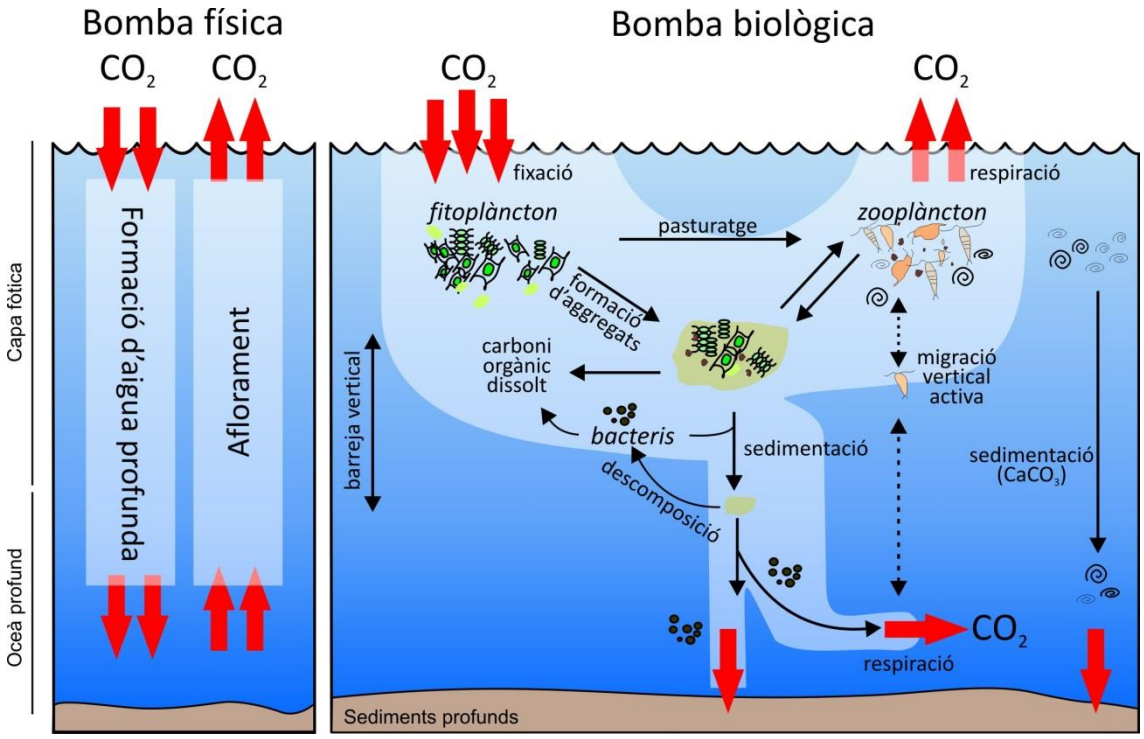

Figura 1.6. Representació esquemàtica simplificada de la bomba física i biològica als oceans. La bomba física (esquerra) és impulsada per processos fisicoquímics. La bomba biològica (dreta) és impulsada per processos biològics. Els nutrients inorgànics i el CO_2 atmosfèric fixats durant la fotosíntesi del fitoplàncton són transportats cap a aigües profundes a través de l'enfonsament tant de compostos orgànics com de biominerals. El zooplàncton, com ara copèpodes, produeixen pèl·lets fecals, els quals poden ser reutilitzats per altres organismes, enfonsats o agregats amb altres partícules, incrementant la velocitat d'enfonsament. Gran part del carboni orgànic que passa a través de la xarxa tròfica és convertit en CO_2 per respiració i retornat a l'atmosfera.

Traçadors de la matèria orgànica. És àmpliament reconegut l'ús de traçadors composicionals i moleculars per tal de caracteritzar i avaluar la contribució relativa de les diferents fonts de matèria orgànica als sediments marins (Meyers, 1994, 1997; Volkman, 2006). La utilitat d'aquests traçadors rau en el fet que cada font, ja sigui marina o terrestre, presenta senyals bioquímiques diferents. No obstant això, mentre que els traçadors composicionals són importants per identificar els orígens generals de la matèria orgànica (p. ex., la ràtio N/C i l'isòtop estable del C), els traçadors moleculars (p. ex., biomarcadors lipídics) s'utilitzen no només per identificar l'origen de la matèria orgànica sinó també per conèixer els precursors biològics específics i avaluar el seu estat de conservació (Eglinton i Eglinton, 2008; Hedges et al., 1997; Meyers, 1997; Volkman, 2006).

Traçadors de la composició general. La proporció de nitrogen total respecte el carboni orgànic (simplificat a ràtio TN/OC) i l'isòtop estable del C ($\delta^{13}C$) s'utilitzen bàsicament per discernir si la matèria orgànica dels sediments prové de plantes vasculars terrestres o d'algues marines. La matèria orgànica marina es caracteritza per tenir alts continguts de N i per tant mostra una relació N/C superior a 0.12, mentre que la matèria orgànica d'origen terrestre té una relació N/C inferior a 0.08 (Hedges i Oades, 1997; Redfield et al., 1963). Aquestes diferències venen explicades per la manca de cel·lulosa $(C_6H_{10}O_5)_n$ i altres biomacromolècules recalcitrants lliures de N i una major quantitat de proteïnes a les algues marines respecte les plantes vasculars terrestres. Els valors de les ràtios N/C es poden veure alterats tant pels processos de diagènesis[1] que degraden preferentment els components proteics (rics en N) com per l'arribada de residus antropogènics com ara el petroli (Friligos et al., 1998; Meyers et al., 1996).

El carboni-12 i carboni-13 (^{12}C i ^{13}C, respectivament) són els dos isòtops estables naturals del carboni, sent el primer el més abundant de la Terra (98.93%). La relació isotòpica del C varia en funció del fraccionament entre l'isòtop pesat (^{13}C) i el lleuger (^{12}C). La proporció de ^{13}C (respecte a la de ^{12}C) a la matèria viva es menor que la que es troba al CO_2 de l'atmosfera, i això és degut a que la fixació biològica de CO_2 discrimina negativament les molècules de CO_2 atmosfèric que tenen l'isòtop pesat. Les diferents vies metabòliques de cada organisme produeixen molècules amb diferent proporció d'isòtop pesat. La matèria orgànica marina generalment és isotòpicament més pesada que la terrestre provinent de les plantes vasculars C3. Així doncs, mentre que la composició típica de $\delta^{13}C$ del fitoplàncton marí d'aigües temperades varia de -18‰ a -22‰ (Gearing et al., 1984; Goericke i Fry, 1994; Harmelin-Vivien et al., 2008), les entrades de material terrestre derivat de les plantes C3 i C4 presenten valors de $\delta^{13}C$ que van des de -25 ‰ a -28 ‰ i des de -12 ‰ a -15 ‰, respectivament (Hedges et al., 1997).

Traçadors específics: biomarcadors lipídics. Els biomarcadors són molècules orgàniques derivades dels organismes, que es troben als sediments i han estat preservades intactes o amb canvis estructurals mínims al llarg dels processos sedimentaris i diagenètics. Aquests compostos contenen informació sobre els seus precursors, les condicions ambientals amb les que van viure els organismes que els van originar i els processos de transformació que han experimentat (Volkman, 2006). Els biomarcadors més emprats són aquells d'origen lipídic. Lípids és un terme general que s'aplica a totes les substàncies produïdes per microorganismes que són insolubles en aigua però poden ser extretes a través d'algun tipus de dissolvent orgànic. Tot i que aquesta

[1] Transformació física, química o biològica dels sediments un cop aquests han estat dipositats.

àmplia definició abasta una gran varietat de compostos, inclosos els pigments fotosintètics, generalment el terme lípid fa referència als greixos i ceres, fosfolípids, glicolípids, esterols i certs hidrocarburs (p. ex., *n*-alcans). Al contrari del que succeeix amb els carbohidrats, proteïnes i àcids nucleics, que no es preserven després de la mort cel·lular, els lípids resisteixen el pas del temps ja que les restes hidrocarbonades hidrofòbiques són difícils de degradar.

L'abundància de brassicasterol ($_{28}\Delta^{5,22E}$), dinosterol ($_{30}\Delta^{22E}$), C30diols&keto-ols i alquenones de cadena llarga als sediments indica presència de diatomees i algues primnesiofícies, algues dinoflagel·lades, microalgues de la classe *Eustigmotophyceae* i algues de la classe *Primnesiophyte* (p. ex., *Emiliana huxleyii*), respectivament (Volkman, 1986). La suma de les concentracions dels biomarcadors lípids que tenen un clar origen marí (algal) es pot calcular de la següent manera:

$$\sum \text{Mar} = \sum ({}_{28}\Delta^{5,22E} + {}_{30}\Delta^{22E} + \text{C}_{30}\text{diols\&keto-ols} + \text{alquenones}) \qquad (1.1)$$

Per contra, l'abundància de colesterol a les partícules sedimentàries posa de manifest l'existència d'organismes consumidors marins com ara el zooplàncton o organismes bentònics (Grice et al., 1998).

La suma de les concentracions dels *n*-alcans (∑TerNa) i *n*-alkanols (∑Tern-OH) més abundants d'alt pes molecular, són els components majoritaris de les ceres epicuticulars de les plantes superiors (Eglinton i Hamilton, 1967; Ohkouchi et al., 1997), i es defineixen com:

$$\sum \text{TerNA} = \sum n\text{-C}_{27,29,31,33} \qquad (1.2)$$

$$\sum \text{TerN-OH} = \sum n\text{-C}_{24,26,28,30} \qquad (1.3)$$

Com que TerNA és més resistent a la degradació que TerN-OH (Eglinton i Hamilton, 1967; Ohkouchi et al., 1997), la relació ∑TerNa/∑Tern-OH s'ha utilitzat com a indicador de la proporció de components terrestres refractaris vs. làbils.

L'abundància de la mescla complexa sense resoldre (UCM) d'hidrocarburs alifàtics, es pot utilitzar com a indicador de la contribució de productes del petroli degradat (Wang et al., 1999).

Els índex de preferència del carboni dels *n*-alcans (CPI_{NA}) i *n*-alcanols ($CPI_{N\text{-}OH}$) de cadena llarga es poden emprar com a indicadors de degradació de la matèria orgànica terrestre. Els valors de CPI típic de fulles fresques és >4 (Collister et al., 1994). La presència d'hidrocarburs de petroli no degradats pot esbiaixar (disminuir) els valors de CPI_{NA} degut a que els compostos *n*-alcans de productes petrolífers tenen valors de CPI_{NA} ~1.

$$\text{CPI}_{\text{NA}} = \frac{\sum([n\text{-C}_{25}]\text{-}[n\text{-C}_{33}])}{\sum([n\text{-C}_{26}]\text{-}[n\text{-C}_{34}])} \qquad (1.4)$$

$$\text{CPI}_{\text{N-OH}} = \frac{\sum([n\text{-C}_{24}]\text{-}[n\text{-C}_{30}])}{\sum([n\text{-C}_{23}]\text{-}[n\text{-C}_{29}])} \qquad (1.5)$$

1.2. Processos i ambients sedimentaris

1.2.1. Processos sedimentaris

En conjunt, els processos que involucren la producció, transport i deposició de sediments s'anomenen *processos sedimentaris* o *sedimentació*. El comportament de les partícules a la columna d'aigua no només depèn de la mida d'aquestes sinó que també de la diferència entra la seva densitat i la de les aigües circumdants (Burd i Jackson, 2009). Les partícules més denses que l'aigua sedimentaran sempre i quan la velocitat del corrent que les transporta no sigui suficient per mantenir-les en suspensió. Per tant, a l'oceà principalment hi ha dos tipus de transport de partícules: el lateral i el vertical (Figura 1.7).

Els processos de **transport lateral** influeixen en la dispersió del material particulat erosionat dels continents cap a l'interior de l'oceà. En general, es poden produir tres tipus de moviment lateral: 1) de rotació o lliscament d'un gra en una superfície; 2) de saltació, salts d'un gra en una superfície; i 3) de suspensió, flotació d'un gra dins d'un fluid (Figura 1.7). Mentre que els grans de mida petita (<sorra fina) i poc densos són fàcils de remoure i resuspendre, arribant lluny del seu lloc d'origen, les partícules més grans/denses requereixen fluxos més energètics (p. ex., intensos vents i corrents) per moure's i s'enfonsen més ràpidament.

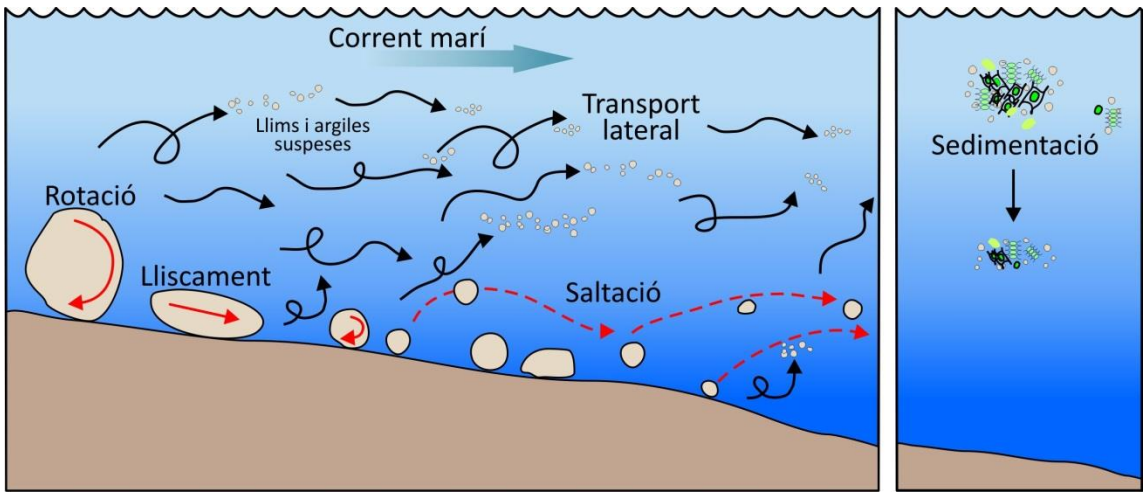

Figura 1.7. Representació esquemàtica del transport lateral (esquerra) i vertical (dreta) de les partícules de sediments sota la influència de corrents marines.

Els **fluxos verticals** de partícules a través de la columna d'aigua (altrament anomenats "neu marina") varien temporalment i espacialment en funció de diferents forçaments biològics i físics (Deuser, 1986), generalment associats a l'estructura i activitat de la comunitat planctònica i a la presència de partícules "llast" com restes calcàries o aerosols. Hi ha certs organismes (com ara les diatomees, radiolaris i coccolitoforis) i partícules d'aerosols que incrementen la taxa d'enfonsament per la seva capacitat d'agregació i seva densitat relativament elevada (Agusti et al., 2015; Guieu et al., 2014). Els fluxos de partícules també es poden veure incrementats per la intensificació de les corrents marines a causa de forçaments atmosfèrics. Un clar exemple es duu a terme als girs oceànics, que són corrents circulars formats per la combinació d'un sistema de

vents dominant i el transport d'Ekman[2]. Aquests remolins tenen un gran impacte en la biogeoquímica de l'oceà superficial, especialment en zones oligotròfiques, a causa de la injecció de nutrients a la capa fòtica (Bibby et al., 2008; Doblin et al., 2016) estimulant l'activitat biològica (McGillicuddy et al., 2007).

L'alteració digenètica, descomposició i dissolució de les partícules durant la sedimentació, controlen, juntament amb la circulació oceànica, la distribució d'oxigen, nutrients, CO_2 i altres constituents traça dins l'aigua. Els fluxos de material particulat a la columna d'aigua i el destí de la matèria orgànica a l'oceà ha intrigat als científics des de fa dècades (Deuser et al., 1988; Honjo, 1996) ja que és clau per comprendre el cicle global del carboni i les pertorbacions antropogèniques del mateix (Siegenthaler i Sarmiento, 1993). És per això que un dels objectius dels estudis de partícules, com és el cas d'aquest treball, consisteix en concretar la quantitat de C i altres components associats que s'exporten en els ecosistemes marins (Honjo, 1996). L'avanç del coneixement sobre els factors que controlen la variabilitat temporal en els fluxos de partícules a l'oceà ha estat possible gràcies a estudis realitzats en diferents ambients marins amb trampes de sediments (veure secció 1.4.1.2.).

Esdeveniments d'alt nivell energètic causats per la interacció i intercanvi d'energia entre l'atmosfera i l'oceà, com per exemple els temporals, les cascades d'aigua densa de plataforma o la formació d'aigua densa a mar obert, poden comportar una intensificació dels transports, tant verticals com laterals, provocant una exportació massiva de sediment i matèria orgànica cap a l'oceà profund (Canals et al., 2006; Ivanov et al., 2004; Sanchez-Vidal et al., 2012; Stabholz et al., 2013). Els temporals són pertorbacions meteorològiques caracteritzades per vents forts que provoquen fort onatge i, si van acompanyades de precipitacions intenses, provoquen l'augment dels cabals dels rius costaners. La resuspensió i redistribució del sediment per l'acció de l'onatge, els corrents associats i les descarregues fluvials elevades produeixen plomalls tèrbols[3], tant en superfície com enganxats al fons. Les cascades d'aigües denses de plataforma, causades per l'enfonsament d'aigües superficials densificades per l'efecte de forçaments externs, són fluxos ràpids (>1 m s^{-1}), turbulents i carregats de sediment i altres materials que discorren sobre el fons a favor de la gravetat (Canals et al., 2006; Durrieu de Madron et al., 2013). La diferència principal d'aquests corrents amb els corrents de terbolesa és que en aquests és el moviment del sediment el que arrossega l'aigua circumdant, mentre que en les cascades és el moviment de l'aigua el que arrossega el sediment.

Un cop arriben al fons, els sediments poden patir diversos processos abans de ser enterrats. D'aquesta manera, els sediments poden 1) ser consumits o processats (bioturbats) per altres organismes que viuen al fons marí (organismes bentònics), 2) patir processos de diagènesis o 3) ser enterrats i preservats.

[2] Model que prediu que, en general, l'aigua es mourà amb un cert angle respecte la direcció del vent.
[3] Sovint s'empra el terme *nefeoloide* o *capa nefeloide* per referir-se a aquests plomalls. Els fins que formen aquestes capes poden romandre en suspensió llargs períodes i distàncies.

1.2.2. Ambients sedimentaris

El fons marí es pot descriure considerant tres unitats fisiogràfiques fonamentals: els marges continentals, les planes batials i abissals i les dorsals oceàniques.

El marge continental és la part de l'escorça continental que es troba submergida sota l'aigua, i inclou la plataforma continental, el talús continental i la base del talús. Més enllà dels marges continentals, a partir de la base del talús, s'hi troben les zones més profundes dels mars i oceans, les planes batials i abissals (Figura 1.8).

Els marges continentals són ambients sedimentaris dinàmics que reben, emmagatzemen i a través dels quals s'exporten grans quantitats de sediments, matèria orgànica i altres elements clau associats (Hedges i Keil, 1995). El talús continental és una pronunciada i estreta franja que separa la zona costanera de l'oceà profund. El talús continental està freqüentment seccionat per canyons submarins (Shepard i Dill, 1966), valls profundes que actuen com conductes preferencials pel transport de matèria, enviant grans volums de sediments des de la plataforma cap a la conca profunda (Canals et al., 2006; Heussner et al., 1999; Palanques et al., 2005; Sanchez-Vidal et al., 2012; Zúñiga et al., 2009). Aquestes condicions específiques contribueixen a que els canyons submarins siguin hàbitat especials amb una elevada biodiversitat en comparació a altres zones de la plataforma o talús continental (De Leo et al., 2010; Vetter et al., 2010).

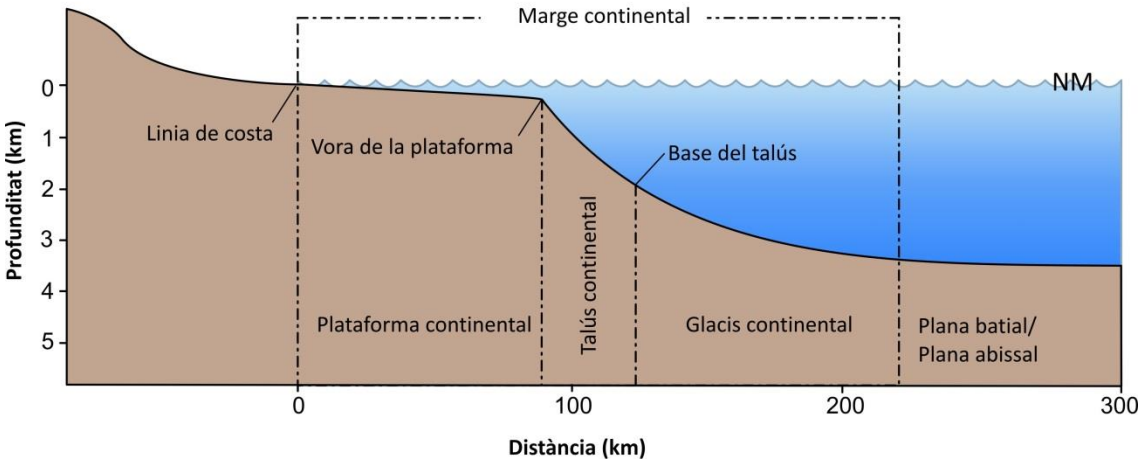

Figura 1.8. Representació esquemàtica de les principals unitats fisiogràfiques d'un marge continental passiu limitant amb una plana batial/abissal. L'escala vertical està exagerada x20 respecte l'escala horitzontal. NM, nivell del mar. Modificada d'Amblas (2012).

En zones costaneres dominen els sediments formats per una mescla de materials terrígens, biogènics i autigènics. A la plataforma continental predominen els depòsits terrígens o, si hi ha poca influència de descàrrega fluvial/deposició atmosfèrica, materials biogènics (carbonatats). La mida de gra d'aquests materials variarà en funció de les condicions energètiques del sistema. Per contra, els sediments marins profunds, en funció dels processos de transport que originen el dipòsit sedimentari es poden classificar en a) sediments hemipelàgics, formats per material que ha estat transportat a través de corrents de fons, o b) sediment pelàgics, constituïts per material que cau verticalment a través de la columna d'aigua.

1.3. Àrea d'estudi: marges continentals i conques de la mar Mediterrània

Tal i com ho suggereix el seu nom, el qual deriva de la paraula llatina *Mediterraneus* que vol dir mar entre terres, la mar Mediterrània està envoltada per tres continents: Europa, Àfrica i Àsia. Té una superfície de $2.5 \cdot 10^6$ km^2 i $46 \cdot 10^3$ km de costa. Malgrat la seva reduïda superfície i volum respecte el total dels oceans (0.7% i 0.25%, respectivament), la mar Mediterrània és considerada un dels ambients marins més complexos de la Terra a causa de la gran varietat de processos físics que hi tenen lloc (Pinardi i Masetti, 2000). Aquesta mar semi-enclosa es formà fa aproximadament 150 milions d'anys, i, durant la crisi de salinitat messiniana (fa uns 5.60 milions d'anys), es va dessecar majoritàriament per evaporació com a conseqüència del tancament de l'Estret de Gibraltar. Fa aproximadament 5.33 milions d'anys, les aigües de l'Atlàntic reomplirien ràpidament la conca formant la mar Mediterrània com el coneixem avui (Garcia-Castellanos et al., 2009).

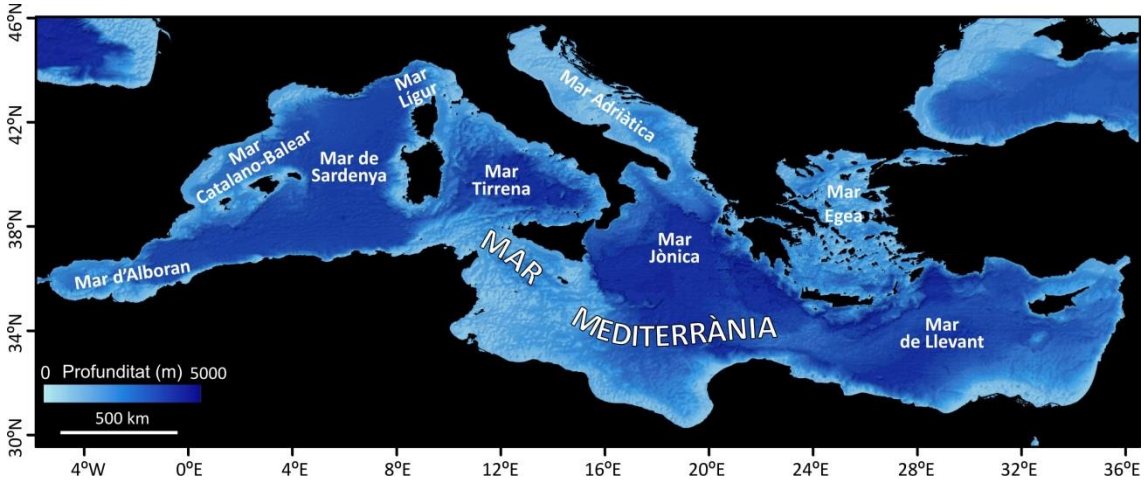

Figura 1.9. Mapa batimètric de la Mar Mediterrània amb la localització de les diferents mars regionals.

Com a conseqüència de la configuració dels continents circumdants i de la seva reduïda extensió, la mar Mediterrània, no posseeix grans sistemes d'afloraments ni marees. Es caracteritza per ser una conca de concentració amb una circulació termohalina, la qual és impulsada per l'excés d'evaporació, vinculada als vents freds i secs, respecte les entrades d'aigua dolça (precipitació i escorrentia fluvial). La circulació termohalina està fortament afectada per dues constriccions circulatòries: 1) l'estret de Gibraltar, de 14 km d'ample i 400 m de profunditat, que és l'únic punt de connexió entre la mar Mediterrània i l'oceà Atlàntic i 2) el canal de Sicília, de 140 km d'ample i 300 m de profunditat, que separa la mar Mediterrània amb dues subconques: la Mediterrània occidental i la Mediterrània oriental (Bergamasco i Malanotte-Rizzoli, 2010; Robinson et al., 2001). Mentre que la subconca occidental es caracteritza per presentar una àmplia i profunda plana abissal, la oriental és molt més accidentada. Aquestes subconques a la vegada contenen diverses mars regionals (d'Alboran, Catalano-Balear, Lígur, Tirrena, Adriàtica, Jònica, Egea i de Llevant) (Figura 1.9). La profunditat mitjana de la Mediterrània és de 1500 m, sent el punt més profund 5267 m, a la mar Jònica.

El dèficit hídric de la mar Mediterrània es compensa a través de l'estret de Gibraltar amb una entrada d'aigua atlàntica (AW, de l'anglès *Atlantic Water*) en superfície (0-200 m), amb una temperatura (T) de 15 ºC, una salinitat (S) de 36.15 psu, i relativament empobrida de nutrients. Aquesta massa d'aigua, la qual viatja cap a la Mediterrània oriental vorejant Àfrica a causa de la força de Coriolis (circulació ciclònica), esdevé més calenta i salada. Un cop arriba al mar de Llevant, durant l'hivern, les pèrdues de calor i evaporació incrementen la densitat de les aigües superficials, propiciant l'enfonsament i generació de l'aigua intermèdia Llevantina (LIW, de l'anglès *Levantine Intermediate Water*, 200-600 m) (Millot i Taupier-Letage, 2005; Schroeder et al., 2012). La LIW flueix cap a la conca mediterrània occidental seguint una ruta complexa i surt a través de l'estret de Gibraltar amb una T de 14.3, S de 38.5 psu i carregada de nutrients (Figura 1.10) (Malanotte-Rizzoli, 2001; Ovchinnikov, 1984). S'estima que una gota d'aigua que entra per l'estret de Gibraltar triga uns 150 anys a completar tot el gir i tornar, amb la seva composició profundament modificada, a l'oceà Atlàntic (Millot, 2009).

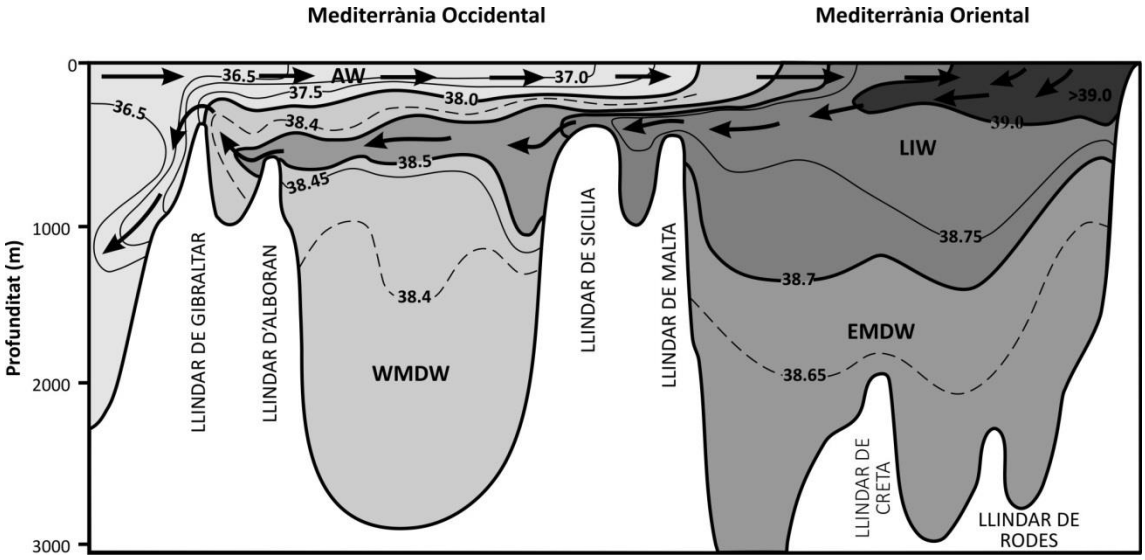

Figura 1.10. Circulació termohalina a l'hivern a la mar Mediterrània. Modificada de Wüst (1961) i Bergamasco i Malanotte-Rizzoli (2010).

La cel·la de circulació de la Mediterrània és impulsada per la LIW i per la formació d'aigua profunda (DWF, de l'anglès *Dense Water Formation*) (Figura 1.10). La DWF ocorre durant l'hivern en àrees molt concretes: al golf de Lleó a la Mediterrània occidental (WMDW, de l'anglès *Western Mediterranean Deep Water*) (Canals et al., 2006), a la mar Tirrena (TDW, de l'anglès *Tyrrhenian Deep Watter*) (Schroeder et al., 2008), a la mar Adriàtica a la Mediterrània oriental (EMDW, *Eastern Mediterranean Deep Water*) (Manca et al., 2002; Mihanović et al., 2013), i en hiverns excepcionalment freds, al mar de Llevant (LDW, *Levantine Deep Water*) (Beuvier et al., 2010). Aquests llocs es caracteritzen 1) per tenir una estabilitat de la columna d'aigua reduïda ja sigui per l'existència d'una circulació ciclònica preexistent o d'una batimetria poc profunda (com és el cas de les plataformes continentals), i 2) per patir fortes pèrdues de calor durant hiverns amb vents especialment freds i secs. La combinació d'aquests factors propicia la pèrdua de flotabilitat de les aigües superficials i el seu enfonsament. La circulació termohalina i els processos de DWF són de gran importància pels cicles biogeoquímics i els ecosistemes marins de la mar Mediterrània (Figura 1.10). La intensa barreja de la columna d'aigua associada als processos de DWF indueix 1) un increment de la producció primària gràcies a la pujada de nutrients a les aigües superficials, 2)

la ventilació (aportació d'oxigen) de la Mediterrània profunda, 3) el transport de sediments i 4) l'exportació de carboni.

Des d'una perspectiva biològica, la mar Mediterrània es defineix com un sistema oligotròfic, amb baix contingut de nutrients i clorofil·la (Sournia, 1973; Mermex group, 2011 i referències allà citades). La mar Mediterrània es caracteritza per tenir un gradient oest-est decreixent de disponibilitat de nutrients, producció primària i exportació de carboni (Moutin i Raimbault, 2002; Wambeke et al., 2002). Les seves aigües profundes presenten una relació N:P peculiarment alta respecte les relacions de Redfield (Redfield, 1934) (N:P 24-27 a la Mediterrània oriental; N:P 20-22 a la Mediterrània occidental; Ribera d'Alcalà, 2003; Krom et al., 2005). La ràtio Si:N també presenta un gradient est-oest, amb valors d'1.0 i >1.3 per a la Mediterrània occidental i oriental, respectivament (Ribera d'Alcalà, 2003). La concentració de clorofil·la a mar obert rarament sobrepassa els 2-3 mg m^{-3}. Tot i que la productivitat de la mar Mediterrània, i especialment la de la conca oriental, ha estat considerada des de fa molts anys limitada pel nutrient P (Krom et al., 1991, 2004), estudis recents suggereixen que existeix una co-limitació del N i P (Thingstad et al., 2005). Mentre que la productivitat primària anual a la Mediterrània occidental arriba a valors de 86 a 232 gC m^{-2} any^{-1} (Marty i Chiav, 2002), a certes zones de la oriental pot arribar a ser només de 29 gC m^{-2} any^{-1} (Siokou-Frangou et al., 2010; Yogev et al., 2011). A la mar Mediterrània, la concentració de fitoplàncton segueix un cicle estacional, amb baixes concentracions a l'estiu i altes a l'hivern, amb increments entre finals d'hivern i principis de primavera (D'Ortenzio i Ribera d'Alcalà, 2009).

En un sistema oligotròfic d'aquest tipus, les entrades externes de nutrients juguen un paper clau en el manteniment de la productivitat marina (Markaki et al., 2003; Pujo-Pay et al., 2011). Les fonts externes més importants de nutrients a la Mediterrània són la descàrrega fluvial (Ludwig et al., 2009) i d'aigües subterrànies (Rodellas et al., 2015), i la deposició atmosfèrica (Guerzoni et al., 1999; Krom et al., 1991). Mentre que la influència de les dues primeres es concentra sobretot a zones properes a la costa i a la conca occidental, l'abast de la deposició atmosfèrica a la conca oriental és molt major, arribant a zones de mar obert. Grans quantitats de pols (1-50 g m^{-2} any^{-1}) procedents de les regions àrides adjacents, del nord d'Àfrica (desert del Sàhara) i Orient Mitjà, es dipositen a la Mediterrània (Figura 1.2) (Guerzoni et al., 1999; Jickells et al., 2005). A més, tot i que en menor mesura, la deposició de cendres provinents d'erupcions volcàniques, principalment del volcà actiu Etna (Sicília), també pot representar una font de nutrients (Olgun et al., 2013).

1.3.1. La plataforma continental de Barcelona i el canyó de Blanes

Tant la plataforma continental de Barcelona com el canyó del Blanes es situen al marge nord-est ibèric (Mediterrània occidental). Aquest està format pel marge nord-català, el marge sud-català i el marge de l'Ebre (Amblàs et al., 2006; Lastras et al., 2011). El marge continental català té una plataforma continental estreta, amb una ruptura de la plataforma ubicada a uns 150 m de profunditat. Els canyons submarins del marge nord-català es van originar durant l'Oligocè-Miocè inferior, generant una profunda incisió a la plataforma i talussos (Tassone et al., 1994). L'actual marge nord-català té més de 100 km de llarg, una superfície d'uns 20000 km^2, i està delimitat pel

canyó de Cap de Creus al nord i el canyó de Blanes, que separa la regió del golf de Lleó i la plataforma continental de Barcelona al marge català del sud (Amblàs et al., 2006).

La plataforma continental de Barcelona té una extensió de 91 km, una amplada mitjana d'uns 15 km, una superfície total de 1317 km^2, i està orientada en una direcció nord-est–sud-oest (Durán et al., 2014). Aquesta plataforma continental consta de tres zones, la plataforma interna, la mitja i l'externa, les quals queden separades per les isòbates de 30-40 i 80 m, respectivament (Liquete et al., 2008). La plataforma consta de dipòsits col·luvials i al·luvials del Quaternari, modulats pels deltes dels rius Tordera, Besós i Llobregat (de nord a sud).

El canyó de Blanes, el qual secciona la plataforma continental de Barcelona i de la Planassa i el talús continental del marge nord-català, es caracteritza per la presència de nombroses incisions a profunditats de fins a 2000 m (Amblàs et al., 2006). Aquest canyó és de tipus erosiu fins al peu del talús, on esdevé deposicional. La capçalera del canyó, que presenta una forma de V, es troba al voltant de 60 m de profunditat, a una distància de menys de 4 km de la costa (Díaz i Maldonado, 1990), on el tortuós llit del riu Tordera i, a vegades, els rierols torrencials de Lloret i Tossa, arriben al mar (Rovira i Batalla, 2006). El canyó de Blanes, de 184 km de llarg, mostra una tendència gairebé nord-sud en el seu incisiu eix. L'amplada del canyó incrementa amb la profunditat fins a arribar a un màxim de 20 km a la part més profunda i plana (Canals et al., 2004). Té un curs sinuós amb un canal pla al fons de la base del pendent, i, finalment, passa a tenir una orientació oest-est, a aproximadament 2600 m (Amblàs et al., 2006; Lastras et al., 2011). El flanc occidental (o sud) del canyó de Blanes és més favorable al transport de partícules en suspensió que el flanc oriental (o nord), on prevalen les condicions hidrodinàmiques no erosives (Lopez-Fernandez et al., 2013; Zúñiga et al., 2009).

La circulació general a la Mediterrània Nord-Occidental és de caràcter ciclònic, amb el corrent del nord (NC, de l'anglès *North Current*) fluint amb meandres de fins a 30 km d'amplada amb una direcció sud–sud-oest vorejant el talús del marge català des del golf de Lleó (Figura 1.11) (Millot, 1999). La NC s'estén des de la superfície del mar fins a 400 metres de profunditat i el seu moviment és forçat per l'entrada d'Aigua Atlàntica (Millot, 1999). La NC té una component baroclínica des de la superfície fins aproximadament 400 m de profunditat, associada a un front de densitat de la plataforma que separa les aigües més dolces sobre la plataforma continental de les aigües més salades de mar obert (Font et al., 1995; Ulses et al., 2008), i una component barotròpica que involucra la columna d'aigua (Flexas et al., 2002). Mentre que la plataforma continental externa i mitja del marge nord-català estan afectades principalment pels meandres de la NC, la plataforma interna i la costa estan influenciats pels corrents derivats de la deriva litoral i forçaments locals, com són les onades generades pel vent.

La Mediterrània nord-occidental està sotmesa a dos tipus de forçaments de caràcter atmosfèric, que causen esdeveniments d'alta energia de curta durada. Un és degut a les tempestes humides de l'est, que presenten precipitacions intenses, forts vents i generació d'onatge amb elevada alçada d'ona (Sanchez-Vidal et al., 2012). L'altre és degut a les tempestes seques de nord, amb vents freds i secs que formen de cascades d'aigua densa (DSWC) (Canals et al., 2006). Aquests esdeveniments estan relacionats amb els principals vents que afecten la zona: el Llevant i la Tramuntana-Mestral, respectivament (Figura 1.11).

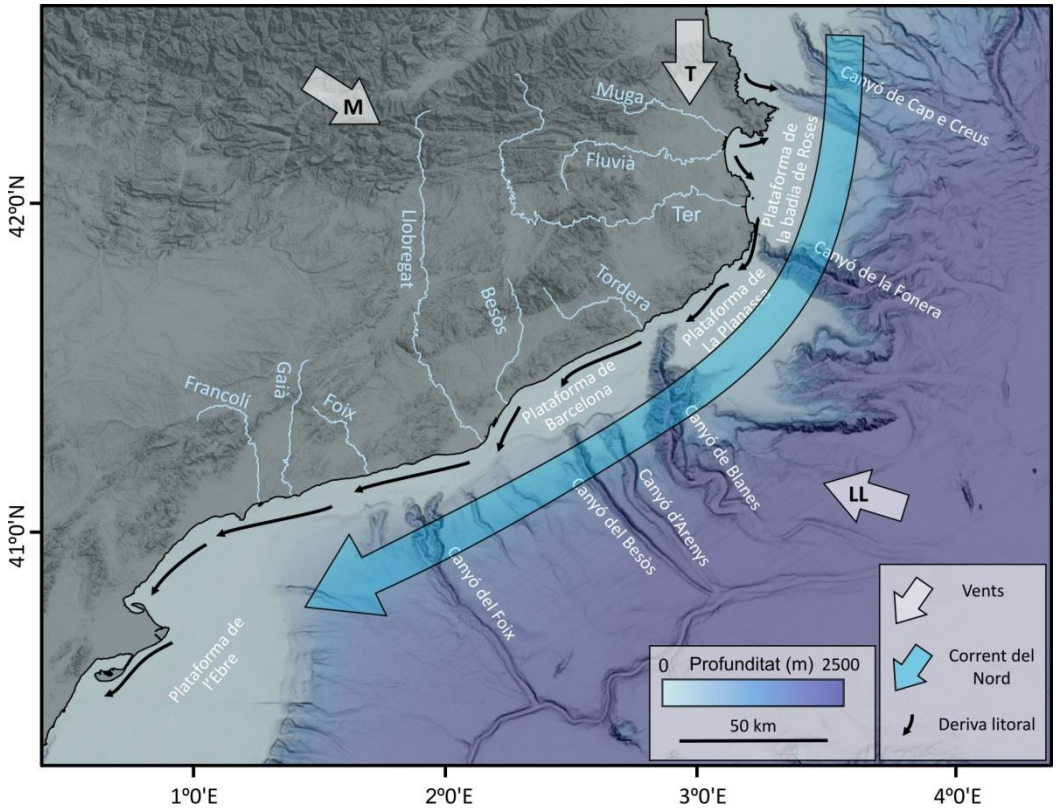

Figura 1.11. Mapa del relleu submarí del marge Catalanobalear, i de les zones emergides properes. En aquest s'hi indiquen la localització dels principals canyons submarins, plataformes continentals i els principals trets oceanogràfics, hidrològics i meteorològics que afecten a la zona. T: vents de Tramuntana, M: vents de Mestral, LL: vents de Llevant. Modificada de Tubau (2015).

A la plataforma continental de Barcelona hi ha dues fonts principals d'aigua dolça i partícules terrígenes: el riu Besós, situat al nord de l'àrea d'estudi, i els desguassos del clavegueram de Barcelona, essencialment l'emissari d'Espigó de Ginebra (Rumolo et al., 2015). La principal font d'aigua dolça i partícules terrígenes del canyó de Blanes és el riu Tordera, situat lleugerament a l'oest de la capçalera del canyó (Amblàs et al., 2006; Lopez-Fernandez et al., 2013).

1.3.2. La mar Mediterrània oriental i la conca de Ierapetra

La mar Mediterrània oriental es caracteritza per una topografia complexa constituïda per una successió de valls, serralades i fosses profundes (Amblàs et al., 2004; Medimap Group, 2007). La mar Jònica, a l'oest, i la mar de Llevant, a l'est, estan connectades longitudinalment i cobreixen la major part de la Mediterrània oriental, i és on es troben les zones més profundes de la Mediterrània (Figura 1.12). La mar Egea i l'Adriàtica es situen a la part més septentrional de la Mediterrània oriental. Mentre que l'Adriàtica està format per una àmplia plataforma i talús de profunditats de fins a 1200 m, l'Egea presenta una topografia particularment complexa amb profunditats de fins a 2500 m (Amblàs et al., 2004; Medimap Group, 2007). Totes aquestes mars

regionals presenten fortes estructures hidrodinàmiques de mesoescala[4], amb girs ciclònics i anticiclònics permanents i/o recurrents (Petihakis et al., 2009; Robinson et al., 2001). Aquests girs poden estar relacionats, entre d'altres, amb els forts vents del nord que bufen sobre la conca (el Bora, a la mar Adriàtica, i Etesià, a la mar Egea). Els girs faciliten els intercanvis entre les aigües de la plataforma continental i les aigües del talús, que al seu torn influeixen en la productivitat primària i amb la distribució de la matèria orgànica paticulada (Danovaro et al., 2010; Millot i Taupier-Letage, 2005).

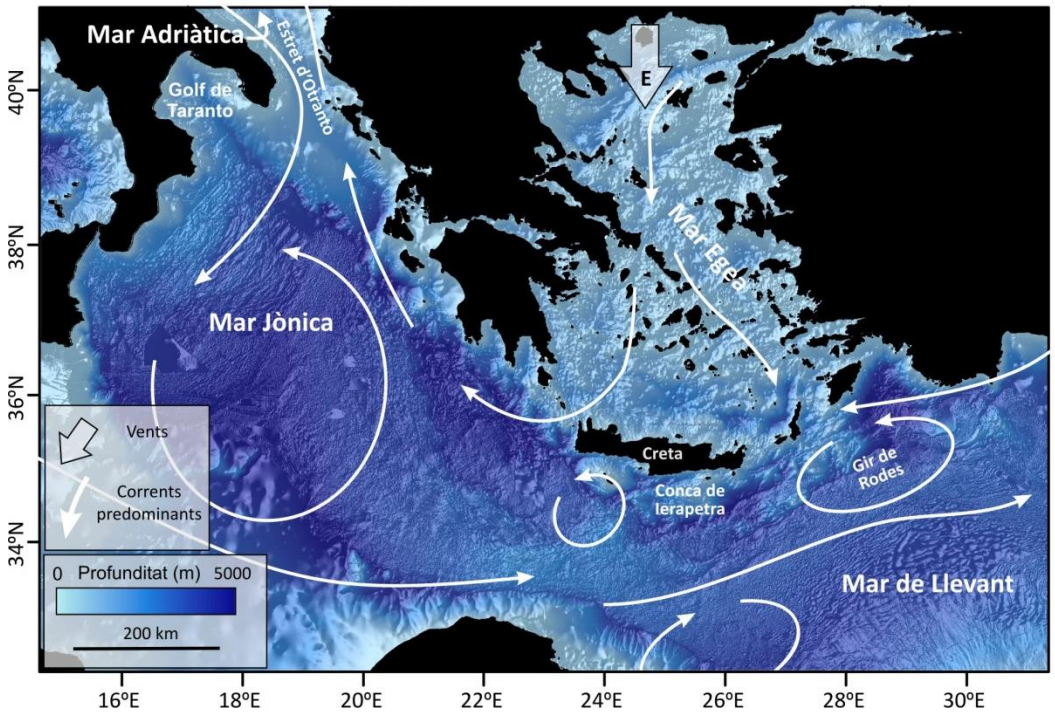

Figura 1.12. Mapa del relleu submarí de la Mediterrània oriental, centrat en la conca profunda de Ierapetra. En aquest s'hi indiquen la localització de les principals mars regionals i dels principals trets oceanogràfics i meteorològics que afecten a la zona. E: vents Etesians.

La mar de Llevant inclou la conca de Ierapetra, la qual és objecte d'especial atenció d'aquesta Tesi. Aquesta es localitza al sud-est de l'Illa de Creta i té una profunditat de fins a 4430 m. En aquesta zona, els vents Etesians (vents de nord) interactuen amb el relleu de l'illa de Creta, formant el que es coneix com el gir anticiclònic de Ierapetra. Aquest gir no és permanent, sinó que té una variabilitat estacional, interanual i fins i tot interdecadal (Larnicol et al., 2002; Theocharis i Kontoyiannis, 1999). El gir ciclònic permanent que afecta la conca de Ierapetra per la seva proximitat és el gir de Rodes, el més rellevant de la Mediterrània oriental ja que té un paper clau per a la formació de la LIW. Al ser un gir ciclònic, les aigües denses profundes i riques amb nutrients tendeixen a aflorar pel seu centre cap a les masses d'aigua superiors, afavorint la producció primària. Aquest procés es reforça durant el període d'hivern per les intenses pèrdues de calor (Napolitano et al., 2000).

[4] Circulació regionals les dimensions espacials de les quals poden arribar a centenars de quilòmetres.

La circulació termohalina i els processos físics que es duen a terme a la Mediterrània oriental propicien que aquesta sigui un dels ambients més oligotròfics del món (Gogou et al., 2014; Psarra et al., 2000; Thingstad et al., 2005). La major part del material particulat sedimentari prové de deposicions atmosfèriques, ja que les aportacions fluvials són limitades i afecten a zones molt localitzades (Guieu et al., 1997; Statham i Hart, 2005).

1.4. Material i mètodes

Disseny de l'experiment

Per tal d'estudiar la composició, transport i acumulació de material particulat (amb especial èmfasi a les partícules orgàniques), a diversos tipus d'ecosistemes marins de la mar Mediterrània, en aquesta Tesi s'ha dut a terme una anàlisi combinada de les característiques dels sediments superficials del fons i el fluxos de partícules, i de les condicions meteorològiques, hidrològiques i oceanogràfiques. Els sediment superficials van ser obtinguts a zones costaneres, marges continentals i conques profundes, tant de la Mediterrània oriental com occidental, mitjançant l'ús d'un multicorer o draga Van Veen durant diferents campanyes oceanogràfiques, realitzades des del gener de 2007 al juny de 2012 (Figura 1.13, Taules 1 i 2 de l'annex). De les mateixes estacions que es van obtenir mostres de sediment del canyó de Blanes i talús adjacent es va registrar la velocitat (m s^{-1}) i direcció de la corrent (º) a prop del fons amb correntímetres Anderaa RCM 7/9 disposats en línies instrumentades des de novembre 2008 fins al novembre 2009. Aquests correntímetres estaven situats a 23 m per sobre del fons i van registrar a intervals de 30 min.

Els fluxos de partícules van ser obtinguts d'una zona batipelàgica de la Mediterrània oriental, la conca profunda de Ierapetra, a 4285 m de profunditat durant 3 anys (des de juny de 2010 a maig de 2013) mitjançant el fondeig d'una línia instrumentada (Figura 1.15).

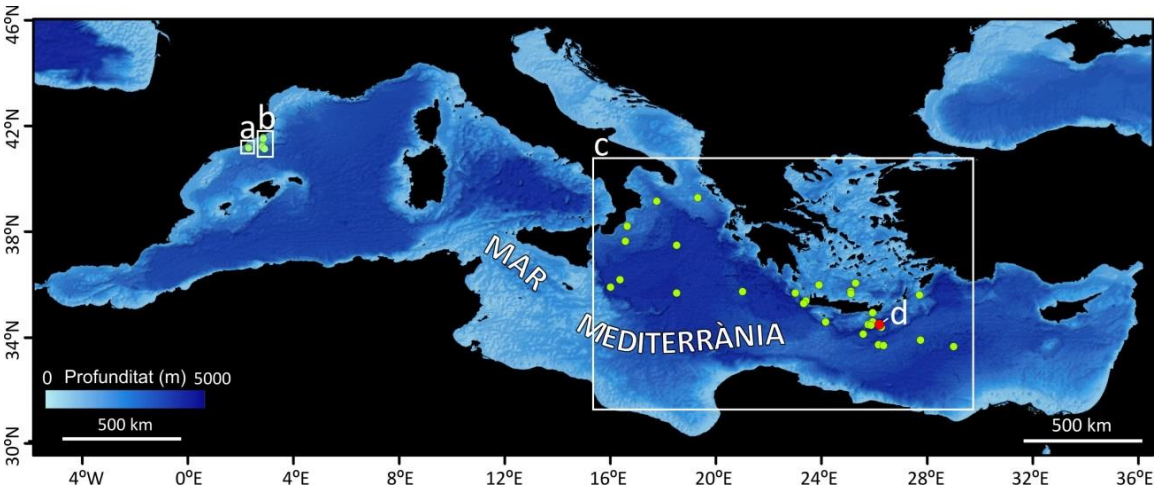

Figura 1.13. Localització dels punts de mostreig. Amb verd s'indiquen les estacions d'on es va obtenir sediments del fons i amb vermell d'allà on es van recol·lectar partícules mitjançant una trampa de sediment. Els requadres mostren les àrees d'estudi que s'han treballat detalladament de mode individualment: a) plataforma continental de Barcelona, b) canyó submarí de Blanes i plataforma i talús adjacent, c) Mediterrània oriental profunda i d) conca profunda de Ierapetra.

1.4.1. Tècniques de mostreig

1.4.1.1. Mostreig de sediment

La metodologia per a l'estudi dels sediments marins fou desenvolupada en el segle XIX. Durant l'expedició de l'H. M. S. Challenger (1872-1873), dirigida per Sir John Murray i Alphonse Renard, es va utilitzar per primer cop un instrument (*tub-ampolla*) que permetia recollir sediment del fons amb aigua superficial. Tot i així, el gran avenç en el disseny de sondes de mostreig no va ser fins l'any 1947 quan l'oceanògraf Kullenberg va utilitzar la pressió hidrostàtica de l'aigua de la mar per produir un buit parcial al tub mostrejador i obtenir mostres de sediment de gran longitud. Aquest buit fa que la mostra no presenti resistència, permetent que el tub s'enfonsi més al llit marí.

Extracció de testimonis de sediment. Durant les campanyes oceanogràfiques els sediment es van obtenir mitjançant un testificador de sediments tubular (multicorer) de 6 tubs (Figura. 1.14) o draga Van Veen. Mentre que el multicorer permet obtenir testimonis de sediment de relativa elevada qualitat (sediment no pertorbat), la draga Van Veen permet obtenir sediment superficial mitjançant el tancament de les seves mandíbules al tocar fons.

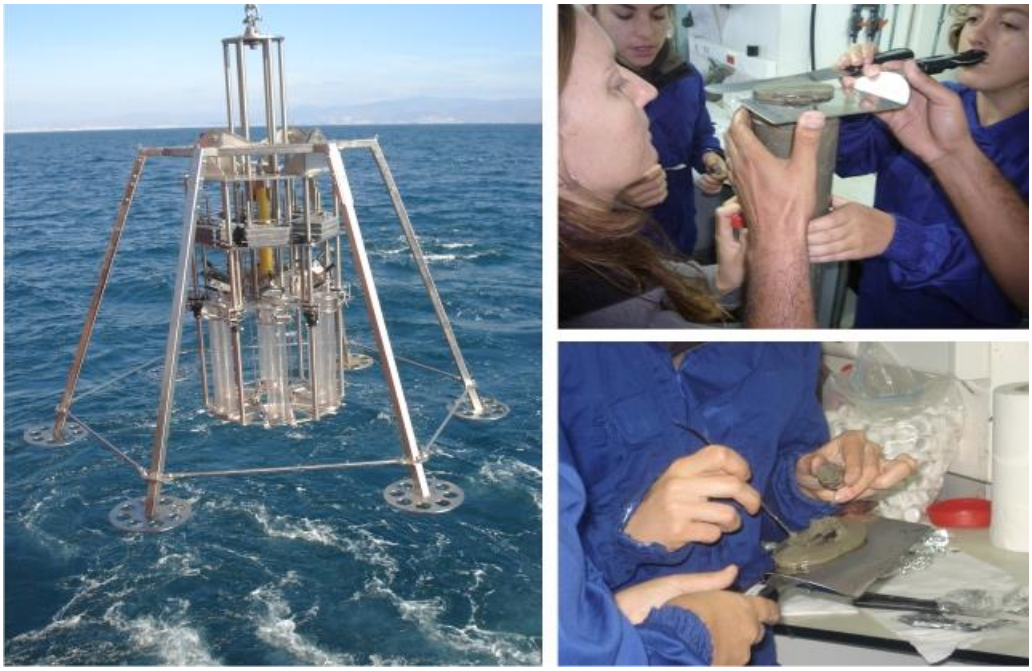

Figura 1.14. Esquerra: Testificador de sediments multicorer de 6 tubs. Dreta: Mostreig del testimoni de sediment a bord d'un vaixell d'investigació.

Tractament de les mostres. Un cop a bord, els testimonis de sediment (o les mostres extretes amb la draga) es descriviren visualment i després es submostrejaren en seccions de 0.5 cm els primers 5 cm i d'1 cm dels 5 cm al final. Les submostres recollides per dur a terme anàlisi de mida de gra, composició elemental i isotòpica s'emmagatzemaren amb bosses de plàstic segellades a 4 ºC. Les mostres recollides per analitzar biomarcadors lipídics s'emmagatzemaren embolicades en alumini precombustionat a -20 ºC. Aquestes mostres un cop al laboratori es pesaren per saber el contingut en aigua, i posteriorment es congelaren i liofilitzaren. En aquesta Tesi només s'ha treballat amb el mig centímetre superficial de cada testimoni.

1.4.1.2. Mostreig de partícules

L'ús de trampes de sediments es remunta a la dècada del 1870 (Bloesch i Burns, 1980; Heim, 1900). Tot i així, no va ser fins els anys 1990 quan es va començar a utilitzar la trampa de sediment de mostreig seqüencial per estudiar l'exportació de partícules des de la superfície fins a l'oceà profund (Honjo, 1996).

La línia instrumentada emprada en aquesta Tesi estava equipada amb una trampa de sediment seqüencial PPS3 Technicap amb 12 ampolles de recollida, una obertura de 0.125 m^2 i una ràtio alçada/diàmetre de 2.5, i amb un correntímetre Aanderaa (RCM 8). La trampa de sediment i el correntímentre estaven situats a 25 m i 23 m sobre el fons, respectivament (Figura 1.15). L'interval de mostreig es fixà a 1 mes per a les trampes i a 1 hora per als mesuradors de corrent. Les ampolletes de recepció de les trampes, netejades amb sabó i HCL, s'ompliren amb una solució formolada al 5% (v/v) (formaldehid al 37-38% amb aigua de mar filtrada a 0.45 µm) neutralitzada amb borat de sodi per obtenir un pH 7.5-8. Es varen obtenir un total de 36 mostres, el que representa un 100% d'èxit.

Figura 1.15. Esquerra: Disseny de la línia instrumentada fondejada a la conca profunda de Ierapetra (Mediterrània oriental) . Aquesta estava composta per una trampa de sediments i un correntímentre, posicionats a 25 m i 23 m sobre el fons marí, respectivament. Mig: fotografia de dues boies i el correntímetre RCM8. Dreta: fotografia de la trampa de sediment.

Eficiència de les trampes de sediments. Els patrons generals de fluxos de partícules derivats de les trampes de sediment seqüencial, com és el cas de la trampa de sediment PPS3 utilitzada en aquesta Tesi, es consideren raonables tot i conèixer que hi ha certs factors que poden esbiaixar els resultats de la seva mesura. Aquestes incerteses de mesura estan associades a la intrusió d'organismes nedadors, a processos de solubilització, i a la pertorbació dels fluxos degut a l'estructura de la trampa (Gardner et al., 1997; Buesseler et al., 2007 i referències allà citades). Conseqüentment, s'ha suggerit que l'eficiència de les trampes de sediment és funció del disseny de la trampa, de la velocitat de la corrent i de les característiques de les partícules sedimentàries. El disseny de la trampa de sediment PPS3 presenta una ràtio alçada/diàmetre que minimitza el balanceig (Heussner et al., 1990). De fet, Bonnin et al (2008) van examinar com la velocitat de la corrent afecta a les trampes de sediment PPS3 mitjançant sensors de pressió posicionats als correntímetres per sobre de les trampes. En aquest estudi van arribar a la conclusió que la inclinació de les trampes de sediment arribava a ser d'aproximadament 15º durant episodis de fortes corrents (fins a 80 cm s^{-1}), els quals no afectaria significativament a l'eficiència de recol·lecció dels fluxos de partícules. Tot i així, durant la majoria de les condicions de flux, gran part de les partícules no es recullen com a resultat de l'enfonsament passiu, sinó degut a processos turbulents generats a la boca de la trampa. Diversos treballs han investigat el biaix hidrodinàmic, però el coneixement de les condicions sota les quals els biaixos de captura de partícules es tornen significatius encara avui en dia és limitat (Buesseler et al., 2007).

La intrusió d'organismes nedadors també pot afectar el flux de partícules. És per aquest motiu que tots els organismes nedadors (definits com aquells que es suposa que han entrat a la trampa de sediment de manera voluntària) de les mostres de les trampes de sediment s'extreuen. Altrament, hi ha processos fisicoquímics, com ara la dissolució de biominerals o agregats orgànics, que també poden esbiaixar el flux de partícules de diferents compostos (Antia, 2005). La solució conservant utilitzada en aquest estudi (formaldehid) sembla la més adequada en termes d'efectivitat i prevenció de fragmentació dels organismes nedadors i per invalidar l'activitat microbiana (Buesseler et al., 2007; Gardner, 1989; Heussner et al., 1990). Tot i que es coneix que l'ús d'aquest conservant pot causar alguns problemes analítics per a la determinació de carboni i nitrogen orgànic dissolt, aquest és àmpliament emprat i acceptat per a la determinació dels compostos orgànics particulats investigats en aquest estudi (Dell'Anno et al., 2002; Tuominen et al., 1994).

Obtenció i tractament de les mostres de la trampa de sediment. Les ampolles de la trampa de sediment, un cop recuperades del carrusel on van subjectades, es precinten i s'emmagatzemen a la foscor a 2-4 ºC fins que es processen al laboratori. El mètode aplicat pel tractament de les mostres obtingudes de les trampes de sediment és una modificació d'aquell descrit per Heussner et al. (1999). Un cop realitzada una fotografia a totes les ampolles de la trampa (Figura 1.16), el primer pas és l'extracció dels organismes nedadors de les mostres. Mentre que els més grans s'extreuen tamisant la mostra amb una malla de niló d'1mm, els més petits d'1mm es retiren manualment amb l'ajut d'una lupa binocular i pinces de precisió. Tots aquests organismes es guarden amb un potet amb formaldehid per potencials posteriors estudis. En el cas que de tenir poc material a la mostra, com és el cas de totes les mostres d'aquesta Tesi excepte una, la totalitat de la mostra ha de ser observada a la lupa binocular i els nedadors han de ser extrets. Quan hi ha molt material, es procedeix a dividir la mostra en submostres de 10-20 mg mitjançant

l'ús d'una bomba peristàltica d'alta precisió. Una part de les submostres són la mostra de treball i l'altre part queda emmagatzemada per arxiu amb formaldehid. Seguidament, la mostra de treball es centrifuga amb Mili-Q freda 3 vegades per tal de rentar el sediment de sal i formol. Finalment, les mostres es liofilitzen, pesen, per tal de determinar la massa total de la mostra, i s'emmagatzemen per a posterior anàlisis.

Tenint en compte que un flux és el resultat de la velocitat de caiguda per l'abundància concentració de partícules (Honjo, 1996), el flux total de les mostres (TMF) es va calcular utilitzant la massa total (MT), l'àrea de la boca de la trampa (0.125 m^2) i els dies de mostreig:

$$TMF = \frac{MT}{A \cdot D} = \frac{g}{m^2 d} \quad (1.6)$$

Figura 1.16. Fotografia de les 12 ampolles de la trampa fondejada a la conca profunda de Ierapetra (Mediterrània oriental) de juny 2012 a maig de 2013.

1.4.2. Tècniques analítiques

1.4.2.1. Anàlisi granulomètrica

La mida de gra és un indicador molt útil ja que determina la velocitat llindar (*threshold velocity*) a la que es mourà una partícula, que es defineix com la velocitat de flux del fluid (aire o aigua) que fa que el sediment es mogui. Mitjançant l'estudi de la distribució granulomètrica dels sediments els oceanògrafs poden determinar com s'han transportat i les condicions en les quals s'han dipositat.

Per determinar la distribució granulomètrica dels sediments es va utilitzar un difractòmetre de raig làser LS230 de Beckman Coulter del laboratori de Sedimentologia del Departament de Dinàmica de la Terra i de l'Oceà de la Universitat de Barcelona. El Coulter LS230 mesura la mida de les partícules d'una mostra segons l'angle de difracció que es produeix al fer passar a través de la mostra en solució un feix de llum monocromàtica (750 nm) (Figura 1.17). Quan l'angle de difracció és baix o alt, es tracta d'una partícula gran o petita, respectivament. Aquesta descomposició, es basa en les teories de dispersió de la llum de Fraunhofer (Teoria de 1814-1817). El valor de la mida de gra que es dóna és el diàmetre equivalent d'una esfera que produís la mateixa difracció que la partícula, veient-la així com un objecte bidimensional. Aquesta informació, mitjançant el software LS32, es presenta la distribució granulomètrica en corbes acumulatives o histogrames de 116 barres, una per cada canal analitzat.

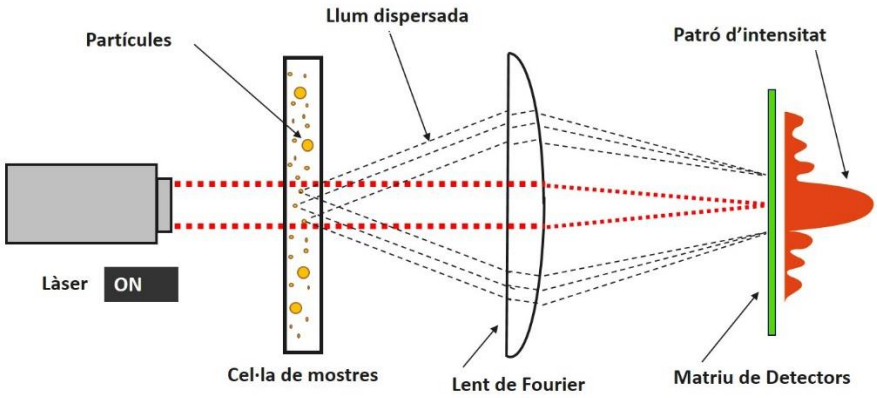

Figura 1.17. Sistema òptic de mesura del Coulter LS230 per difracció de llum.

El Coulter mesura el percentatge en volum de les partícules, i els seus límits de detecció es situen entre 0.04 i 2000 µm. Les mostres amb fracció >2000 µm cal corregir-les. En el cas de la presència de fraccions superiors a 2000 µm a la mostra, s'ha de tamisar en diferents mides de malla i, mitjançant unes correccions específiques, hi ha la possibilitat d'introduir els valors obtinguts al software i obtenir els paràmetres estadístics, corbes acumulatives i histogrames de la mostra total. Els avantatges d'aquest instrument es basen en la bona reproductibilitat de les anàlisis, la realització d'una única anàlisi per obtenir un ampli rang de mides, la petita quantitat de mostra que es necessita, la informació detallada de la granulometria que s'obté i l'obtenció dels resultats directament en format digital.

Per dur a terme aquesta anàlisi s'utilitzà una quantitat variable de sediment, entre 0.3 i 5 g en funció de la quantitat necessària per obtenir l'obturació òptima del feix del làser. Els compostos orgànics tendeixen a unir-se amb altres partícules formant agregats que sedimenten més ràpidament que les partícules individuals. Per aquest motiu, en primer lloc, la matèria orgànica de la mostra s'oxidà amb H_2O_2 al 10%. A continuació, com que en estudis oceanogràfics és interessant conèixer tant la distribució granulomètrica de la fracció no carbonatada (fracció litogènica) com la de la carbonatada (mostra total), la mostra es va dividir amb dues parts, dels quals una es tractà amb HCl 1 M per eliminar els carbonats. Seguidament, per evitar la formació d'agregats o flocs durant la manipulació de les mostres, les dues mostres es dispersaren en ≈20 cm^3 d'aigua i un dispersant químic (polifosfat de sodi) i es sacsejà durant 4 hores. Finalment, cada mostra fou introduïda al Coulter usant un tamís de 2 mm per retenir partícules gruixudes ocasionals que puguin obstruir el circuit de flux de l'instrument. En la present Tesi Doctoral, l'espectre de mida de partícula mesurat es presenta com a percentatge de volum en una escala logarítmica i s'han considerat 4 divisions de mida de gra i) sorra (>63 micres), ii) llim groller (63-40 micres) iii) llim mitjà-fi (40-4 micres) i iv) argila (<4 micres). Per a la caracterització de les distribucions granulomètriques s'ha emprat el paràmetre d50, que és el diàmetre de gra mitjà de les partícules, on el 50% de la mostra de sediment és més fi i l'altre 50% és més groller.

1.4.2.2. Mètode de fraccionament per mida de gra

Durant aquesta Tesi s'ha desenvolupat una nova metodologia per fraccionar mostres de sediment en funció de 4 mides de gra: sorra (>63 µm), llim groller (63-40 µm), llim mitjà-fi (40-4 µm) i argiles (<4 µm) (Figura 1.18).

Primerament, la mostra de sediment es va suspendre i disgregar amb polifosfat de sodi durant 2 hores. Seguidament, per tal d'obtenir la fracció sorra i llim groller es tamisà la mostra amb tamisos d'acer inoxidable de 63 µm i 40 µm, respectivament. Per dividir el material <40 µm, es va procedir a centrifugar aquesta fracció de la mostra 7 min a 1000 rpm. Les partícules que sedimentaren corresponien al llim mitjà fi, mentre que les contingudes al sobrenedant era la fracció argila. El procés de centrifugació i extracció de sobrenedant es repetí dues vegades per assegurar que no quedessin argiles atrapades entre els llims. Les argiles del sobrenedant es concentraren centrifugant-lo 15 min a 5000 rpm. Per tal d'ajustar i validar el mètode i poder establir quines eren les condicions de temps i velocitat de centrifugació idònies per separar les fraccions 40-4 i <4 µm, el sobrenedant es va analitzar diverses vegades amb el Coulter LS230. Un cop acabat aquest procediment, cada submostra es liofilitzà, i es molturà a pols fina per posteriorment poder realitzar anàlisis específiques a cada fracció de sediment.

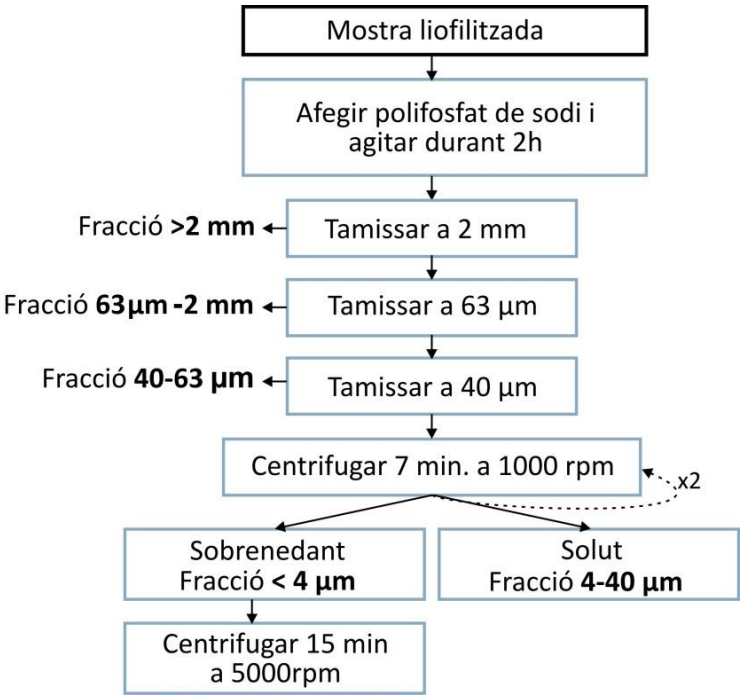

Figura 1.18. Representació esquemàtica del procediment per dur a terme la separació per mida de gra.

1.4.2.3. Anàlisi de la composició elemental i isòtops estables del C

Les anàlisis de carboni total (TC), nitrogen total (TN), carboni orgànic (OC) i la seva relació isotòpica ($\delta^{13}C$) es realitzaren amb un analitzador elemental (Flash 1112 EA) acoblat a un espectròmetre de masses Delta C Finnigan MaT dels Centres Científics i Tecnològics de la Universitat de Barcelona. Les incerteses analítiques per a la composició elemental foren inferiors a 0.1%, mentre que pels resultats de $\delta^{13}C$ va ser inferior a 0.05 ‰. El funcionament d'aquest analitzador es basa amb una combustió de la mostra en una atmosfera enriquida amb O_2 a altes temperatures (900-1800 ºC). El gas portador per arrossegar els gasos generats (CO_2, NO_X i HO_2) cap als reactors és l'heli. Finalment, un cop reduït el NO_X a N_2 i extreta l'aigua, el N_2 i el CO_2 es separen mitjançant una columna de cromatografia de gasos i passen a ser quantificats.

Per a l'obtenció de la composició elemental i isotòpica es pesaren entre 5 i 20 mg de mostra prèviament liofilitzada i molturada i es procedí al seu encapsulament amb capsules d'estany (per analitzar el TC i el TN) o de plata (per analitzar el OC i $\delta^{13}C$), addicionant V_2O_5 com a catalitzador (Figura 1.19). Per la determinació de l'OC i $\delta^{13}C$ la mostra, un cop a la càpsula d'Ag, s'atacà amb alíquotes de 50 µL d'HCL al 25% i s'assecà a l'estufa a 60 ºC. Aquest procés es repetí fins que no s'observaren efervescències assegurant la total descarbonatació (Nieuwenhuize et al., 1994). Finalment, abans d'afegir V_2O_5 i tancar la càpsula es netejà repetidament amb alíquotes d'aigua Milli-Q.

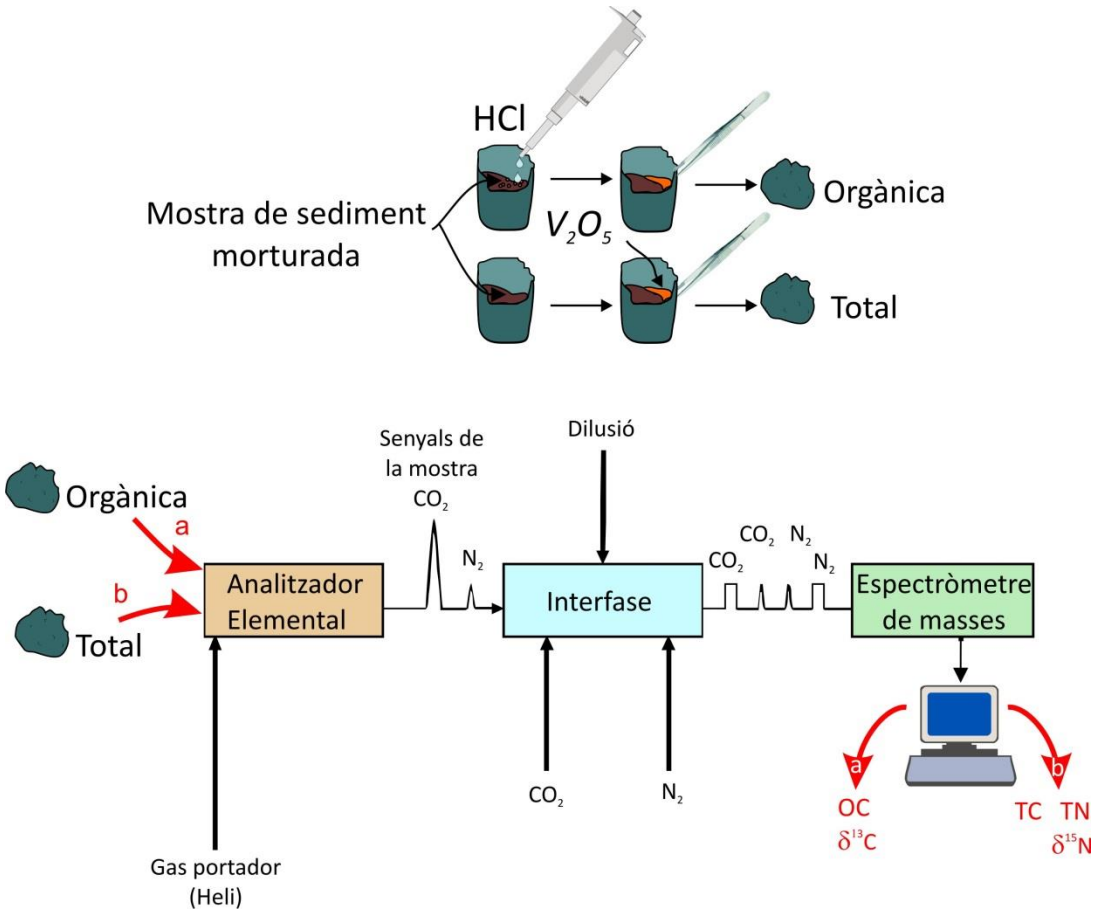

Figura 1.19. Representació esquemàtica simplificada del procediment analític per a la determinació de la composició elemental i isotòpica.

El contingut de carboni inorgànic (IC) es va calcular mitjançant una resta simple on:

$$IC = TC - OC \quad (1.7)$$

Assumint que tot el IC contingut a les mostres era carbonat càlcic ($CaCO_3$), el contingut de $CaCO_3$ es va calcular multiplicant l'IC per la massa molecular del $CaCO_3$ (100/12). El contingut de matèria orgànica es va obtenir multiplicant el contingut de l'OC per 2 (per ex., Heussner et al., 1996; Masqué et al., 2003). La ràtio molar TN/OC també es va calcular. En aquesta Tesi, s'ha utilitzat la ràtio molar TN/ OC en lloc de la ràtio OC/TN amb la finalitat de limitar les ràtios de mostres empobrides de N (és a dir, TN/OC≈0 en lloc d'OC/TN≈∞) (Goñi et al., 2006) i evitar la subestimació de la fracció de carboni terrestre (Perdue i Koprivnjak, 2007).

La concentració de $\delta^{13}C$ obtingut de les anàlisis s'expressa en parts per mil (‰). Aquests enriquiments (δ) representen la relació de l'isòtop pesant de la mostra respecte el valor del material de referència. Actualment el material de referència emprat internacionalment és el NBS-19, que és un carbonat de calci de roca calcària. A causa de que antigament s'utilitzava un altre carbonat (Vienna Pee Dee Belemnite, VPDB), el calibratge mitjançant NBS-19 està referit a l'escala (VPDB). Per tant:

$$\delta^{13}C = \left(\frac{\left(\frac{^{13}C}{^{12}C}\right)_{mostra}}{\left(\frac{^{13}C}{^{12}C}\right)_{VPDB}} - 1 \right) * 1000‰ \quad (1.8)$$

1.4.2.4. Anàlisi d'òpal

La concentració d'òpal (sílice biogènica) es determinà mitjançant l'ús d'un espectròmetre d'emissió òptica de plasma acoblat inductivament (ICP-OES) Perkin-Elmer Optima 3200RL dels Centres Científics i Tecnològics de la Universitat de Barcelona. La tècnica es basa amb la vaporització, dissociació, ionització i excitació dels diferents elements químics d'una mostra (en aquest cas Si i Al) a l'interior d'un plasma d'Ar. Un corrent d'Ar és introduït en un camp de radiofreqüència on l'energia cinètica de l'Ar^+ pot generar temperatures de fins a 8000 ºC. Durant el procés de desexcitació del àtoms i ions presents a l'interior del plasma, es produeixen emissions de radiació electromagnètica de la zona de l'UV-visible. Aquestes radiacions, característiques de cada element, es separen en funció de la seva longitud d'ona i finalment es mesura la seva intensitat per tal d'obtenir les quantificacions.

A causa de que la sílice present en els sediments pot ser tant biogènica com litogènica (aluminosilicats, com les argiles), el principal problema de la determinació de l'òpal és conèixer quina fracció hi ha de cada de tipus de Si (Kamatani i Oku, 2000). Com que la sílice biogènica es dissol més ràpidament que i els aluminosilicats, la determinació de la quantitat d'òpal es va dur a terme mitjançant 2 digestions de 2 hores a 85 ºC en una solució de carbonat de sodi (Na_2CO_3) 0.5 M (Fabres et al., 2002; Ragueneau et al., 2005). Els lixiviats obtinguts de les dues digestions es

centrifugaren i analitzaren a l'ICP-OES. Durant la primera digestió, es produeix la dissolució total de la sílice biogènica i part dels aluminosilicats. Per contra, durant la segona digestió el Si prové únicament dels aluminosilicats, el que permet calcular la relació Si/Al atribuïda a les argiles de la mostra. Aquesta relació és emprada com a factor de correcció per conèixer la concentració de Si biogènic:

$$Si_{bio}=Si_1-Al_1\times\left(\frac{Si_2}{Al_2}\right) \qquad (1.9)$$

on, Si_1 i Al_1 són les concentracions d'aquests elements en el lixiviat de la primera digestió i Si_2 i Al_2 ho són de la segona. Com que la Si_{bio} dels sediment marins és Si hidratada amorfa ($SiO_2{\cdot}0.4H_2O$), la concentració d'òpal es calculà multiplicant el valor obtingut de Si_{bio} per 2.4 (Mortlock i Froelich, 1989).

Tenint en compte que la composició total d'una mostra és la suma dels components biogènics i dels litogènics, el percentatge de material litogènic es va obtenir assumint la següent relació:

$$\%\text{litogènic} = 100 - (\%\text{matèria orgànica}\% + \%CaCO_3 + \%\text{òpal}) \qquad (1.10)$$

1.4.2.5. Anàlisi de biomarcadors lipídics

L'anàlisi de la concentració del biomarcadors orgànics (*n*-alcans, hidrocarburs aromàtics policíclics (PAH), alquenones de cadena llarga, *n*-alcanols i esterols) dels sediments es va realitzar mitjançant l'ús de cromatografia de gasos acoblada a espectrometria de masses (GC-MS) i cromatografia de gasos amb detector d'ionització de flama (GC-FID) de les instal·lacions de l'Hellenic Centre for Marine Research a Atenes, Grècia (Figura 1.20). En cromatografia de gasos, la mostra s'injectà a la fase mòbil (gas He) i es passà a través d'una columna situada a dins un forn on la velocitat de migració de cada component, i en conseqüència el seu temps de retenció a dins la columna, varià en funció de la seva afinitat amb la columna.

Figura 1.20. Fotografies del procediment analític seguir per a la determinació de biomarcadors lipídics. Esquerra: Extracció de la fracció orgànica dels sediments. Mig: Dissolvents orgànics preparats per a l'extracció de la fraccions. Dreta: Cromatògraf de gasos.

El procediment analític que es seguí per a la determinació dels biomarcadors lipídics és el descrit en detall per (Gogou et al., 1998). Primerament els sediments liofilitzats s'enriquiren amb una barreja d'estàndards interns i seguidament es sonificaren tres vegades amb una mescla de dichlorometà:metanol (4:1, v/v) per a l'extracció de les substàncies orgàniques. El fraccionament de l'extracte es va dur a terme en una columna de sílice gel (Figura 1.20). El grup de solvents que es va utilitzar per separar els diferents compostos va ser el següent: 1) *n*-hexà (fracció F1, hidrocarburs alifàtics), 2) diclorometà/*n*-hexà (fracció F2, compostos carbonil) i 3) etil acetat/*n*-hexà (fracció F3, alcohols i esterols). Totes les fraccions es concentraren per evaporació rotatòria al buit i es transferien en vials d'1.5 mL de color ambre. Mentre que les fraccions F1 i F3 s'analitzaren amb GC-MS, la fracció F2 es va fer amb GC-FID.

Els lípids individuals van ser identificats mitjançant la comparació dels temps de retenció obtinguts de la cromatografia de gasos amb els estàndards, així com també la comparació dels espectres de massa obtinguts amb els espectres de compostos patró. La quantificació es basà amb la resposta del GC-MS o GC-FID i la comparació de les àrees dels pics amb les quantitats conegudes d'estàndards afegit abans de l'extracció dels sediments.

Els biomarcadors lipídics utilitzats en aquesta Tesi van ser els *n*-alcans, *n*-alcanols, diols i quetols de cadena llarga i un conjunts d'esterols, juntament amb índex lipídics com a indicadors de fonts de la matèria orgànica i/o degradació (veure secció 1.3.2).

1.4.2.6. Anàlisi microestructural

Per determinar la morfologia i composició de les partícules es va utilitzar un microscòpic electrònic de rastreig (SEM J 7100 FE) equipat amb espectrometria d'energia dispersiva (EDS), el qual va permetre l'anàlisi semi-quantitatiu dels principals element químics de les partícules. El microscopi electrònic de rastreig es fonamenta en la interacció d'un feix primari d'electrons amb la mostra que es vol estudiar. Aquests electrons interaccionen amb la superfície de la mostra, es dispersen, es localitzen mitjançant un detector i es projecten a la pantalla.

1.4.3. Altres paràmetres i eines de suport

L'ús de dades hidrològiques, meteorològiques i oceanogràfiques ha estat essencial per estudiar els factors ambientals que modulen el transport i deposició de material particulat a la zona d'estudi.

Per als estudis de la plataforma continental de Barcelona i el canyó de Blanes, els valors de les descàrregues fluvials (m^3 s^{-1}) del riu Besós i del riu Tordera, respectivament, s'obtingueren de les estacions d'aforament de l'Agència Catalana de l'Aigua (ACA) de Santa Coloma de Gramenet i de Fogars de la Selva, respectivament (Figures 2.1 i 2.11). Les dades de precipitació, pressió i velocitat i direcció del vent foren extretes de les estacions meteorològiques de les estacions meteorològiques de Barcelona-El Raval per a l'estudi de la plataforma de Barcelona i de Malgrat de Mar per l'estudi del canyó de Blanes i de Barcelona-El Raval per a l'estudi de la plataforma de

Barcelona. Aquestes estacions són gestionades pel Servei Meteorològic de Catalunya (SMC) i formen part de la Xarxa d'Equipaments Meteorològics de la Generalitat de Catalunya (XEMEC).

Per a l'estudi de la plataforma interna de Barcelona les dades d'onatge s'extragueren d'una boia costanera (Barcelona–II) gestionada per *Puertos del Estado* del Ministeri de Foment (Figura 2.1). Les dades d'onatge s'obtingueren, en el cas de l'estudi del canyó de Blanes, d'una boia situada prop de les desembocadura del riu Tordera (Figura 2.11). Aquesta formava part de la malauradament desapareguda Xarxa d'Instrumentació Oceanogràfica i Meteorològica (XIOM) de la Generalitat de Catalunya. Les alçades d'ona que s'han utilitzat en aquesta Tesi són les significants, $H_{1/3}$ (que és la mitjana del terç de les onades més altes d'un registre horari).

Per la descripció de les condicions oceanogràfiques i el seu potencial efecte als sediments s'ha emprat el programa Sedtrans05. Aquest empra un model de transport de sediments de plataforma continental i estuaris que prediu la mobilització de sediments en un punt en funció de la profunditat de l'aigua, el tipus de sediment, el règim de corrents i l'onatge (model *single point*) (Neumeier et al., 2008). El model simula taxes d'erosió i sedimentació en règim de corrents constants o la influència combinada del temps d'onatge i corrents. El llindar dels moviments es calcula en funció de la mida de gra, la densitat dels sediments, la salinitat i temperatura de l'aigua.

Les dades de temperatura superficial de l'aigua (SST, ºC) i concentració superficial de clorofil·la-a (Chl-a, mg m^{-3}) utilitzades foren obtingudes gràcies al sensor *Moderate Resolution Imaging Spectoradiometer* (MODIS) instal·lat al satèl·lit Aqua. Les dades dels fluxos de calor aire-mar emprats (calor sensible SHF i latent LHF) provenen d'un satèl·lit de la NASA *Modern Era Retrospective-analysis for Reaearch and Applications* (MERRA). Les concentracions de diòxid de sofre (SO_2, 1 Dobson Unit = 0.029 g m-2, (Spinei et al., 2010)) a la troposfera i estratosfera (quantitat total de la columna) s'obtingué del producte OMI/Aura Level-3e SO2 Data Product OMSO2e (Versió 003) (Krotkov i Li, 2012). Totes aquestes dades van ser adquirides de la base de dades de *NASA's Goddard Earth Sciences* (GES) *Data and Information Services Center* (DISC) *Interactive Online Visualization ANd aNalysis Infrastructure* (GIOVANNI).

Les concentracions d'oxigen dissolt molecular (O_2), nitrat (N) i fosfat (P) al límit de la capa fòtica es van obtenir del model *Biogeochemical Flux Model* (OPATM-BFM) (Lazzari et al., 2010, 2012, 2016). Per contra, les dades de Si s'obtingueren del model *PELAgic biogeochemistry for Global Simulations* (PELAGOS025) (Vichi et al., 2013). Totes aquestes dades són distribuïdes a través de *Copernicus Marine Environment Monitoring Service* (MyOcean)

La deposició atmosfèrica total de partícules a la zona d'estudi va ser facilitada pel Centre de Supercomputació de Barcelona (BSC) a partir del model BSC-DREAM8b (Basart et al., 2012; Pérez et al., 2006a, 2006b). Aquest model simula els principals processos del cicle atmosfèric de la pols erosionada dels deserts i prediu els principals esdeveniments de deposició atmosfèrica sobre Europa (Pérez et al., 2006b).

Capítol 2

Resultats

2.1. Distribution and sources of organic matter in size-fractionated nearshore and inner-shelf sediments of the NW Mediterranean

Lucía Quirós-Collazos[a,b,1], Rut Pedrosa-Pàmies[a,1], Anna Sanchez-Vidal[a*], Jorge Guillén[b], Ruth Durán[b]

[a] GRC Geociències Marines, Departament de Dinàmica de la Terra i l'Oceà, Universitat de Barcelona, Martí i Franquès s/n, 08028 Barcelona, Catalonia, Spain

[b] Institut de Ciències del Mar (ICM-CSIC), Passeig Marítim de la Barceloneta, 37-49, 08003 Barcelona, Catalonia, Spain

[1]These authors contributed equally to this work.

Submitted April 2016. Estuarine, Coastal and Shelf Science.

Abstract

Continental shelves are recognized to play a key role in the biogeochemical cycle of carbon, linking terrestrial and marine carbon reservoirs. In this study we investigate the physical and biogeochemical processes that control the source, transport and fate of organic carbon (OC) in the continental shelf off Barcelona city, in the NW Mediterranean Sea. Surface sediment samples were collected from depths of 10 to 40 m during late summer and autumn 2012. Grain size and biogeochemical parameters such as OC, its stable isotope $\delta^{13}C$, total nitrogen (TN) and OC/TN ratios were analysed in size-fractionated sediments. The influence of environmental factors over the study area was determined using hydrological and oceanographic time series, together with video images of the Barcelona coast line and nearshore region.

We have found a wide range of OC contents, from 0.13 to 8.68%, depending on water depth and sediment particle size. The highest OC concentration was always found in the clay fraction (<4 μm), followed by the sand fraction (>63 μm) that contained terrestrial plant debris. Wave activity, discharge of the Besòs River and the "Espigó de Ginebra" outfall were the main mechanisms that controlled the sorting of sediments by their grain size and thus the distribution of OC in the inner shelf off Barcelona. In addition, we observed that the organic matter in clay particles was progressively degraded seawards, probably because these particles remain suspended in the water column much more time compared to those that are heavier and, therefore, they are exposed for longer time periods to oxygenated conditions. Both OC/TN ratios and $\delta^{13}C$ values found suggest that the OM that was preserved was predominantly land supplied.

2.1.1. Introduction

Despite continental margins account for only 10% of the total ocean area, they play a major role in the global cycle of organic carbon (OC) (Wollast, 1991; Hedges and Keil, 1995; Bauer et al., 1998; Macdonald et al., 1998). Large amounts of nutrients and particles derived from river watersheds arrive to the continental shelf through riverine discharges. These large nutrient-rich supplies, which are typically loaded with terrestrial organic matter (OM) including plant detritus, soil eroded particles and freshwater algae (Gordon and Goñi, 2004; Bianchi et al., 2009; Sanchez-Vidal et al., 2013), act as a trigger mechanism increasing marine primary production (Malej et al., 1995; Lohrenz et al., 1997; Iriarte et al., 2012). The burial and preservation of OM in marine sediments is tightly coupled to the remineralisation and early diagenetic processes such as microbial degradation, photooxidation or meiofauna consumption (Miller, 1997; Grant et al., 1997; Accornero et al., 2003; Hernes and Banner, 2003; Arnosti, 2011; Kujawinski, 2011). Therefore, a small fraction of this OM can be accumulated and buried in shelf sediments, while another fraction is exported towards the outer-shelf and the continental slope to reach the deep basin (Wollast 1991; Hedges et al., 1997; Accornero et al., 2003; Pedrosa-Pàmies et al., 2013). The continental shelf and in particular the nearshore and the inner-shelf is highly influenced by local meteorological, hydrological and topographic conditions, which cause the transport of sediments and determine its spatial distribution. Some studies demonstrate that storm events play a key role in sediment dynamics. For example, in the NW Mediterranean Sea, the occurrence of strong easterly and southeasterly winds with long fetch cause increased wave height, high bottom stress and resuspension of fine grained sediments from the shelf that are transported towards deeper areas (Ferré et al., 2005; Guillén et al., 2006). Thus, the inner-shelf, which receives both terrigenous and marine OC, largely acts as a bypass zone for unconsolidated sediments.

Coastal areas under fresh water influences are prone to accumulate high amounts of OM, not only because the contribution of matter loadings being washed down by rivers from land to shelf (Roussiez et al., 2005; Dagg et al., 2004), but because flocculation processes take place at the fresh water-sea water mixing boundary (Geyer et al., 2004; Hunter and Liss, 1982; Sholkovitz, 1976). In such scenario, woody vascular plant material has been observed to be an important component of OC discharged by rivers (Leithold and Hope, 1999; Tesi et al., 2007; Kuzyk et al., 2008; Tesi et al., 2016). This type of OC source, which behaves like fine sand and tends to be retained near river mouths, is highly affected by bacterial consumption (Nuwer and Keil, 2005). The microbial community likely turns the plant debris into very refractory materials buried and stored in shelf sediments (Leithold and Hope, 1999). On the other hand, flocculation processes play a key role during mixing of fresh and salty water since aggregates glue OM with fine mineral particles (Eisma, 1986; Dyer and Manning, 1999).

One of the most important jigsaw pieces to understand the distribution of OC in marine sediments is the link between mineral particles and OC. A strong correlation of OC content and mineral grain size was found in many marine environments (Mayer, 1994a; Keil et al., 1997; Secrieru and Oaie, 2009). Indeed, several studies have demonstrated that clay sediments are the most efficient store of OM (e.g., Mayer, 1994a; Keil and Cowie, 1999) being organic-mineral aggregates and sorption suggested as the main mechanisms for OM protection against degradation (Ransom et al., 1998; Arnarson and Kiel, 2001; Mead and Goñi, 2008; Kennedy et al., 2014). Accordingly, sorption of marine OC in clay minerals has been identified as the major

mechanism allowing effective dispersion and preservation of carbon not only in the shelf but also over large distances during high energy episodic hydrodynamic events such as eastern storms in the Catalan margin (Sanchez-Vidal et al., 2012; Pedrosa-Pàmies et al., 2013).

Overall, despite many studies have investigated particulate OC production, transport and accumulation in the Catalan margin (Lopez-Fernandez et al., 2013; Martin et al., 2006; Puig and Palanques, 1998; Pedrosa-Pàmies et al., 2013; Sanchez-Vidal et al., 2012; Zúñiga et al., 2009), the processes that affect the OC in the nearshore areas remain poorly documented. The objective of this paper is to evaluate the distribution, sources and cycling of particulate OC in surface sediments in a shallow environment off Barcelona city, in the Catalan margin. Our focus has been to assess the interaction between mineral grains and OC through the analysis of OC and total nitrogen (TN) contents, together with the stable isotopic composition of the OC ($\delta^{13}C$) and OC/TN ratios. Furthermore, meteorological, hydrological and oceanographic time-series data has also been investigated in order to assess the impact of environmental conditions (waves and river discharges) on sediment and OC transport. This study will contribute to establishing the link between the nearshore environment, a source region of sedimentary particles and OC, and the deep basin, which is the final carbon sink.

2.1.2. Study area

2.1.2.1. Geographic and geological setting

The study area is located in the inner continental shelf off Barcelona city (NW Mediterranean Sea) (Fig. 2.1a), in front of the Somorrostro beach (Fig. 2.1b). The Somorrostro beach is an artificially embayed beach of 522 m long, 89 m averaged wide, and NE-SW oriented. The beach borders are the Olympic harbour on the northeast and the "Espigó de Ginebra" (a breakwater also known as "Espigó del Gas") on the southwest. Periodic protection works of sand nourishment have been performed in this beach and the beaches along the surrounding coast line due to chronical erosion (Ojeda et al., 2011; Sancho-García et al., 2013). The grain size of the sediment (d50) on these beaches ranges between 430 µm (at 5 meter depth) and 1500 µm (on the dry beach) (Ojeda et al., 2011).

This area occupies the central stretch of the section bounded by the Foix Canyon offshore the southern limit of the Llobregat Delta to the south, and the Blanes Canyon to the north (Liquete et al., 2007) (Fig. 2.1a). The Barcelona continental shelf extends along a straight distance of 91 km, covers a total area of 1317 km^2 and is oriented in a NE-SW direction (Durán et al., 2012). The shelf width is approximately 10 km in front of Somorrostro beach, but its average width is ~15 km. The shelf edge depth is 130 m in straight line off the sampled region. Despite the average shelf slope gradient is low (0.7°) north of Barcelona, in the study area it is 1.5º. The Barcelona shelf consists of an inner, middle and outer-shelf separated by the 30-40 and the 80 m isobaths, respectively (Liquete et al., 2008). The low-lying coastline stretches that extend along the Barcelona shelf are colluvial and alluvial deposits of Quaternary age and are shaped by the deltas of Tordera, Besòs and Llobregat rivers from north to south. The construction of the modern river-fed continental shelf and slope in the study area was modulated by the Plio-Quaternary glacio-eustatic sea level

changes leading to alternating phases of accumulation and erosion of the continental shelf (Liquete et al., 2008; Durán et al., 2012). The most important features are paleodeltas, narrow ridges, abrupt steps, prodeltas and infralittoral prograding wedges. The last one is the main geological relief in the inner-shelf, where the studied region in located.

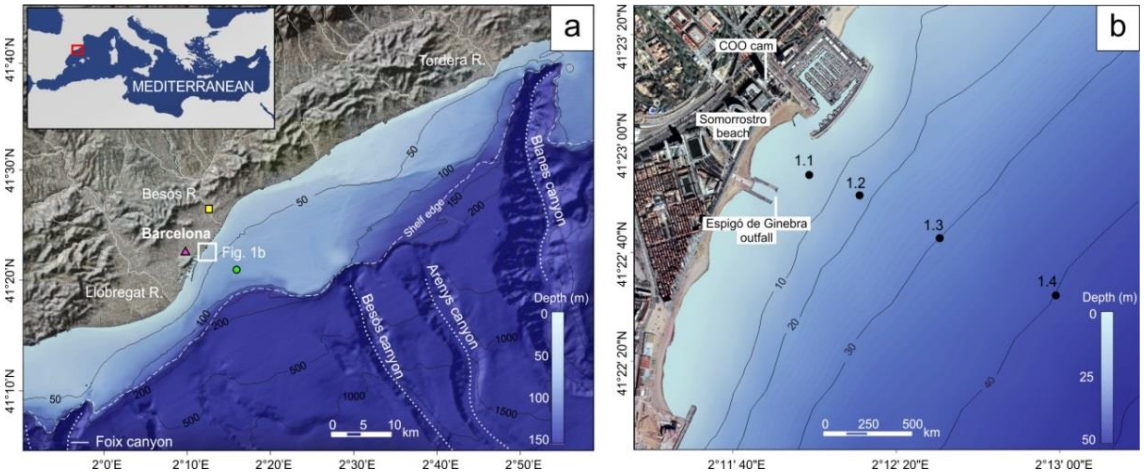

Figure 2.1. (a) General bathymetric map of the study area with grey contours every 50 m. Green dot, pink triangle, yellow square and white rectangle show the position of the Barcelona II wave buoy, the meteorological station, the gauge station on the Besòs River and the location of sampling stations, respectively. The small fitted map highlights this area of the Catalan margin (red cell) within the Mediterranean Sea. (b) Location of sampling stations 1.1 (10 m depth), 1.2 (20 m), 1.3 (30 m) and 1.4 (40 m) are shown in black dots. Isobaths are displayed every 10 m (black lines). Location of Somorrostro beach, "Espigó de Ginebra" outfall and the COO videocam are also indicated. Georeferenciated image from "Institut Cartogràfic de Catalunya" (ICC).

2.2.2.2. Oceanographic, meteorological and hydrological settings

The general circulation in the NW Mediterranean Sea is characterized by a south-westwards flow named the Northern Current (NC), which flows cyclonically along the Gulf of Lions and the Catalan margin bordering the slope (Millot, 1991). The current structure changes seasonally, with less mesoscale variability in summer and developing relatively intense mesoscale meanders during winter (Millot, 1999). The NC represents a density barrier between continent-influenced shelf waters onshore of the current and denser open sea saline waters (Font, 1988; Salat et al., 1992). Because the continental shelf is micro-tidal affected, the main dominant factors in the mid and outer shelf currents are the meandering of the NC. However, inner-shelf and surf zone is highly shaped by constant south-westward littoral drift currents and local forcings such as wind-generated waves. Indeed, our study area is located within the most affected region by a southward net littoral drift north of the Llobregat River, as reported by Durán el al. (2012). Such an alongshore current triggers a sediment transport of 80000 to 180000 m^3y^{-1} within the Besòs-Llobregat coastal stretch (Durán et al., 2012; DGPC., 1986). In addition, Grifoll et al. (2012, 2013) observed that during springtime local wind stress in short time scales and synoptic-scale pressure gradients are the main controls over the currents, mainly depending on Coriolis acceleration and stratification of the water column rather than bottom stress influence.

The main winds in the study area are the northerly "Tramuntana" and the easterly "Llevant". The "Llevant" induces increased significant wave height due to the orientation of the coastline and long fetch. The climate report by "Puertos del Estado 2004-2011" shows that mean wave direction in the study area is E-SE with predominance of significant wave heights <1 m and peak periods >6 s. However, 5% of significant wave heights are higher than 2 m with an easterly direction, likely corresponding to easterly wind storm events. In this near coast area, flow intensifications episodes (up to 1.4 m s^{-1} of flow speed has been recorded) of more than 12h have been attributed to the strong prevailing easterly and north-easterly winds concomitant with the channelling effect due to topographic steering and the narrowing of the coastal shelf (Mestres et al., 2016).

There are two main sources of fresh water and sediment discharges in the study area: the Besòs River, northwards of the study area, and the outfalls of the Barcelona drainage system (Fig. 2.1a). The Besòs River runs along an alluvial and non-alluvial detrital watershed with 1038 km^2 basin area and its 10 year average discharge is 4.31 m^3 s^{-1} (Fig. 2.1a). The outfalls along the Barcelona city contain a lift station which pumps water collected by the local storm drain systems towards the Besòs wastewater treatment plant. However, the lift station capacity (1260 m^3 h^{-1}) can be surpassed by some heavy rainfall events, thus delivering the water excess to the sea through an outfall. The "Espigó de Ginebra" outfall is located off the sampling stations of this study (Fig. 2.1b). Another potential freshwater source would be the Llobregat River, south-westward the study area, but it has little influence on our study area due to the general south-westward littoral drift (Fig. 2.1a).

2.1.3. Material and methods

2.1.3.1. Sample collection and analytical methods

Surface sediment samples were obtained during four cruises in August, September, October and November of 2012. These cruises were carried out within the frame of the Coastal Ocean Observatory (COO) from the Institute of Sea Science (ICM-CSIC), which is collecting a long time series of monthly surface sediment samples and water column profiles since October 2003. During each cruise, surface sediment samples were collected using a stainless Van Veen dredge in four stations distributed along a transect perpendicular to the coastline of ~1.2 km long (Fig. 2.1b). The stations were located at 10 m (station 1.1), 20 m (station 1.2), 30 m (station 1.3) and 40 m water depth (station 1.4). After recovery, samples were stored in sealed plastic bags at 4 ºC until processed in the laboratory.

Each bulk sediment sample was fractionated in four grain-size divisions which included sand (63 µm-2 mm), coarse silt (40-63 µm), fine silt (4-40 µm) and clay (<4 µm) following Pedrosa-Pàmies et al. (2013). Briefly, each sediment sample was suspended and disaggregated with sodium polyphosphate for 2 h. Then the fractions larger than 40 µm were separated using wet sieving, while sediment fraction smaller than 40 µm were extracted by centrifugation. A centrifugation at 1000 rpm during 7 minutes was performed to concentrate the 4-40 µm fraction, and the supernatant was centrifuged twice at 5000 rpm for 15 minutes to finally concentrate de clay (<4

μm) fraction. Each fraction was visually inspected under a binocular microscope and then freeze-dried before grounding it into fine powder.

OC and N contents and the stable isotopic composition of OC ($\delta^{13}C$) were analysed on each of the grain-size fractions. The analyses were performed at "Centres Científics i Tecnològics de la Universitat de Barcelona" (CCiT-UB) using an elemental analyser Flash 1112 EA interfaced to a Delta C Finnigan MAT isotope ratio mass spectrometer. Between 3 and 15 mg of the ground sample were weighed into Ag capsules and de-carbonated using repeated additions of 25% HCl, drying the sample at 60 ºC after each dose until no effervescence was observed. The Ag capsule, together with an oxidizer (vanadium pentoxide V_2O_5), was wrapped in a tin bundle. Then OC and N contents and $\delta^{13}C$ were measured, and OC/TN atomic ratios were calculated. The δ notation is defined as $\delta^{13}C = [(R_{sample}/R_{standard}) - 1] \times 1000$, where R is the isotopic ratio of $^{13}C/^{12}C$. The isotopic ratios of the samples (R_{sample}) are expressed relative to those of a standard ($R_{standard}$) which was Pee Dee Belemnite. In order to assess the contribution of OC to the bulk sample, we summed the product of the OC concentration in each grain-size fraction multiplied by the proportion of the corresponding grain-size fraction. All these results where expressed in % of dry weight of the bulk sediment sample.

A Coulter LS230 laser particle size analyser was used to determine particle size spectra of the bulk sediment sample. First, the >2 mm fraction was discarded using a sieve to prevent occasional coarse particles to obstruct the flow circuit of the instrument. After that, OM of the freeze-dried sample was oxidized with 10% H_2O_2 in order to eliminate the influence of organic particles and aggregates. The influence of carbonates was determined by comparison between a half of the sample being only treated with H_2O_2 and the other half being also treated with 1M HCl to remove carbonates. Before the analysis, both samples were mechanically shacked for 4 hours in a solution of water and sodium polyphosphate.

2.2.3.2. External forcing parameters

Information on wave conditions was acquired from Barcelona-II coastal buoy, located at 41.32º N and 2.21º E, belonging to "Puertos del Estado" of "Ministerio de Fomento" (Fig. 2.1b, green dot). Significant wave height (H_s, m), which is the average height of the highest one-third of waves in a given time period, and peak period (T_z, s), which is the average zero down-crossing wave period, were obtained with a temporal resolution of 1 hour. In addition, this data was propagated shoreward and then processed using the sediment transport model SEDTRANS05 (Li and Amos, 2001; Neumeier et al., 2008) to estimate the wave influence on seafloor sediments at each sampled depth. To this purpose, the orbital velocity parameter (u, m s^{-1}), given a particular wave condition (H_s, T_z) and a specific bottom depth was calculated.

Local weather data including precipitation (mm) and wind speed (m s^{-1}) were obtained with a frequency of 30 minutes in the Barcelona-El Raval meteorological station belonging to "Servei Meteorològic de Catalunya" (Fig. 2.1a, pink triangle). Daily water discharge (m^3 s^{-1}) of the Besòs River was obtained from the gauging station of Santa Coloma de Gramanet belonging to "Agència Catalana de l'Aigua" (Fig. 2.1a, yellow square).

Video images of the study area were obtained with a camera (Argus System) located at the top of a 142 m tall building in Barcelona (Mapfre Building) (Fig. 2.1b). This device belongs to a video cameras network of the Coastal Ocean Observatory (COO) from ICM-CSIC. Video images were used to observe the Besòs River and the "Espigó de Ginebra" outfall plumes over the study area, and also to compare measured data (precipitation and water discharge, which for the "Espigó de Ginebra" are not always correlated due to its discharge mechanism) and visual data of environmental conditions.

Time-series of 8-day averaged sea surface chlorophyll-a (chl-a) concentration (mg m^{-3}) were obtained from the Moderate Resolution Imaging Spectroradiometer (MODIS) onboard the Aqua satellite as a tool to measure the presence of marine photosynthetic organisms. The Goddard Earth Sciences Data and Information Services Centre (GES DISC) provides the processed and arranged data. Data was obtained from a grid limited by the coast: from 41º21'N to 41º24'N and from 2º11'E to 2º14'E.

2.1.4. Results

2.1.4.1. Forcing conditions

The studied period was characterized by relatively low average wind speeds never surpassing 5 m s^{-1} (Fig. 2.2b) and H_s below 2 m (Fig. 2.2a). Following the definition of a storm event by Mendoza and Jimenez (2009), which is an event in which the H_s exceeded 2 m for more than 6 hours, four storm events occurred in late September, mid and late October and mid November 2012 (Fig. 2.2a and shaded areas) in the study area. As far as river discharge is concerned, we define a flood when a river discharges more than 5 times its usually daily discharging rate over a steady period, based on the criteria used by Guillén et al. (2006). Two steady periods are distinguished with an average daily discharge rate of 1.8 m^3 s^{-1} during August and September and 7.7 m^3 s^{-1} during October and November 2012. Three flood events were observed in the Besòs River with such characteristics on 6 August, 29 September (the major water discharge) and 31 October 2012 (Fig. 2.2c). On the other hand, chlorophyll-a concentration recorded in surface waters was relatively stable below 0.16 mg m^{-3} during August and September 2012, while afterwards it progressively increased peaking at 0.56 mg m^{-3} in late October.

During the first storm event, in 28-29 September 2012, eastern winds with a long fetch triggered H_s up to 2.5 m and T_z up to 6.1 s, and the Besòs River discharged up to 46 m^3 s^{-1} (~26 fold its mean daily discharge), which was the major flood of the whole study period (Fig. 2.2a and d). Due to the coincidence of the storm waves and the high river discharge, this can be classified as an eastern wet storm (Guillén et al., 2006). The second storm took place during 18-20 October 2012, when winds blew mainly from an E-NE direction and caused waves surpassing 2 m for 44 hours (H_s 3.5 m and T_z 8 s). The storm, which occurred without relevant continental runoff, can be classified as an eastern dry storm (Guillén et al., 2006). The strongest storm took place in 31 October - 1 November 2012. This storm lasted for 29 h, with maximum H_s of 3.3 m and maximum T_z of 10.5 s (Fig. 2.2a). Winds were highly variable, they started blowing from the NE and were turning and increasing its intensity until 1 November, when an average wind velocity of 5.1 m s^{-1} (Fig. 2.2b) was recorded from the W direction. Furthermore, the Besòs River discharged 44 m^3 s^{-1} (~6 fold its

mean daily discharge), coinciding with the highest peak of chlorophyll (0.56 mg m^{-3}) at the study area for the whole study period (Fig. 2.2c). Therefore, this storm has been classified as a northern wet storm. Finally, the last storm took place in 14 November 2012, it lasted for 14 h and it was characterized by H_s of 2.2 m and T_z of 8.7 s (Fig. 2.2a). No increase in water discharge above the mean daily discharge was observed, thus being classified as an eastern dry storm.

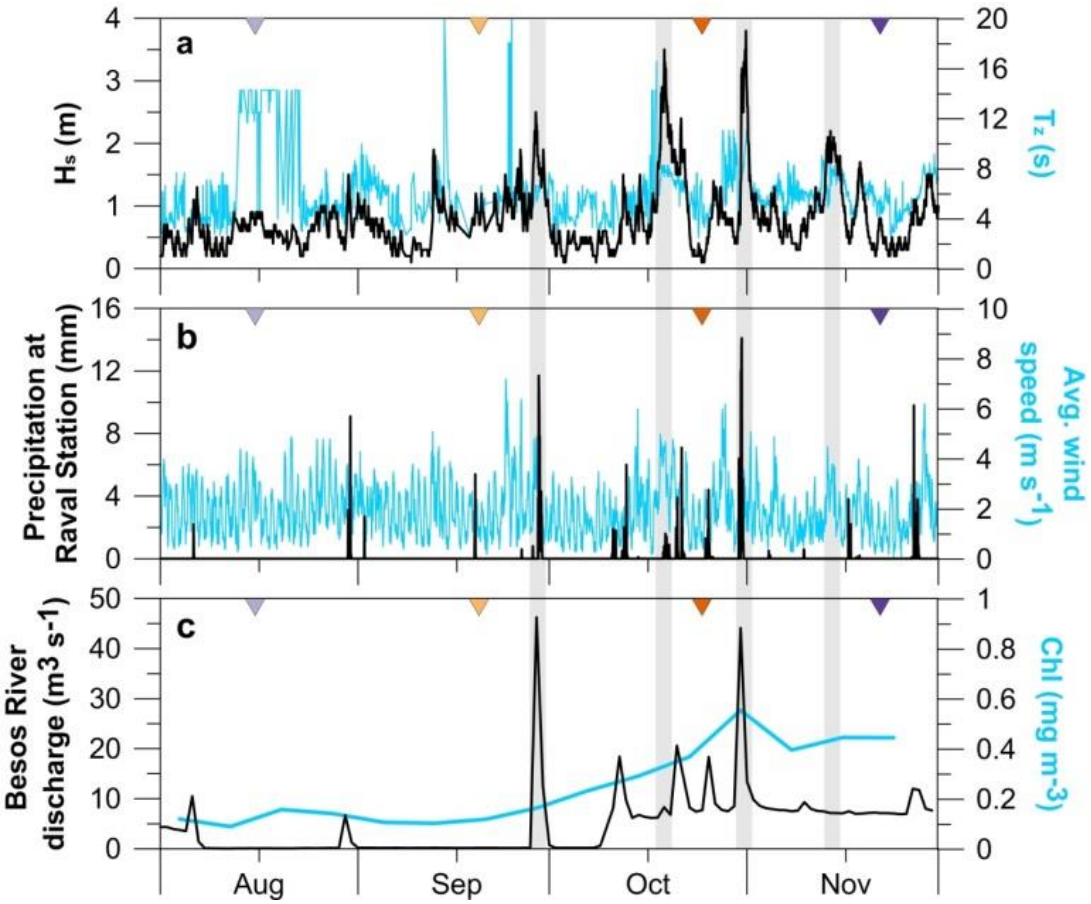

Figure 2.2. Time series of oceanographic, meteorological and fluvial variables from August to November 2012. (a) Significant wave height (H_s) (black line) and peak period (T_z) (blue line) at the Barcelona II buoy. (b) Precipitation (mm) (black line) and average wind speed (m s^{-1}) (blue line) at the Raval station. (c) Besòs River water discharge (m^3 s^{-1}) (black line) and chlorophyll-a concentration (mg m^{-3}) (blue line). Inverted triangles show sediment sampling dates where different colours correspond to August, September, October and November, agreeing with the colour code in Fig. 2.3. Shaded areas highlight the most important storms of the study period.

2.2.4.2. Grain-size

The grain-size distributions of decarbonated and non-decarbonated samples show no significant differences (data not shown). As a result of the irrelevant role of carbonates, we will only discuss the grain-size spectra of the samples without including the carbonate fraction.

Grain-size distribution of surface sediments in the study area evidence a significant seawards decrease of the grain size median (Table 2.1), as illustrated by the significant negative correlation

found between d50 and water depth (R-squared= 0.93, p-value $<2.1 \cdot 10^{-9}$). Surface sediments were predominantly composed of sand and shifting to a more silty composition at 40 m depth.

During the study period, we found three significant temporal variations in the grain-size spectra at the shallow (10 m and 20 m) and the deep (40 m) stations (see below) (Fig. 2.3).

Surface sediments at 10 m depth were well-sorted and showed a unimodal distribution with a narrow peak around 450-550 µm in August, September and October 2012, and a peak at 160 µm in November 2012 (Fig. 2.3a). This decrease in grain size is also shown by the strongest shift in the d50 value of these samples (Table 2.1). Time-averaged grain-size distribution shows that 97±1% of sediments at 10 m depth were sand-sized (Table 2.1).

Sediments at 20 m depth were sorted with a bimodal distribution peaking around 110-140 µm and 370-410 µm, respectively (Fig. 2.3b). Grain-size distribution shifted towards coarser values in October 2012 as shown by a shift in the d50 from 146 to 164 µm. Time-averaged grain-size distribution shows a decrease in the percentage of sand (84±3%) when compared with the 10 m samples, due to an evident increase in the silt and clay fractions (Table 2.1).

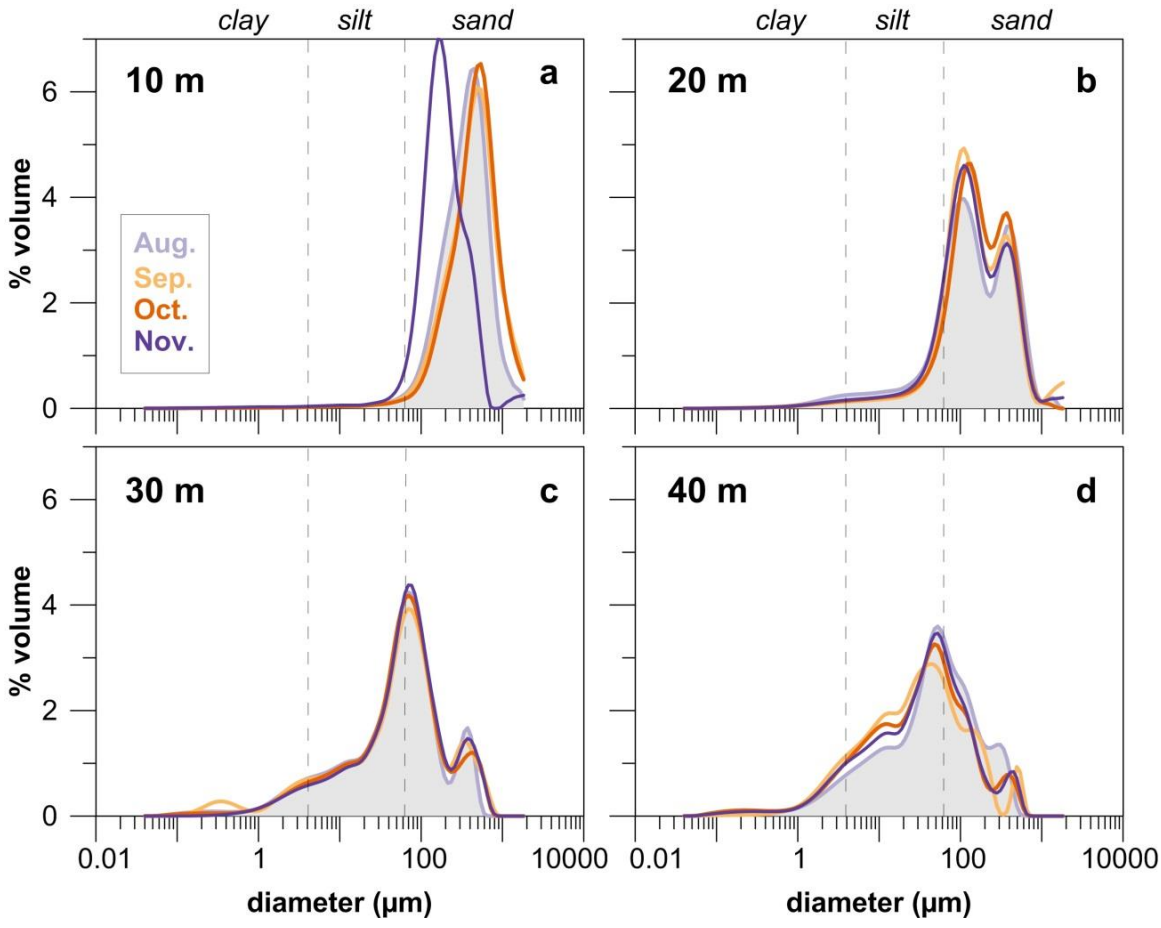

Figure 2.3. Grain size distribution of surface sediments at (a) 10 m, (b) 20 m, (c) 30 m and (d) 40 m depth, corresponding to de-carbonated samples. The grain-size spectra in August 2012 is shadowed in order to ease comparison with the grain-size at the beginning of the study period. Fine dashed vertical lines separate clay (<4 µm), silt (4-63 µm) and sand (>63 µm) sizes.

Sediments at 30 m depth show no variability with time. The sediment samples were bimodal sorted with the main mode at 70 µm and a secondary mode at 340-410 µm (Fig. 2.3c). The sand fraction followed its generally offshore decrease down to 50±2% and silt and clay fractions increased at this depth to 50±3% showing the transition to a muddy zone (Table 2.1).

Finally, samples collected at 40 m depth were mostly composed of fine sediments. The silt and clay fractions accounted for 56±6% and 10±1%, respectively, and the sand fraction dropped down to 34±5% (Table 2.1). Grain-size profiles show a not well-sorted population, but a main mode could be distinguished at 43-52 µm shifting to finer sizes in September 2012(Fig. 2.3d).

Month and station	Depth (m)	Clay (%)	Fine Silt (%)	Coarse silt (%)	Sand (%)	d50 (µm)
August						
1.1	10	0.53	1.38	0.72	97.4	386
1.2	20	2.90	10.0	6.43	80.6	143
1.3	30	8.79	29.6	13.5	48.1	60.7
1.4	40	8.15	36.8	14.0	41.1	50.2
September						
1.1	10	0.49	1.40	0.60	97.5	465
1.2	20	1.77	6.07	5.40	86.8	146
1.3	30	10.2	27.4	12.7	49.7	63.0
1.4	40	10.9	48.9	11.2	29.0	31.6
October						
1.1	10	0.41	1.19	0.53	97.9	488
1.2	20	2.09	6.86	4.42	86.6	164
1.3	30	7.53	28.8	13.9	49.8	63.2
1.4	40	11.1	45.3	12.8	30.9	35.6
November						
1.1	10	0.91	1.88	1.49	95.7	189
1.2	20	2.12	7.92	6.29	83.7	142
1.3	30	6.41	27.1	13.5	53.1	67.9
1.4	40	10.6	42.8	13.6	33.0	39.4

Table 2.1. Grain size distribution of surface sediments collected in August to November 2012 at 10, 20, 30 and 40 m of water depth.

2.2.4.3. Organic matter content and stable isotope ratios

In terms of absolute amount of OC in the bulk sample, the OC ranged from 0.17 to 2.9 mg OC/100 mg sample of dry weight ($\%OC_{size}/\%OC_{bulk}$,Table 2.2). The maximum OC values were always found at 40 m depth (2.40±0.45 mg OC/100 mg sample), followed by 10 m depth (1.47±0.97 mg OC/100 mg sample). Sand fraction was the main contributor to the total OC with values ranging from 50 to 97%, decreasing with water depth (Table 2.2). The rest OC was predominantly contained in fine silt and clay fraction with up to 23.8% and 25.3%, respectively, and being the coarse silt the minimum contributor (up to 7.28%).

In the different size-fractions the OC and TN concentration ranged from 0.13 to 8.68% and from 0.02 to 1.47%, respectively (Fig. 2.4a, b and Table 2.2). As demonstrated by the strong correlation between OC and TN, with the Pearson's correlation coefficient ranging from 0.81 to 0.93 (p-value $<10^{-4}$) in the different grain-size fractions, TN contents exhibit a very closely parallel trend (Fig. 2.4a, b). The highest OC concentration was always recorded in the clay fraction, reaching maximum values at 10 m depth (8.68%), followed by the sand fraction with the maximum OC concentration at 40 m depth (5.23%). Visual inspection of the samples exhibit an important

presence of strands and plant detritus in the 40 m-depth sand fractions, while that was not observed in the rest of the fractions and depths (data not shown). The OC concentrations of fine and course silt fractions were lower with values up to 2.06% at 10 m depth and 1.06% at 40 m depth, respectively (Fig. 2.4a and Table 2.2).

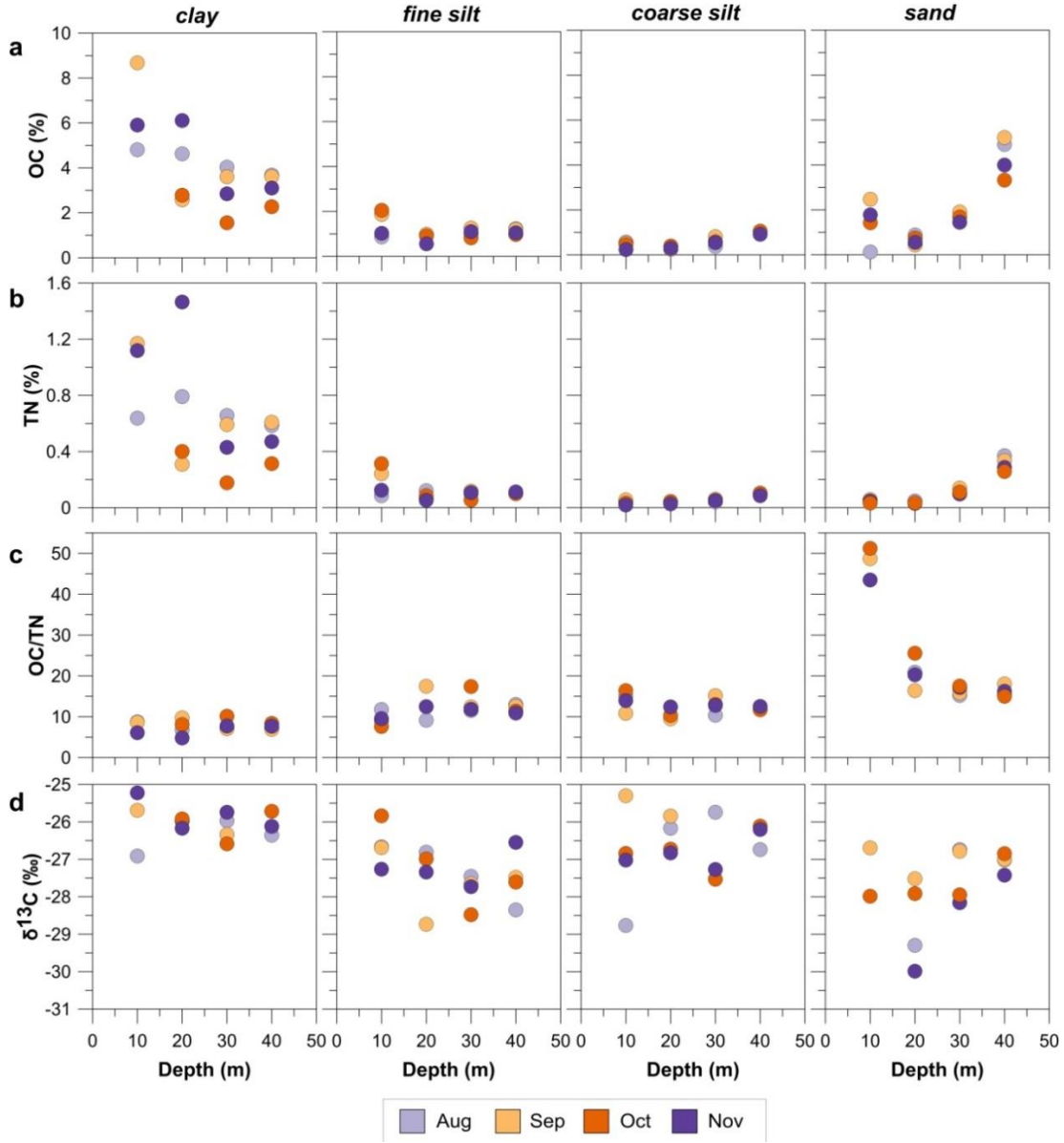

Figure 2.4. (a) %OC, (b) %TN, (c) OC/TN ratio and (d) $\delta^{13}C$ versus depth for each grain-size fraction.

Several important variations are clearly seen from the time series. At 10 m depth there was a significant enrichment of the total OC content (Table 2.2) in September 2012 due to the increase of OC concentration in the clay fraction (from 4.81 to 8.68%), fine silt fraction (from 0.88 to 1.88%) and sand fraction (from 0.13 to 2.48%). Afterwards, in November 2012, OC concentrations in clay and fine silt fractions were similar to those recorded in August 2012 (Fig. 2.4a). At 20 m depth, the lowest total OC contents was recorded during September 2012 (Fig. 2.4a) due to a drop in OC concentration in the clay (2.59%) and sand (0.44%) fractions. At 30 m and 40 m depth, the most significant changes were in October 2012 with the decrease of the OC concentration of clay and sand fractions (Fig. 2.4a). The N content also showed these same temporal oscillations (Fig. 2.4b and Table 2.2).

Month and station	Size fraction	OC_{bulk} (%)	OC_{size} (%)	$\%OC_{size}/\%OC_{bulk}$ (%)	OC/TN	$\delta^{13}C$ (‰)
August						
1.1	<4 µm	0.17	4.81	14.9	8.79	-26.9
	4 - 40 µm		0.88	7.09	11.8	-26.7
	40 - 63 µm		0.57	2.39	15.1	-28.8
	63 µm - 2 mm		0.13	75.6	n.d.	-25.9
1.2	<4 µm	0.96	4.64	13.9	6.83	-26.0
	4 - 40 µm		0.96	9.96	9.17	-26.8
	40 - 63 µm		0.30	1.98	10.3	-26.2
	63 µm - 2 mm		0.89	74.1	20.9	-29.3
1.3	<4 µm	1.40	4.04	25.3	7.16	-26.0
	4 - 40 µm		1.00	21.1	11.6	-27.5
	40 - 63 µm		0.38	3.67	10.4	-25.7
	63 µm - 2 mm		1.45	49.9	15.3	-26.7
1.4	<4 µm	2.91	3.68	10.3	7.32	-26.4
	4 - 40 µm		1.24	15.7	13.1	-28.3
	40 - 63 µm		0.93	4.48	11.8	-26.7
	63 µm - 2 mm		4.92	69.5	15.5	-27.0
September						
1.1	<4 µm	2.49	8.68	1.71	8.64	-25.7
	4 - 40 µm		1.88	1.05	9.01	-26.7
	40 - 63 µm		0.53	0.13	10.9	-25.3
	63 µm - 2 mm		2.48	97.1	48.8	-26.7
1.2	<4 µm	0.50	2.59	9.11	9.74	-26.0
	4 - 40 µm		1.00	12.0	17.5	-28.7
	40 - 63 µm		0.25	2.66	9.52	-25.8
	63 µm - 2 mm		0.44	76.2	16.5	-27.5
1.3	<4 µm	1.77	3.61	20.7	7.10	-26.3
	4 - 40 µm		1.27	19.7	12.5	-27.6
	40 - 63 µm		0.82	5.86	15.2	n.d.
	63 µm - 2 mm		1.92	53.8	15.9	-26.8
1.4	<4 µm	2.60	3.62	15.1	6.93	-26.1
	4 - 40 µm		1.20	22.5	12.6	-27.5
	40 - 63 µm		0.92	3.99	11.9	-26.1
	63 µm - 2 mm		5.23	58.3	18.1	-27.0
October						
1.1	<4 µm	n.d.	n.d.	n.d.	n.d.	n.d.
	4 - 40 µm		2.06	1.71	7.66	-25.8
	40 - 63 µm		0.46	0.17	16.4	-26.8
	63 µm - 2 mm		1.43	98.1	51.3	-28.0
1.2	<4 µm	0.79	2.79	7.35	8.11	-25.9
	4 - 40 µm		0.92	7.96	12.5	-27.0
	40 - 63 µm		0.40	2.24	10.4	-26.7
	63 µm - 2 mm		0.76	82.5	25.6	-27.9
1.3	<4 µm	1.28	1.56	9.20	10.2	-26.6
	4 - 40 µm		0.83	18.7	17.4	-28.5
	40 - 63 µm		0.58	6.31	13.1	-27.5
	63 µm - 2 mm		1.69	65.8	17.5	-27.9
1.4	<4 µm	1.86	2.28	13.6	8.43	-25.7
	4 - 40 µm		0.98	23.8	11.4	-27.6
	40 - 63 µm		1.06	7.28	11.8	-26.1
	63 µm - 2 mm		3.33	55.3	15.0	-26.8
November						
1.1	<4 µm	1.79	5.91	3.00	6.15	-25.2
	4 - 40 µm		1.03	1.09	9.60	-27.3
	40 - 63 µm		0.24	0.20	14.0	-27.0
	63 µm - 2 mm		1.79	95.7	43.6	n.d.
1.2	<4 µm	0.66	6.11	19.6	4.86	-26.2
	4 - 40 µm		0.57	6.79	12.5	-27.3
	40 - 63 µm		0.30	2.85	12.5	-26.8
	63 µm - 2 mm		0.56	70.8	20.3	-30.0
1.3	<4 µm	1.33	2.86	13.8	7.75	-25.7
	4 - 40 µm		1.11	22.5	11.9	-27.7
	40 - 63 µm		0.55	5.58	12.8	-27.3
	63 µm - 2 mm		1.45	58.1	17.2	-28.2
1.4	<4 µm	2.23	3.11	14.8	7.69	-26.1
	4 - 40 µm		1.06	20.4	10.9	-26.5
	40 - 63 µm		0.92	5.62	12.6	-26.2
	63 µm - 2 mm		4.00	59.2	16.3	-27.4

Table 2.2. OC concentration of the bulk sample (OC_{bulk}) and OC concentration in each grain size $\%OC_{size}/\%OC_{bulk}$, OC/TN ratios and $\delta^{13}C$ of OC in each of the fractions. n.d.: no data.

The OC/TN atomic ratio varied between 4.86 and 51.3 with a tendency to increase towards coarser fractions (or, alternatively, to decrease towards finer fractions) (Figs. 2.5 and 2.6a). The lowest ratio recorded was 4.86 in the clay fraction at 20 m depth, and the highest ratio was 51.3 in the sand faction at 10 m depth (Fig. 2.4c and Table 2.2). The most significant spatial variability was found in the sand fraction with an OC/TN ratio decrease from 10 to 20 m depth (Fig. 2.4c and Table 2.2), while no remarkable temporal variations were observed. The OC/TN ratio showed significant grain-size fraction dependence with a slope of the regression lines varying from a 4.56 recorded in the clay fraction, to 5.25 in the fine silt, 10.2 in the coarse silt and 12.5 in the sand fraction (Fig. 2.5).

The $\delta^{13}C$ of OC ranged between -30.0 and -22.4‰ (Fig. 2.4d and Table 2.2). OC in the clay fraction showed the highest and more clustered values, with $\delta^{13}C$ ranging from -26.9 to -25.2‰, while in the other fractions a wider and sparser range was observed: -28.7 to -25.8‰ in the fine silt fraction, -28.8 to -25.3‰ in the coarse silt fraction and -30.0 to -26.7‰ in the sand fraction (Fig. 2.4d and Table 2.2).

2.1.5. Discussion

2.1.5.1. Grain-size distribution and variability in surface sediments

Wave activity, storm events and fluvial input are the main environmental factors that most likely contribute to sediment supply, bottom sediment resuspension and advective transport in the Barcelona inner-shelf (Copeiro, 1982; DGPC, 1986; Durán et al., 2009; Ercilla et al., 2010; Antonijuan et al., 2012; Durán et al., 2012; Sanchez-Vidal et al., 2012). Our results suggest that the grain-size distribution of surface sediments during the study period is mainly determined by the very efficient dispersion of the particles by wave action under relatively calmed weather conditions. Therefore, under these conditions, the main disturbing factors appeared to be the floods from the outfalls and dry storm events both providing and removing, respectively, sediment particles to this coastal scenario.

The spatial distribution of surface sediment grain size found in late summer-autumn 2012 shows the typical trend for grain size to decrease seawards (Fig. 2.3 and Table 2.1), which is mainly caused by decreasing wave energetic disturbance of seafloor sediments with increasing water depth (Dufois et al., 2008; Dalyander et al., 2013). In order to know the impact of wave energy in the studied area, we applied the linear wave propagation (Vincent and Demirbilek, 2002) to the wave data obtained from the Barcelona-II buoy, and then we calculated orbital velocities at 10, 20, 30 and 40 m depth. The decreasing seawards trend of the orbital velocities occurred between 10 and 40 m depth in the Barcelona inner shelf is illustrated in Figure 2.6. Thus, particles supplied to the nearshore by outfalls and riverine discharge might have suffered a natural sorting mainly controlled by wave strength which is in turn controlled by depth (Table 2.1). From 10 to 20 m depth, most of clay sized particles and light fragments such as plant debris would not have even settled down to the bottom due to wave activity and mainly heavier grains would have remained at these shallower stations. From 30 to 40 m depth, the fine and/or light particles, which are able to travel on the water column to deeper and calmer areas (Guillen et al., 2006), would have been deposited on the seafloor.

Orbital motion and bottom current activity associated with storm waves can exert important effects on the sediment sorting in non-tidal nearshore sandy environments (Ogston et al., 2000). During the study period, in the Barcelona coast, however, there was no record of any dramatic event or major storm causing intense reworking and remobilization of nearshore sediments such as those recorded in the NW Mediterranean in November 2001 or December 2008, with maximum H_s surpassing 7 m and return periods of several decades (Ojeda and Guillén, 2008; Sanchez-Vidal et al., 2012). Nonetheless, there were small but detectable temporal variations in the grain-size distribution of seafloor sediments along the study period (Fig. 2.3).

The first noticeable shift in grain-size distribution, was a significant enrichment of the fine silt fraction at 40 m of water depth in September 2012, lowering the d50 from ~50 to ~30 µm and maintaining around this value in October and November samplings (Fig. 2.3d and Table 2.1). This change was probably caused by fine particles derived from the "Espigó de Ginebra" outfall, Indeed, the day before obtaining the sediments in the September survey, outfalls along Barcelona coast discharged significant amounts of water (and sediment) due to increased precipitation (Fig. 2.2b). This is clearly seen in the image obtained from the COO, which shows a plume of suspended sediment flowing out of the outfall (Fig. 2.5a). Relatively calmed conditions at the offshore station may have allowed particles to settle and remain there. Despite we also analysed Besòs River floods as a potential source of fine particles getting into our monitored area, the COO images of the main flood (on 30 August) of this time interval show a Besòs River plume too small during this period to arrive at the sampled region.

A second shift in the median grain size took place in October 2012 at 10 and 20 m depth. The d50 increased from 465 and 146 (in September 2012) to 488 and 164 µm, respectively (Fig. 2.3d and Table 2.1). Since the relative abundance of grain size fractions remains almost the same, it is assumed a coarsening of the sand fraction of the sediment, which could have been triggered by the strongest storm of the study period, occurred on 18-20 October 2012. Large waves generated during the storm might have produced the shear stress necessary to mobilize sediment and transport it along and across the shelf; afterwards, when waves height decrease, bottom stress decrease and sediment is redeposited (Guillén et al., 2006).

Finally, the last relevant shift in grain-size occurred at 10 m depth between October and November 2012, when the main mode at 540 µm decreased to a mode of 160 µm. The d50 showed also a significant decrease from 488 to 189 µm (Fig. 2.3a and Table 2.1). Coinciding with these results, the COO device detected an important plume getting out from the "Espigó de Ginebra" outfall, which drifted alongshore over the 10 m-isobath station two days before sample acquisition (Fig. 2.5b).

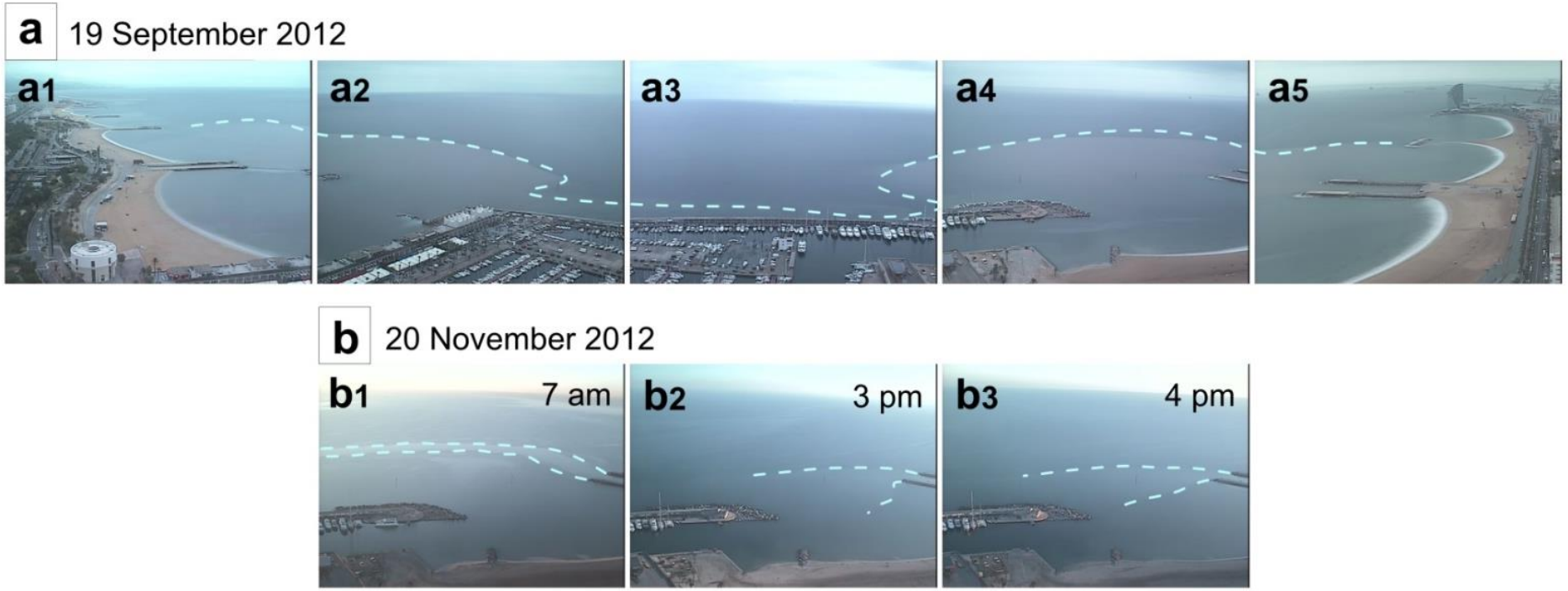

Figure 2.5. (a) Panoramic view of the Barcelona coast line on 19 September 2012 at 11 a.m.; a1 and a2 show water discharge from the outfalls northward of the study area, a2 and a3 show the Olympic harbour, a4 show the sampled area, and a5 show Somorrostro (foreground) and Barceloneta (background) beaches separated by the "Espigó de Ginebra" breakwater. The dashed line indicates the front of the flow loaded with suspended material. (b) Panoramic view of the Barcelona coast line on 20 November 2012 where it is evident the plume getting out from the "Espigó de Ginebra" outfall at 7 a.m. (b1), 3 p.m. (b2) and 4 p.m. (b3). The dashed line highlights the visual boundaries of the plume. Images are from the Coastal Ocean Observatory (ICM-CSIC).

2.2.5.2. Organic matter distribution and variability among the grain-size fractions

The results of our study indicate that the amount of OC is different in each grain size fraction of the sediment, which is not apparent from analyses of bulk sediments. Thus, hydrodynamic grain size sorting affects the distribution and amount of OC in surface sediments (Fig. 2.4).

The sand-sized particles, which dominated the bulk sediment composition at almost every depth, accounted for the major contribution to the total OC along the studied transect, with the highest values at 10 m and the lowest at 40 m, where finer particles are more abundant (Tables 2.1 and 2.2). The opposite trend was observed, however, in the OC concentration of this fraction which increased with water depth (Fig. 2.4a and Table 2.2). The shoreward stations (10 and 20 m) were located in a permeable bed sand zone where light OM non-adsorbed within mineral particles can be easily winnowed due to the persistent wave-induced resuspension (Fig. 2.6) (Huettel et al., 2013). At 40 m depth, where the highest OC concentration in the sand fraction is found (Fig. 2.4a), calm wave conditions likely favoured the settling of organic light sand-sized particles sourced from the river and the outfalls located along the coast. This was witnessed by a high and constant presence of large fragments of plant debris in the samples collected. Moreover, we noticed a steep seawards decrease in the OC/TN ratio found within the sand fractions (Fig. 2.4c). We interpret this fact as an incorporation of exogenous nitrogen to typically nitrogen-poor plant debris. Some studies suggest that microbial communities are fed with these vegetal particles, which might have been progressively enriched due to bacterial incorporation of nitrogen from the water to the bacterial cell walls (Nuwer and Keil, 2005; Tesi et al., 2007; Fernandes et al., 2014).

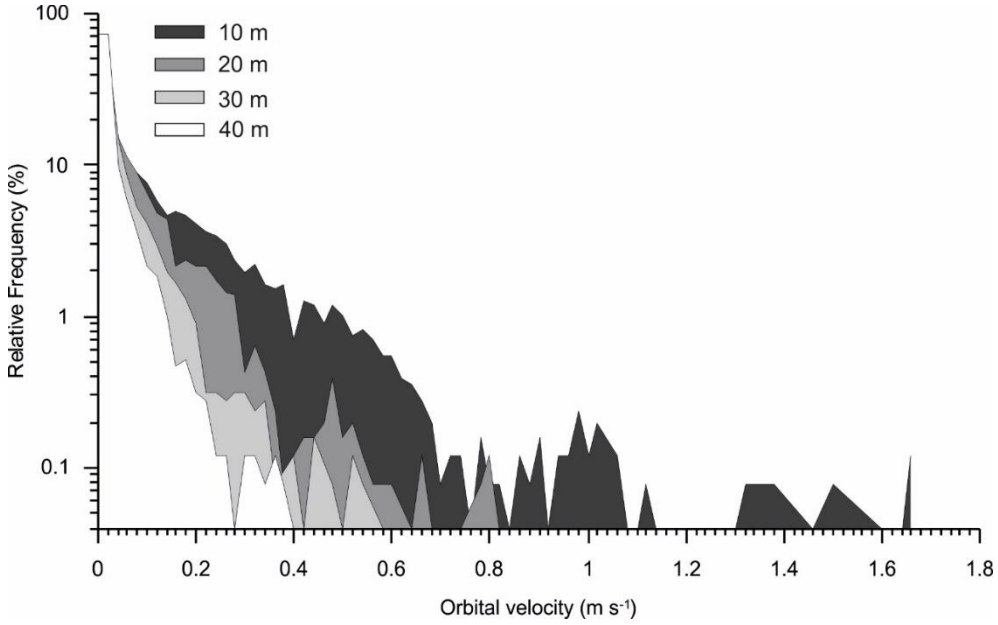

Figure 2.6. Relative frequency distribution of orbital velocities of the study period at 10 m, 20 m, 30 m and 40 m depth.

Clay fraction also played an important role in the OC distribution. Despite this fraction was the less abundant at the shallower stations (Table 2.1), it had the highest %OC content and it was the second major contributor to the total OC (Table 2.2). Our results add to the growing body of evidence that OM is mostly associated to clay fraction as mineral-OM aggregates (e.g., Bock and

Mayer, 2000). This correlation is caused by the high specific surface area of fine-grained particles, which have a higher capacity for adsorption of OM (Mayer, 1994b; Hedges and Keil, 1995). In contrast to the sand fraction, the concentration of OC in the clay fraction decreased with increasing water depth from a maximum of 6.5±2.0% (10 m) to a minimum of 3.0±1.1% (30 m) and 3.2±0.6% (40 m), meaning that OC in the clay fraction was somehow "lost" seawards. This can be explained because at the shallower stations, in the interface between fresh and sea water, the coastal environments are prone to the flocculation by aggregating very small organic and mineral particles which settle down as flocks that are larger than the constituent particles (Shalkovitz, 1976; Burban et al., 1989; Lick et al., 1993). This is in agreement with the high OC concentrations found at the 10 m-depth (Fig. 2.4a), which might not have remained much time suspended in the water column and only a small proportion of that OM might have been remineralized (Arnarson et al., 2007). Conversely, the suspended organic and mineral particles that remain in the water column and settle in deeper areas suffer a longer oxygen exposure time and thus OM oxidation (Arnarson et al., 2007). Plot of OC vs. OC/TN ratio in the clay fraction (Fig. 2.7b) shows an inverse lineal correlation, which suggests that samples with lower OC content had lost the more labile compounds (N-rich) (Cowie and Hedges, 1994). Thus, there has been a preferential loss of N during early remineralisation of OM, pointing to increased OM degradation between the 10-30 m depth (Fig. 2.4a, b). Therefore, fine particles with both lower OC and TN may have been deposited at deeper areas. Accordingly, bacterial reworking of particulate OM has been detected along the water column at coastal and shelf environments (Bourgoin and Tremblay 2010; Fernandes et al., 2014). In these environments, the more reactive N-rich compounds are preferentially consumed and recycled while OM is travelling towards deeper regions as well as settling down to seafloor, which usually turns out into a rise in the OC/TN ratio, as observed in our study (Fig. 2.7). Overall, the clay fraction together with the organic sand-sized particles, are the lighter particles which are susceptible to be transported in the water column and contribute to the OC budget of the deepest studied area.

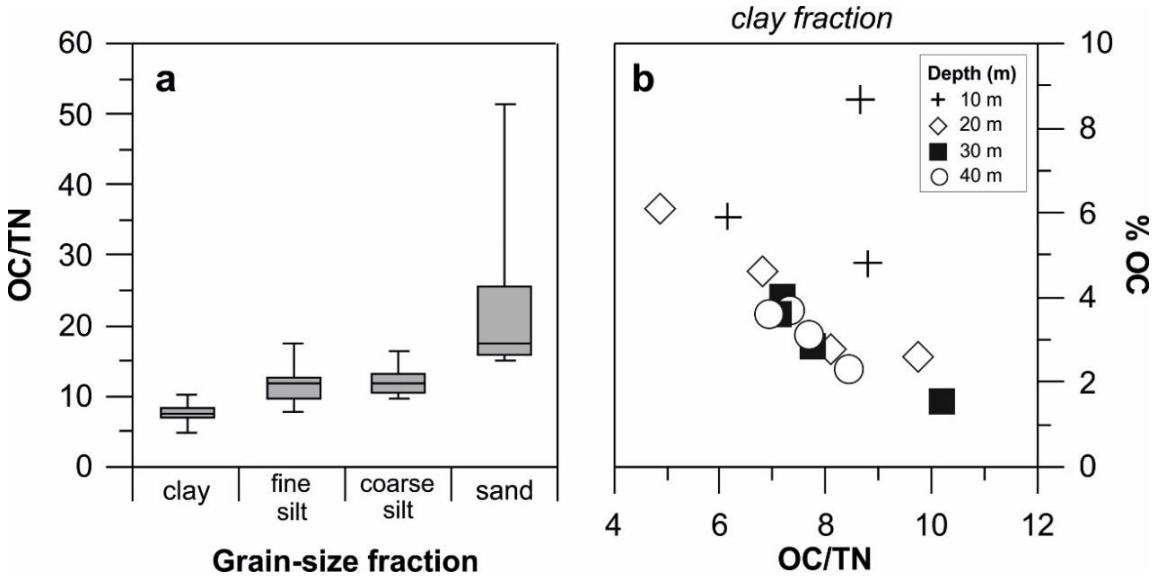

Figure 2.7. (a) OC/TN in each grain-size fraction. The whiskers at the end of each box correspond to extreme values, while the box is defined by the lower and upper quartiles and the horizontal line within each box represents the median. (b) Relation of OC concentration versus OC/TN ratios for the clay grain-size fraction through the studied depths.

Our results reveal significant temporal variability of the OM distribution in surface sediments due to the impact of the different external forcing conditions. In September 2012, the OC concentration increased at 10 m depth (Fig. 2.4a) likely due to the arrival of sand sized organic debris and enhancement of aggregates formation occurring in the very first phase of the fresh and salty water mixing process during the strongest flood recorded in the Barcelona city outfalls during the study period (Fig. 2.5). At 40 m depth, despite we observed an arrival of fine particles (Fig. 2.3d and Table 2.1), OC loadings remained very similar to the values of August (Fig. 2.4a and Table 2.2).

In October 2012, the decrease in OC content of the sand fraction at 10 and 40 m depth (Fig. 2.4a and Table 2.2), was most probably caused by the impact of the strongest dry storm recorded during the whole study period (18-20 October 2012, Fig. 2.2). The strong wave shear stress of this storm may have triggered a significant reworking causing a winnowing of the smaller particles at 10 and 20 m-depth (Fig. 2.3) and also of the previously deposited OC-rich sand-size particles such as plant debris delivered by the outfalls and the Besòs River a few days ago, both at shallower (10 m) and deeper (40 m) stations, (Fig. 2.2c).

Finally, between October and November 2012, the main changes in OC, as well as in grain-size distribution (see section 5.1), occurred at 10 and 20 m depth. In absence of any obvious explanation to this behaviour it is hypothesized that fine mineral particles likely sourced from outfalls made the d50 to sharply decrease at 10 m depth (Fig. 2.5b). These mineral particles might have been poorly loaded in OC, which could explain the OC decrease in the fine silt fraction at 10 m depth. However, the apparently opposite trend of the clay fraction at 20 m depth could have been caused by flocculation processes at the fresh-salty water interface.

2.2.5.3. Organic matter sources from nearshore to lower slope

Bulk geochemical proxies such as elemental (TN/OC) and stable isotopic ratios of OC ($\delta^{13}C$) have been widely used in marine environments as a first provenance tracers to elucidate the relative contribution from different sources (Fry and Sherr, 1984; Meyers, 1994; Goñi et al., 2003). $\delta^{13}C$ values of terrestrial OC depend on the dominant vegetation of the watersheds, ranging from -28 to -23‰ or from -14 to -10‰ if C3 or C4 are the dominant constituents, respectively (Fry and Sherr, 1984). Sanchez-Vidal et al. (2013) recorded $\delta^{13}C$ values of -33 to -26‰ for terrestrial OC entering the North Catalan margin through the Tordera River, about 50 km north from our study area. The TN/OC ratio of terrestrial OM usually have low values (<0.06) due to the dominance of N-free biomacromolecules in the terrestrial vascular plants (Hedges et al., 1997). In contrast, OM from temperate marine phytoplankton have heavier $\delta^{13}C$ values (from -22 to -19‰) with N-enriched compounds (TN/OC >0.12), which are more labile and easily degradable (Fry and Sherr, 1984; Goñi and Hedges, 1995; Hedges et al., 1997).

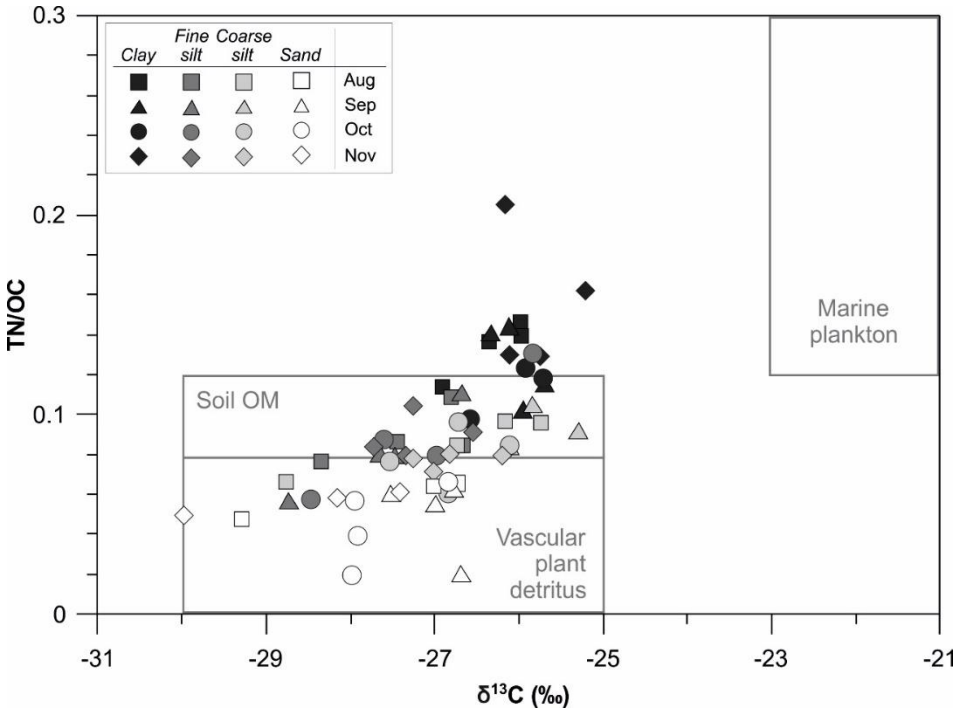

Figure 2.8. TN/OC versus $\delta^{13}C$ in each size fraction (clay in black, fine silt in dark grey, coarse silt in light grey, sand in white) and in each month (filled squares, triangles, circles and diamond correspond to August, September, October, and November, respectively). The compositional ranges of different end members are included in the plot for ease of reference, based on Hedges et al. (1997), Sanchez-Vidal et al. (2013) and Pedrosa-Pàmies et al. (2013).

To estimate the relative contributions of different OC sources in each size fraction in the studied coastal zone, either terrestrial or marine, $\delta^{13}C$ values are plotted against the TN/OC ratios (TN/OC~0 rather than OC/TN~∞, following Goñi et al., 2006) (Fig. 2.8). Our results reveal significant variability in OC/TN ratios and $\delta^{13}C$ values in the different size fractions of the surface sediments (Figs. 2.4c-d and 2.6a). The OM reaching the study area is mostly of terrestrial origin (Fig. 2.8), although each of the grain-size fractions may have a distinct terrigenous provenance (Fig. 2.9). Indeed, previous studies have found that the most labile compounds tends to be stored in the clay fraction; pollen grains and soil eroded OM tend to be associated to the silt fraction; and vascular plant debris is related to sand fraction (Keil et al., 1998; Tesi et al., 2007; Pedrosa-Pàmies et al., 2013; Sanchez-Vidal et al., 2013; Rumolo et al., 2015). $\delta^{13}C$ values found in our study are more depleted than those found by Rumolo et al. (2015) at depths beyond 60 m in the Barcelona continental margin, clearly reflecting the major impact and influence of the river and outfall terrestrial inputs at shallower depths.

Despite the high terrigenous influence in the studied surface sediment, relatively higher phytoplankton contribution can be inferred in the clay fractions in November 2012 (Fig. 2.8). Accordingly, between October and November 2012 the highest values of chlorophyll-a concentration of the study period (Fig. 2.2c) were recorded in the study area, up to 0.56 mg m^{-3}. This could have been enhanced by the arrival of nutrient-rich waters from a series of minor Besòs river discharges that took place in early November (Fig. 2.2c).

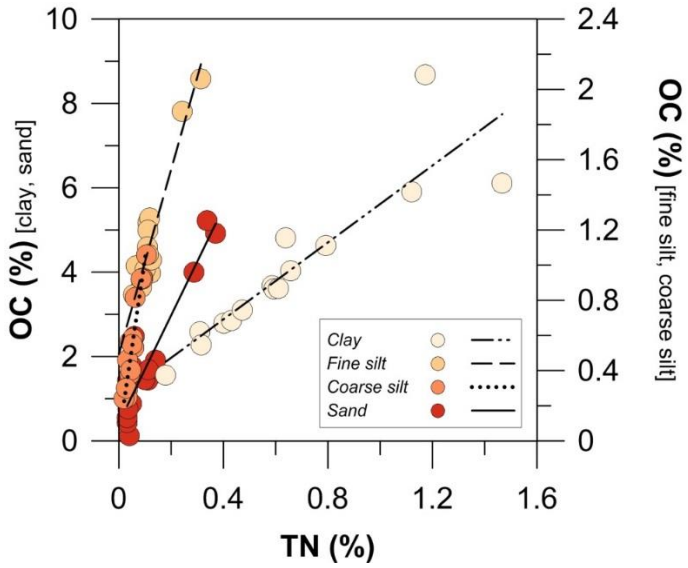

Figure 2.9. OC versus TN in the different grain-size fraction. Different style lines show the linear fit for each grain size fraction (see legend): y=4.6x+1.1 (r^2=0.81, clay), y=5.3x+0.5 (r^2=0.90, fine silt), y=10.2x (r^2=0.93, coarse silt) and y=12.5x+0.4 (r^2=0.88, sand). Data of clay and sand fractions are referred to the left y-axis, while fine and coarse silt are referred to the right y-axis.

Finally, further insights into OC fate and transport in the marine environment is provided if we plot our data from the nearshore environment with that obtained by Pedrosa-Pàmies et al. (2013) in a similar study performed in the continental shelf about 50 km north of our study area and the nearby Blanes submarine canyon (Fig. 2.10). If we build a virtual section across the margin, covering a depth range from 10 m (inner-shelf) to 1500 m (open slope and Blanes Canyon), the only remarkable change is a seawards loss of OC in the clay fraction (Fig. 2.10). In the Catalan margin, fine particles are transported to the lower slope and deep basin by intermediate and near bottom nepheloid layers (Puig et al., 2001), which may be reinforced in case of extreme events such as dense shelf water cascading or eastern storms (Sanchez-Vidal et al., 2012; Canals 2013; Puig et al., 2013).

Fine sediments from the near shore show the highest OC loadings, and decrease across the continental margin and towards the lower slope to a baseline value of ~1% (Fig. 2.10). This suggests that successive remobilization and advective transport of OC-rich fine sediments from the inner-shelf to the outer shelf and upper slope and towards the deep-sea decrease OC loading by a factor of up to 10. Surprisingly, this is in agreement with a similar study performed in a very different margin, the Siberian margin, by Tesi et al. (2016), where an average OC loss of 90% was detected due to cross-shelf transport from the coast to the outer shelf. This highlights that the processes which modulated our study area are likely quite ubiquitous in shelf environments. Furthermore, Pedrosa-Pàmies et al. (2013) and Rumolo et al. (2015) found that fine sediments ultimately buried in the deep open slope of Catalan margin show heavier $\delta^{13}C$ values than those from the nearshore environment, thus marine carbon may have been also added to clay sized particles while travelling towards deeper areas.

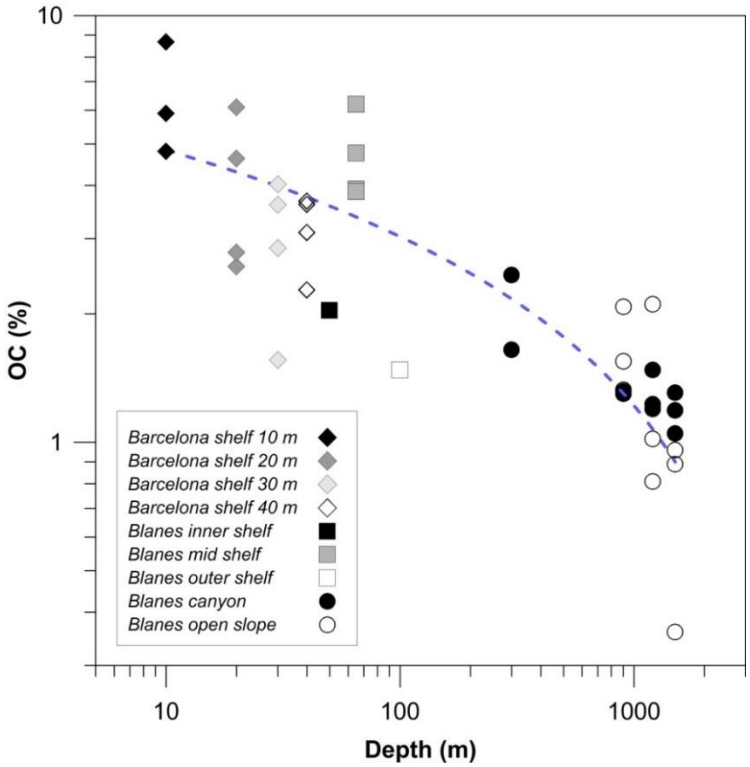

Figure 2.10. OC content in the clay fraction of samples from the inner-shelf off Barcelona (10-40 m depth) (this study), from the inner (50 m depth), mid (60-70 m) and outer-shelf (100 m) off Blanes, and from the Blanes submarine canyon axis (300, 900, 1200 and 1500 m) and its adjacent open slope (900, 1200 and 1500 m depth) (data from Pedrosa-Pàmies et al., 2013) (symbols in the upper-right box). Data fits to a potential function (OC= -0.79 ln(depth)+6.66, r=0.79, dashed blue line).

2.1.6. Conclusions

The grain size distribution and OC content of surface sediments across a nearshore environment off Barcelona city is mainly influenced by the terrestrial input of sediments (through the Besòs River and the urban outfalls) and the sediment redistribution by wave activity, that sorts and transports fine and light sediments offshore. Therefore, in spite of a clear predominance of coarse grain size across the whole transect, sediment grain-size distribution shows the typical seaward decrease of sand content and increase of the clay fraction with water depth.

In terms of the total OM budget, the OC turns out to be mainly accumulated at the shallowest (10 m) and deepest (40 m) stations, with sandy fraction as the most relevant OC contributor across this nearshore region. However, the study of OC concentration in four distinctive grain-size fractions led us deepen in the fate of the OC arriving to our study zone. Each of the different grain-size fractions is loaded with different amounts of OC, thus hydrodynamic perturbations have an influence on the redistribution of OM in surface sediments. The highest OC loadings are recorded in the clay and sand fractions in the form of organic matter adsorbed to clay minerals and terrestrial plant debris, respectively. In the clay fraction, OC concentration decreases seawards, probably due to successive remobilization and transport events which increase oxygen exposure times and oxidize OM. In contrast, the seaward increase in the OC loading in the

coarsest fraction is mainly caused by the offshore transport and deposition of floods-sourced woody debris, suggesting that the Besòs River and the urban outfalls are a significant continental source of OC in the study area.

Our results have significant implications for the understanding of the role of OC in shelf sediments and its transfer and ultimately burial in the deep environment. Adding our results to those obtained in deeper areas by Pedrosa-Pàmies et al. (2013) suggests that, despite a significant amount of OC is degraded before reaching the continental slope, the shelf acts as a source of fine particles carrying OC for deeper regions.

2.1.7. Acknowledgments

This research has been supported by PERSEUS (FP7-OCEAN-2011-3-287600) and Coastal Ocean Observatory (ICM-CSIC) projects, and the Generalitat de Catalunya (Consolidated Research Groups grants 2014 SGR 1068). We are grateful to A. Calafat for fruitful discussions and M. Guart, N. Maestro, and O. Mulet who assisted with the field and laboratory work. AS is supported by a “Ramon y Cajal” contract from MICINN and RD is supported by the JAE Programme from the CSIC.

2.1.8. References

Accornero, A., Picon, P., Bovée, de F., Charrière, B., Buscail, R., 2003. Organic carbon budget at the sediment-water interface on the Gulf of Lions continental margin. Continental Shelf Research 23, 79-92. DOI: 10.1016/S0278-4343(02)00168-1.

Antonijuan, J., Guillén, J., López, L., Simarro, G. 2012. Near-bottom sediment dynamics on highly-protected beaches: The Coastal Ocean Observatory of Barcelona. A: IEEE Instrumentation and Measurement Technology Conference. "IEEE Instrumentation and Measurement Technology Conference", 403-406.

Arnarson, T.S. and Keil, R.G., 2001. Organic-mineral interactions in marine sediments studied using density fractionation and X-ray photoelectron spectroscopy. Organic Geochemistry 32, 1401-1415. DOI: 10.1016/S0146-6380(01)00114-0.

Arnarson, T.S. and Keil, R.G., 2007. Changes in organic matter-mineral interactions for marine sediments with varying oxygen exposure times. Geochimica et Cosmochimica Acta 71, 3545-3556. DOI: 10.1016/j.gca.2007.04.027.

Arnosti, C., 2011. Microbial Extracellular Enzymes and the Marine Carbon Cycle. Annual Review of Marine Science 3, 401-425. DOI: 10.1146/annurev-marine-120709-142731.

Bauer, J.E., Druffel, E.R.M., Wolgast, D.M., Griffin, S., Masiello, C.A., 1998. Distributions of dissolved organic and inorganic carbon and radiocarbon in the eastern North Pacific continental margin. Deep Sea Research Part II: Topical Studies in Oceanography 45, 689-713. DOI: 10.1016/S0967-0645(97)00098-2.

Bianchi, T.S. and Allison, M.A., 2009. Large-river delta-front estuaries as natural ''recorders'' of global environmental change. Proceedings of the National Academy of Sciences of the United States of America 106, 8085-8092. DOI: 10.1073/pnas.0812878106.

Bock, M.J., Mayer, L.M., 2000. Mesodensity organo-clay associations in a near-shore sediment. Marine Geology 163, 65-75. DOI: 10.1016/S0025-3227(99)00105-X.

Bourgoin, L. and Tremblay, L., 2010. Bacterial reworking of terrigenous and marine organic matter in estuarine water columns and sediments. Geochimica et Cosmochimica Acta 74, 5593-5609. DOI: 10.1016/j.gca.2010.06.037.

Burban, P., Wilbert, L., Lick, J., 1989. The flocculation of fine-grained sediments in estuarine waters. Journal of Geophysical Research 94, 8323-8330. DOI: 10.1029/JC094iC06p08323

Canals, M., Company, J.B., Martín, D., Sànchez-Vidal, A., Ramírez-Llodrà, E., 2013. Integrated study of Mediterranean deep canyons: Novel results and future challenges. Progress in Oceanography 118, 1-27. DOI: 10.1016/j.pocean.2013.09.004.

Copeiro, E., 1982. Playas y obras costeras en España. Rev. Obras Públicas, 531-547.

Cowie, G.L. and Hedges, J.I., 1994. Biochemical indicators of diagenetic alteration in natural organic matter mixtures. Nature 369, 304-307. DOI:10.1038/369304a0.

Dagg, M., Benner, R., Lohrenz, S., Lawrence, D., 2004. Transformation of dissolved and particulate materials on continental shelves influenced by large rivers: plume processes. Continental Shelf Research 24, 833-858. DOI: 10.1016/j.csr.2004.02.003.

Dalyander, P.S., Butman, B., Sherwood, C.R., Signell, R.P., Wilkin, J.L., 2013. Characterizing wave- and current- induced bottom shear stress: U.S. middle Atlantic continental shelf. Continental Shelf Research 52, 73-86. DOI: 10.1016/j.csr.2012.10.012.

DGPC (Direcció General de Protecció Civil), 1986. Investigación tecnológica de las acciones a tomar para la estabilidad de las playas del Maresme. Generalitat de Catalunya, Barcelona, Spain.

Dufois, F., Garreau, P., Hir, P. Forget, P., 2008. Wave- and current-induced bottom shear stress distribution in the Gulf of Lions. Continental Shelf Research 28, 1920-1934. DOI: 10.1016/j.csr.2008.03.028

Durán, R., Nuez, M., Alonso, B., Ercilla, G., Estrada, F., Casas, D., Farrán, M., 2009. Assessment of sand trapped by coastal structures towards better management. El Masnou (Maresme, Catalunya). Geotemas 10, 511–514.

Durán, R., Canals, M., Sanz, J.L., Lastras, G., Amblas, D., Micallef, A., 2012. Morphology and sediment dynamics of the northern Catalan continental shelf, northwestern Mediterranean Sea. Geomorphology 204, 1-20. DOI: 10.1016/j.geomorph.2012.10.004.

Dyer, K.R. and Manning, A.J., 1999. Observation of the size, settling velocity and effective density of flocs, and their fractal dimensions. Journal of Sea Research 41, 87-95. DOI: 10.1016/S1385-1101(98)00036-7.

Eisma, D., 1986. Flocculation and de-flocculation of suspended matter in estuaries. Netherlands Journal of Sea Research 20, 183-199. DOI: 10.1016/0077-7579(86)90041-4.

Ercilla, G., Estrada, F., Casas, D., Durán, R., Nuez, M., Alonso, B., Farràn, M., 2010. The El Masnou infralittoral sedimentary environment (Barcelona province, NW Mediterranean Sea): morphology and Holocene seismic stratigraphy. ScientiaMarina 74, 179-196. DOI: 10.3989/scimar.2010.74n1179.

Fernandes, L., Garg, A., Borole, D.V., 2014. Amino acid biogeochemistry and bacterial contribution to sediment organic matter along the western margin of the Bay of Bengal. Deep Sea Research Part I: Oceanographic Research Papers 83, 81-92. DOI: 10.1016/j.dsr.2013.09.006.

Ferré, B., Guizien, K., Durrieu de Madron, X., Palanques, A., Guillén, J., Grémare, A., 2005. Fine-grained sediment dynamics during a strong storm event in the inner-shelf of the Gulf of Lion (NW Mediterranean). Continental Shelf Research 25, 2410-2427. DOI: 10.1016/j.csr.2005.08.017.

Font, R., 1988. Compression zone effect in batch sedimentation. American Institute of Chemical Engineers Journal 34, 229-238. DOI: 10.1002/aic.690340207.

Fry, B. and Sherr, E.B., 1984. $\delta^{13}C$ measurements as indicators of carbon flow in marine and freshwater ecosystems. Contributions to Marine Science 27, 13-47.

Geyer, W.R., Hill, P.S., Kineke, G.C., 2004. The transport, transformation and dispersal of sediment by buoyant coastal flows. Continental Shelf Research 24, 927-949. DOI:10.1016/j.csr.2004.02.006.

Goñi, M.A. and Hedges, J.I., 1995. Sources and reactivities of marine-derived organic matter in coastal sediments as determined by alkaline CuO oxidation. Geochimica et Cosmochimica Acta 59, 2965-2981. DOI: 10.1016/0016-7037(95)00188-3.

Goñi, M.A., Monacci, N., Gisewhite, R., Ogston, A., Crockett, J., Nittrouer, C., 2006. Distribution and sources of particulate organic matter in the water column and sediments of the Fly River Delta, Gulf of Papua (Papua New Guinea). Estuarine, Coastal and Shelf Science 69, 225-245. DOI: 10.1016/j.ecss.2006.04.012.

Gordon, E.S. and Goñi, M.A., 2004. Controls on the distribution and accumulation of terrigenous organic matter in sediments from the Mississippi and Atchafalaya river margin. Marine Chemistry 92, 331-352. DOI: 10.1016/j.marchem.2004.06.035.

Grant, J., Cranford, P., Emerson, C., 1997. Sediment resuspension rates, organic matter quality and food utilization by sea scallops (Placopecten magellanicus) on Georges Bank. Journal of Marine Research 55, 965-994. DOI: 10.1357/0022240973224193.

Grifoll, M., Aretxabaleta, A.L., Espino, M., Warner, J.C., 2012. Along-shelf current variability on the Catalan inner-shelf (NW Mediterranean). Journal of Geophysical Research 117, C09027. DOI: 10.1029/2012JC008182.

Grifoll, M.; Aretxabaleta, A.L.; Pelegri, J.L.; Espino, M.; Warner, J.C.; Sanchez-Arcilla, A., 2013. Seasonal circulation over the Catalan inner-shelf (northwest Mediterranean Sea). Journal of Geophysical Research-Oceans 118, 5844-5857. DOI: 10.1002/jgrc.20403.

Guillén, J., Bourrin, F., Palanques, A., Durrieu de Madron, X., Puig, P., Buscail, R., 2006. Sediment dynamics during wet and dry storm events on the Têt inner shelf (SW Gulf of Lions). Marine Geology 234, 129-142. DOI: 10.1016/j.margeo.2006.09.018.

Hedges, J.I. and Keil, R.G., 1995. Sedimentary organic matter preservation: an assessment and speculative synthesis. Marine Chemistry 49, 81-115. DOI: 10.1016/0304-4203(95)00008-F.

Hedges, J.I., Keil, R.G., Benner, R., 1997. What happens to terrestrial organic matter in the ocean? Organic Geochemistry 27, 195-212. DOI: 10.1016/S0146-6380(97)00066-1.

Hernes, P.J. and Banner, R., 2003. Photochemical and microbial degradation of dissolved lignin phenols: Implications for the fate of terrigenous dissolved organic matter in marine environments. Journal of Geophysical Research 108, 3291. DOI: 10.1029/2002JC001421.

Huettel, M., Berg, P., Kostka, J.E., 2014. Benthic exchange and biogeochemical cycling in permeable sediments. Annual Review of Marine Science 6, 23-51. DOI: 10.1146/annurev-marine-051413-012706.

Hunter, K.A. and Liss, P.S., 1982. Organic matter and the surface charge of suspended particles in estuarine waters. Limnology and Oceanography 27, 322-335.

Iriarte, J.L., Vargas, C.A., Tapia, F.J., Bermúdez, R., Urrutia, R.E., 2012. Primary production and plankton carbon biomass in a river-influenced upwelling area off Concepción, Chile. Progress in Oceanography 92-95, 97-109. DOI: 10.1016/j.pocean.2011.07.009.

Keil, R.G., Mayer, L.M., Quay, P.D., Richey, J.E., Hedges, J.I., 1997. Loss of organic matter from riverine particles in deltas. Geochimica et Cosmochimica Acta 61, 1507-1511. DOI: 10.1016/S0016-7037(97)00044-6.

Keil, R.G., Tsamakis, E., Giddings, J.C., Hedges, J.I., 1998. Biochemical distributions (amino acids, neutral sugars, and lignin phenols) among size-classes of modern marine sediments from the Washington coast. Geochimica et Cosmochimica Acta 62, 1347-1364. DOI: 10.1016/S0016-7037(98)00080-5.

Keil, R.G. and Cowie, G.L., 1999. Organic matter preservation through the oxygen-deficient zone of the NE Arabian Sea as discerned by organic carbon: mineral surface area ratios. Marine Geology 161, 13-22. DOI: 10.1016/S0025-3227(99)00052-3.

Kennedy, M.J., Löhr, S.C., Fraser, S.A., Baruch, E.T., 2014. Direct evidence for organic carbon preservation as clay-organic nanocomposites in a Devonian black shale; from deposition to diagenesis. Earth and Planetary Science Letters 388, 59-70. DOI: 10.1016/j.epsl.2013.11.044.

Kujawinski, E.B., 2011. The impact of microbial metabolism on marine dissolved organic matter. Annual Review of Marine Science 3, 567-599. DOI: 10.1146/annurev-marine-120308-081003Li, M.Z. and Amos, C.L., 2001. SEDTRANS96: the upgraded and better calibrated sediment-transport model for continental shelves. Computers & Geosciences 27, 619-645. DOI: 10.1016/S0098-3004(00)00120-5.

Kuzyk, Z.Z.A., Goñi, M.A., Stern, G.A., Macdonald, R.W., 2008. Sources, pathways and sinks of particulate organic matter in Hudson Bay: Evidence from lignin distributions. Marine Chemistry 112, 215-229. DOI: 10.1016/j.marchem.2008.08.001.

Leithold, E.L. and Hope, R.S., 1999. Deposition and modification of a flood layer on the northern California shelf: lessons from and about the fate of terrestrial particulate organic carbon. Marine Geology 154, 183-195. DOI: 10.1016/S0025-3227(98)00112-1.

Li, M.Z. and Amos, C.L., 2001. SEDTRANS96: the upgraded and better calibrated sediment-transport model for continental shelves. Computers & Geosciences 27, 619-645. DOI: 10.1016/S0098-3004(00)00120-5.

Lick, W., Huang, H.N., Jepsen, R., 1993. Flocculation of fine-grained sediments due to differential settling. Journal of Geophysical Research-Oceans 98, 10279-10288. DOI: 10.1029/93JC00519.

Liquete, C., Canals, M., Lastras, G., Amblas, D., Urgeles, R., De Mol, B., De Batist, M., Hughes-Clarke, J.E., 2007. Long-term development and current status of the Barcelona continental shelf: A source-to-sink approach. Continental Shelf Research 27, 1779-1800. DOI: 10.1016/j.csr.2007.02.007.

Liquete, C., Canals, M., De Mol, B., De Batist, M., Trincardi, F., 2008. Quaternary stratal architecture of the Barcelona prodeltaic continental shelf (NW Mediterranean). Marine Geology 250, 234-250. DOI: 10.1016/j.margeo.2008.01.014.

Lohrenz, S.E., Fahnenstiel, G.L., Redalje, D.G., Lang, G.A., Chen, X., Dagg, M.J., 1997. Variations in primary production of northern Gulf of Mexico continental shelf waters linked to nutrient inputs from the Mississippi River. Marine Ecology Progress Series 155, 45-54. DOI: 10.3354/meps155045.

Lopez-Fernandez, P., Bianchelli, S., Pusceddu, A., Calafat, A.M., Sànchez-Vidal, A., Danovaro, R., 2013. Bioavailability of sinking organic matter in the Blanes canyon and the adjacent open slope (NW Mediterranean Sea). Biogeosciences 10, 3405-3420. DOI: 10.5194/bg-10-3405-2013.Macdonald, R.W., Solomon, S.M., Cranston, R.E., Welch, H.E., Yunker, M.B., Gobeil, C., 1998. A sediment and organic carbon budget for the Canadian Beaufort Shelf. Marine Geology 144, 255-273. DOI: 10.1016/S0025-3227(97)00106-0.

Malej, A., Mozetič, P., Malačič, V., Terzić, S., Ahel, M., 1995. Phytoplankton responses to freshwater inputs in a small semi-enclosed gulf (Gulf of Trieste, Adriatic Sea). Marine Ecology Progress Series 120, 111-121. DOI: 10.3354/meps120111.

Martin, J., Palanques, A., Puig, P., 2006. Composition and variability of downward particulate matter fluxes in the Palamós submarine canyon (NW Mediterranean). Journal of Marine Systems 60, 75-97. DOI: 10.1016/j.jmarsys.2005.09.010.

Mayer, L.M., 1994a. Relationships between mineral surfaces and organic carbon concentrations in soils and sediments. Chemical Geology 114, 347–363. DOI: 10.1016/0009-2541(94)90063-9.

Mayer, L.M., 1994b. Surface area control of organic carbon accumulation in continental shelf sediments. Geochimica et Cosmochimica Acta 58, 1271-1284. DOI: 10.1016/0016-7037(94)90381-6.

Mead, R.N. and Goñi, M.A., 2008. Matrix protected organic matter in a river dominated margin: A possible mechanism to sequester terrestrial organic matter? Geochimica et Cosmochimica Acta 72, 2673-2686. DOI: 10.1016/j.gca.2008.03.007.

Mendoza, E.T. and Jiménez, J., 2009. Regional vulnerability analysis of Catalan beaches to storms. Proceedings of the Institution of Civil engineers-Maritime Engineering 162, 127-135. DOI: 10.1680/maen.2009.162.3.127.

Mestres, M., Grifoll, M., Sánchez-Arcilla, A., 2016. Analysis of current intensification in the Northwest Mediterranean shelf. Continental Shelf Research 114, 29-40. DOI: 10.1016/j.csr.2015.12.011.

Miller, W.L. and Mora, M.A.,1997. Interaction of photochemical and microbial processes in the degradation of refractory dissolved organic matter from a coastal marine environment. Limnology and Oceanography 42, 1317-1324. DOI: 10.4319/lo.1997.42.6.1317

Millot, C., 1991. Mesoscale and seasonal variabilities of the circulation in the Western Mediterranean. Dynamics of Atmospheres and Oceans 15, 179-214. DOI: 10.1016/0377-0265(91)90020-G.

Millot, C., 1999. Circulation in the western Mediterranean Sea. Journal of Marine Systems 20, 423-442. DOI: 10.1016/S0924-7963(98)00078-5.

Neumeier, U., Ferrarin, C., Amos, C.L., Umgiesser, G., Li, M.Z., 2008. SEDTRANS05: An improved sediment-transport model for continental shelves and coastal waters with a new algorithm for cohesive sediments. Computers & Geosciences 34, 1223-1242. DOI: 10.1016/j.cageo.2008.02.007.

Nuwer, J.M. and Keil, R.G., 2005. Sedimentary organic matter geochemistry of Clayoquot Sound, Vancouver Island, British Columbia. Limnology and Oceanography 50, 1119-1128.

Ogston, A.S., Cacchione, D.A., Sternberg, R.W., Kineke, G.C., 2000. Observations of storm and river flood-driven sediment transport on the northern California continental shelf. Continental Shelf Research 20, 2141–2162.

Ojeda, E., Guillén, J., Ribas, F., 2011. Dynamics of single-barred embayed beaches. Marine Geology 280, 76-90. DOI: 10.1016/j.margeo.2010.12.002.

Pedrosa-Pàmies, R., Sanchez-Vidal, A., Calafat, A., Canals, M., Durán, R., 2013. Impact of storm-induced remobilization on grain size distribution and organic carbon content in sediments from the Blanes Canyon area, NW Mediterranean Sea. Progress in Oceanography 118, 122-136. DOI: 10.1016/j.pocean.2013.07.023.

Puertos del Estado - Ministerio de Fomento, 2004-2011. Clima medio de oleaje: boya de Barcelona (conjunto de datos REDCOS). Banco de datos oceanográficos de Puertos del Estado. Área de Medio Físico.

Puig, P. and Palanques, A., 1998. Temporal variability and composition of settling particle fluxes on the Barcelona continental margin (Northwestern Mediterranean). Journal of Marine Research 56, 639-654. DOI: 10.1357/002224098765213612

Puig, P., Company, J.B., Sarda, F., Palanques, A., 2001. Responses of deep-water shrimp populations to intermediate nepheloid layer detachments on the Northwestern Mediterranen continental margin. Deep Sea Research Part I: Oceanographic Research Papers 48, 2195-2207. DOI: 10.1016/s0967-0637(01)00016-4.

Puig P., de Madron X. D., Salat J., Schroeder K., Martin, J., Karageorgis A. P., Palanques A., Roullier, F., Lopez-Jurado, J.L., Emilianov, M., Moutin, T., Houpert, L., 2013. Thick bottom nepheloid layers in the western mediterranean generated by deep dense shelf water cascading. Progress in Oceanography 111, 1-23. DOI: doi:10.1016/j.pocean.2012.10.003.

Ransom B., Kim D., Kastner M. and Wainwright S., 1998. Organic matter preservation on continental slopes: Importance of mineralogy and surface area. Geochimica et Cosmochimica Acta 62, 1329-1345. DOI: 10.1016/S0016-7037(98)00050-7.

Roussiez, V., Aloisi, J.C., Monaco, A., Ludwig, W., 2005. Early muddy deposits along the Gulf of Lions shoreline: A key for a better understanding of land-to-sea transfer of sediments and associated pollutant fluxes. Marine Geology 222-223, 345-358. DOI: 10.1016/j.margeo.2005.06.023.

Rumolo, P., Cartes, J.E., Fanelli, E., Papiol, V., Sprovieri, M., Mirto, S., Gherardi, S., Bonanno, A., 2015. Seasonal variations in the source of sea bottom organic matter off Catalonia coasts (western Mediterranean): links with hydrography and biological response. Journal of Oceanography 71, 325-343. DOI: 10.1007/s10872-015-0291-7.

Salat, J., Tintore, J., Font, J., Wang, D.P., Vieira, M., 1992. Near-inertial motion on the shelf-slope front off notheast Spain. Journal of Geophysical Research-Oceans 97, 7277-7281. DOI: 10.1029/92JC00588.

Sanchez-Vidal, A., Canals, M., Calafat, A.M., Lastras, G., Pedrosa-Pàmies, R., Menéndez, M., Medina, R., Company, J.B., Hereu, B., Romero, J., Alcoverro, T., 2012. Impacts on the deep-sea ecosystem by a severe coastal storm. Plos One 7, e30395. DOI: 10.1371/journal.pone.0030395.

Sanchez-Vidal, A., Higueras, M., Martí, E., Liquete, C., Calafat, A., Kerhervé, P., Canals, M., 2013. Riverine transport of terrestrial organic matter to the North Catalan margin, NW Mediterranean Sea. Progress in Oceanography 118, 71-80. DOI: 10.1016/j.pocean.2013.07.020.

Sancho-García, A., Guillén, J., Ojeda, E., 2013. Storm-induced readjustment of an embayed beach after modification by protection Works. Geo-Marine Letters 33, 159-172. DOI: 10.1007/s00367-012-0319-6.

Secrieru, D. and Oaie, G., 2009. The relation between the grain size composition of the sediments from the NW Black Sea and their total organic carbon (TOC) content. Geo-eco-marina 15/2009, 5-11.

Sholkovitz, E.R., 1976. Flocculation of dissolved organic and inorganic matter during the mixing of river water and seawater. Geochimica et Cosmochimica Acta 40, 831-845. DOI: 10.1016/0016-7037(76)90035-1.

Tesi, T., Miserocchi, S., Goñi, M.A., Langone, L., 2007. Source, transport and fate of terrestrial organic carbon on the western Mediterranean Sea, Gulf of Lions, France. Marine Chemistry 105, 101-117. DOI: 10.1016/j.marchem.2007.01.005.

Tesi, T., Semiletov, I., Dudarev, O., Andersson, A., Gustafsson, Ö., 2016. Matrix association effects on hydrodynamic sorting and degradation of terrestrial organic matter during cross-shelf transport in the Laptev and East Siberian shelf seas. Journal of Geophysical Research: Biogeosciences 121. DOI: 10.1002/2015JG003067

Vincent, L. and Demirbilek, Z., 2002. Water Wave Mechanics. Coastal Engineering Manual, Part II, Hydrodynamics, Chapter II-2, Engineer Manual 1110, 2-1100. U.S. Army Corps of Engineers, Washington, DC.

Wollast, R., 1991. The coastal organic carbon cycle: fluxes, sources and sinks. Ocean Margin Processes in Global Change. John Wiley, New York, 365-381.Zimmerman, A.R., Goyne, K.W., Chorover, J., Komarneni, S., Brantley, S.L., 2004. Mineral mesopore effects on nitrogenous organic matter adsorption. Organic Geochemistry 35, 355-375. DOI: 10.1016/j.orggeochem.2003.10.009.

Zúñiga, D., Flexas, M.M., Sànchez-Vidal, A., Coenjaerts, J., Calafat, A.M., Jordà, G., García-Orellana, J., Puigdefàbregas, J., Canals, M., Espino, M., Sardà, F., Company, J.B., 2009. Particle fluxes dynamics in Blanes submarine canyon (Northwestern Mediterranean). Progress in Oceanography 82, 239-251. DOI: 10.1016/j.pocean.2009.07.002.

2.2. Impact of storm-induced remobilization on grain size distribution and organic carbon content in sediments from the Blanes Canyon area, NW Mediterranean Sea

Pedrosa-Pàmies, R., Sanchez-Vidal, A., Calafat, A., Canals, M., Durán., R.

GRC Geociències Marines, Dept. d'Estratigrafia, Paleontologia i Geociències Marines, Universitat de Barcelona, E-08028 Barcelona, Spain

2013 Progress Oceanography 118, 122-136. doi:10.1016/j.pocean.2013.07.023.
Copyright © 2013 Elsevier Ltd. All rights reserved

Abstract

Interactions between organic carbon and mineral particles are known to play a key role for the preservation of organic carbon in marine sediments. In this study we combine meteorological, hydrological and oceanographic information with grain size and geochemical analyses (organic carbon, OC, its stable isotope $\delta^{13}C$, and the nitrogen to OC ratio) in different grain size fractions of surface sediments to determine the impact of a major storm on organic matter redistribution in a deep continental margin of the NW Mediterranean Sea. Sediment cores were obtained from the continental shelf, along the axis of the Blanes submarine canyon (BC), and in the adjacent southern open slope before (November 2008) and after (February and May 2009) the occurrence of one of the most severe coastal storms recorded in the last century in the study area.

The storm occurred the 26 of December 2008 and dramatically impacted the North Catalan coast and its offshore area. The high shear stress produced by this event on the shelf floor led to sediment erosion and, subsequently, to its transport and deposition into BC. While sand and gravel-sized particles up to 2500 μm in diameter were deposited at 300 m of water depth in the canyon head, the finer particles (<4 μm) were transported farther offshore towards the deep margin reaching at least 1500 m depth.

The results obtained show that the hydrodynamic processes that controlled the sorting and differential deposition of particles according to their grain size also controlled the redistribution of particles with different loads of OC. Thus, whereas coarse particles transported to the canyon head were poorly loaded with OC, fine particles reaching greater depths were relatively rich in OC, a significant proportion of which was of marine origin (i.e. derived from marine primary production). This adds to evidence that the physical action of waves and currents during storms plays a key role in determining the amount of OC stored in surface sediments not only in the shelf but also in the deep margin and possibly deeper.

2.2.1. Introduction

Continental margins receive large amounts of organic carbon (OC) and minerals from terrestrial sources and are sites of high OC primary production by marine algae. Although continental margins account for only 10% of the total ocean area, most of the OC burial occurs in sediments depositing on deltas, continental shelves, and upper continental slopes (Berner, 1989; Hedges and Keil, 1995, 1997). Burial of OC is the ultimate long-term sink in the global carbon cycle, as it isolates this material from the quickly cycling carbon pools (Berner, 1989). The mechanisms that regulate OC burial in continental margins are heterogeneous, and areas with high sediment accumulation and OC preservation (due to high riverine discharge and/or high primary production) can be found next to areas with intense physical mixing that remobilizes and/or effectively degrades OC (Goñi et al., 2005; Blair et al., 2012). Interactions between OC and the mineral fraction appear also to be highly relevant for OC preservation in sediments as they can make it more or less susceptible to degradation (Hedges and Keil, 1995). Direct correlations between OC and mineral surface area have been commonly observed and attributed to aggregation processes and/or adsorption of OC within small pores on mineral surfaces (Keil et al., 1994; Mayer, 1994a, b; Ransom et al., 1998; Arnarson and Kiel, 2007; Goñi et al., 2008). Clay-sized particles with high surface area are, for instance, proposed as one of the key controls on OC burial efficiency in deltaic and continental shelf and slope sediments (Mayer, 1994a, b; Hedges and Keil, 1995; Keil et al., 1997). Therefore, physical processes that sort particles on the basis of their size (such as hydrodynamic sorting) may thus remobilize sediments with different loadings of OC. Thus, to understand environmental conditions that control OC burial on a global basis it is necessary to gain in depth knowledge of OC load, sediment transport and deposition processes in continental margins.

Meteorology and climate, regional circulation, local hydrodynamics, bottom topography and sediment sources and types control sediment transport and deposition over the continental margin (Ross et al., 2009). Intense hydrodynamic processes, such as storms with associated waves and wind driven currents, are the primary drivers of shelf bed erosion, remobilization and off-shelf export and winnowing of sediment and OC (Hedges and Keil, 1995; Blair et al., 2004; Goñi et al., 2006; Dail, 2007). Storms are especially relevant for the cycles of resuspension, transport and deposition of sediment, thereby increasing the concentration of particulate material in the water column and facilitating its downslope transport (Ross et al., 2009). Under these circumstances, hydrodynamic sorting of particles by size and/or density may play a major role in OC transport and determine whether OC is going to be eventually (and ultimately) deposited and buried (Prahl, 1985; Keil et al., 1994, 1998; Goñi et al., 1998; Leithold and Hope, 1999; Bianchi et al., 2002, 2007; Wakeham et al., 2009).

The aim of this work is to improve our knowledge of sediment and OC dynamics in the Blanes Canyon (BC) area, located in the North Catalan margin, NW Mediterranean Sea, and to analyze the sequence of forcing processes and resulting near-bottom shelf-to-canyon sediment and OC transport during a major storm. Several studies carried out in and nearby the study area, such as in the Gulf of Lion, have described the main mechanisms that control cross-slope exchanges of OC (Canals et al. 2006; Heussner et al. 2006, among others), and the biogeochemical characteristics of the organic material transferred (Fabres et al., 2008; Sanchez-Vidal et al., 2008, 2009). These studies have shown that extreme events such as coastal storms and also dense shelf water

cascading (a type of marine current driven exclusively by seawater density contrast) resuspend and transport large quantities of sediments and OC to the deep margin and basin. However, the loading and provenance of OC among grain size fractions has not been examined in detail so far. In this study we combine meteorological, hydrological and oceanographic datasets to determine how one of the most extreme storms in the NW Mediterranean Sea in the last 100 years redistributed sediments and OC over a continental margin incised by a large submarine canyon. The analysis of OC content, its stable isotope $\delta^{13}C$ and TN/OC ratios in sediments from the BC and adjacent open slope allowed us to assess the influence of transport and deposition processes on the hydrodynamic sorting and the OC loading of different grain size fractions.

2.2.2. Study area

2.2.2.1. Geographical and geological settings

The ~110 km long North Catalan margin displays a complex geomorphology, with three large submarine canyon systems deeply incised in the continental shelf and slope. These are, from north to south, Cap de Creus (CCC), La Fonera (LFC, also known as Palamós) and Blanes (BC) canyons (Canals et al., 2004b; Lastras et al., 2007, 2011) (Fig. 2.11). The continental shelf width varies from 0.8 km shoreward of LFC head to 30 km off Roses bay in between CCC and LFC heads; the shelf break is located at 110-140 m depth and the continental rise reaches up to 2600 m in depth.

BC, the largest of the three , is 184 km long and displays a nearly N-S trending upper course that it is incised up to 1500 m into the continental shelf (Amblas et al., 2006). The canyon axis shows a concave long-profile, starting with a slope gradient of 20º that rapidly decreases to 10º after a few tens of meters in distance. It then gradually decreases to 3º approximately 3.5 km away from the tip of the canyon head. The canyon walls show contrasting morphologies. While the eastern wall is relatively smooth, the western one is heavily gullied (Canals et al., 2004a; Lastras et al., 2011) (Fig. 2.11).

The shelf-incised reach of BC has an average width of 8 km and is 21.7 km long from the head, at 70 m water depth (Lastras et al., 2011). The tip of the canyon head is parallel to the nearby coastline, which is located at less than 4 km (Díaz and Maldonado, 1990). Tordera River and Lloret and Tossa torrents open to the sea at the coastline close to BC head (Fig. 2.11). Tordera River is the largest river in terms of both drainage area and fluvial discharge with its mouth only 5 km west of BC tip. Its sediment input has led to the development of a ~30 m thick delta and prodelta (Serra et al., 2007). The Tordera prodelta extends mainly southwestwards of the river mouth. Seawards, BC intersects several large relict sediment bodies formed on the mid and outer Maresme shelf (Lastras et al., 2011; Durán et al., 2013).

2.2.2.2. Oceanographic setting

Regional currents and their interaction with the topography mainly govern hydrodynamics along the North Catalan margin. The area is tideless and there is no persistent wind field that could

eventually lead to coastal upwelling (Alvarez et al., 1996; Masó and Tintoré, 1991). Mesoscale circulation is characterized by the cyclonic Northern Current (NC), which forms a 30 km wide meandering stream that flows S and SW over the continental slope (Millot, 1999). The NC extends from the sea surface down to at least 400 m depth (Millot, 1999) and its motion is forced by the surface entrance of Atlantic Water through Gibraltar Strait and its cyclonic circulation around the Western Mediterranean Sea. The NC is associated to a permanent shelf-slope density front that separates less saline and continent-influenced shelf waters from saltier and denser open sea saline waters (Font et al., 1988). Such density front constrains the circulation over the continental shelf, influences shelf-slope exchanges and mediates the advection of suspended matter (Font et al., 1995; Lapouyade and Durrieu de Madron, 2001; Ulses et al., 2008).

Atmospheric forcing in the NW Mediterranean region can lead to two types of high-energy, short-lived events: Eastern wet storms and Northern dry storms with episodic dense shelf water cascading (DSWC). Eastern storms develop when humid winds blowing from the east generate swell and high waves over the continental shelf favored by a long fetch (Ferré et al., 2005; Guillén et al., 2006; Bourrin et al., 2008). These storms cause wave-induced resuspension of sediment in the inner shelf and, in association with the littoral drift and the NC effects, result in a dominant southwards along-shelf sediment transport (Puig et al., 2001; Guillén et al., 2002, 2006; Palanques et al., 2002). Northern storms and DSWC develop under the influence of cold and dry winds from the continent that cool and evaporate shelf superficial waters causing an increase in their density and subsequent sinking. This dense shelf water overflows the shelf edge and cascades downslope, mainly along submarine canyons, thus enhancing intermediate and deep-water ventilation and the transport of sediments, OC and pollutants to the deep (Canals et al., 2006; Heussner et al., 2006; Palanques et al., 2006; Sanchez-Vidal et al., 2009, Salvadó et al., 2012). Eastern storms are able to erode the coastline and inner shelf (Sanchez-Vidal et al., 2012), while DSWC events can lead to extensive sediment erosion and remobilization down to the outer shelf and upper continental shelf, the later mainly inside submarine canyons (Canals et al., 2006; Lastras et al., 2007, 2011; Puig et al., 2008).

2.2.3. Material and methods

2.2.3.1 Sediment sample collection

Sediment cores were obtained with a multicorer sampler during three cruises onboard R/V Garcia del Cid in November 2008 (cruise PROMETEO I), February 2009 (PROMETEO II) and May 2009 (PROMETEO III). Sediment samples were recovered from the axis of BC at 300 m (BC300), 900 m (BC900), 1200 m (BC1200) and 1500 m (BC1500) of water depth, in the adjacent outer shelf at 100 m (P6), in the open slope at 900 m (OS900), 1200 m (OS1200) and 1500 m (OS1500) of water depth, and in the mid continental shelf from 50 to 70 m of water depth (P1-P5) (Fig. 2.11). Sediments from the outer shelf were only sampled in November 2008 while those from the mid shelf were sampled just in May 2009. Sediment samples from BC300 and BC900 were recovered only in November 2008 and May 2009. Once onboard, multicorer tubes were visually described and sliced at 0.5 cm intervals. Samples were stored in sealed plastic bags at 4 ºC until they were processed in the laboratory. Only the upper 0-0.05 cm of sediment samples was used in this study.

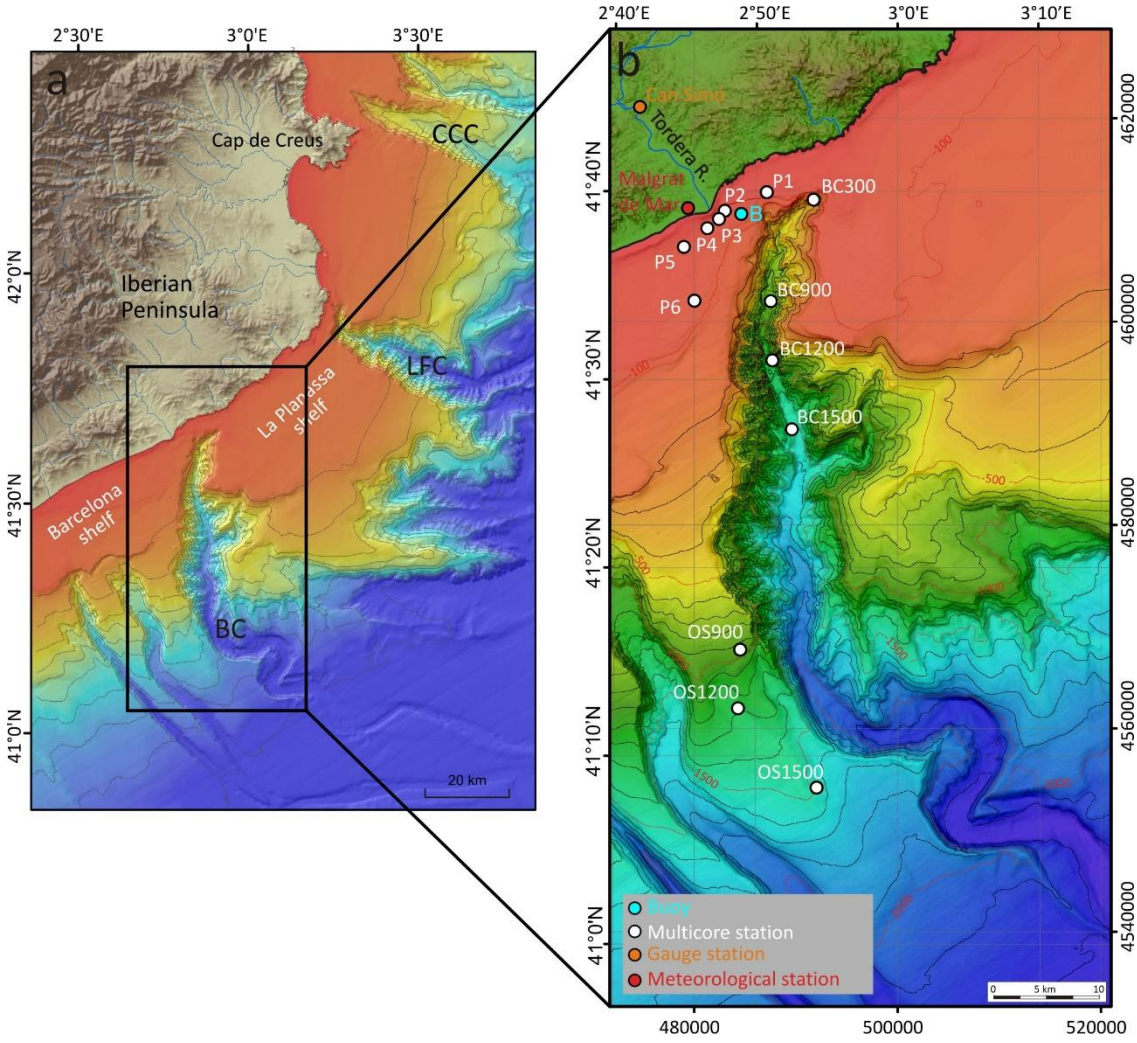

Figure 2.11. (a) General bathymetric map of the study area with black contours every 200 m. It shows from north to south, Cap de Creus (CCC), La Fonera (LFC) and Blanes (BC) canyons. (b) Location of sampling stations on the shelf (P1-P6, 50 to 100 of water depth), along the axis of Blanes Canyon (BC) at 300, 1000 and 1500 m depth, and on the adjacent southern outer shelf and open slope (OS) at 900 and 1500 m depth. Sampling stations at 900, 1200 and 1500 m depth in the axis and the adjacent open slope correspond also to the position of mooring stations equipped with near-bottom current meters (white dots). Contours are every 100 m (black lines) and 500 m (red lines) except for the 100 m contour that is also red colored. Blue, red and orange dots show the position of the Blanes wave buoy, the meteorological station and the gauge station in the Tordera River. Bathymetric data from Canals et al. (2004b).

2.2.3.2. Analytical methods

Particle size spectra were determined with a Coulter Counter LS230 laser analyzer. Between 0.3 and 5 g of freeze-dried sediment was used, depending on the amount needed to obtain the optimal obscuration of the laser beam. Organic matter in the samples was first oxidized with 10% H_2O_2. Each sample was then split in two parts, of which one was treated with 1M HCl to remove carbonates. Subsequently, both samples were dispersed in approximately 20 cm^3 of water and sodium polyphosphate (a chemical dispersant) and mechanically shaken for 4 hours. Each sample was then introduced into the particle size analyzer after using a 2000 µm

sieve to retain rare coarser particles that might obstruct the flow circuit of the instrument. The measured particle size spectrum is presented as volume percentage in a logarithmic scale, where volume is calculated from particle diameter, assuming spherical shapes. D50 has been calculated as the average equivalent diameter, which is the diameter where 50% of the sediment sample has a larger equivalent diameter, while the other 50% has a smaller equivalent diameter.

Another portion of the sediment sample was divided into four size fractions: sand (2 mm-63 µm), coarse silt (63-40 µm), medium-fine silt (40-4 µm) and clay (<4 µm). Each sediment sample was suspended and disaggregated with sodium polyphosphate for 2 h and then the >63 µm and the 40-63 µm fractions were separated using stainless-steel sieves. Centrifugation techniques were utilized to extract the fraction smaller than 40 µm. The 4-40 µm fraction was concentrated by centrifuging seven minutes at 1000 rpm, and the supernatant containing the <4 µm fraction was then recovered. This step was repeated twice. The supernatant was concentrated by centrifuging 15 minutes at 5000 rpm. To adjust and validate the method, we verified with the particle size analyzer that the supernatant included only the <4 µm fraction. Each fraction was then freeze-dried and grounded to fine powder.

Total carbon (TC), total nitrogen (TN), OC contents and the stable isotopic composition of OC ($\delta^{13}C$) were measured on the bulk sediment sample and on each of the size fractions with an elemental analyzer Flash 1112 EA interfaced to a Delta C Finnigan MAT isotope ratio mass spectrometer at "Centres Científics i Tecnològics de la Universitat de Barcelona". Samples for OC and $\delta^{13}C$ were first de-carbonated using repeated additions of 25% HCl with 60 ºC drying steps in between until no effervescence was observed (Nieuwenhuize et al., 1994). From the values thus obtained, $CaCO_3$ was calculated as (TC-OC) x100/12 assuming all inorganic carbon is in the form of $CaCO_3$.

The OC loading of each of the size fractions vs. the total OC of the bulk sample were calculated and used to determine where OC concentrated in the sediment. TN/OC atomic ratios were also calculated. We plot TN/OC ratios rather than OC/TN ratios in order to constrain the elemental ratios of N-depleted samples (e.g. TN/OC ~0 rather than OC/TN ~∞) following Goñi et al. (2006).

2.2.3.3. Meteorological, hydrological and oceanographic data

Local weather data, including precipitation (mm), pressure (hPa), wind speed (m s^{-1}) and direction (º), were obtained from the Malgrat de Mar station from "Servei Meteorològic de Catalunya" (Fig. 2.11, blue dot). In addition, European weather data used to interpret atmospheric situations have been obtained from the European Centre for Medium-Range Weather Forecasts (ECMWF).

Daily water discharge (m^3 s^{-1}) of the Tordera River was obtained from the gauging station of Can Simó (Fogars de la Selva) from "Agència Catalana de l'Aigua" (Fig. 2.11, orange dot).

Time-series of chlorophyll-a (Chl-a) concentration (mg m^{-3}) were obtained from the Goddard Earth Sciences (GES) Data and Information Services Center (DISC), using as a source the Moderate Resolution Imaging Spectoradiometer (MODIS) onboard the Aqua satellite. For our study, Chl-a concentration has been gridded including the BC area from 41.00 to 41.36º N; and from 2.40 to 3.10º E.

Wave height data were obtained from two different buoys, a scalar DATAWELL Waverider Buoy located near the mouth of Tordera River (Blanes buoy, Fig. 2.11, blue dot) and a Triaxys directional Wave Buoy located 6 km SE of Palamós, (41.83º N, 3.19º E, Palamós buoy, not shown). The first buoy is part of the unfortunately recently disappeared oceanographic monitoring network "Xarxa d'Instrumentació Oceanogràfica i Meteorològica" (XIOM) of the Catalan government, while the second belongs to "Puertos del Estado" of the Spanish government. The parameters utilized in this study are significant wave height (H_s, m), which is the average of the highest one-third of waves that occur in a given period, and zero crossing period (T_z, s), defined as the mean time interval between upward or downward zero crossings on a wave record.

Near-bottom current speed (m s^{-1}) and direction (º) were obtained from Aanderaa RCM7/9 current meters moored at 23 m above the bottom and recording at a sampling interval of 30 min at the same stations where sediment samples were obtained.

In order to investigate sediment transport we have used the Sedtrans05 program (Li and Amos, 2001; Neumeier et al., 2008) that predicts sediment mobilization at a point depending on water depth, sediment type and the system of currents and waves including current speed, H_s and T_z. Bottom shear stress (τ, Pa) was estimated using H_s and T_z measurements, current speed at 23 m above bottom and wave–current angle, with the values of the slope angle and the bottom roughness resulting from the sediment grain-size d50 and the maximum grain size of each sample.

2.2.4. Results

2.2.4.1. Forcing conditions

The November 2008 to May 2009 study period was characterized by a meteorologically unstable, cold, windy and wet autumn and winter. According to Mendoza and Jimenez (2009), a storm is defined as an event in which H_s exceeds a threshold value of 2 m during a minimum period of 6 h. The application of the selected H_s threshold criteria allowed to identify a total number of 4 storms during the study period, classified as significant, severe-extreme, moderate-significant and weak (Mendoza and Jimenez 2009) in November 2008, December 2008, January 2009 and April 2009, respectively.

The first storm occurred on 27-30 November 2008 and was driven by north and northwesterly winds. During this dry storm winds were strong reaching maximum velocities of 6.1 m s^{-1}, wind gusts of 14.3 m s^{-1}, H_s up to 4.1 m and wave peak periods of 8.7 s (Fig. 2.12a-b). The current meters located at the head of BC (Fig. 2.12d) and in the open slope (data not shown) didn't record increased down-canyon current speeds, but a slight increase was recorded along the canyon axis at 900 m,1200 m (both up to 0.3 m s^{-1}) and 1500 m (up to 0.2 m s^{-1}) (Fig. 2.12e-g). All these increased current speeds lie above the 99th percentile of total data recorded at each location.

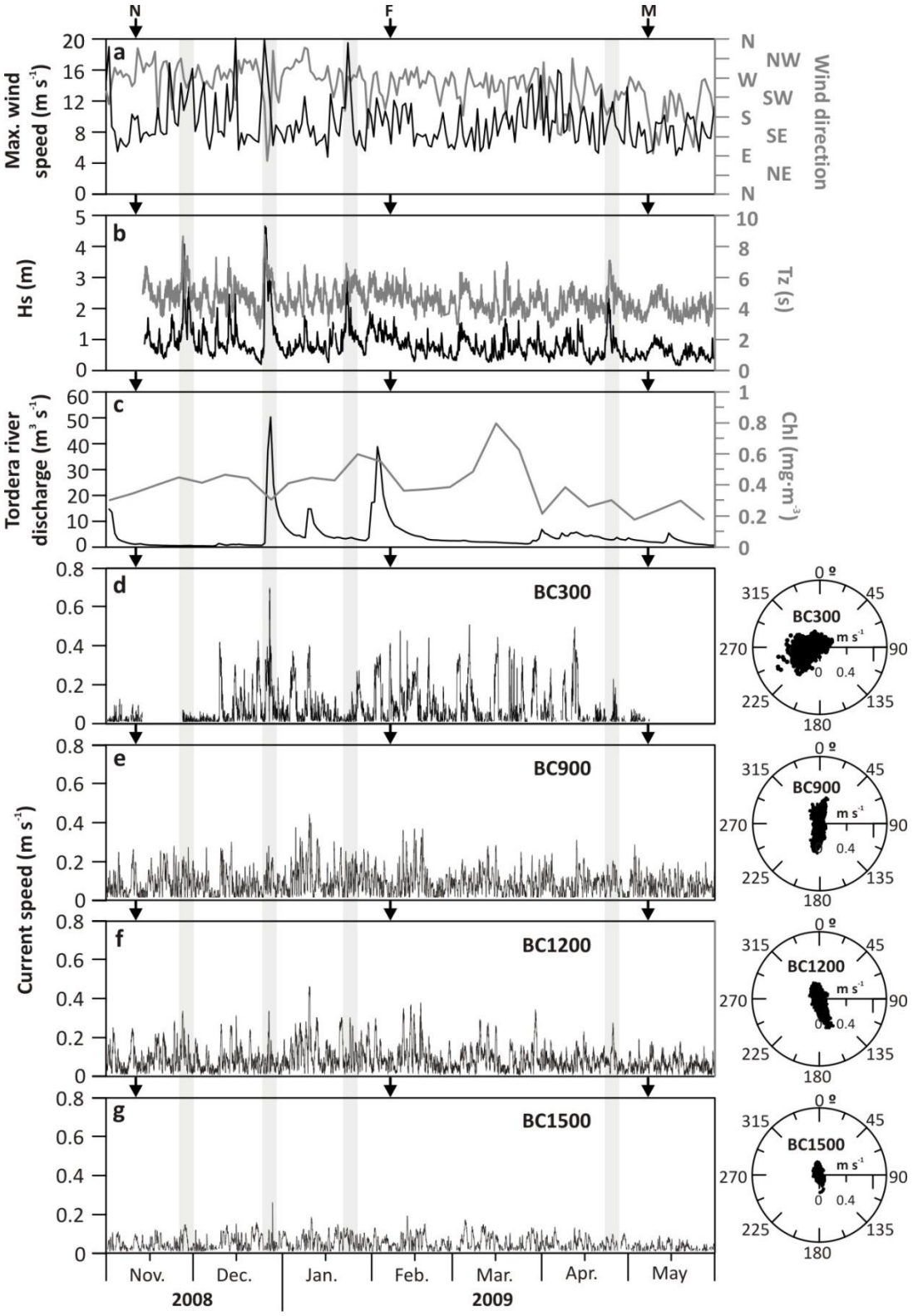

Figure 2.12. Time series of meteorological, fluvial and oceanographic variables from November 2008 to May 2009. (a) Maximum wind speed (m s^{-1}) (black line) and wind direction (^{o}) (grey line). (b) Significant wave height (Hs) (black line) and period (Tz) (grey line). (c) Tordera River discharge (m^3 s^{-1}) (black line) and chlorophyll a concentration (mg m^{-3}) (grey line). (d-g) Near-bottom currents (m s^{-1}) along the axis of Blanes Canyon (BC) at 300, 900, 1200 and 1500 m depth. Polar graphs next to current plots show current direction (^{o}) at 300, 900, 1200 and 1500 m. depth. Arrows show sediment sampling dates, and the shaded area shows the storms of the study period.

The second storm was the most severe and occurred at the end of December 2008. An intense high-pressure system with up to 1044 hPa moving to the NE of Europe led to E-NE cold air fluxes flowing over the Western Mediterranean region. As a result, a northerly flow through the Rhône Valley forced cold, dry continental air over a warmer Western Mediterranean Sea, generating a strong cyclogenesis over the Gulf of Genoa. The storm moved then west towards the Catalan coast where it made landfall on 26 December 2008. During a period of 18 hours easterly winds reached 7.4 m s^{-1}, with wind gusts of 19.9 m s^{-1} (Fig. 2.12a), leading to H_s of 4.7 m and wave peak periods of 8.8 s (Fig. 2.12b), maximum wave heights of 8 m offshore Blanes (reaching 14.4 m at the Palamós buoy, further north) and wave peak periods of 14.3 s. Twenty-five years of wave data from the Blanes and Palamós buoys allow to roughly calculating a return period for the storm of 18 years near Blanes, and in excess of 100 years at Palamós. This indicates that the storm impacted more violently the continental shelf north of the BC. Due to increased rainfall during the previous three days, the Tordera River discharged from 27 to 29 December 2008 (only 3 days) an amount of 9635.6 kt of water and 0.6 kt of sediment (Sanchez Vidal et al., 2013) (Fig. 2.12c). At the same time that the storm was causing increased wave height in the shelf, higher current speeds were recorded in deep waters of the BC. The maximum near-bottom current at the head of the BC during this event (measured on 27 December 2008) was of 0.7 m s^{-1}, i.e. the highest value recorded throughout the study period (Fig. 2.12d). After this peak, currents around 0.3 m s^{-1} were also recorded at 900 m, 1200 m and 1500 m depth (Fig. 2.12e-g). In the open slope, increased near-bottom current speeds were recorded at 900 m and 1500 m depth (both up to 0.2 m s^{-1}) (Lopez-Fernandez et al., 2013). All these increased current speeds lie above the 99th percentile of total data recorded at each location.

The other two events, driven by westerly winds, were of lower intensity. They occurred on 24 January 2009 and 25-26 April 2009 (Fig. 2.12), when low-pressure systems formed over the Cantabrian Sea moved over the NW Mediterranean Sea. These instabilities did not lead to high rainfall along the North Catalan coast and thus river discharge did not increase (Fig. 2.12c). During the January event westerly winds were particularly strong reaching maximum velocities of 5.3 m s^{-1}, wind gusts of 19.5 m s^{-1}, H_s up to 3.3 m and wave peak periods of 6.6 s (Fig. 2.12a-b). During April 2009 storm, southwesterly winds reached 4.6 m s^{-1}, with wind gusts of 10.1 m s^{-1} (Fig. 2.12a), leading to H_s of 2.37 m and wave peak periods of 4.8 s (Fig. 2.12a-b). In both events increased near-bottom current speed were recorded along the canyon axis (up to 0.3 m s^{-1}).

2.2.4.2. Grain-size and calcium carbonate distribution

Surface sediments in the study area show a significant decrease in grain size from the shelf to the deepest locations, as illustrated by the exponential decrease of d50 with increased water depth (Pearson correlation coefficient r=0.93)(Fig. 2.13).

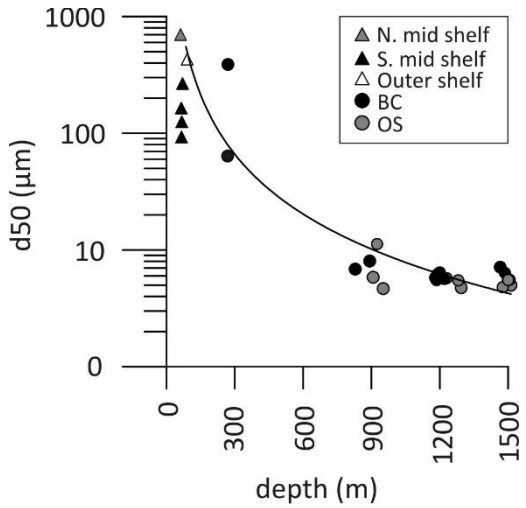

Figure 2.13. d50 (µm) versus depth in seafloor sediment samples. N. mid shelf: Northernmost mid shelf. S. mid shelf: Southernmost mid shelf. BC: Blanes Canyon axis. OS: Southern open slope.

In P1, the northernmost mid shelf station at 50 m water depth, in May 2009 the sediment was predominantly composed of well-sorted coarse sand and gravel-sized biogenic particles, with the main mode at 623 µm and a maximum grain size ($Ø_{max}$) of 3000 µm (Fig. 2.14a and Table 2.3). Samples from southernmost mid shelf stations P2, P3, P4 and P5 also collected in May 2009 at 60 to 70 m of water depth were composed of medium and fine bimodal sorted sands with biogenic particles, with the main modes at 97-140 µm (P2, P4 and P5) and 400 µm (P3) and $Ø_{max}$ of 2000 µm (Fig. 2.14a and Table 2.3). Sediment from the outer shelf station P6 sampled in November 2008 showed well sorted biogenic particles with a main mode at 517 µm and $Ø_{max}$ of size >2000 µm, though the de-carbonated fraction was poorly sorted (Fig. 2.14b and Table 2.3). The biogenic character of P6 was further evidenced by the difference in grain size distribution amongst samples treated and non-treated with HCl (Fig. 2.14b).

Sediment grain size in BC and the adjacent open slope underwent significant changes in some stations before and after the occurrence of the storms in late November 2008, late December 2008 and January 2009 (hereafter stormy period). In November 2008 sediments at station BC300 were poorly sorted, with a unimodal size peak at 250 µm and $Ø_{max}$ of 410 µm. After the stormy period, in May 2009, sediments were predominantly composed of sorted medium and coarse sand, with a bimodal distribution with the main mode size at 300 µm and a second mode at 1500 µm and $Ø_{max}$ >2000 µm. These two lognormal populations in sediments collected after the stormy period were not observed in sediments from water depths in excess of 300 m. Therefore, there was a significant change (p-value <0.0001, α=0.05) in the grain size distribution of canyon head surface sediments from November 2008 to May 2009, with a decrease of silt and clay content and a relative increase of sand sized grains (Fig. 2.14c and Table 2.3). In addition, after this stormy period there was an increase in the $CaCO_3$ content in the BC300 station (Fig. 2.14c and Table 2.3).

Surface sediments along the axis of the BC (BC900, BC1200 and BC1500) in November 2008 were predominantly composed of well-sorted medium-fine silt and clay. Medium-fine silts accounted for 55-64% of the sediment, whilst clays accounted for most of the remaining sediment, with typical abundances of 32-40%. The sand-sized fraction was the least abundant, representing less than 4% of the total volume. The fine-grained dominating fraction showed main modes at 9-14 µm and small secondary modes at 20-30 µm with $Ø_{max}$ equal to 111 µm. After the stormy period

no significant variations in grain size distributions were observed, excepting an 11% increase of the clay fraction in station BC1500 in February 2009 (Fig. 2.14d-f and Table 2.3). Stations BC900 and BC1500 showed also a peak of carbonates at 50-100 µm in May 2009, in accordance with the increase of 5% in $CaCO_3$ content at BC1500 (Fig. 2.14d-f and Table 2.3).

Station	Sand (%)	Coarse silt (%)	Medium fine silt (%)	Clay (%)	d50 (µm)	OC (%)	$CaCO_3$ (%)	TN/OC	$\delta^{13}C$ (‰)
Shelf									
N. Mid Shelf									
P1-May	98.54	0.25	0.71	0.50	728.9	0.47	38.7	0.04	-22.4
S. Mid Shelf									
P2- May	89.96	2.90	4.94	2.20	157.7	0.60	21.5	0.06	-24.2
P3- May	86.30	3.38	7.70	2.61	256.5	0.69	12.8	0.15	-24.0
P4- May	74.36	6.23	14.29	5.12	121.7	0.62	15.8	0.10	-24.8
P5- May	64.38	10.09	19.02	6.51	90.2	0.89	14.3	0.07	-24.4
Outer Shelf									
P6- Nov.	85.74	2.07	8.04	4.15	435.5	0.42	63.6	0.25	-26.4
Blanes canyon									
BC300- Nov.	50.05	4.08	27.56	18.31	64	0.77	31.2	0.08	-23.1
BC900- Nov.	3.14	3.99	55.64	37.23	6.9	1.32	21.1	0.08	-24.0
BC1200- Nov.	1.78	3.59	54.80	39.82	5.8	0.86	25.3	0.12	-23.3
BC1500- Nov.	1.59	2.82	64.01	31.58	7.1	1.20	21.5	0.08	-23.1
BC1200-Feb.	1.00	2.80	54.65	41.55	5.7	0.90	24.8	0.11	-23.2
BC1500- Feb.	1.42	3.30	52.95	42.33	5.6	1.02	22.1	0.09	-22.6
BC300- May	93.42	0.51	3.26	2.81	388.6	0.96	34.6	0.03	-23.7
BC900- May	7.16	3.38	56.23	33.24	8.1	1.24	20.4	0.08	-24.9
BC1200- May	1.44	3.78	56.40	38.38	6.3	0.91	23.7	0.11	-23.2
BC1500- May	6.42	3.65	52.76	37.17	6.4	0.54	26.0	0.18	-22.3
Open slope									
OS900-Nov.	0.02	1.63	51.57	46.77	4.7	1.23	20.9	0.09	-22.2
OS1200- Nov.	0.45	2.20	51.49	45.86	4.8	0.67	25.4	0.13	-22.6
OS1500-Nov.	1.20	2.46	52.28	44.06	5.0	0.70	27.1	0.12	-23.2
OS900- Feb.	10.80	4.98	60.99	23.23	11.2	1.14	22.4	0.10	-22.7
OS1200- Feb.	2.00	3.97	53.24	40.79	5.5	0.66	33.4	0.20	-23.1
OS1500-Feb.	0.30	0.76	59.14	39.80	5.5	0.97	24.5	0.10	-22.5
OS900- May	1.30	2.24	58.61	37.85	5.8	0.68	25.4	0.11	-23.7
OS1200- May	3.38	2.23	54.70	39.68	5.5	0.92	25.2	0.12	-22.4
OS1500- May	0.15	2.66	51.89	45.30	4.8	0.54	29.6	0.22	-22.9

Table 2.3. Grain size and geochemical data for sediment samples collected in the shelf, along the Blanes Canyon axis and in the adjacent open slope, before (November 2008) and after (February and May 2009) the stormy period. N. mid shelf: Northernmost mid shelf. S. mid shelf: Southernmost mid shelf.

In the adjacent open slope at stations OS900, OS1200 and OS1500 m, the seafloor in November 2008 was predominantly composed of well-sorted medium-fine silts and clays with a main mode at 4-10 µm, a secondary mode at 20-30 µm and $Ø_{max}$ equal to 70 µm (Fig. 2.14g-i). Medium-fine silt and clay fractions accounted for 52% and 44-47%, respectively, and the sand fraction accounted for less than 2% of the volume (Table 2.3). After the stormy period no significant variations in grain size distributions were observed excepting at OS900 in February 2009, where an increase in the coarse fraction was recorded ($Ø_{max}$ equal to 194 µm) (Fig. 2.14G, Table 2.3). At the other open slope stations the sediments were still predominantly composed of sorted fine silt and clay, with main modes at 5-10 µm and $Ø_{max}$ equal to 147 µm. Stations OS900 and OS1200 showed a peak of carbonates at 50-100 µm in May 2009, in accordance with the increase of 2-8% in $CaCO_3$ content (Fig. 2.14g-h and Table 2.3).

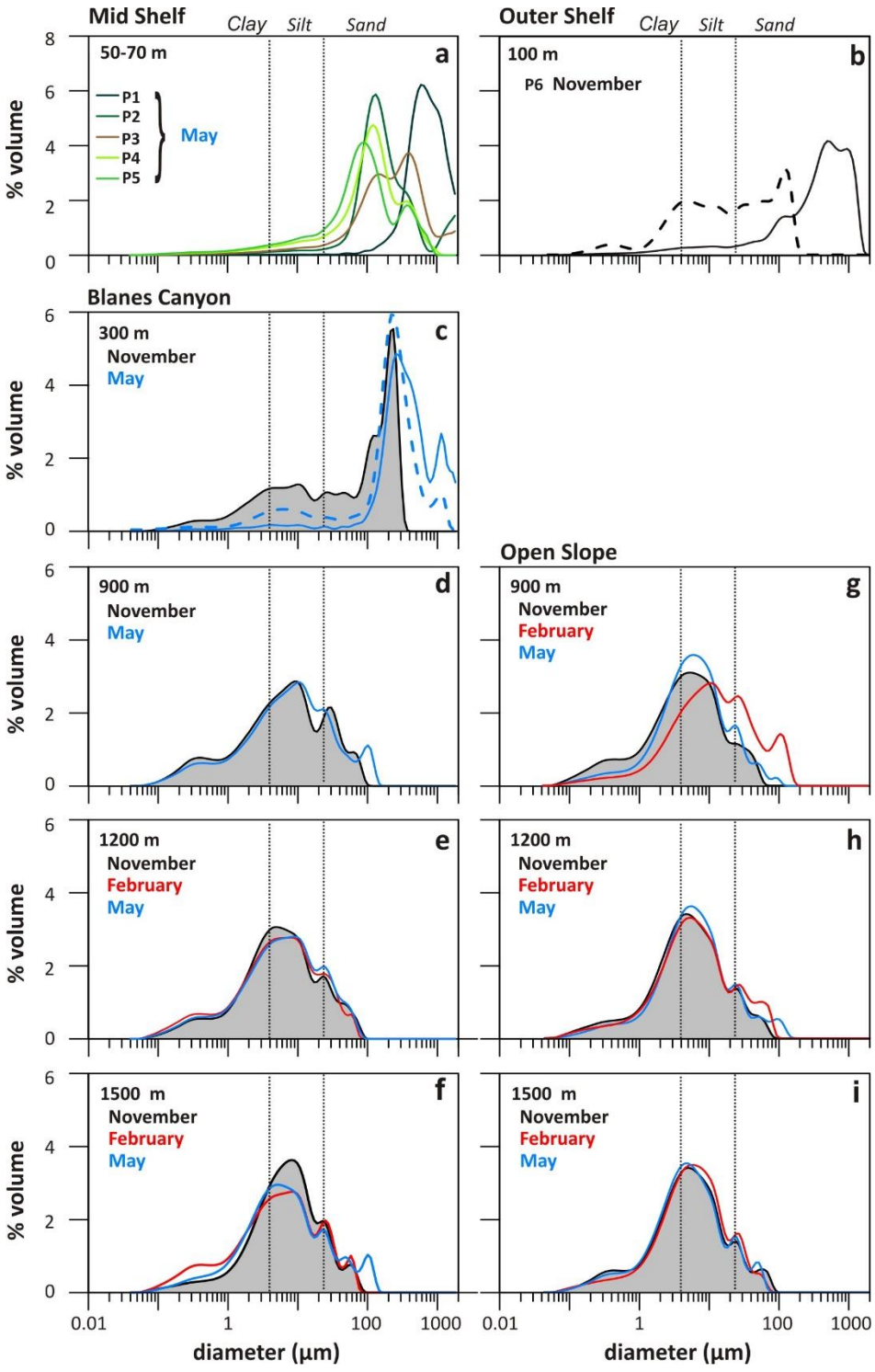

Figure 2.14. Sediment grain size in (a) the mid shelf stations P1 to P5, (b) the outer shelf, (c to f) along the axis of Blanes Canyon, and (g to i) across the southern open slope, before (N, November 2008, black line) and after (F and M, February and May 2009, red and blue lines, respectively) the stormy period. Dashed lines correspond to de-carbonated samples (dashed lines were not plotted when no significant changes amongst the bulk and de-carbonated samples were observed). Fine dotted vertical lines separate clay (<4 µm), silt (4-63 µm) and sand (>63 µm) sizes. Note the different Y-axis for shelf sample plots. Location of sampling stations shown in Figure 2.11.

2.2.4.3. OC, TN/OC and $\delta^{13}C$

The OC content in all bulk samples from the study area ranged from 0.42 to 1.24% (Table 1), while the OC content in the different size fractions ranged from 0.03 to 6.21% (Fig. 2.15a-c and Table 2.4). The TN/OC ratio ranged from 0.03 to 0.25 in the bulk sample (Table 2.3) and from 0.03 to 0.29 in the various size fractions (Fig. 2.16a-b and Table 2.4). Finally $\delta^{13}C$ varied from -26.4 to -22.5‰ in the bulk sample (Table 2.3), and from -27.6 to -21.9‰ in the various size fractions (Figs. 2.15a-c and 2.16a-b and Table 2.4). Therefore, while geochemical parameters measured in the bulk sediment sample were tightly clustered (Table 2.3), a much wider range appeared in the different grain size fractions (Fig. 2.15 and Table 2.4).

In the continental shelf, OC contents in bulk samples were relatively low (0.4-0.9% OC), the TN/OC ratio ranged from 0.07 to 0.25, and $\delta^{13}C$ oscillated from -26.4 to -22.4‰ (Table 2.3). The lowest OC values were recorded in the northernmost mid (P1) and outer (P6) shelf, while the highest values were found in the southernmost mid shelf (P2-P5) (Table 2.3). The highest OC contents were always recorded in the clay fraction (Fig. 2.15a), reaching maximum values in the southernmost mid shelf (Table 2.4). In the mid shelf $\delta^{13}C$ values were high in both clay and sand sized fractions (-24.8 to -22.2‰) and low mainly in the coarse silt fractions (-27.2 to -24.3‰) (Table 2.4). In contrast, in the outer shelf the sand sized fractions showed a very low value (-27.6‰) while high values were recorded in the fine size fractions of medium-fine silt and clay (-22.5 and -22.4‰, Table 2.4). The highest TN/OC ratios were recorded in the mid shelf in the fine size fractions (0.15 to 0.21, Table 2.4).

Bulk sediments from the BC300 canyon head station before the stormy period, in November 2008, showed a %OC of 0.8%, a TN/OC ratio of 0.08 and a $\delta^{13}C$ of -23.12‰ (Table 2.3). The same parameters measured in May 2009 after the occurrence of the storms in late November 2008, late December 2008 and January 2009 yielded values of 1.0%, 0.03 and -23.7‰, respectively, thus indicating the lack of major changes (Table 2.3). While analyzing the different fractions in November 2008, it became evident that all the three parameters, %OC, TN/OC and $\delta^{13}C$, were higher in the clay fraction and relatively lower in the coarser (sand and coarse silt) grain sizes (Table 2.4). Furthermore, after the stormy period there was a decrease in $\delta^{13}C$ values and an increase in the %OC contents in the fine sediment fraction (Figs. 2.15b, 2.15e and 2.16a), even though the relative contribution of this fraction to the total OC content (OC clay vs. OC bulk in Table 2.4) was lower because of the smaller proportion of fine sediments after the stormy period (Table 2.3).

Bulk samples from BC900, BC1200 and BC1500 into the canyon in November 2008 showed OC contents of 1.3%, 0.9% and 1.2% respectively, while TN/OC ranged from 0.08 to 0.12 and $\delta^{13}C$ from -27.7 to -22.1‰ (Table 2.3). After the stormy period bulk samples showed OC contents from 0.5 to 1.2 % (Table 2.3). In November 2008, the higher values of all three parameters always corresponded to the clay fraction and the lowest to the coarser silt fraction (Figs. 2.15b, 2.15e and 2.16a and Table 2.4). In February and May 2009 the same pattern was observed, but high $\delta^{13}C$ values were also found in the coarser fractions (Figs. 2.15b, 2.15e and 2.16a and Table 2.4). It should be noted that along the BC canyon transect TN/OC ratios and $\delta^{13}C$ values correlated significantly (Pearson's r=0.60).

Station	Fraction	OC (%)	$\%OC_{size}/\%OC_{bulk}$	TN/OC	$\delta^{13}C$
Shelf					
N. Mid Shelf					
P1- May	2 mm - 63 µm	0.11	0.09	0.15	-22.3
	63-40 µm	0.53	0.26	n.d	-26.0
	40-4 µm	0.10	0.05	0.16	-22.2
	<4 µm	2.04	0.60	n.d	-22.2
S. Mid Shelf					
P2- May	2 mm - 63 µm	0.22	0.16	0.14	-23.2
	63-40 µm	0.42	0.18	0.09	-27.2
	40-4 µm	0.38	0.17	0.10	-24.1
	<4 µm	6.21	0.49	0.07	-24.4
P3- May	2 mm - 63 µm	0.32	0.20	0.09	-24.1
	63-40 µm	0.55	0.21	0.12	-27.1
	40-4 µm	0.66	0.26	0.21	-23.4
	<4 µm	4.77	0.34	0.14	-24.5
P4- May	2 mm - 63 µm	0.28	0.20	0.14	-24.0
	63-40 µm	0.41	0.17	0.12	-26.1
	40-4 µm	0.59	0.24	0.17	-26.9
	<4 µm	3.93	0.40	0.15	-24.4
P5- May	2 mm - 63 µm	0.40	0.19	0.15	-24.2
	63-40 µm	0.39	0.11	0.13	-24.3
	40-4 µm	1.16	0.33	0.10	-27.0
	<4 µm	3.87	0.37	0.20	-24.8
Outer Shelf					
P6- Nov.	2 mm - 63 µm	0.05	0.03	0.12	-27.6
	63-40 µm	0.03	0.02	0.19	-23.4
	40-4 µm	0.12	0.07	0.10	-22.4
	<4 µm	1.48	0.88	0.17	-22.5
Blanes Canyon					
BC300- Nov.	2 mm - 63 µm	0.26	0.09	0.12	-23.7
	63-40 µm	0.40	0.13	0.11	-24.9
	40-4 µm	0.86	0.27	0.11	-25.4
	<4 µm	1.65	0.51	0.15	-22.6
BC900- Nov.	2 mm - 63 µm	1.50	0.27	0.03	-24.9
	63-40 µm	1.38	0.27	0.03	-26.7
	40-4 µm	1.14	0.22	0.09	-24.8
	<4 µm	1.30	0.24	0.18	-22.6
BC1200- Nov.	2 mm - 63 µm	0.88	0.27	0.03	-26.4
	63-40 µm	0.61	0.17	0.06	-24.9
	40-4 µm	0.75	0.23	0.11	-23.4
	<4 µm	1.20	0.33	0.18	-22.7
BC1500- Nov.	2 mm - 63 µm	1.76	0.34	0.04	-27.4
	63-40 µm	1.00	0.21	0.05	-26.8
	40-4 µm	0.88	0.19	0.12	-22.6
	<4 µm	1.19	0.25	0.16	-23.0
BC1200- Feb.	2 mm - 63 µm	0.61	0.18	0.11	-22.4
	63-40 µm	0.61	0.17	0.09	-23.2
	40-4 µm	0.92	0.25	0.11	-22.8
	<4 µm	1.48	0.40	0.15	-22.8
BC1500- Feb.	2 mm - 63 µm	0.92	0.24	0.10	-23.2
	63-40 µm	0.64	0.15	0.06	-24.2
	40-4 µm	1.21	0.29	0.10	-22.8
	<4 µm	1.31	0.32	0.17	-23.0
BC300- May	2 mm - 63 µm	0.36	0.13	0.07	-23.9
	63-40 µm	1.36	0.47	0.09	-27.6
	40-4 µm	1.06	0.35	0.10	-26.4
	<4 µm	2.47	0.05	0.10	-26.2
BC900- May	2 mm - 63 µm	1.19	0.15	0.10	n.d
	63-40 µm	0.98	0.27	0.12	-24.3
	40-4 µm	1.08	0.25	0.10	-27.1
	<4 µm	1.32	0.33	0.28	n.d
Blanes Canyon					
BC1200- May	2 mm - 63 µm	0.92	0.27	0.08	-25.0
	63-40 µm	0.69	0.19	0.09	-23.2
	40-4 µm	0.84	0.23	0.12	-23.0
	<4 µm	1.23	0.31	0.18	-23.0
BC1500- May	2 mm - 63 µm	0.39	0.28	0.26	-22.5
	63-40 µm	0.52	0.22	0.20	-24.6
	40-4 µm	0.48	0.21	0.21	-23.3
	<4 µm	1.05	0.29	0.21	n.d
Open Slope					
OS900-Nov.	2 mm - 63 µm	1.18	0.29	0.10	-26.4
	63-40 µm	1.14	0.26	0.07	-25.1
	40-4 µm	1.08	0.27	0.10	-22.2
	<4 µm	2.08	0.17	0.14	-23.0
OS1200-Nov.	2 mm - 63 µm	0.64	0.24	0.05	-27.4
	63-40 µm	0.43	0.17	0.08	-26.8
	40-4 µm	0.86	0.32	0.08	-22.6
	<4 µm	0.81	0.27	0.18	-22.9
OS1500-Nov.	2 mm - 63 µm	0.73	0.19	n.d	-25.9
	63-40 µm	0.57	0.19	0.12	-25.0
	40-4 µm	0.58	0.18	0.13	-23.2
	<4 µm	0.96	0.43	0.26	-22.7
OS900- Feb.	2 mm - 63 µm	0.87	0.18	0.13	-22.3
	63-40 µm	1.00	0.23	0.11	-22.2
	40-4 µm	1.17	0.25	0.10	-22.5
	<4 µm	1.55	0.33	n.d	-22.1
OS1200- Feb.	2 mm - 63 µm	0.32	0.12	0.13	-22.9
	63-40 µm	0.60	0.27	0.13	-23.4
	40-4 µm	0.72	0.25	0.13	-23.4
	<4 µm	1.02	0.36	0.18	-22.8
OS1500- Feb.	2 mm - 63 µm	1.12	0.30	0.07	-22.5
	63-40 µm	0.95	0.25	0.09	-21.9
	40-4 µm	0.89	0.24	0.10	-23.1
	<4 µm	0.89	0.21	0.18	-22.8
OS900- May	2 mm - 63 µm	0.47	0.26	0.27	-23.7
	63-40 µm	0.62	0.20	0.18	-24.0
	40-4 µm	0.49	0.16	0.28	-24.1
	<4 µm	1.33	0.39	0.27	-22.0
OS1200- May	2 mm - 63 µm	1.09	0.12	0.12	-23.8
	63-40 µm	1.32	0.20	0.09	-26.1
	40-4 µm	0.93	0.25	0.12	-24.1
	<4 µm	2.11	0.43	0.29	-22.4
OS1500- May	2 mm - 63 µm	0.51	0.24	0.21	-22.6
	63-40 µm	0.54	0.25	0.19	-22.4
	40-4 µm	0.44	0.20	0.23	-23.8
	<4 µm	0.36	0.31	0.27	-22.5

Table 2.4. OC content, OC size/OC bulk, TN/OC ratio and $\delta^{13}C$ isotopic composition of sand (2 mm - 63 µm), coarse silts (63-40 µm), medium-fine silt (40-4 µm) and clay (<4 µm) sediment size fraction before (November 2008) and after (February and May 2009) the stormy period. N. mid shelf: Northernmost mid shelf. S. mid shelf: Southernmost mid shelf.

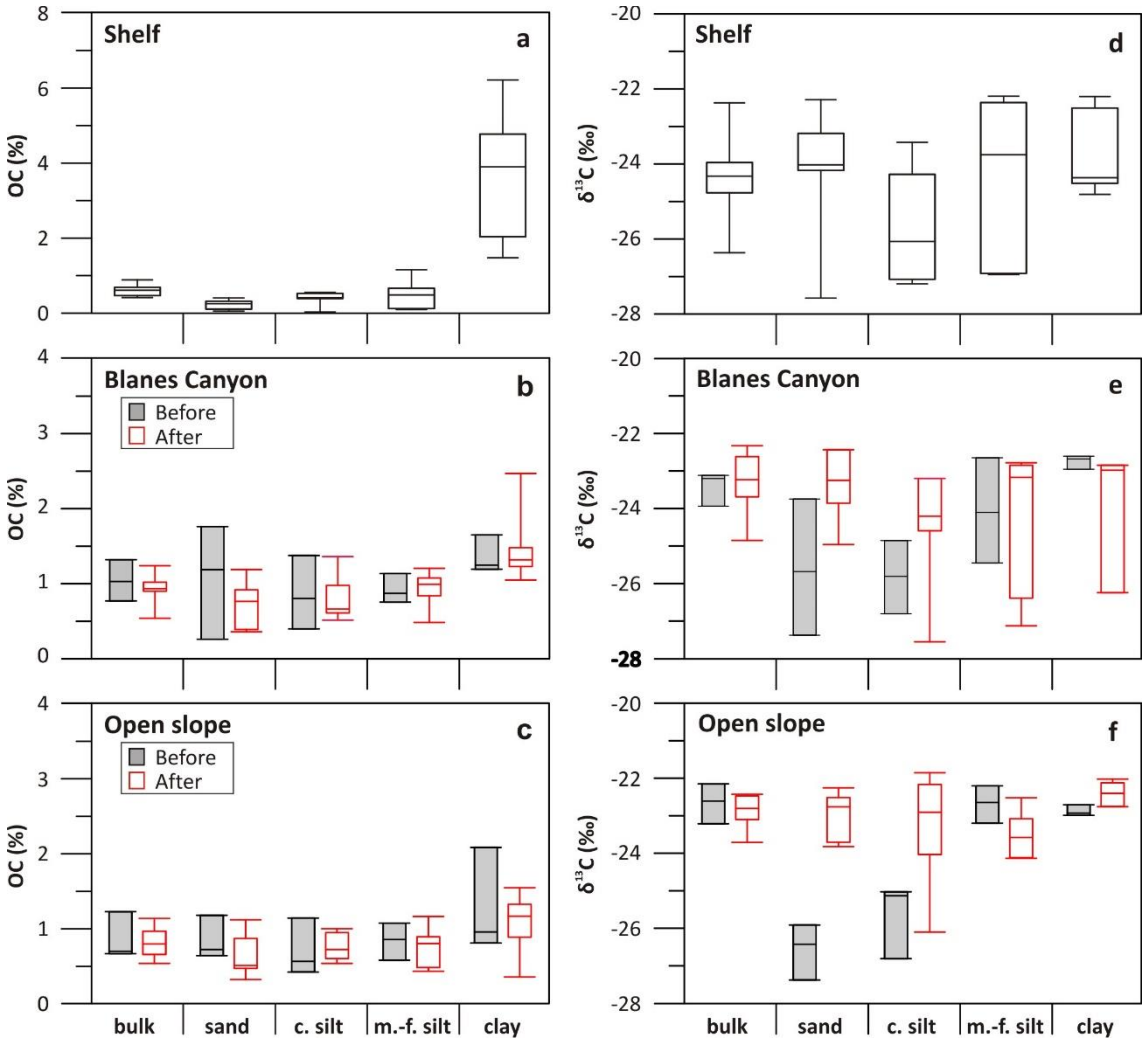

Figure 2.15. % OC (a-c) and $\delta^{13}C$ (d-f) in the bulk and size fractions from sand to clay before (grey) and after (red) the stormy period. The whiskers at the end of each box correspond to extreme values, while the box is defined by the lower and upper quartiles and the horizontal line within each box represents the median.

OC contents in bulk samples from open slope stations OS900, OS1200 and OS1500 in November 2008 were 1.2%, 0.7% and 0.7%, and no significant variations were observed after the stormy period (Table 2.3). TN/OC and $\delta^{13}C$ ranged from 0.09 to 0.13 and from -23.7 to -22.2‰, respectively (Table 2.3). Before the stormy period, in November 2008, the higher OC content and $\delta^{13}C$ were recorded in the clay fraction, with the lowest in the coarse fractions (Figs. 2.15c, 2.15f and 2.16b and Table 2.4). Again, a relative increase of $\delta^{13}C$ was recorded in the coarser fractions after stormy period (Figs. 2.15f and 2.16b and Table 2.4), while no significant changes were observed in the OC content (Fig. 2.15c and Table 2.4).

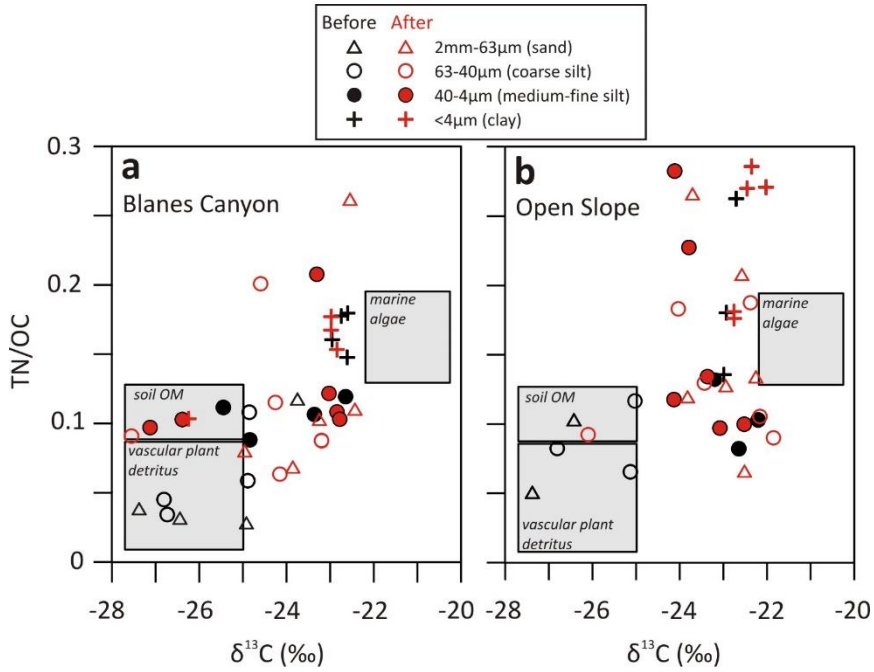

Figure 2.16. $\delta^{13}C$ versus TN/OC in the Blanes Canyon (a) and the adjacent open slope (b). Samples before (black) and after (red) the stormy period, and size fractions (symbols in upper box) are differentiated. The compositional ranges of different end members are included in the plot for ease of reference, based on Meyers (1994), Goñi and Hedges (1995), Hedges et al. (1997) and Sanchez-Vidal et al. (2013).

2.2.5. Discussion

The impact of the storms that hit the Catalan coast in autumn 2008 and winter 2009 on the oceanographic conditions (near-bottom current speeds), the physical properties of surface sediments (grain size) and the sediment geochemistry (OC content and origin) in the Blanes submarine canyon area is discussed in the following sections, where special attention is paid to the major storm of December 2008.

2.2.5.1. *Storm impact on near-bottom currents, sediment transport and grain size distribution*

It is well known that in the NW Mediterranean pressure variations due to the passage of atmospheric fronts and winds coming from the E-SE trigger large swell and high shore breaking waves that can contribute significantly to increase near-bottom currents and bottom shear stress all over the continental shelf (Guillén et al., 2006; Bolaños et al., 2009; Ulses et al., 2008). For surface waves with H_s>5 m and T_s>9 s, the resulting bottom shear stress is able to resuspend sediments, thus increasing the density of shelf waters and inducing them to flow down across the continental slope (Puig et al., 2001; Guillén et al., 2002; Palanques et al., 2002, 2006; Ulses et al., 2008). Eastern storms mostly occur during autumn and winter, though their frequency shows a large interannual variability. Autumn 2008 and winter 2009 was characterized by high storminess with a severe-extreme storm in December 2008. Because of its extreme character, changes in

surface sediments in the study area before and after the stormy period should be mostly attributed to the occurrence of the December 2008 storm. Indeed scuba divers observed the erosion of large volumes of coarse coastal sediments causing serious damage to benthic communities, which highlights the extraordinary magnitude of the December 2008 storm. This includes the abrasion and removal of sea urchins from rocky substrates (Hereu et al., 2012) and the burial and uprooting of *Posidonia oceanica* shoots that up to date have not recovered (Alcoverro et al., 2012). The surface waves developed in December 2008 over the shelf at 50 m water depth near the BC generated a bottom shear stress (τ) in excess of 0.60 Pa as calculated from the SEDTRANS model (Li and Amos, 2001), which is indeed significantly higher than the τ limit to define a storm in the nearby stormy Gulf of Lion (τ >0.12 Pa) (Guillén et al., 2006). Besides increasing bottom shear stress, the strong shoreward eastern winds piled up water against the shore along the Catalan coast. This accumulation of water, together with the permanent southwards flowing littoral drift and NC, and the increased density of the same water due to loading by resuspended sediment, should have further reinforced the alongshore and shelf sediment transport (Sanchez-Vidal et al., 2012). The shelf incising head of BC naturally interrupted this massive flow of remobilized sediment, which was subsequently trapped into the canyon and forced to flow down under the drive of gravity and canyon floor morphology, while reaching velocities of up to 0.7 m s^{-1} in the canyon head at 300 m of water depth. We know that this topographically constrained down canyon flow reached at least 1500 m depth (Fig. 2.12e-g).

The data obtained indicate that waves and near-bottom currents during the December 2008 storm substantially modified the grain size distribution of seafloor sediments over the continental shelf and slope in the study area. The presence of particles larger than 2000 µm in the upper reaches of the BC after the stormy period stormy period suggests that the strong near-bottom current speeds recorded during the storm of December 2008 carried coarse shelf sediments and light shells into the canyon. Indeed, the dominance of coarse sand sizes in the northernmost mid shelf and medium sand sizes in the southernmost mid and outer shelf (Fig. 2.14a-b) are indicative of environments with high average kinetic energy. The associated dynamics leads to the winnowing of the clay and silt fraction, which remains suspended in the water column thus easing its offshore transfer, and the near-bottom transport of the coarse fraction (Wiberg, et al., 1993; Ogston et al., 2004; Guillén et al., 2006). Relict carbonate shells are a major contributor to outer shelf floor sediments (Fig. 2.14b), reflecting the presence of paleoshorelines, a quite common feature at these depths in the NW Mediterranean Sea (Liquete et al., 2007; Durán et al., 2012). Also, on the outer shelf surrounding the BC head there is a prominent relict sand bar that constitutes the northernmost extension of large sand bodies formed during the Last Glacial Maximum and early post-glacial transgression (Díaz and Maldonado, 1990; Lastras et al., 2011; Durán et al., 2013).

According to the SEDTRANS model of Li and Amos (2001), the near-bottom current speed needed to initiate bed load transport by particle rolling, sliding and saltation and suspended load transport of such coarse (>700 µm) shelf sediments is 0.5 m s^{-1} and 0.8 m s^{-1}, respectively. This suggests that the wave generated flow over the shelf during the December 2008 storm was sufficient to remobilize coarse sand and light biogenic carbonate debris from the shelf into the BC. Current speeds recorded within the canyon at BC300 also exceeded the critical threshold for suspended load transport of coarse sediments (i.e. >300 µm). Furthermore, the currents recorded

at BC300 station in the canyon head were strong (up to 0.7 m s^{-1}) and persistent enough (speeds above 0.3 m s^{-1} for 48h) to resuspend and transport finer material farther downcanyon. Indeed, the disappearance of the finer fractions (<100 μm) from canyon head sediments (Fig. 2.14c) is an indication of winnowing, sorting and progressive exhaustion of the most resuspendable sizes due to the storm-induced currents (Ferré et al., 2005). The transport of coarse particles (i.e. >300 μm) to the head of BC by those currents is consistent with the grain size of settling particles caught by a sediment trap deployed 25 m above the bottom at the same location (Sanchez-Vidal et al., 2012). These authors recorded up to 71% of sand sized particles in the canyon head fluxes during the December 2008 storm and also noticed an increase of near-bottom suspended sediment concentrations (up to 28 g m^{-3}) as deep as 1200 m inside the canyon. These observational evidences support both the mobilization of coarse sediments in the canyon head and the down canyon transport of suspended fine particles by storm-generated currents. Furthermore, the sampling of particles of up to 200 μm at OS900 m also points to the shelf edge spillover of coarse material beyond BC head down to the open upper continental slope during the December 2008 storm.

In contrast with the canyon head and the upper slope, only minor grain size variations were observed deeper along the canyon axis and in the lower slope after the stormy period. The high similarity of grain size distributions at 900, 1200 and 1500 m depth along the BC and in the open slope deeper than 900 m suggests that hydrodynamic conditions did not change that much in those locations, and that attenuation of current speeds with increasing depths triggered a similar selective deposition of clay and silt particles along the canyon and the open slope.

The appearance of up to 200 μm sized scattered shells of calcareous organisms such as foraminifera at 900 and 1500 m along the canyon axis and in the open slope in May 2009, which were not noticed in February 2009, points to the arrival of calcareous primary production remains from surface waters, probably associated to the 2009 late winter-spring bloom (Fig. 2.12c). Silty aggregates of about the same size, incorporating terrigenous and biogenic material, were also noticed.

2.2.5.2. Impact of the storm on OC transport and provenance

OC content of surface sediments in the study area are comparable to those earlier reported for other submarine canyons in the Western Mediterranean Sea (Durrieu de Madron et al., 1999; Cartes et al., 2002; Accornero et al., 2003; Martín et al., 2008). In the bulk sediments OC content averaged 0.84%, with a standard deviation of ±0.26%, while the average OC content of the different size fractions was of 1.00%, with a standard deviation of ±0.90%. This wider range of OC contents agrees with the premise that geochemical analyses of size-fractionated sediments provide substantially greater return of information than studies of bulk sediments alone (Wakeham et al., 2009).

Our results reveal significant differences in OC content and $\delta^{13}C$ values in the different size fractions of the sediments, as well as before (November 2008) and after (February and May 2009) the stormy period (Fig. 2.15). To investigate in which size fractions OC preferentially concentrates and which its origin we have plotted $\delta^{13}C$ vs. TN/OC from different size fractions (Fig. 2.16), so

that we could discriminate OC sources (Ember et al., 1987; Fogel et al., 1989; Middelburg et al., 1997). The two main sources of sedimentary organic matter in continental margins are terrestrial, usually imported from river watersheds, and marine, resulting from primary production of marine algae. While marine OC from temperate phytoplankton has a $\delta^{13}C$ value ranging from -22 to -19‰, terrestrial OC shows low $\delta^{13}C$ values (from -30 to -23‰) if C3 plants are the dominant constituent, and high $\delta^{13}C$ values (from -15 to -12‰) if C4 plants dominate (Fry and Sherr, 1984; Hedges et al., 1997). Accordingly, Sanchez-Vidal et al. (2013) show that terrestrial OC entering the North Catalan margin through the Tordera River present $\delta^{13}C$ values of -33 to -26‰. Whereas organic matter derived from vascular plants is generally depleted in TN, yielding a TN/OC ratio <0.06, the tendency of vascular plant detritus to preferentially gain nitrogen during soil microbial decay increases the TN/OC ratio up to 0.12 (Hedges et al., 1997). Organic matter from phytoplankton and bacterioplankton is characterized by higher TN contents and TN/OC >0.12 (Goñi and Hedges, 1995). The relative contributions of the marine vs. terrestrial sources of OC over the study area during the monitoring period has been evaluated by means of a simple $\delta^{13}C$-based binary mixing model (Fig. 2.17), where a marine $\delta^{13}C$ value of -20.1‰ (Harmelin-Vivien et al., 2008) and a terrestrial $\delta^{13}C$ value of -28.1‰ (Sanchez-Vidal et al., 2013) are assumed:

$$\text{marine OC} = \frac{\left(\delta^{13}C + 28.1\right)}{(-20.1 + 28.1)} \qquad (2.1)$$

$$\text{terrestrial OC} = 1 - \text{marine OC} \qquad (2.2)$$

We observed that OC contents and provenance differed amongst grain size fractions (Figs. 2.15 and 2.16). The highest OC contents were always found in the clay fraction (<4 μm) and there was a clear tendency towards decreasing OC contents with increasing particle size (Fig. 2.15a-c and Table 2.4). This is in agreement with previous studies by Mayer (1994a, 1994b), Hedges and Keil (1995) and Keil et al. (1998), which highlighted the close association between OC and the finest mineral fraction of the sediment. This has been attributed to incorporation or adsorption of OC into mineral structures such as pores and laminae (Curry et al., 2007) and aggregation of OC with mineral grains (Arnarson and Keil, 2005), which protect OC from remineralization thus controlling its preservation in marine sediments (Mayer, 1994; Hedges and Keil, 1995). The decrease of the amount of OC contained in the clay fraction in the head of the canyon after the stormy period (lowering the %OC clay/%OC bulk to less than 5%, Table 2.4) can be explained by the winnowing of the fine, OC-rich particles by the strong currents of the storm of December 2008, which lowered the inventory of OC in the fine fraction accumulating on the canyon head. Therefore, in addition of increasing its preservation potential, the sorption of marine OC in clay minerals (Fig. 2.16) allows its effective dispersion over large distances (Inthorn et al., 2006) until the level of energy in the environment decreases and clays are deposited.

Also to be noticed is the decreasing %OC in the clay fraction with increasing water depth, with values in excess of 6% in the mid shelf and 1-2% in the deeper stations. A relative increase in $\delta^{3}C$ in the clay fraction also parallels water depth increase, with values around -24.8‰ in the shelf and values near -22.5‰ in the deep canyon and slope sediments. A similar situation has been also reported from other continental margin environments, which was attributed to dilution of the terrestrially derived OC by sorption of marine derived material to sediments (Bergamaschi et al., 1997). It should be noted that the addition of marine organic matter to sediments can increase

the decomposition of the terrestrial OC through poorly understood coupled decomposition processes (see review in Blair and Aller, 2012), which at the same time may lower to some extent the OC content of the clay fractions .

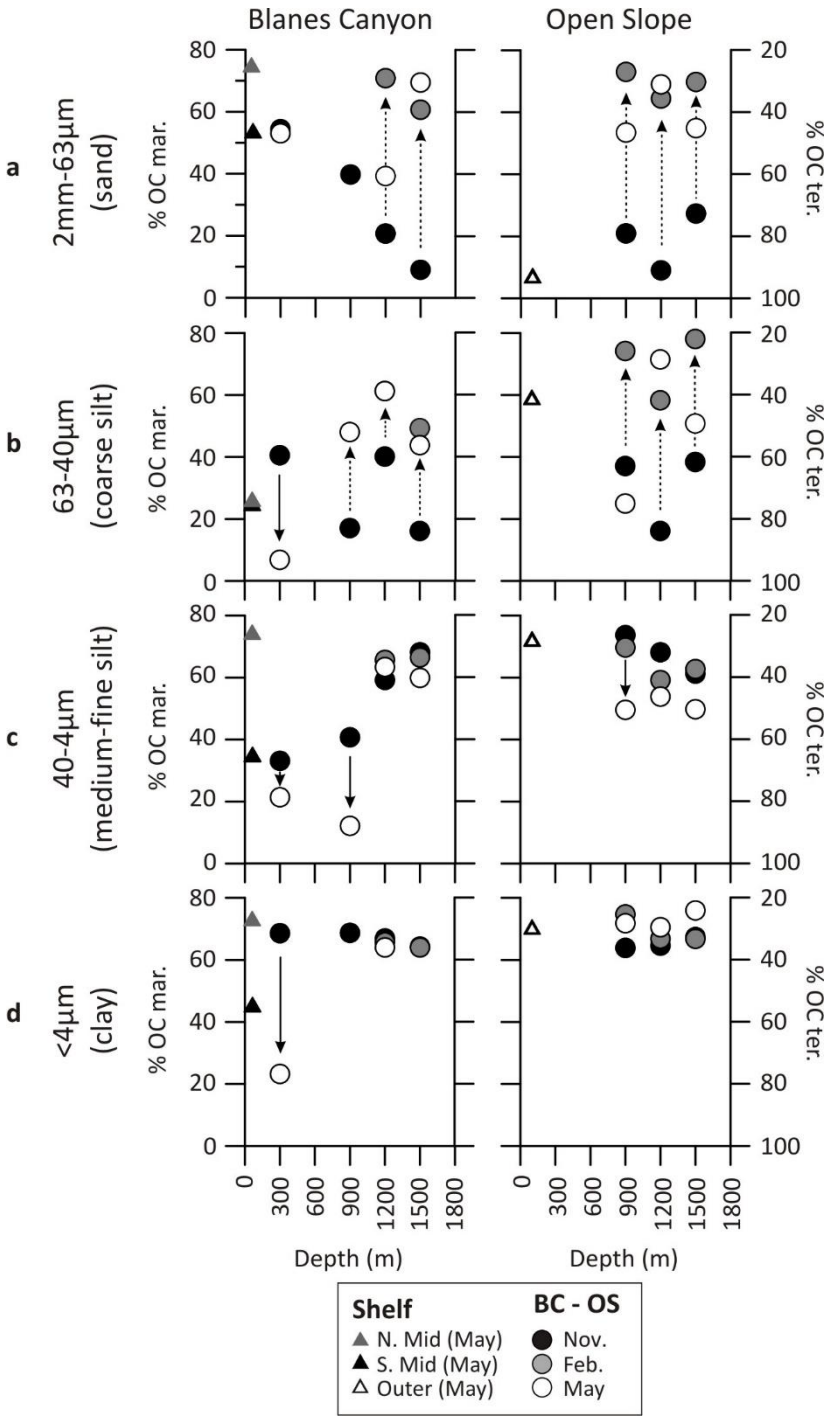

Figure 2.17. Marine and terrestrial OC distribution in shelf, canyon and slope environments and size fractions (a-d), before and after the stormy period. Data from the southernmost mid shelf stations have been averaged. Solid arrows indicate the largest decreases in marine OC (or increase in OC terrestrial), and dotted arrows indicate the largest increases in marine OC. N. mid: Northernmost mid shelf. S. mid: Southernmost mid shelf. BC: Blanes Canyons' axis. OS: Southern open slope.

In contrast to clays, coarser particles show lower OC contents but a wide range of $\delta^{13}C$ values (Figs. 2.15 and 2.16 and Table 2.4). In the northernmost mid shelf P1 station contributions of marine OC reaches 74% (Fig. 2.17a), which may be attributed to the main microphytoplankton components of the phytoplanktonic communities inhabiting surface waters (Rau et al., 1990; Rolff and Elmgren, 2000; Harmelin-Vivien et al., 2008). In the southernmost mid shelf P2 to P5 stations contributions of terrestrial OC are higher (up to 87%), which may be due to the proximity of Tordera River inputs (Fig. 2.11). The higher terrestrial OC content in the silt fraction of P2 to P5 the shelf sediments (Figs. 2.17b-c) agrees with the well sorted silt size dominance in suspended particles from the Tordera River (6.7% clay, 74.5% silt and 18.8% sand) (Sanchez-Vidal et al., this 2013). Sand and coarse silt particles at deeper stations in sediments collected in February and May 2009 show also a relative enrichment in $\delta^{13}C$ (Figs. 2.15e-f, 2.17a-b), suggesting the arrival of pelagic primary production detritus resulting from the spring bloom (Fig. 2.12c). Overall, this means that sand and coarse silt sized sediments from the shelf carry little of the OC in the bulk sediment (Table 2.4), even though this can be either marine or terrestrial derived OC (Figs. 2.16 and 2.17). This is also observed in the BC axis and the adjacent open slope sediments as shown by the wide range of $\delta^{13}C$ in the sand and coarse silt fractions (Fig. 2.16).

The principal processes involved in OC transport and deposition over the shelf, canyon and adjacent open slope in the Blanes submarine canyon area are summarized in the conceptual sketch of Figure 2.18. Grain size is a relevant parameter in controlling the distribution of OC in surface sediments, itself reflecting kinetic energy levels, which is in agreement with the findings of Bergamaschi et al. (1997). The factors governing grain size thus play a crucial role in determining the type and amount of OC accumulating in the sediments. In our study area this is especially the case of the shelf and canyon head environments, where the impact of high energy episodic hydrodynamic events is particularly noticeable and leads to textural heterogeneity. The storm in December 2008 caused the arrival at shallower depths of silt-sized particles carrying terrestrial OC largely resulting from the discharge of Tordera River (Figs. 2.12, 2.17 and 2.18, blue arrows in Fig. 2.18). It also led to the mobilization and transport of sand and coarse silt fractions that overall was poorly loaded with OC from the shelf to the upper reaches of the submarine canyon (Fig. 2.16, brown arrows in Fig. 2.18). The winnowing of a significant amount of marine OC-rich clay particles from the canyon head steered their arrival to deeper stations downcanyon (Figs. 2.14 and 2.16, yellow arrows in Fig. 2.18 and Table 2.3). Also, off-canyon shelf-edge spillover processes could have had similar effects on the open slope, though the associated fluxes where lower. This involves rapidly shifting the accumulation of continental and marine OC from shallower to deeper settings as found in other continental margins of the world, thus leading to the long-term sequestration of carbon in the deep sea (Inthorn et al., 2006).

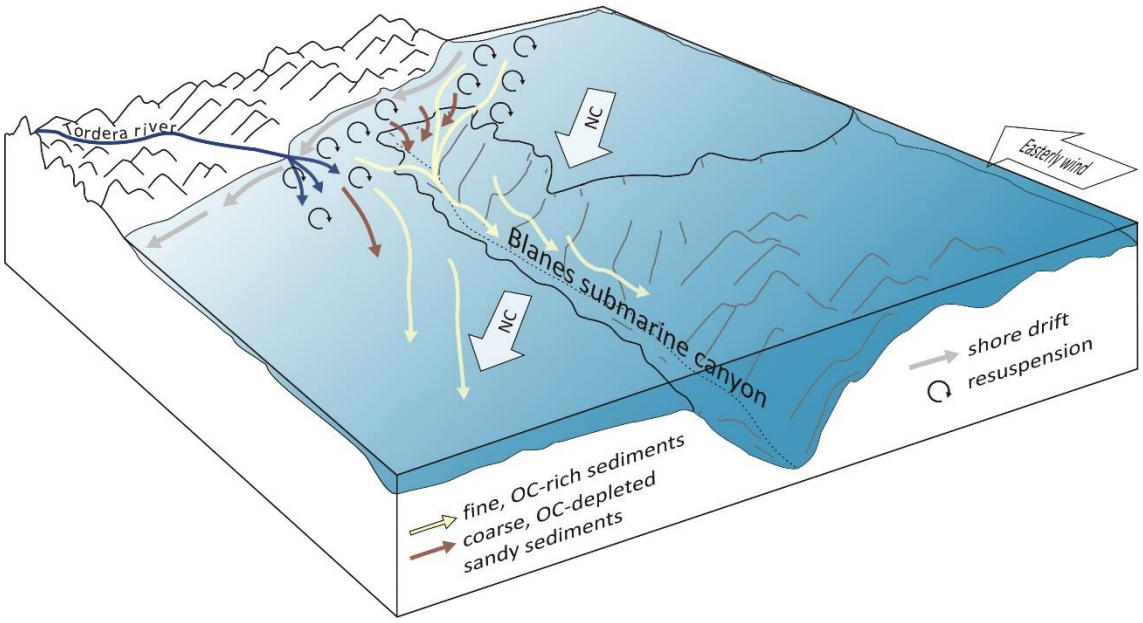

Figure 2.18. Conceptual model of the Blanes Canyon environment showing the main processes and sediment and OC transport pathways that were activated during the major storm of December 2008. Arrows point towards the direction of transport. NC: Northern Current.

2.2.6. Conclusions

Seafloor sediments collected before and after the autumn 2008 and winter 2009 stormy period were examined to understand how the high kinetic energy levels reached in and around the Blanes Canyon affected grain size distribution and the transfer of OC to the deep. During the December 2008 storm, high waves (up to 8 m with Hs up to 4.7 m), strong currents (up to 0.7 m s^{-1} into the canyon head at 300 m depth) and intense bottom shear stress at the shelf floor (in excess of 0.60 Pa) occurred. The associated flows triggered the transport of sand particles poorly loaded with OC from shelf to canyon head environments, and also the down slope transport of OC-rich fine particles. The storm thus proved to be efficient at transporting OC from shallow to deeper environments, with the submarine canyon acting as a preferential conduit. OC contents and types (terrestrial vs. marine) were differently distributed among the various grain size fractions, which were in turn affected by erosion, resuspension, transport, sorting and deposition processes activated by the storm-related near-bottom currents.

Our results show that in the study area atmosphere-driven coastal oceanographic events are able to influence the sedimentary dynamics and grain size distribution not just over the continental shelf and upper canyon but also much deeper into a major submarine canyon and the adjacent open slope. The same events controlling the sorting and differential deposition of particles according to their grain size and density also control the redistribution of OC loaded into such particles. This likely may have a strong impact on the deep-sea ecosystem and living resources, as previously demonstrated for other high-energy events such as DSWC also occurring in the study area (Canals et al., 2006; Company et al., 2008). Quick changes of environmental parameters, such as increased near bottom current speeds and deposition of coarse, OC-poor particles at the

upper reaches of the canyon vs. the winnowing and deposition of OC-rich fine sediments down canyon, may have functional consequences and alter the dynamics of the benthic ecosystem. Our results have also significant implications for understanding particle dynamics and thus for modeling the global carbon cycle. An improved knowledge of the environmental factors driving the transfer of OC from shallow to deep ocean compartments is essential to understand the role of the continental margin dynamic processes in the global carbon budget.

2.2.7. Acknowledgements

We thank the crew of R/V Garcia del Cid for their help and dedication during the sea work. We also thank G. Lastras who kindly provided Figure 2.11, and A. Micallef who reviewed an earlier version of the manuscript. We thank the two anonymous reviewers for their constructive comments. This research has been supported by DOS MARES (ref. CTM2010-21810-C03-01), ReDEco (ref. CTM2008-04973-E/MAR), GRACCIE (CSD2007-00067, Consolider-Ingenio Program), and PERSEUS (GA 287600) research projects, and by a Generalitat de Catalunya "Grups de Recerca Consolidats" grant (2009 SGR 1305). R.P. is supported by a predoctoral F.P.U. grant from the Spanish government, and A.S. and R.D by "Ramon y Cajal" and "Juan de la Cierva" postdoctoral contracts.

2.2.8. References

Accornero, A., Picon, P., De Bovée, F., Charrière, B., Buscail, R., 2003. Organic carbon budget at the sediment-water interface on the Gulf of Lions continental margin. Continental Shelf Research 23, 79-92.

Alcoverro, T., Pagès, J., Gera, A., Farina, S., Roca, G., Pérez, M., Romero, J., 2012. The effects of 26th December 2008 storm on Costa Brava Posidonia oceanica ecosystems. Final Report Proyecto Intramural Especial Cofinanciado CEAB-CSIC PIEC 200430E599, 147-156.

Alvarez, A., Tintoré, J., Sabatés, A., 1996. Flow modification and shelf-slope exchange induced by a submarine canyon off the northeast Spanish coast. Journal of geophysical research 101, 043-12.

Amblas, D., Canals, M., Urgeles, R., Lastras, G., Liquete, C., Hughes-Clarke, J.E., Casamor, J.L., Calafat, A.M., 2006. Morphogenetic mesoscale analysis of the northeastern Iberian margin, NW Mediterranean Basin. Marine Geology 234, 3-20.

Arnarson, T.S., Keil, R.G., 2005. Influence of organic-mineral aggregates on microbial degradation of the dinoflagellate Scrippsiella trochoidea. Geochimica et Cosmochimica Acta 69, 2111-2117.

Arnarson, T.S., Keil, R.G. 2007. Changes in organic matter-mineral interactions for marine sediments with varying oxygen exposure times. Geochimica et Cosmochimica Acta 71, 3545-3556.

Bergamaschi, B. A., Tsamakis, E., Keil, R.G., Eglinton, T.I., Montluçon, D.B., Hedges, J.I., 1997. The effect of grain size and surface area on organic matter, lignin and carbohydrate concentration,

and molecular compositions in Peru Margin sediments. Geochimica et Cosmochimica Acta 61, 1247-1260.

Berner, A., Canfield, E., 1989. A new model for atmospheric oxygen over phanerozoic time. American Journal of Science 289, 333-361

Bianchi, T.S., Rolff, C., Widbom, B., Elmgren, R., 2002. Phytoplankton pigments in Baltic Sea seston and sediments: seasonal variability, fluxes, and transformations. Estuarine, Coastal and Shelf Science 55, 369-383.

Bianchi, T.S., Galler, J.J., Allison, M.A., 2007. Hydrodynamic sorting and transport of terrestrially derived organic carbon in sediments of the Mississippi and Atchafalaya Rivers. Estuarine, Coastal and Shelf Science 73, 211-222.

Blair, N.E., Leithold, E.L., Aller, R.C., 2004. From bedrock to burial: the evolution of particulate organic carbon across coupled watershed-continental margin systems. Marine Chemistry 92, 141-156.

Blair, N.E., Aller, R.C. 2012. The fate of terrestrial organic carbon in the Marine environment. Annual Review of Marine Science 4, 401-423.

Bolaños, R., Jorda, G., Cateura, J., Lopez, J., Puigdefabregas, J., Gomez, J., Espino, M., 2009. The XIOM: 20 years of a regional coastal observatory in the Spanish Catalan coast. Journal of Marine Systems 77, 237-260.

Bourrin, F., Durrier de Madron, X., Heussner, S., Estourne, C., 2008. Impact of winter dense water formation on shelf sediment erosion (evidence from the Gulf of Lions, NW Mediterranean). Continental Shelf Research 28, 1984-1999.

Canals, M., Casamor, J.L., Lastras, G., Monaco, A., Acosta, J., Berne, S., Loubrieu, B., Weaver, P.P.E., Grehan, A., Dennielou, B., 2004a. The role of canyons on strata formation. Oceanography 17, 80-91.

Canals, M., Casamor, J.L., Urgeles, R., Farrán, M., Calafat, A.M., Amblás, D., Willmott, V., Estrada, F., Sánchez, A., Arnau, P., Frigola, J. and Colás, S., 2004b. Mapa del relleu submarí de Catalunya (Seafloor relief map of Catalonia), 1:250 000. Institut Cartogràfic de Catalunya, 1 map.

Canals, M., Puig, P., de Madron, X.D., Heussner, S., Palanques, A., Fabres, J. 2006. Flushing submarine canyons. Nature 444, 354-357.

Cartes, J.E., Grémare, A., Maynou, F., Villora-Moreno, S., Dinet, A., 2002. Bathymetric changes in the distributions of particulate organic matter and associated fauna along a deep-sea transect down the catalan sea slope (Northwestern Mediterranean). Progress in Oceanography 53, 29-56.

Company, J.B., Puig, P., Sarda, F., Palanques, A., Latasa, M., Scharek, R., 2008. Climate influence on deep sea populations. Plos One 3, e1431.

Curry, K.J., Bennett, R.H., Mayer, L.M., Curry, A., Abril, M., Biesiot, P.M., Hulbert, M.H., 2007. Direct visualization of clay microfabric signatures driving organic matter preservation in fine-grained sediment. Geochimica et Cosmochimica Acta 71, 1709-1720.

Dail, M., 2007. Assessing the importance of tropical cyclones on continental margin sedimentation in the Mississippi delta region. Continental Shelf Research 27, 1857-1874.

Díaz, J.I., Maldonado, A., 1990. Transgressive sand bodies on the Maresme continental shelf, western Mediterranean Sea. Marine Geology 91, 53-72.

Durán, R., Canals, M., Sanz, J.L., Lastras, G., Amblas, D., Micallef, A., 2012. Morphology and sediment dynamics of the northern Catalan continental shelf, northwestern Mediterranean Sea. Geomorphology 204, 1-20.

Durán, R., Canals, M., Lastras, G., Micallef, A., Amblas, D., Pedrosa-Pàmies, R., 2013. Sediment dynamics of the continental shelf around the Blanes submarine canyon head (NW Mediterranean). Progress in Oceanography 118, 28-46.

Durrieu de Madron, X., Radakovitch, O., Heussner, S., Loye-Pilot, M.D., Monaco, A., 1999. Role of the climatological and current variability on shelf-slope exchanges of particulate matter: evidence from the Rhône continental margin (NW Mediterranean). Deep Sea Research Part I: Oceanographic Research Papers 46, 1513-1538.

Ember, L.M., Williams, D.F., Morris, J.T., 1987. Processes that influence carbon isotope variations in salt marsh sediments. Marine Ecology Progress Series 36, 33-42.

Fabres, J., Tesi, T., Velez, J., Batista, F., Lee, C., Calafat, A., Heussner, S., Palanques, A., Miserocchi, S., 2008. Seasonal and event-controlled export of organic matter from the shelf towards the Gulf of Lions continental slope. Continental Shelf Research 28, 1971-1983.

Ferré, B., Guizien, K., Durrieu de Madron, X., Palanques, A., Guillén, J., Grémare, A., 2005. Fine-grained sediment dynamics during a strong storm event in the inner-shelf of the Gulf of Lion (NW Mediterranean). Continental Shelf Research 25, 2410-2427.

Fogel, M.L., Sprague, E.K., Gize, A.P., R.W. Frey, R.W., 1989. Diagenesis of organic matter in georgia salt marshes. Estuarine, Coastal and Shelf Science 28, 211-230.

Font, R. 1988. Compression zone effect in batch sedimentation. American Institute of Chemical Engineers Journal 34, 229-238.

Font, J., Garcia-Ladona, E., Gorriz, E.G., 1995. The seasonality of mesoscale motion in the Northern Current of the western Mediterranean: several years of evidence. Oceanologica Acta 18, 207-219.

Goñi, M.A., Hedges, J.I., 1995. Sources and reactivities of marine-derived organic matter in coastal sediments as determined by alkaline CuO oxidation. Geochimica et Cosmochimica Acta 59, 2965-2981.

Goñi, M.A., Ruttenberg, K.C., Eglinton, T.I., 1998. A reassessment of the sources and importance of land-derived organic matter in surface sediments from the Gulf of Mexico. Geochimica et Cosmochimica Acta 62, 3055-3075.

Goñi, M.A., Yunker, M.B., Macdonald, R.W., Eglinton, T.I., 2005. The supply and preservation of ancient and modern components of organic carbon in the Canadian Beaufort Shelf of the Arctic Ocean. Marine Chemistry 93, 53-73.

Goñi, M.A., Monacci, N., Gisewhite, R., Ogston, A., Crockett, J., Nittrouer, C., 2006. Distribution and sources of particulate organic matter in the water column and sediments of the Fly River Delta, Gulf of Papua (Papua New Guinea). Estuarine, Coastal and Shelf Science 69, 225-245.

Goñi, M.A., Monacci, N., Gisewhite, R., Crockett, J., Nittrouer, C., Ogston, A., Alin, A.R., Aalto, R., 2008. Terrigenous organic matter in sediments from the Fly River delta-clinoform system (Papua New Guinea). Journal of Geophysical Research 113.

Guillén, J., Jiménez, J.A., Palanques, A., Gracia, V., Puig, P., Sánchez-Arcilla, A., 2002. Sediment resuspension across a microtidal, low-energy inner shelf. Continental Shelf Research 22, 305-325.

Guillén, J., Bourrin, F., Palanques, A., Durrieu de Madron, X., Puig, P., Buscail, R., 2006. Sediment dynamics during wet and dry storm events on the Tęt inner shelf (SW Gulf of Lions). Marine Geology 234, 129-142.

Harmelin-Vivien, M., Loizeau, V., Mellon, C., Beker, B., Arlhac, D., Bodiguel, X., Ferraton, F., Hermand, R., Philippon, X., Salen-Picard, Ch., 2008. Comparison of C and N stable isotope ratios between surface particulate organic matter and phytoplankton in the Gulf of Lions (NW Mediterranean). Continental. Shelf Research 28, 1911-1919.

Hedges, J.I., Keil, R.G., 1995. Sedimentary organic matter preservation: an assessment and speculative synthesis. Marine Chemistry 49, 81-115.

Hedges, J.I., Keil, R.G., Benner, R., 1997. What happens to terrestrial organic matter in the ocean? Organic Geochemistry 27, 195-212.

Hereu, B., Garcia-Rubies, A., Linares, C., Navarro, L., Bonaviri, C., Cebrian, E., Diaz, D., Garrabou, J., Teixidó, N., Zabala, M., 2012. Impact of the Sant Esteve's storm (2008) on the algal cover in infralittoral rocky photophilic communities. Final Report Proyecto Intramural Especial Cofinanciado CEAB-CSIC PIEC 200430E599, 123-134.

Heussner, S., Durrieu de Madron, X., Calafat, A., Canals, M., Carbonne, J., Delsaut, N., Saragoni, G., 2006. Spatial and temporal variability of downward particle fluxes on a continental slope: Lessons from an 8-yr experiment in the Gulf of Lions (NW Mediterranean). Marine Geology 234, 63-92.

Inthorn, M., Wagner, T., G. Scheeder, G., M. Zabel, M., 2006.Lateral transport controls distribution, quality and burial of organic matter along continental slopes in high-productivity areas. Geology 34 (3), 205-208.

Keil, R.G., Montluçon, D.B., Prahlt, F.G., Hedges, J.I., 1994. Sorptive preservation of labile organic matter in marine sediments. Nature 370, 549-552

Keil, R.G., Mayer, L.M., Quay, P.D., Richey, J.E., Hedges, J.I., 1997. Loss of organic matter from riverine particles in deltas. Geochimica et Cosmochimica Acta 61, 1507-1511.

Keil, R.G., Tsamakis, E., Giddings, J.C., Hedges, J.I., 1998. Biochemical distributions (amino acids, neutral sugars, and lignin phenols) among size-classes of modern marine sediments from the Washington coast. Geochimica et Cosmochimica Acta 62, 1347-1364.

Lapouyade, A., Durrieu de Madron, X., 2001. Seasonal variability of the advective transport of particulate matter and organic carbon in the Gulf of Lion (NW Mediterranean). Oceanologica Acta 24, 295-312.

Lastras, G., Canals, M., Urgeles, R., Amblas, D., Ivanov, M., Droz, L., Dennielou, B., Fabrés, J., Schoolmeester, T., Akhmetzhanov, A., Orange, D., García-García, A., 2007. A walk down the Cap de Creus canyon, northwestern Mediterranean Sea: Recent processes inferred from morphology and sediment bedforms. Marine Geology 246 (2-4), 176-192.

Lastras, G., Canals, M., Amblas, D., Lavoie, C., Church, I., De Mol, B., Duran, R., Calafat, A.M., Hughes-Clarke, J.E., 2011. Understanding sediment dynamics of two large submarine valleys from seafloor data: Blanes and La Fonera canyons, northwestern Mediterranean Sea. Marine Geology 280, 20-39.

Leithold, E.L.. Hope R. S., 1999. Deposition and modification of a flood layer on the northern California shelf: lessons from and about the fate of terrestrial particulate organic carbon. Marine Geology 154, 183-195.

Li, M.Z., Amos, C.L., 2001. SEDTRANS96: the upgraded and better calibrated sediment-transport model for continental shelves. Computers & Geosciences 27, 619-645.

Liquete, C., Canals, M., Lastras, G., Amblas, D., Urgeles, R., De Mol, B., De Batist, M., Hughes-Clarke, J.E., 2007. Long-term development and current status of the Barcelona continental shelf: A source-to-sink approach. Continental Shelf Research 27, 1779-1800.

Lopez-Fernandez, P., Calafat, A., Sanchez-Vidal, A., Canals, M., Flexas, M., Cateura, J. and Company, J.B. Multiple drivers of particle fluxes in the Blanes submarine canyon and southern open slope: Results of a year round experiment. Progress in Oceanography 118, 95-107.

Martín, J., Puig, P., Palanques, A., Masqué, P., García-Orellana, J., 2008. Effect of commercial trawling on the deep sedimentation in a Mediterranean submarine canyon. Marine Geology 252, 150-155.

Masó, M., Tintoré, J., 1991. Variability of the shelf water off the northeast Spanish coast. Journal of Marine Systems 1, 441-450.

Mayer, L.M., 1994a. Relationships between mineral surfaces and organic carbon concentrations in soils and sediments. Chemical Geology 114, 347-363.

Mayer, L.M., 1994b. Surface area control of organic carbon accumulation in continental shelf sediments. Geochimica et Cosmochimica Acta 58, 1271-1284.

Mendoza, E.T., Jiménez, J., 2009. Regional vulnerability analysis of Catalan beaches to storms. Proceedings of the Institution of Civil Engineers-Maritime Engineering 162, 127-135.

Meyers, P. A., 1994. Preservation of elemental and isotopic source identification of organic matter. Chemical Geology. 144, 289–302. Middelburg, J. J., Nieuwenhuize, J., Lubberts, R. K., Van de Plassche, O., 1997. Organic carbon isotope systematics of coastal marshes, Estuarine, Coastal and Shelf Science, 45, 681-687.

Millot, C., 1999. Circulation in the western Mediterranean Sea. Journal of Marine Systems 20, 423-442.

Neumeier, U., Ferrarin, C., Amos, C.L., Umgiesser, G., Li, M.Z., 2008. Sedtrans05: An improved sediment-transport model for continental shelves and coastal waters with a new algorithm for cohesive sediments. Computers & Geosciences 34, 1223-1242.

Nieuwenhuize, J., Maas, Y.E.M., Middelburg, J.J., 1994. Rapid analysis of organic carbon and nitrogen in particulate materials. Marine Chemistry 45, 217–224.

Ogston, A.S., Guerra, J.V., Sternberg, R.W., 2004. Interannual variability of nearbed sediment flux on the Eel River shelf, northern California. Continental Shelf Research 24, 117-136.

Palanques, A., Puig, P., Guillén, J., Jimenez, J., Gracia, V., Sanchez-Arcilla, A., Madsen, O., 2002. Near-bottom suspended sediment fluxes on the microtidal low-energy Ebro continental shelf (NW Mediterranean). Continental Shelf Research 22, 285-303.

Palanques, A., Durrieu de Madron, X., Puig, P., Fabres, J., Guillén, J., Calafat, A., Canals, M., Heussner, S., Bonnin, J., 2006. Suspended sediment fluxes and transport processes in the Gulf of Lions submarine canyons. The role of storms and dense water cascading. Marine Geology 234, 43-61.

Prahl, F.G., 1985. Chemical evidence of differential particle dispersal in the southern Washington coastal environment. Geochimica et Cosmochimica Acta 49, 2533-2539.

Puig, P., Palanques, A., Guillén, J., 2001. Near-bottom suspended sediment variability caused by storms and near-inertial internal waves on the Ebro mid continental shelf (NW Mediterranean). Marine Geology 178, 81-93.

Puig, P., Palanques, A., Orange, D.L., Lastras, G., Canals, M., 2008. Dense shelf water cascades and sedimentary furrow formation in the Cap de Creus Canyon, northwestern Mediterranean Sea. Continental Shelf Research 28, 2017-2030.

Salvadó, J.A., Grimalt, J.O., López, J.F., Durrieu de Madron, X., Heussner, S., Canals, M., 2012. Transformation of PBDE mixtures during sediment transport and resuspension in marine environments (Gulf of Lion, NW Mediterranean Sea). Environmental Pollution 168, 87-95.

Ransom, B., Shea, K.F., Burkett, P.J., Bennett, R.H., Baerwald, R., 1998. Comparison of pelagic and nepheloid layer marine snow: implications for carbon cycling. Marine Geology 150, 39-50.

Rau, G.H., Teyssie, J.L., Rassoulzadegan, F., Fowler, S.W., 1990. $^{13}C/^{12}C$ and $^{15}N/^{14}N$ variations among size-fractionated marine particles: implications for their origin and trophic relationships. Marine Ecology Progress Series 59, 33-38.

Rolff, C., R. Elmgren, R., 2000. Use of riverine organic matter in plankton food webs of the Baltic Sea. Marine Ecology Progress Series 197, 81–101

Ross, C.B., Gardner, W.D., Richardson, M.J., Asper, V.L., 2009. Currents and sediment transport in the Mississippi Canyon and effects of Hurricane Georges. Continental Shelf Research 29, 1384-1396.

Sanchez-Vidal, A., Pasqual, C., Kerhervé, P., Calafat, A., Heussner, S., Palanques, A., Durrieu de Madron, X., Canals, M., Puig, P., 2008. Impact of dense shelf water cascading on the transfer of organic matter to the deep western Mediterranean basin. Geophysical Research Letters 35, .

Sanchez-Vidal, A., Pasqual, C., Kerhervé, P., Heussner, S., Calafat, A., Palanques, A., De Madron, X.D., Canals, M., Puig, P., 2009. Across margin export of organic matter by cascading events traced by stable isotopes, northwestern Mediterranean Sea. Limnology and Oceanography 54, 1488-1500.

Sanchez-Vidal, A., Canals, M., Calafat, A.M., Lastras, G., Pedrosa-Pàmies, R., Menéndez, M., Romero, J., Hereu, B., Alcoverro, T., 2012. Impacts on the deep-sea ecosystem by a severe coastal storm. Plos One 7(1): e30395.

Sanchez-Vidal, A., Higueras, M., Martí, E., Liquete, C., Calafat, A., Kerhervé, P., Canals, M., 2013. Riverine transport of terrestrial organic matter to the North Catalan margin, NW Mediterranean Sea. Progress in Oceanography 118, 71-80.

Serra, J., Valois X., Parra, D., 2007. Estructura del prodelta de la Tordera (costa del Maresme, NO Mediterráneo) a partir del análisis sísmico de alta resolución. Geogaceta 41, 211-214.

Ulses, C., Estournel, C., Durrieu de Madron, X., Palanques, A., 2008. Suspended sediment transport in the Gulf of Lions (NW Mediterranean): Impact of extreme storms and floods. Continental Shelf Research 28, 2048-2070.

Wakeham, S.G., Lee, C., Peterson, M.L., Liu, Z., Szlosek, J., Putnam, I., Xue, J., 2009. Organic compound composition and fluxes in the Twilight Zone—time series and settling velocity sediment traps during MEDFLUX. Deep-Sea Research II: Topical Studies in Oceanography 66, 1420-1436.

Wiberg, P., Dungan Smith, J., 1983. A comparison of field data and theorical models for wave-current interactions at the bed on the continental shelf. Continental Shelf Research 2, 147-162.

2.3. Composition and sources of sedimentary organic matter in the deep eastern Mediterranean Sea

R. Pedrosa-Pàmies[a,b], C. Parinos[b], A. Sanchez-Vidal[a], A. Gogou[b], A. Calafat[a], M. Canals[a], I. Bouloubassi[c], N. Lampadariou[d]

[a]GRC Geociències Marines, Departament d'Estratigrafia, Paleontologia i Geociències Marines, Universitat de Barcelona. Barcelona, Catalonia.

[b]Hellenic Centre for Marine Research (HCMR), Institute of Oceanography. Anavyssos, Attiki, Greece.

[c]Laboratoire d'Océanographie et du Climat: Expérimentation et Approches Numériques (LOCEAN), CNRS – Université Pierre et Marie Curie. Paris, France.

[d]Hellenic Centre for Marine Research (HCMR), Institute of Oceanography, Heraklion, Crete, Greece.

2015 Biogeosciences 12, 7379-7402. doi:10.5194/bgd-12-9935-2015.

Abstract

Surface sediments collected from deep slopes and basins (1018-4087 m depth) of the oligotrophic Eastern Mediterranean Sea have been analysed for bulk elemental and isotopic composition of organic carbon, total nitrogen and selected lipid biomarkers, jointly with grain size distribution and other geochemical proxies. The distribution and sources of sedimentary organic matter (OM) have been subsequently assessed and general environmental variables, such as water column depth and physical circulation patterns, have been examined as causative factors of deep-sea sediment characteristics. Lithogenic and biogenic carbonates are the dominant sedimentary fractions, accounting for up to 85.4% and 66.5% of the total weight, respectively. The low OC and TN contents in the surface sediments of the study area, that ranged from 0.15 to 1.15% and 0.06 to 0.11%, respectively, reflect the oligotrophic character of the EMS. Both bulk and molecular organic tracers reflect a mixed contribution from autochthonous and allochthonous sources for the sedimentary OM, as indicated by relatively degraded marine OM, terrestrial plant waxes and anthropogenic OM e.g., degraded petroleum by-products, respectively. Wide regional variations have been observed amongst the studied proxies, which reflect the multiple factors controlling sedimentation in the deep Eastern Mediterranean Sea. Our findings highlight the role of deep Eastern Mediterranean basins as depocentres of organic-rich fine-grained sediments (mean 5.4±2.4 μm), with OM accumulation and burial being attributed to aggregation mechanisms and hydrodynamic sorting. A multi-proxy approach is applied aiming to investigate the biogeochemical composition of sediment samples, which sheds new light on the sources and transport mechanisms along with the impact of preservation vs. diagenetic processes on the composition of sedimentary OM in the deep basins of the oligotrophic Eastern Mediterranean Sea.

2.3.1. Introduction

The burial of organic matter (OM) in marine sediments constitutes the main link between "active" pools of carbon in the oceans, atmosphere and landmasses, and carbon pools that cycle on much longer, geological, time scales (Burdige, 2007). Therefore, investigating the processes that control the composition of sedimentary OM that is buried in deep-sea sediments is crucial for understanding carbon cycling on a global scale.

The deep sea receives inputs of organic particles from multiple sources, both autochthonous (e.g., biogenic particulate matter from primary production in ocean surface waters) and allochthonous (i.e. land-sourced OM from soils, plant debris, riverine phytoplankton and man-made compounds transported by runoff and atmospheric deposition into the marine domain) (Bouloubassi et al., 1997; Durrieu de Madron et al., 2000; Kaiser et al., 2014). Consequently, sedimentary OM constitutes an heterogeneous and complex mixture of organic compounds with a wide range of chemical and physical properties (Mayer, 1994; Hedges and Oades, 1997; Hedges et al., 1997; Goñi et al., 1998). Therefore, the combined use of bulk geochemical indicators such as total nitrogen (TN) to organic carbon (OC) ratios, stable isotope of OC ($\delta^{13}C$), and molecular proxies such as lipid biomarkers can aid to gain knowledge on the origin, delivery and preservation of OM in marine sediments (Bouloubassi et al., 1997; Meyers, 1997; Goñi et al., 2003; Volkman, 2006).

The biogeochemical composition of sediments in deep basins of the oligotrophic Eastern Mediterranean Sea (EMS), as well as the sources, transport and preservation of sedimentary OM, have been scarcely investigated so far. Previous studies have shown that the composition of surficial sediments is principally controlled by the geochemical characteristics of the source areas, the prevailing metoceanic conditions on the adjacent shelves, the contribution of atmospheric aerosols and the dominant regional circulation (e.g., Weldeab et al., 2002; Ehrmann et al., 2007; Hamann et al., 2008). Nevertheless, the factors involved in the supply, distribution and fate of sedimentary OM are still poorly known.

In the present study, surface sediments collected from deep slopes and basins of the EMS have been analysed for physical and geochemical parameters such as grain size distribution, lithogenic, calcium carbonate ($CaCO_3$), opal, OC and TN contents, along with molar TN/OC ratios, stable isotopic ratios of OC ($\delta^{13}C$) and selected lipid biomarkers. Our main goal is to investigate the spatial distribution and main sources of sedimentary OM and to evaluate the impact of autochthonous vs. allochthonous contributions in the study area. We also examine whether and up to which point general environmental factors, such as water mass circulation patterns and water column depth, could explain the observed deep-sea sediment geochemical properties.

2.3.2. Oceanographic setting

The EMS is a land-locked sea with a complex topography including shelves, slopes, ridges, seamounts, trenches and four main basins: the Adriatic Sea, the Ionian Sea, the Aegean Sea and the Levantine Sea (Fig. 2.19) (Amblàs et al., 2004; Medimap Group, 2007). The Ionian Sea to the west and the Levantine Sea to the east are longitudinally connected and cover most of the EMS area. They are also the deepest basins of the EMS, with the maximum depth (5267 m) located at

the Hellenic Trench, south of the Cretan Arc. The Aegean Sea and the Adriatic Sea represent the northern extensions of the EMS. Both are relatively shallow, in particular the Adriatic Sea, which is dominated by a broad shelf and a slope sub-basin shallower than 1200 m. In the Aegean Sea, which has a particularly complex topography with tens of depressions, highs and islands, water depths up to 2500 m are found north of the island of Crete (Amblàs et al., 2004; Medimap Group, 2007). The southern Aegean Sea (Cretan Sea) is the sea area comprised between the Cyclades Archipelago to the north and the island of Crete to the south, which also includes the western Cretan Straits.

The general circulation pattern of the EMS is anti-estuarine, which results from interactions between basin, sub-basin and mesoscale flows (Bethoux, 1979). The EMS communicates with the Western Mediterranean Sea through the Sicily Strait, with an inflow of low-salinity Modified Atlantic Water (MAW) at the upper 100-150 m of the water column (Rabitti et al., 1994; Malanotte-Rizzoli et al., 1997). MAW flows in an easterly direction getting progressively saltier and warmer till transforming into Levantine Intermediate Water (LIW) into the Levantine Sea where it sinks to mid depths (Milliff and Robinson, 1992; Lascaratos et al., 1993).

The Eastern Mediterranean Deep Water (EMDW) is a relatively well oxygenated water mass, likely as a result of the formation and sinking of warm deep-water that ventilates the deepest levels in the EMS (Schlitzer et al., 1991; Roether and Well, 2001; Meador et al., 2010). Waters from the Adriatic Sea (Adriatic Deep Waters, ADW) have been considered as the main contributor of deep and bottom waters to the EMS (Malanotte-Rizzoli and Hecht, 1988). Nevertheless, the Aegean Sea constitutes a sporadically significant contributor to EMDW through the Cretan Deep Water (CDW), as in the case of the Eastern Mediterranean Transient (EMT) anomaly in the 1990s (Lascaratos et al., 1999; Theocharis et al., 1999). Additionally, the Aegean Sea constitutes a possible secondary source of intermediate waters to the adjacent Ionian and Levantine seas, through outflows across the Cretan Arc straits (Robinson et al., 2001).

Key factors that control the exchanges through the Cretan Arc straits are the thermohaline properties of water masses and mesoscale variability. For example, the Ierapetra anticyclonic gyre, which is located off the southeast corner of Crete (Ierapetra Basin), exhibits a strong seasonal signal that is linked to variations of the outflow across the eastern Cretan Arc straits (Theocharis et al., 1993; Larnicol et al., 2002). Actually, the several permanent and/or recurrent eddies in each of the EMS sub-basins enhance exchanges between continental shelf and slope waters (Robinson et al., 1992; Malanotte-Rizzoli et al., 1997; Millot and Taupier-Letage, 2005), which in turn influence primary productivity and the settling of OM to the deep-sea floor (Danovaro et al., 2010).

Thermohaline circulation and overall environmental conditions make the EMS one of the most ultra-oligotrophic environments of the world ocean (Psarra et al., 2000; Krom et al., 2005; Thingstad et al., 2005; Gogou et al., 2014a). Annual primary production in the EMS averages between 121 and 145 g C m^{-2} y^{-1} (Bosc et al., 2004; Gogou et al., 2014b). However, the fraction of primary production exported below 2000 m of water depth averaged 0.3% (Gogou et al., 2014b). The low autochthonous contribution to OM fluxes in the deep open EMS is counterbalanced by allochthonous inputs resulting from long-range atmospheric transport and deposition by aerial dust (Jickells, 1995; Gogou et al., 1996; Tsapakis and Stephanou, 2005). The overall sedimentation

rate in the deep areas of the open EMS is low (i.e. 2-5 cm kyr^{-1}) (Van Santvoort et al., 1996, 2002; Garcia-Orellana et al., 2009; Stavrakakis et al., 2013).

2.3.3. Material and methods

2.3.3.1. Sampling

Short sediment cores were collected with a multicorer at 29 stations, ranging from 1018 to 4087 m water depth, during six oceanographic cruises in the Ionian Sea, the southern Aegean Sea (Cretan Sea) and the northwestern Levantine Sea from January 2007 to June 2012 (Fig. 2.19 and Table 2.5). Once onboard, multicores were visually described and sliced at 1-cm intervals. Sub-samples collected for grain size, elemental and stable isotopic composition were stored in sealed plastic bags at 4 ºC, while those collected for the analysis of lipid biomarkers were stored in pre-combusted aluminium foils at -20 ºC. Only the undisturbed top centimetre of each sediment core is considered in this study.

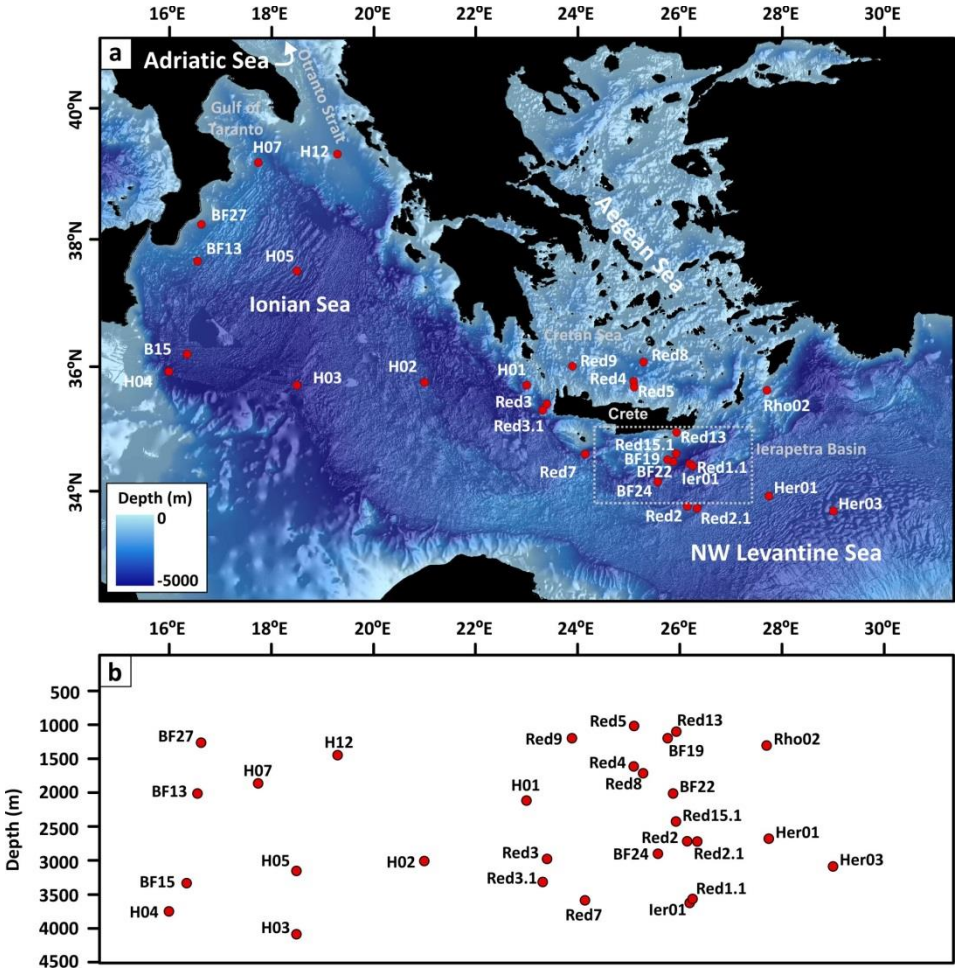

Figure 2.19. (a) Location of sampling sites across the open Eastern Mediterranean Sea (see also Table 2.5). The map was produced using GEBCO Digital Atlas (IOC, IHO and BODC, 2003). (b) Plot of longitude vs. water depth of sampling stations.

Sample Code	Latitude (N)	Longitude (E)	Water depth (m)	Date of collection	Physiographic regions
Ionian Sea					
North					
H12	39.30	19.30	1450	Jan-07	Otranto Valley
H07	39.17	17.75	1866	Jan-07	Taranto Valley
Central					
BF27	38.22	16.63	1264	juny-09	Calabrian Slope
BF13	37.66	16.56	2012	juny-09	Calabrian Arc
BF15	36.20	16.35	3335	juny-09	Ionian Basin
H04	35.92	16.00	3750	Jan-07	Ionian Basin
West					
H02	35.75	21.00	3008	Jan-07	Ionian Basin
H05	37.50	18.50	3154	Jan-07	Ionian Basin
H03	35.70	18.50	4087	Jan-07	Ionian Basin
S. Aegean Sea (Cretan Sea)					
Red5	35.68	25.10	1018	May-10	Cretan Trough
Red9	36.00	23.89	1200	May-11	Cretan Trough
Red4	35.76	25.10	1615	May-10	Cretan Trough
Red8	36.07	25.28	1715	May-11	Cretan Trough
W Cretan Straits					
H01	35.70	23.00	2117	Jan-07	Kithira Strait
Red3	35.40	23.40	2976	May-10	Antikithira Strait
Red3.1	35.30	23.32	3317	May-10	Antikithira Strait
Red7	34.60	24.15	3589	May-11	Ptolemy Strait
NW Levantine Sea					
Ierapetra Basin					
Red13	34.95	25.93	1101	juny-12	Cretan-Rhodes Ridge
BF19	34.51	25.76	1200	juny-09	Hellenic Trench
BF22	34.48	25.87	2015	juny-09	Hellenic Trench
Red15.1	34.61	25.92	2428	juny-12	Hellenic Trench
Red1.1	34.40	26.25	3568	juny-12	Hellenic Trench
Ier01	34.44	26.19	3626	Jan-07	Hellenic Trench
Open Sea					
Rho02	35.62	27.70	1305	Jan-07	Rhodes Strait
Her01	33.92	27.74	2680	Jan-07	EM Ridge
Red2	33.74	26.15	2717	May-10	EM Ridge
Red2.1	33.71	26.34	2720	May-10	EM Ridge
BF24	34.15	25.57	2902	juny-09	Pliny Trench
Her03	33.67	29.00	3090	Jan-07	Herodotus Basin

Table 2.5. Location, depth and collection date of sediment samples. January 2007 samples were collected during the M71 (Leg 3) cruise onboard the R/V Meteor (University of Hamburg, Germany), June 2009 samples during the Biofun1 cruise onboard the R/V Sarmiento de Gamboa (CSIC-UB, Spain), and May 2010, 2011 and June 2012 samples during the ReDEco cruises onboard the R/V Aegaeo (HCMR, Greece).

2.3.3.2. Analytical procedures

2.3.3.2.1. Particle size characterization

The grain size distribution of sediment samples was determined using a Coulter LS230 Laser Diffraction Particle Size Analyzer, which measures sizes between 0.04 and 2000 µm. Prior to analysis, freeze-dried samples were oxidized with a 10% H_2O_2 (v/v) solution in order to remove OM. Each sample was then divided into two sub-samples, one of which was treated with 1M HCl

to remove carbonates and thus obtain the grain size distribution of lithogenic (siliciclastic) particles. Subsequently, both bulk and lithogenic fractions were dispersed into 20 cm^3 of a 5% NaPO5 (v/v) solution and mechanically shaken for 4 hours, and then introduced into the particle size analysed after using a 2000 µm sieve to retain occasional coarse particles that might obstruct the flow circuit of the instrument.

The measured particle size spectrum is presented as % volume in a logarithmic scale, where volume is calculated from particle diameter, assuming spherical shapes. Results were recalculated to percentages of clay (<4 µm), silt (4-63 µm) and sand (63 µm-2 mm).

2.3.3.2.2. Elemental and stable isotopic analysis of carbon and nitrogen

For the determination of total carbon (TC), TN, OC contents and stable isotopic composition of OC ($\delta^{13}C$) freeze-dried and ground sediments were analysed using a Flash 1112 EA elemental analyser interfaced to a Delta C Finnigan MAT isotope ratio mass spectrometer. Samples 108nalysed for %OC and $\delta^{13}C$ were initially de-carbonated using repetitive additions of a 25% HCl (v/v) solution, separated by 60 ºC drying steps, until no effervescence was observed (Nieuwenhuize et al., 1994). Stable isotope data are reported using the conventional per thousand $\delta^{13}C$ notation relative to the Pee Dee Belemnite standard. Uncertainties for elemental composition were lower than 0.1%, while uncertainty for $\delta^{13}C$ was lower than 0.05‰.

In consistency with published data in the Mediterranean Sea we assumed OM as twice the OC content (e.g., Heussner et al., 1996; Masqué et al., 2003). The inorganic carbon content was calculated from the difference between TC and OC measurements. Assuming all inorganic carbon is contained within calcium carbonate, $CaCO_3$ content was determined using the molecular ratio of 100/12.

Molar TN/OC ratios were also calculated. TN/OC is plotted in order to constrain the elemental ratios of N-depleted samples (i.e. TN/OC ≈ 0 rather than OC/TN≈∞) following Goñi et al. (2006), and to avoid the underestimation of the terrestrial-derived carbon fraction (Perdue and Koprivnjak, 2007).

2.3.3.2.3. Biogenic opal and lithogenic fraction analysis

The biogenic silica content was analysed using a two-step 2.5 h extraction with a 0.5M Na_2CO_3 solution, separated by centrifugation of the leachates. Si and Al contents of both leachates were analysed with a Perkin-Elmer Optima 3200RL Inductive Coupled Plasma Optical Emission Spectrometer (ICP-OES), correcting the Si content of the first leachate by the Si/Al ratio of the second one. All values are reported as opal ($SiO_2 \cdot 0.4H_2O$), a parameter defined by 2.4 times the weight percentage of biogenic Si content determined for each sample (Mortlock and Froelich, 1989). The opal detection limit, associated to the detection limit of the ICP-OES system, is approximately 0.2%.

The lithogenic fraction was estimated by subtracting the concentration of the major constituents from total dry weight (%lithogenic= 100 – [%OM + $\%CaCO_3$ + %opal]). This fraction represents the

residual component of particles such as quartz, feldspars, clay minerals and aluminosilicates (Mortlock and Froelich, 1989).

2.3.3.2.4. Lipid biomarkers analysis and definitions of molecular indices

The analytical procedure followed for the determination of lipid biomarkers has been previously presented in detail (Gogou et al., 1998, 2000, 2007). Briefly, freeze-dried sediment samples were initially solvent-extracted three times by sonication with a dichloromethane: methanol mixture (4:1, v/v). Combined extracts were subsequently separated into different compound classes by column chromatography using silica gel that had been activated for 1 hour at 150 °C. The following solvent systems were used to elute different compound classes: (1) *n*-hexane (fraction F_1, aliphatic hydrocarbons), (2) dichloromethane/*n*-hexane (fraction F_2, carbonyl compounds) and (3) ethyl acetate/*n*-hexane (fraction F_3, alcohols, sterols).

F_1 and F_3 fractions were analysed by Gas Chromatography-Mass Spectrometry (GC-MS) while F_2 fractions were analysed by Gas Chromatography using Flame Ionization Detection (GC-FID). Hydroxyl-bearing compounds (fraction F_3) were derivatized to the corresponding trimethylsilyl ethers prior to GC-MS analysis using N,O-bis-(trimethylsilyl)-trifluoroacetamide (BSTFA) + 1% trimethylchlorosilane (TMCS) for 1 hour at 80^{o}C. Details regarding the GC instrumental parameters are presented elsewhere (Gogou et al., 2007; Parinos et al., 2013).

The individual lipids were identified by a combination of comparison of GC-retention times to authentic standards and comparison of their mass spectral data to those in the literature. Quantification was based on the GC-MS or GC-FID response and comparison of peak areas with those of known quantities of standards added prior to the extraction of the sediment samples ([$^{2}H_{50}$]*n*-tetracosane for *n*-alkanes, *n*-hexatriacontane for long-chain alkenones, 5α-androstan-3β-ol for sterols and heneicosanol for *n*-alkanols). The signal of the Unresolved Complex Mixture (UCM) of aliphatic hydrocarbons was defined by the chromatographic area (fraction F_1) between the solvent baseline and the curve defining the base of resolved peaks. UCM quantification was performed relatively to [$^{2}H_{50}$]*n*-tetracosane using the average response factor of *n*-alkanes.

Procedural blanks processed in parallel to the samples were found to be free of contamination. Reproducibility of the analytical method based on multiple extractions of sediments was better than 6% in all cases.

A range of selected lipid biomarkers are considered in this study, namely long chain *n*-alkanes and *n*-alkanols, long-chain alkenones, long-chain diols & keto-ols and a suite of sterols, along with lipid biomarkers' indices, as proxies of organic matter sources and/or degradation. As OC can vary due to the supply of inorganic material (dilution effect) the concentrations of the reported lipid compounds were normalized to OC contents.

The sum of the concentrations of the most abundant high molecular weight *n*-alkanes and *n*-alkanols, which are major components of epicuticular higher plant waxes (Eglinton and Hamilton, 1967; Ohkouchi et al., 1997), are defined, respectively, as:

$$\sum \text{TerNA} = \sum n\text{-}C_{27,29,31,33} \qquad (2.3)$$

$$\sum \text{TerN-OH} = \sum n\text{-}C_{24,26,28,30} \quad (2.4)$$

The sum of the concentrations of the considered lipid biomarkers having a clear marine (algal) origin (see Sect. 5.1.2) was calculated as follows:

$$\sum \text{Mar} = \sum ({}_{28}\Delta^{5,22E} + {}_{30}\Delta^{22E} + C_{30}\text{diols\&keto-ols} + \text{alkenones}) \quad (2.5)$$

The abundance of the Unresolved Complex Mixture (UCM) of aliphatic hydrocarbons, a commonly observed persistent contaminant mixture in marine sediments consisting of branched alicyclic hydrocarbons (Gough and Rowland, 1990), is used as an indicator of the contribution from degraded petroleum products, i.e. chronic oil pollution in the study area (Wang et al., 1999).

The Carbon Preference Indices of long chain *n*-alkanes (CPI_{NA}) and *n*-alkanols ($CPI_{N\text{-}OH}$) have been used as indicators of terrestrial OM degradation with CPI values in fresh leaves being typically >4 (Collister et al., 1994). However, the abundance of non-degraded petroleum hydrocarbons could potentially bias (lower) CPI_{NA} values with increasing petroleum contribution, since *n*-alkane compounds of petroleum products present CPI_{NA} values ~1 (Wang et al., 1999). The indices were calculated, respectively, as:

$$CPI_{NA} = \frac{\sum([n\text{-}C_{25}]\text{-}[n\text{-}C_{33}])}{\sum([n\text{-}C_{26}]\text{-}[n\text{-}C_{34}])} \quad (2.6)$$

$$CPI_{N\text{-}OH} = \frac{\sum([n\text{-}C_{24}]\text{-}[n\text{-}C_{30}])}{\sum([n\text{-}C_{23}]\text{-}[n\text{-}C_{29}])} \quad (2.7)$$

Finally, the abundance ratio of ∑TerNA to ∑TerN-OH is used as a proxy of the proportion of refractory vs. labile terrestrial components, since ∑TerNA are more resistant to degradation than their alcohol counterparts (Eglinton and Hamilton, 1967; Ohkouchi et al., 1997). The ratio is defined as:

$$\frac{[\text{NA}]}{[\text{N-OH}]} = \frac{[\sum \text{TerNA}]}{[\sum \text{TerN-OH}]} \quad (2.8)$$

2.3.3.2.5. Data analysis and presentation

Statistical treatment of grain size data was carried out using the GRADISTAT v. 8.0 software (Blott and Pye, 2001). Median diameter (d50), sorting and skewness were calculated geometrically (in metric units) following the approach of Folk and Ward (1957), which is most appropriate when data are non-normally distributed, as in the case of polymodal sediments from the study area.

D50 was calculated as the average equivalent diameter, which is the diameter where 50% of the sediment sample has a larger equivalent diameter and the other 50% has a smaller equivalent diameter. Sorting (expressed by the standard deviation) indicates the fluctuation in the degree of kinetic energy and the depositional regime on grain size characteristics. Skewness measures the degree of asymmetry onto particle distribution. The skewness for a normal distribution is zero, and any symmetric data should have skewness near zero. Positive values indicate skewness towards the finer grain sizes (skewed left) while negative values indicate skewness towards the

coarser grain sizes (skewed right). The results of grain size distribution analysis were hierarchically clustered (using IBM SPSS Statistics 18.0) according to the above statistical parameters (autoscaled prior to cluster analysis), in order to determine the similarity of samples within each station measuring the squared Euclidean distance.

Principal component analysis (PCA) was performed on standardized grain size and elemental composition data (%clay and sorting of lithogenic and bulk fractions, lithogenic, $CaCO_3$, OC and TN contents), on standardized bulk organic matter signatures (molar TN/OC ratios and $\delta^{13}C$) and on standardized indices and mass-normalized concentrations of lipid biomarkers. A subroutine, the Varimax rotation, was applied to the first three factors in order to maximize or minimize loadings within each factor, and thus simplify the visual interpretation of PCA projections. Correlation analysis was also performed using the same variables. In certain occasions during correlation analysis, the singular stations that were clearly out of the trend were excluded in order to strengthen the evident trends of the examined variables. These stations are explained in detail in the discussion section (see Sect. 5.2).

The spatial distribution of the various geochemical parameters' contents, bulk OM signatures and selected lipid biomarkers' concentrations/indices considered in this study were visualized using Ocean Data View (ODV) (Schlitzer, 2011).

2.3.4. Results

2.3.4.1. Grain size characteristics

The grain size composition (% clay, silt and sand) and the sedimentary parameters (d50, sorting and skewness) are presented in Table 2.6, while the statistical dendrogram, type-averaged grain size spectrum and spatial distributions of grain size types are presented in Figure 2.20.

Silt- and clay-sized particles dominate the bulk sediment, accounting for up to 76.7% and 57.1% of the total weight, respectively (Table 2.6). The lowest values (<40%) for the silt fraction are found in the upper slope of the western Cretan Straits (station Red3) and the northwestern Levantine Sea (station BF19), while the highest values (>65%) correspond to the Ionian Sea (stations H12 and H03). The lowest clay contents (<20%) are also found in the upper slope of the western Cretan Straits (station Red3) but also in the northeastern Ionian Sea (station H12), while maximum values (>55%) are recorded at the northwestern Levantine Sea (station Red1.1 in Ierapetra Basin) and the western Cretan Straits (station H01). Sand contents show large variations, i.e. from 0 to 47.7% (station Red3 in the upper slope of western Cretan Straits), with values less than 2% in most of the stations (Table 2.6). Relatively high values (>10%) are also obtained in the northwestern Levantine Sea (stations Red2, BF19 and BF24). D50 values range between 3.5 and 56.6 μm (Table 2.6).

Sample Code	$Clay_{bulk}$ (% ,<4 μm)	$Silt_{bulk}$ (%, 4-63 μm)	$Sand_{bulk}$ (%, 63 μm-2 mm)	$Sorting_{bulk}$	$Sorting_{litho}$	$Skewnes_{bulk}$	$d50_{bulk}$ (μm)	Lithogenic (%)	$CaCO_3$ (%)	Opal (%)	OC (%)	TN/OC	$\delta^{13}C$ (‰)	OC_{mar} (%)	OC_{terr} (%)
Ionian Sea															
North															
H12	18.1	76.7	5.24	3.47	3.31	-0.13	14.6	71.2	28.5	0.03	0.15	0.08	-24.2	42.3	57.7
H07	41.2	58.8	0.00	3.01	4.12	-0.07	5.34	75.7	22.0		1.15	0.08	-24.4	40.2	59.8
Central															
BF27	52.8	46.1	1.04	3.38	2.83	-0.04	3.97	80.8	17.8	0.16	0.64	0.12	-23.0	60.0	40.0
BF13	50.8	48.1	1.08	3.41	2.92	-0.05	4.17	76.7	22.0	0.21	0.58	0.12	-22.9	62.7	37.3
BF15	39.1	57.0	3.98	4.01	2.91	0.03	5.88	77.9	21.6		0.28	0.14	-22.5	68.8	31.2
H04	41.6	58.4	0.04	4.69	3.53	-0.23	5.52	85.4	13.2	0.04	0.65	0.13	-23.6	50.9	49.1
West															
H02	53.3	46.7	0.00	2.99	6.16	-0.07	3.92	47.7	51.3	0.04	0.45	0.10	-22.5	68.6	31.4
H05	41.6	58.4	0.00	2.98	3.48	-0.01	5.34	60.7	38.2		0.57	0.11	-23.7	50.2	49.8
H03	34.5	65.5	0.08	3.11	3.49	-0.04	7.03	77.6	21.0	0.11	0.63	0.10	-24.6	35.8	64.2
S. Aegean Sea (Cretan Sea)															
Red5	54.0	46.0	0.00	3.32	3.61	-0.01	3.88	32.5	66.5	0.24	0.39	0.10	-22.4	69.2	30.8
Red9	50.1	49.9	0.00	3.24	3.28	-0.01	4.23	46.6	52.2	0.15	0.55	0.12	-22.6	67.4	32.6
Red4	52.6	47.4	0.00	3.26	3.58	-0.06	4.00	39.3	59.8	0.09	0.42	0.12	-22.2	73.0	27.0
Red8	53.1	46.9	0.00	3.12	3.36	-0.03	3.97	44.0	55.3	0.08	0.33	0.15	-22.0	75.5	24.5
W Cretan Straits															
H01	55.1	44.9	0.00	4.74	4.77	-0.11	3.65	42.8	56.6		0.29	0.12	-22.6	66.5	33.5
Red3	14.5	37.9	47.7	5.23	4.54	-0.45	56.6	59.2	39.9	0.15	0.37	0.08	-18.3		
Red3.1	37.7	61.5	0.88	4.32	3.82	-0.07	6.74	55.7	43.0	0.12	0.58	0.09	-22.9	62.4	37.6
Red7	36.0	63.5	0.59	3.55	3.57	-0.01	6.37	61.4	37.5	0.07	0.51	0.12	-22.7	64.7	35.3
NW Levantine Sea															
Ierapetra Basin															
Red13	50.1	49.3	0.66	4.84	3.07	-0.15	4.23	59.1	39.8	0.22	0.46	0.11	-22.3	71.1	28.9
BF19	51.1	38.5	10.4	4.98	3.43	0.27	4.12	39.4	59.9		0.34	0.14	-22.6	67.3	32.7
BF22	47.5	44.0	8.53	4.71	3.34	0.20	4.56	57.7	41.7		0.26	0.15	-21.2	87.7	12.3
Red15.1	47.5	51.8	0.73	4.60	2.77	-0.03	4.59	51.8	46.9	0.80	0.61	0.08	-23.3	56.1	43.9
Red1.1	57.1	42.8	0.15	3.73	2.61	-0.13	3.53	51.8	47.1	0.05	0.54	0.10	-21.5	83.8	16.2
Ier01	49.1	50.4	0.00	3.84	2.67	0.03	4.35	55.6	43.3	0.06	0.52	0.12	-21.7	80.2	19.8
Open Sea															
Rho02	43.0	55.9	1.11	4.43	3.25	-0.14	5.24	58.4	40.6	0.16	0.47	0.12	-22.7	65.2	34.8
Her01	48.2	51.8	0.00	3.88	4.89	0.04	4.44	35.8	63.4	0.13	0.31	0.15	-22.7	65.5	34.5
Red2	32.4	53.2	14.4	4.95	3.85	-0.01	11.1	45.0	53.9	0.07	0.5	0.09	-24.0	46.2	53.8
Red2.1	48.7	51.1	0.21	4.30	3.92	0.11	4.42	44.2	55.0	0.10	0.37	0.11	-22.4	70.5	29.5
BF24	43.1	45.0	11.9	5.25	3.51	0.20	5.34	55.0	44.3	0.11	0.29	0.16	-22.3	70.6	29.4
Her03	39.8	60.2	0.00	4.05	3.20	-0.19	5.81	48.2	50.7	0.11	0.49	0.11	-22.4	70.2	29.8

Table 2.6. Bulk composition and sedimentological parameters of the investigated surface sediments.

Sorting of bulk sediment ranges from 3.0 to 5.2 (Table 2.6). Most of the northwestern Levantine Sea and western Cretan Straits' stations are very poorly sorted and all stations within the southern Aegean Sea and most of the Ionian Sea are poorly sorted (Fig. 2.20a and Table 2. 6). Skewness values for the investigated samples range from −0.45 to 0.27 (Table 2.6), varying from a very clear negative skewness in the upper slope of the western Cretan Straits (station Red3), to positive skewness in the northwestern Levantine Sea (stations Red2.1, BF19, BF22 and BF24).

The hierarchical cluster analysis of all bulk sediment samples resulted into seven grain-size types (Fig. 2.20a). Most of the samples group into cluster types I (n=11), II (n=6) and III (n=6), with grain size profiles almost symmetrical and poorly sorted, and a dominance of clay and silt fractions. Type V includes three very poorly sorted and positive skewed samples from the northwestern Levantine Sea, which consist mainly of clay and silt fractions. Types IV, VI and VII include only one sample each (Red2, H12 and Red3, respectively). Samples Red2 and Red3, dominated by coarse silt fractions (d50 11.1 µm and 56.61 µm, respectively), are both very poorly sorted but with different types of skewed distributions (symmetrical and negatively skewed, respectively). Finally, sample H12, composed mostly of fine silt, is poorly sorted and slight positive skewness.

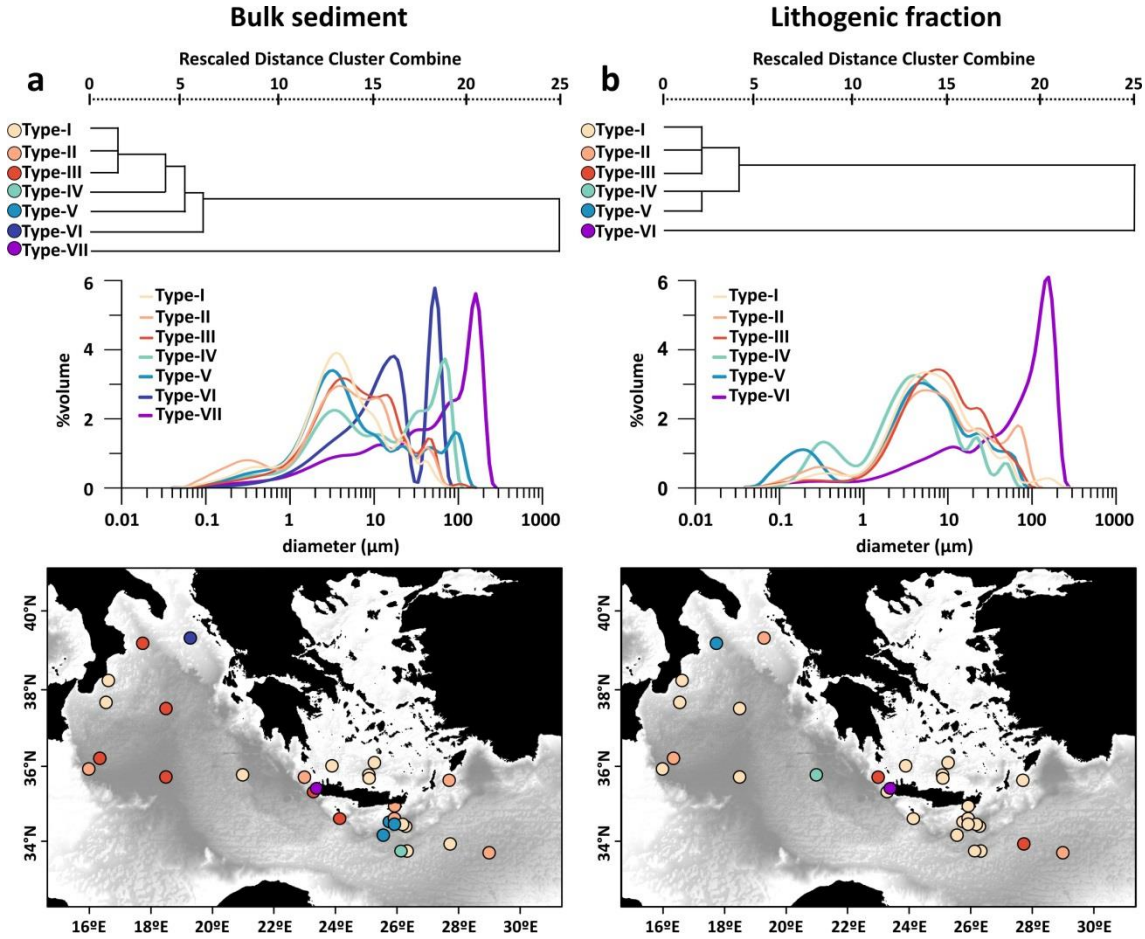

Figure 2.20. Statistical dendrogram of type-averaged grain-size profiles and geographical distribution of grain-size compositional types for a) the lithogenic fraction and b) the bulk fraction of the investigated sediments.

As in the bulk sediment, silt- and clay-sized particles dominate the lithogenic fraction, accounting for up to 73.5% and 50.8% of the total weight, respectively. The hierarchical cluster analysis of the lithogenic fraction identified six grain size types (clusters) (Fig. 2.20b). A majority of samples are highly similar (types I-V), with an average composition of 35.2±5.6% clay, 63.5±5.3% silt and 1.3±2.3% sand, a d50 of 6.6±1.3 µm and a bimodal or trimodal, symmetrical, poorly sorted grain size distribution. Sample Red3 from the upper slope of western Cretan Straits is an exception, in which belongs to type VI. The composition of its lithogenic fraction is 10.3% clay, 34.6% silt and 55.1% sand, with a d50 of 78.1 µm and a bimodal, very poorly sorted and negatively skewed grain size distribution (Fig. 2.20b and Table 2.6).

2.3.4.2. Bulk geochemical sediment composition

The spatial variability of lithogenics, $CaCO_3$, OC and TN contents within the study area is presented in Figure 2.21a-c.

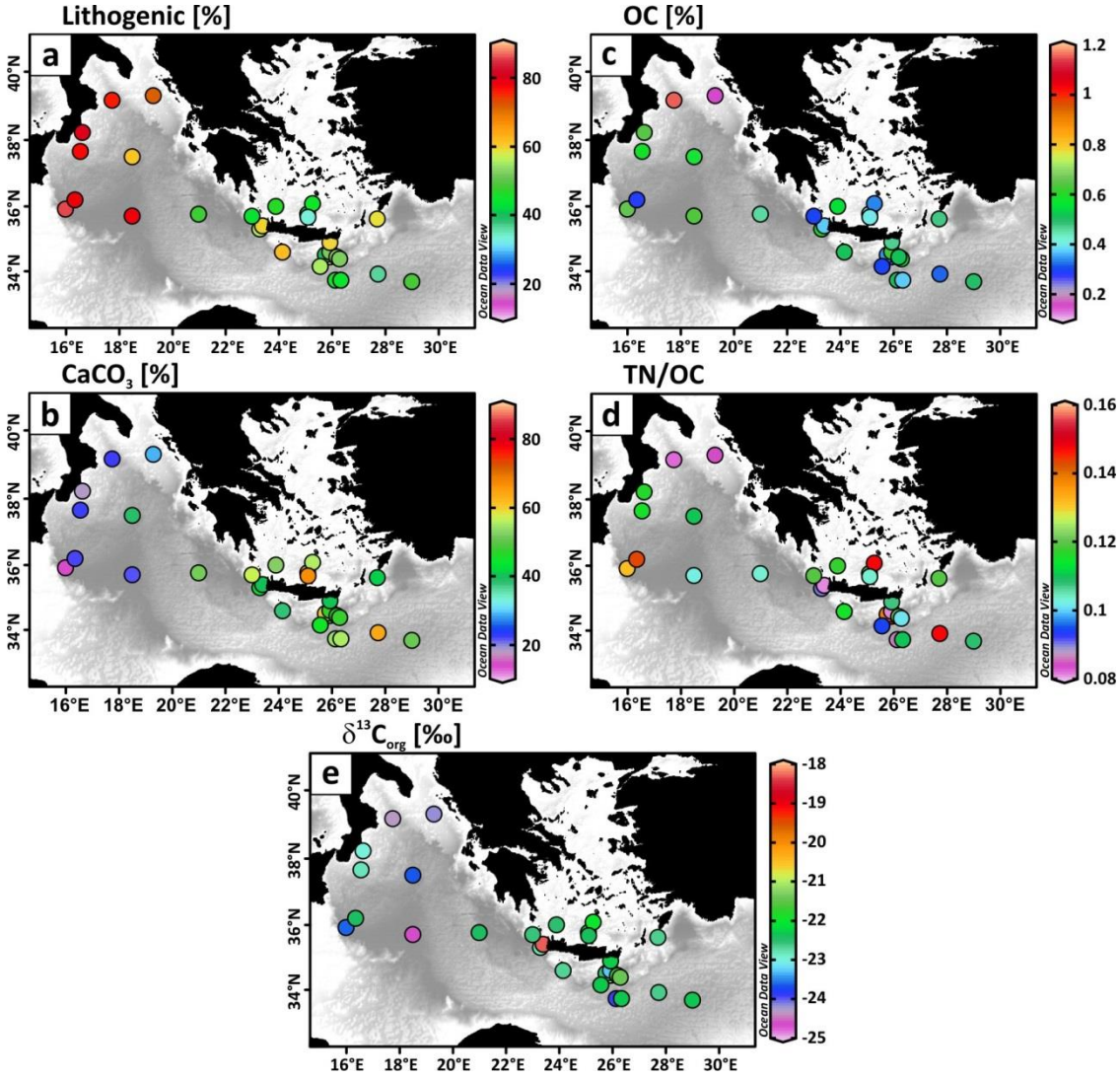

Figure 2.21. Spatial distribution of (a) lithogenics, (b) $CaCO_3$ contents, (c) OC contents, (d) molar TN/OC ratios, and (e) $\delta^{13}C$ values in surface sediments of the deep Eastern Mediterranean Sea.

The lithogenics content in the analyzed surface sediments range between 32.5 and 85.4% (Fig. 2.21a). Higher percentages (>70%) are found in stations of the Ionian Sea (with the exception of station H02), while the lowest percentages (<40%) are found in the southern Aegean (stations Red4 and Red5) and northwestern Levantine seas (stations Her01 and BF19) (Table 2.6). The $CaCO_3$ contents also show a wide range of values throughout the study area, from 13.2 to 66.5% (Fig. 2.21b and Table 2.6). Stations in the western Ionian Sea (H04, BF27, H03, BF15, BF13 and H07) have the lowest $CaCO_3$ contents (<22%), whereas most stations in the southern Aegean and northwestern Levantine seas and in the western Cretan Straits have elevated $CaCO_3$ contents (>40%).

Opal contents are very low, ranging from below detection limits to a maximum of 0.24% in the southern Aegean and northwestern Levantine seas (stations Red5 and Red13) (Table 2.6). Since opal contents are very close to the detection limits, those values can be considered as negligible. Therefore inorganic geochemical fraction of the investigated deep EMS sediments consists only of lithogenic (terrigenous) and carbonate components.

OC contents in the studied samples range from 0.15 to 1.15%, with an average value of 0.47% (Table 2.6). The lowest values are recorded in the northeastern Ionian Sea, south of Otranto Strait (station H12), while the highest values are found off the Gulf of Taranto (station H07), followed by stations in the Ionian Sea (stations BF27, H04 and H03). TN contents range from 0.01 to 0.11% with an average value of 0.06%. TN display a pattern similar to OC, also with the highest values recorded off the Gulf of Taranto (station H07) and the lowest south of Otranto Strait (station H12), both in the northern Ionian Sea.

2.3.4.3. Elemental and stable isotopic composition of sedimentary OM

The spatial distribution of molar TN/OC ratios and $\delta^{13}C$ within the study area is presented in Figure 2.21d-e.

Molar TN/OC ratios of the sedimentary OM range from 0.08 to 0.16 (Fig. 2.21d and Table 2.6). The highest molar TN/OC ratios values (>0.14) are recorded in the southern Aegean (station Red8) and northwestern Levantine (stations Her01, BF22 and BF24) seas, whereas the lowest molar TN/OC ratios (<0.09) are recorded in stations from the northwestern Levantine Sea (station Red15.1), the western Cretan Straits (stations Red3 and Red3.1) and the northern Ionian Sea (stations H07 and H12). However, there is no clear spatial trend (Fig. 2.21d).

The spatial distribution of $\delta^{13}C$ values shows that relatively lower values are more common in the Ionian Sea than in the northwestern Levantine Sea, the southern Aegean Sea and the south Ionian Sea (Fig. 2.21e). $\delta^{13}C$ values range from -18.3 to -24.6‰ (Fig. 2.21e and Table 2.6), with stations from the Ionian Sea (stations H03, H07 and H12) yielding relatively depleted $\delta^{13}C$ values (<-24‰) and stations from the western Cretan Straits (station Red3) and the northwestern Levantine Sea (Ierapetra Basin, stations BF22, Red1.1 and Ier01) having relatively enriched $\delta^{13}C$ values (>-22‰).

2.3.4.4. Lipid biomarkers

The analysed sedimentary aliphatic hydrocarbons comprise of a series of resolved compounds, mainly n-alkanes, and a UCM (Parinos et al., 2013). The UCM dominate amongst aliphatic hydrocarbons in concentrations ranging between 0.50 and 6.64 mg g OC^{-1} (Fig. 2.22a and Table 2.7). Maximum concentrations (>5 mg g OC^{-1}) are recorded in the northwestern Levantine Sea (station Red2.1) followed by the deep central Ionian Sea (station H03). The lowest UCM values (<1.0 mg g OC^{-1}) are obtained in the northern Ionian Sea (station H12) and in the western Cretan Straits (station H01), while rather low values are also recorded in the southern Aegean Sea and west of Crete.

The molecular profile of the *n*-alkanes is dominated by long chain homologues ($C_n \geq 24$), maximizing at *n*-C_{31}, with elevated CPI_{NA} values (4.9±1.6) (Table 2.7). ∑TerNA range between 40.8 and 483 μg g OC^{-1}, with an average value of 172 μg g OC^{-1} (Fig. 2.22b and Table 2.7). The station with the highest concentration (station Red2.1) is found in the northwestern Levantine Sea, while the stations with the lowest ones (<110 μg g OC^{-1}) are located in the northern Ionian Sea (stations H07 and H12) and in the southern Aegean Sea (station Red9). Furthermore, relatively elevated ∑TerNA concentrations (>210 μg g OC^{-1}) are recorded at the deep station of the western Cretan Straits' (station Red3.1) and the deep central Ionian Sea (stations H03 and H05).

The aliphatic alcohol fraction is dominated by a series of *n*-alkanols ranging from *n*-C_{22} to *n*-C_{30}, with maxima at *n*-C_{26}, and elevated $CPI_{N\text{-}OH}$ values (4.5±0.8) (Table 2.7). ∑TerN-OH range from 13.4 to 105 μg g OC^{-1}, with an average of 40.4 μg g OC^{-1}, displaying similar distribution with ∑TerNA (Fig. 2.22c and Table 2.7). The [NA]/[N-OH] ratios for the analysed sediments range between 2.9 and 6.9, with an average of 4.3±0.9 (Table 2.7).

Long-chain di- and tri-unsaturated C_{37} and C_{38} methyl ketones and C_{38} ethyl ketones, commonly referred to as long-chain alkenones, are present in all samples with total concentrations ranging from 3.41 to 30.5 μg g OC^{-1}, 13.0 μg g OC^{-1} on average. The major C_{27}-C_{30} sterols considered in this study, i.e. cholesterol (cholest-5-en-3β-ol; $_{27}\Delta^{5}$), brassicasterol (24-methylcholesta-5,22-dien-3β-ol; $_{28}\Delta^{5,22}$), β-sitosterol (24-ethylcholesta-5-en-3β-ol; $_{29}\Delta^{5}$) and dinosterol (4α,23,24-trimethyl-5α(H)-cholest-22(E)-en-3β-ol $_{-30}\Delta^{22}$), have total concentrations ranging between 10.3 and 62.4 μg g OC^{-1}, averaging 31.7 μg g OC^{-1}. Long-chain C_{30} *n*-alkan-1,15-diols and the corresponding C_{30} keto-ols are also found in concentrations ranging from 7.30 to 35.81 μg g OC^{-1}, with an average of 20.3 μg g OC^{-1} (Table 2.7).

∑Mar range between 18.2 to 72.6 μg g OC^{-1}, 43.6 μg g OC^{-1} on average (Fig. 2.22d and Table 2.7), displaying a generally increasing eastward trend with maximum concentrations (>55 μg g OC^{-1}) recorded in the deep northwestern Levantine Sea (stations Red2.1, Her01, Ier01 and Red7). Elevated ∑Mar values are also recorded at stations Red3 in the upper slope of the western Cretan Straits, but also stations H04 and H05 in the deep Ionian Sea. The lowest values (<40 μg g OC^{-1}) are obtained in the southern Aegean Sea (stations Red8, Red9), the northern Ionian Sea (station H12) and the western Cretan Straits (station H01).

Station	∑TerNA[a] (μg g^{-1} OC)	∑TerN-OH (μg g^{-1} OC)	∑Mar (μg g^{-1} OC)	∑Alkenones[b] (μg g^{-1} OC)	∑C_{30} diols&keto-ols[c] (μg g^{-1} OC)	∑Sterols[d] (μg g^{-1} OC)	$_{27}\Delta^{5}$ (μg g^{-1} OC)	$_{28}\Delta^{5,22}$ (μg g^{-1} OC)	$_{29}\Delta^{5}$ (μg g^{-1} OC)	$_{30}\Delta^{22}$ (μg g^{-1} OC)	CPI_{NA}[a]	CPI_{N-OH}	[NA]/ [N-OH]
Ionian Sea													
North													
H12	54.9	19.0	29.4	6.75	14.7	62.4	29.7	3.22	24.8	4.72	4.14	4.00	2.90
H07	40.8	13.4	34.5	5.97	14.6	35.6	6.77	5.52	14.9	8.37	4.39	4.14	3.03
Central													
BF27													
BF13													
BF15													
H04	169	52.1	54.1	12.3	21.5	59.6	10.6	8.57	28.6	11.7	4.04	5.95	3.24
West													
H02	176	35.2	34.2	8.14	19.7	17.1	3.67	2.36	7.06	3.96	3.57	3.73	5.00
H05	211	42.8	47.2	12.5	25.0	24.2	4.12	3.43	10.4	6.28	4.07	3.63	4.93
H03	214	37.0	35.7	8.77	17.4	25.2	6.04	3.65	9.62	5.92	2.80	4.08	5.78
S. Aegean Sea (Cretan Sea)													
Red5	206	50.7	45.3	20.1	15.9	40.1	10.8	4.74	20.0	4.51	5.07	4.89	4.06
Red9	101	14.7	22.2	9.85	7.30	17.7	3.77	2.66	8.83	2.42	7.25	5.12	6.88
Red4	196	48.4	41.0	17.4	14.8	38.6	11.5	4.63	18.3	4.15	5.36	5.21	4.05
Red8	127	29.4	35.5	16.8	12.3	26.3	5.62	3.23	14.2	3.20	6.40	4.97	4.32
W Cretan Straits													
H01	127	26.2	18.2	3.41	11.3	10.3	2.22	1.35	4.55	2.22	6.64	6.13	4.84
Red3	120	30.4	70.1	21.2	28.1	34.4	7.85	9.33	5.79	11.4	2.90	4.27	3.93
Red3.1	218	50.0	29.0	10.8	11.8	20.7	3.87	3.15	10.4	3.30	3.63	4.02	4.37
Red7	184	43.7	59.2	30.5	19.4	28.6	6.17	3.61	13.1	5.69	3.99	4.63	4.21
NW Levantine Sea													
Ierapetra Basin													
Red13	156	36.8	38.8	14.1	16.1	34.5	10.2	4.97	15.8	3.60	7.95	5.82	4.24
BF19													
BF22													
Red15.1	126	28.3	32.6	11.5	14.1	21.3	4.20	3.21	10.1	3.88	5.26	5.03	4.44
Red1.1	166	38.6	36.9	14.1	14.7	23.9	5.14	3.67	10.7	4.39	6.07	4.79	4.30
Ier01	206	44.4	59.0	11.1	35.0	29.8	4.94	4.69	11.9	8.30	6.37	3.68	4.63
Open Sea													
Rho02	166	49.9	51.2	5.92	33.2	30.2	5.56	4.90	12.6	7.17	6.88	4.68	3.33
Her01	195	52.2	66.3	14.2	35.8	46.5	11.3	7.59	18.9	8.71	4.43	3.70	3.74
Red2													
Red2.1	483	105	72.6	23.6	35.5	47.8	7.86	6.54	26.4	6.97	1.93	4.23	4.59
BF24													
Her03	157	39.7	45.7	7.95	29.5	22.2	4.57	3.05	9.39	5.23	3.69	3.49	3.96

*empty cell = not determined

[a] reported by Parinos et al., 2013

[b] Sum of the concentrations of C37:3M, C37:2M, C36:2FAME, C38:3Et, C38:3M, C38:2Et, C38:2M (the corresponding unsaturated homologues are indicated with the number of their carbon atoms (n) and the number of double bonds (x)-(Cn:x); M: methyl; Et: Ethyl; FAME: Fatty acid methyl ester).

[c] Sum of the concentrations of long-chain C_{30} *n*-alkan-1,15-diols and C_{30} keto-ols

[d] Sum of the major C_{27}-C_{30} sterols considered in this study i.e., cholesterol (cholest-5-en-3β-ol; $_{27}\Delta^{5}$), brassicasterol (24-methylcholesta-5,22-dien-3β-ol; $_{28}\Delta^{5,22}$), β-sitosterol (24-ethylcholesta-5-en-3β-ol; $_{29}\Delta^{5}$) and dinosterol (4α,23,24-trimethyl-5α(H)-cholest-22(E)-en-3β-ol $_{30}\Delta^{22}$)

Table 2.7. Concentrations (OC-normalized) and indices of the considered lipid biomarkers

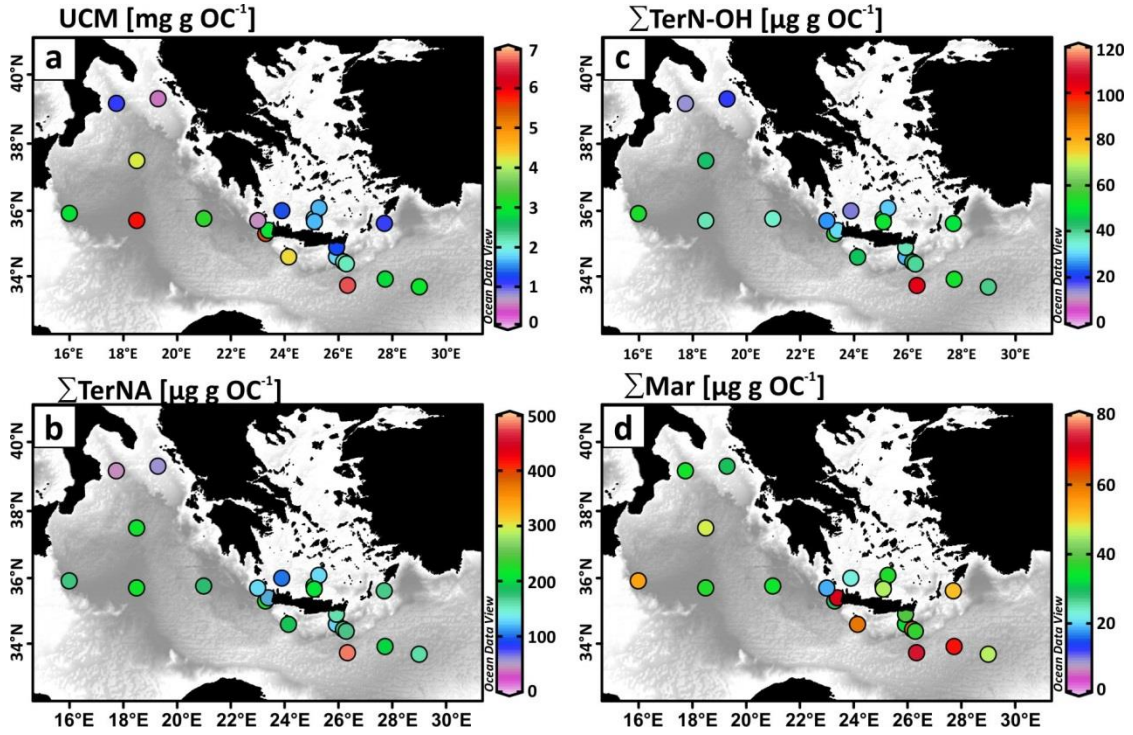

Figure 2.22. Spatial distributions of the OC-normalized concentrations of (a) Unresolved Complex Mixture (UCM), (b) ∑TerNA, (c) ∑TerN-OH and (d) ∑Mar in surface sediments of the deep Eastern Mediterranean Sea. Abbreviations of lipid biomarkers are defined in the text.

2.3.4.5. Multivariate analysis of geochemical parameters

Three main principal components (PCs) are identified from PCA, accounting for 64.3% of the variation within the data set (23.8%, 22.8% and 17.7% for PC1, PC2 and PC3, respectively). PC1 is characterised by positive loadings for water depth, ∑TerNA, ∑TerN-OH, ∑Mar, UCM and negative loadings for CPI_{NA} and $CPI_{N\text{-}OH}$. The highest positive loadings on PC2 are associated to $\%CaCO_3$, %clay in the bulk sediment and TN/OC values, while negative loadings are associated to %lithogenics. Finally, the geochemical parameters with high positive loadings on PC3 are %OC, %TN, and %clay of the lithogenic fraction, while those with negative loadings are $\delta^{13}C$ and sorting of bulk sediment (Fig. 2.23a).

Factor scores on each PC display significant variability amongst the studied stations, both within the same area and from one area to another (Fig. 2.13b). High positive factor scores on PC1 are observed both in stations to the west (Ionian Sea) and east (western Cretan Straits and northwestern Levantine Sea). For PC2, an eastward increasing contribution of positive factor score values seems to exist, with the highest ones located in the southern Aegean Sea and the northwestern Levantine Sea. In contrast, the prevalence on PC3 is recorded in stations of the Ionian Sea and in parts of the northwestern Levantine Sea (Ierapetra Basin).

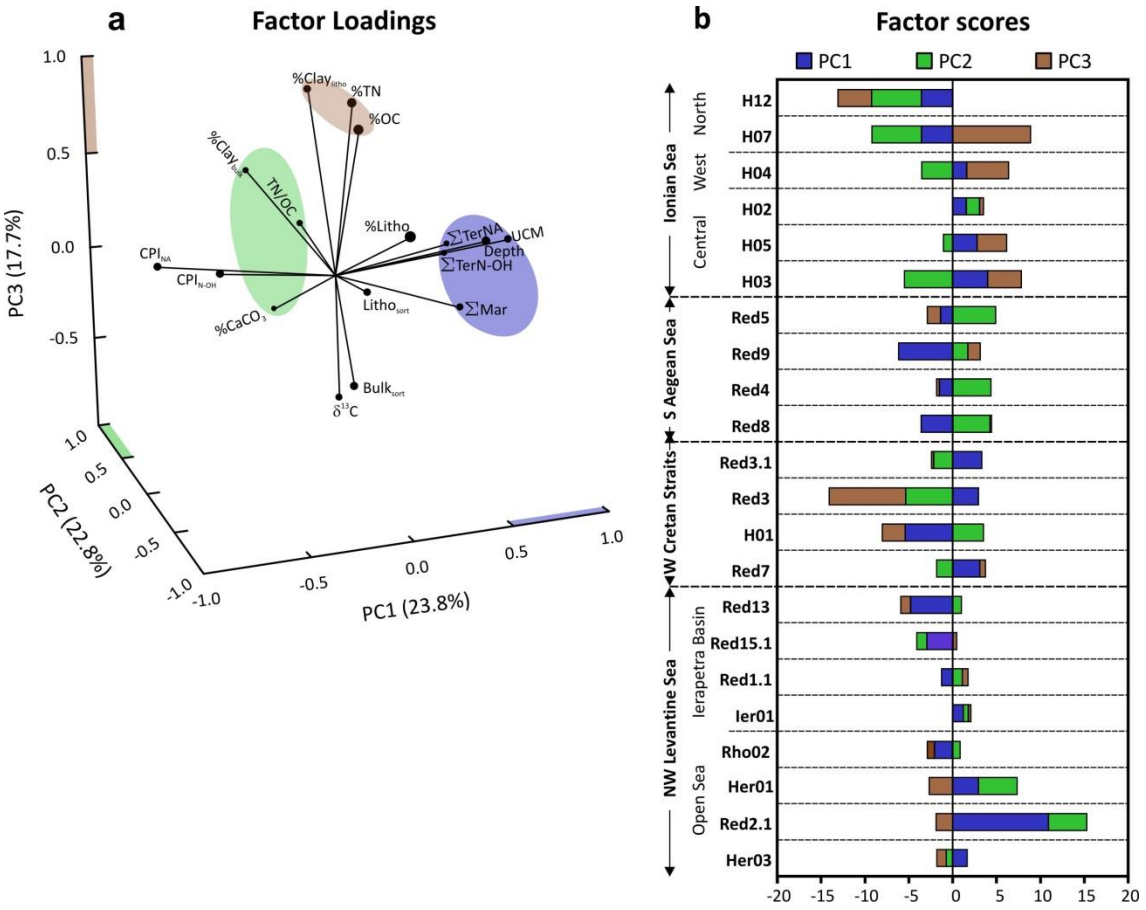

Figure 2.23. (a) Scatter plot of the factor loadings of the three principal components obtained in the Principal Component Analysis, and (b) plot of the scores found at each station. Abbreviations of lipid biomarkers are defined in the text.

The contents of $CaCO_3$ show an increasing north-south and west-east gradient (Figs. 2.21b and 2.23). In the southern Aegean Sea, the northwestern Levantine Sea and the western Cretan Straits' stations, $CaCO_3$ contents are positively correlated to %clay of the bulk sediment ($r=0.48$, $p<0.05$) and to alkenone concentrations ($r=0.62$, $p<0.05$). Lithogenic contents are higher in the north and west (Ionian Sea) while being significantly positively correlated to OC and TN contents ($r=0.65$ and $r=0.72$, $p<0.05$, respectively, excluding stations BF15, H07 and H12 of the Ionian Sea). Furthermore, OC and TN contents of stations deeper than 2100 m show a significant positive correlation to water depth ($r=0.54$ and $r=0.70$, respectively, $p<0.05$). However, this is not highlighted by the PCA. A significant positive correlation is also observed for OC and TN contents in the analysed samples ($r=0.87$, $p<0.0001$) (Fig. 2.24a).

Surface sediments of the Ionian Sea show a significant ($p<0.05$) positive correlation of OC and TN contents to %clay ($r=0.80$ and $r=0.73$), and a negative correlation to %silt ($r=-0.75$ and $r=-0.65$) and d50 of the lithogenic fraction ($r=-0.79$ and $r=-0.83$). $\delta^{13}C$ values (excluding station Red3 of the western Cretan Straits) are significantly ($p<0.05$) and positively correlated to $CaCO_3$ contents ($r=0.53$), %clay of the bulk sediment ($r=0.65$) and molar TN/OC ratios ($r=0.53$), and negatively correlated to %OC ($r=-0.46$), %silt ($r=-0.66$) and d50 ($r=-0.59$) of the bulk sediment.

Terrestrial lipid biomarkers concentrations (∑TerNA and ∑TerN-OH) display a significant positive correlation amongst them (r=0.95, p<0.0001), but also to %clay (both with r=-0.55, p<0.05) and d50 (r=0.62 and r=0.58, respectively, p<0.01) of the bulk lithogenic fraction. Moreover, ∑TerNA and ∑TerN-OH show a significant positive correlation (p<0.05) to β-Sitosterol ($_{29}\Delta^{5}$) (r=0.71 and r=0.56, respectively, excluding stations H07 and H12 of the Ionian Sea). ∑TerNA and ∑TerN-OH (not normalized to OC contents) are also significantly correlated to OC (r=0.81 and r=0.76, respectively, p<0.001), again excluding stations H07 and H12 of the Ionian Sea. ∑Mar (not normalized to OC contents) display a significant positive correlation with OC (r=0.7, p<0.001), while a significant positive correlation (r>0.65, p<0.005 in all cases) is evident amongst the concentration of cholesterol ($_{27}\Delta^{5}$) and marine algal markers ($_{28}\Delta^{5,22E}$, $_{30}\Delta^{22E}$, C_{30} diols&keto-ols and alkenones; see Sect. 5.2.1).

2.3.5. Discussion

2.3.5.1. Sources of sedimentary material in the deep Eastern Mediterranean Sea

Clearly, the surface sediments of the deep EMS mostly consist of lithogenics and carbonates, have low OC contents while opal is nearly absent (Table 2.6). The range of lithogenics, carbonates and opal contents recorded in the investigated samples are similar to those previously reported for the Eastern Mediterranean Sea (Emelyanov and Shimkus, 1986; Bethoux, 1989; Cros, 1995; Kemp et al., 1999; Rutten et al., 2000; Struck et al., 2001). OC contents reach values slightly above 1% and are also comparable to those found in the Eastern Mediterranean Sea (0.56-1.51%, Danovaro et al., 1993; 0.23-0.99%, Bianchi et al., 2003; 0.30-0.82%, Gogou et al., 2000; 0.25-1.73%, Polymenakou et al., 2006), and relatively lower than those found in the Western Mediterranean Sea (0.80-1.60%, Kaiser et al., 2014; 0.47-1.53%, Masqué et al., 2003; 0.23-1.85%, Roussiez et al., 2006). Values found are comparable to the typical hemipelagic sediments found in continental slopes (Rullkötter, 2006) and slightly higher than those in deep basin areas (Seiter et al., 2004).

2.3.5.1.1. Lithogenics and carbonate

The grain size of the lithogenic fraction found in the studied sediments is very similar to that of Saharan dust particles, which mainly consist of clayey silts and silty clays with diameters ranging from 0.5 to 60 μm (d50 ~5 μm) and two main modes at 3-4 μm and 60 μm (Ratmeyer et al., 1999; Guerzoni and Molinaroli, 2005 and references therein). This strongly suggests that the Sahara desert is the main source of lithogenics to the deep EMS. This is further supported by observations pointing to Saharan dust transported by southerlies blowing over the great North African desert as the main lithogenic input to the EMS (Guerzoni et al., 1999; Weldeab et al., 2002). The Saharan dust spreads rather uniformly across the EMS (Rutten et al., 2000; Jickells et al., 2005). Furthermore, but to a lesser extent, volcanic ash deposition into the EMS represents another external source of fine-grained particles (<5-50 μm) (Kelepertsis et al., 2003). Mount Etna, located on the island of Sicily, generates volcanic ash plumes that are transported by the wind reaching as far as Greece and Libya (Olgun et al., 2013 and references therein).

Riverine inputs have a rather minor influence onto the open EMS sedimentation as they are small and localized (Weldeab et al., 2002; Statham and Hart, 2005). The relatively higher lithogenic contents found in most of the Ionian Sea stations (Fig. 2.21a and Table 2.6) points to fluvial inputs reaching the area from the Adriatic Sea. The main source of riverine inputs is the Po River, opening into the northernmost end of the Adriatic Sea, although inputs from smaller rivers draining the Apennines could be also relevant (Weldeab et al., 2002). In the Ionian Sea, river-sourced particles are carried by both surface and deep currents flowing southwards along the Italian Peninsula as part of the overall anticlockwise circulation in the Adriatic Sea (Orlic et al., 1992). It should be noted that dense water formation takes place seasonally in the Adriatic Sea, which triggers episodes of fast-flowing, sediment-loaded dense near-bottom currents that cascade into the deeper Meso Adriatic depression before passing through the Otranto Strait, subsequently spreading into the Ionian Sea where their particle load settles to the bottom (e.g., Zoccolotti and Salusti, 1987; Manca et al., 2002; Canals et al., 2009).

The grain-size variability of the carbonate particles recorded in the studied sediment samples is indicative of calcareous skeletons of primary producers. While the abundance of particles <8 μm is attributable to coccoliths, which is the most abundant primary producer in the EMS (Emelyanov and Shimkus, 1986), coarser carbonate particles mostly correspond to shells and fragments of calcareous dinoflagellates and planktonic foraminifers, in agreement with Ziveri et al. (2000) and Frenz et al. (2005). Although part of the carbonate fraction might also have a terrestrial provenance as transported, for instance, with Saharan dust (Chester et al., 1977; Correggiari et al., 1989; Rutten et al., 2000), this does not seem to be the case with the investigated samples. Like other 121eolian particles, 121eolian carbonates are typically better sorted than those formed in situ, as shown by a well-sorted unimodal distribution due to gravitational settling during atmospheric transport (Skonieczny et al., 2013). The predominance of very poorly sorted grain-size distributions within the bulk sediment samples (Fig. 2.20a) and the highly variable $CaCO_3$ contents (Fig. 2.21b) in the investigated samples, suggests that even within such a highly oligotrophic environment biogenic carbonates are the main source of $CaCO_3$ in the deep EMS.

2.3.5.1.2. Sources of sedimentary organic matter

Bulk geochemical proxies such as elemental (TN/OC) and stable isotopic ratios of OC ($\delta^{13}C$) have been widely used to assess the sources of OM in marine sediments (Meyers, 1994; Goñi et al., 2003; Hu et al., 2006). Sedimentary molar TN/OC ratios and $\delta^{13}C$ values determined in this study are consistent with values previously reported for surface sediments of the deep EMS (Tesi et al., 2007b; Meyers and Arnaboldi, 2008; Carlier et al., 2010; Goudeau et al., 2013).

Marine-derived OM is characterized by high TN contents yielding TN/OC ratio values >0.12, while vascular plants are N-depleted yielding TN/OC ratio values <0.08 (Redfield et al., 1963; Hedges and Oades, 1997). $\delta^{13}C$ values in marine algae from low- to mid- latitude temperate seas vary from -18‰ to -22‰ (Goericke and Fry, 1994; Meyers, 1994; Harmelin-Vivien et al., 2008), whereas most terrestrial OM inputs from C3 plants show depleted $\delta^{13}C$ values ranging from -25‰ to -28‰ (Hedges et al., 1997).

In order to constrain the origin of sedimentary OM and assess the spatial variability in its marine-to-terrestrial blend molar TN/OC ratios were plotted against $\delta^{13}C$ values. Plots show that the elemental and isotopic composition of sedimentary OM fall out of the typical compositional ranges of the potential sources (Fig. 2.24b). Excluding station Red3, located in the upper slope of western Cretan Straits, an overall positive relationship for molar TN/OC ratios and $\delta^{13}C$ values ($r=0.53$, $p<0.05$) becomes apparent (Fig. 2.24b), thus indicating that the composition of the OM in the studied sediment samples could be explained as a mixture of terrigenous (low TN/OC and $\delta^{13}C$) and marine (high TN/OC and $\delta^{13}C$) derived materials.

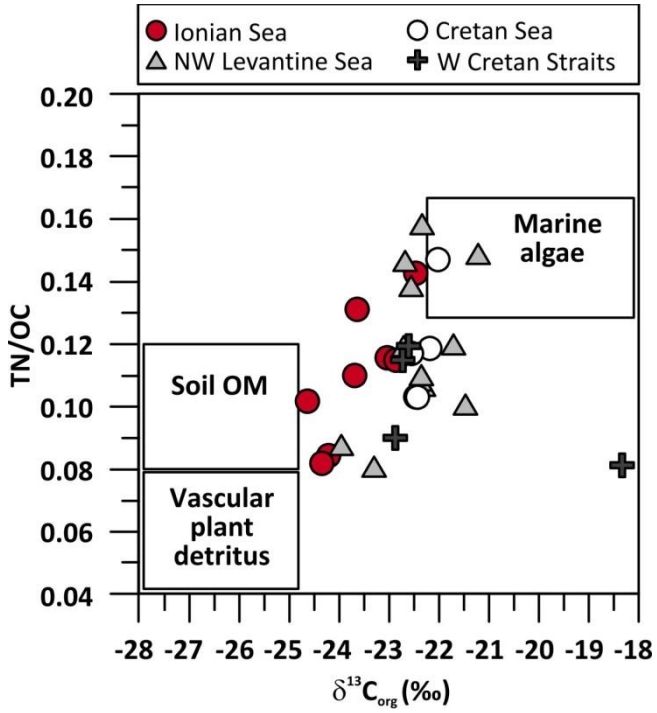

Figure 2.24. (a) Co-plot of the weight percent content of nitrogen (TN) vs. organic carbon (OC) for the deep-sea surface sediments analysed. The linear fit of the data is shown (dotted line) along with the Redfield ratio N_{16}/C_{106} associated with the fresh marine phytoplankton (0.17 wt. /wt.). (b) Plot of molar TN/OC ratios vs. $\delta^{13}C$, in surface sediments of the deep Eastern Mediterranean Sea. The compositional ranges of organic matter sources illustrated in plots (boxes) derive from previously published studies (see section 5.1).

Additionally, the relative contribution of the marine vs. terrestrial sources of OC over the study area has been evaluated by means of a simple $\delta^{13}C$ –based binary mixing model (Table 2.6), where a marine $\delta^{13}C$ value of -20.4‰ and a terrestrial $\delta^{13}C$ value of -27.0‰ (Tesi et al., 2007a) are assumed, considering that the contribution of C4 vascular plants ($\delta^{13}C$ from -12 to -15‰) can be considered negligible throughout the study area (e.g., Collatz et al., 1998).

As evident in Table 2.6, sediments from the Ionian Sea are characterized by elevated contributions of terrestrial OC (OC_{terr}), reaching up to 64.2%. In contrast, W Cretan Straits, Cretan Sea and NW Levantine Sea stations show low OC_{terr} contributions and marine OC (OC_{mar}) peaks of 87.7% (see also section 5.2). The elevated OC_{terr} values recorded in the Ionian Sea suggest that

terrigenous OM entering the Adriatic Sea escapes towards the deep Ionian basins. Indeed, during energetic dense shelf water cascading events, lateral flux prevails over the vertical flux in the southern Adriatic Sea and the contribution of soil-derived OC increases up to ~60% (Turchetto et al., 2007; Tesi et al., 2008). Despite the relatively high OC_{terr} found preserved in the deep Ionian Sea, values are lower than those recorded in areas impacted by extreme events such as storms that enhance the export of organic matter from the shelf to the deep environment, for example in the western Mediterranean (up to 78% of OC_{terr}) (Pedrosa-Pàmies et al., 2013) and the East China Sea (up to 90%) (Selvaraj et al., 2015).

Lipid biomarkers have often been used as molecular proxies to identify specific biological precursors of sedimentary OM (Meyers, 1997; Volkman, 2006). The concentrations of the sedimentary lipid biomarkers determined in this study are fairly comparable to those previously reported in areas devoid of significant fluvial influence both in the Eastern and Western Mediterranean basins (Grimalt and Albaigés, 1990; Gogou et al., 2000; Gogou and Stephanou, 2004; Kaiser et al., 2014).

The patterns of long-chain n-alkanes and n-alkanols with elevated CPI_{NA} and $CPI_{N\text{-}OH}$ values (Sect 4.4; Table 2.7), respectively, indicate the presence of allochthonous natural (terrigenous) inputs from epicuticular higher plant waxes (Eglinton and Hamilton, 1967). Saharan dust is probably the main vector for the transport of small charcoal-like fragments of burnt vegetation, leaf wax-derived lipids absorbed on clays, and cuticular fragments into the open EMS, given the relatively minor direct influence of riverine inputs (Gogou et al., 1996; Eglinton et al., 2002).

Lipid biomarkers preserved in the surface sediments of the study area also highlight the contribution from autochthonous marine OM derived from *in situ* phytoplankton production. More specifically, the abundance of brassicasterol ($_{28}\Delta^{5,22E}$) reveals the presence of diatoms and prymnesiophytes, while dinosterol ($_{30}\Delta^{22E}$) is a major compound in dinoflagellates (Volkman, 1986). The presence of long-chain alkenones reflects the productivity from algal species of the *Prymnesiophyte* class, e.g., *Emiliania huxleyii* (Marlowe et al., 1984), which constitute the dominant primary producers across the Mediterranean Sea (Ziveri et al., 2000; Triantaphyllou, 2004). Regarding the long-chain C_{30} *n*-alkan-1,15-diols and the corresponding C30 keto-ols, although their major sources remain unknown, microalgae of the genus Nannochloropsis (class *Eustigmatophyceae*) are potential sources, while C_{30} keto-ols might result from oxidation of the corresponding C_{30} diols (Volkman, 1986; Volkman et al., 1999; Rampen et al., 2012).

In addition, while the abundance of cholesterol ($_{27}\Delta^{5}$) highlights the existence of marine consumer organisms such as zooplankton and benthic animals (Grice et al., 1998), β-sitosterol ($_{29}\Delta^{5}$) may derive from both terrigenous and marine sources (Volkman, 1986). In the study area however, the positive correlation between ∑TerNA (and ∑TerN-OH) and β-sitosterol argues for a dominant terrestrial origin for this compound.

Aside from natural sources, the abundance of UCM indicates a contribution of anthropogenic OM resulting in chronic oil pollution of the investigated sediments (Parinos et al., 2013). UCM levels recorded in the deep EMS are comparable to those reported for surface sediments in unpolluted coastal and/or open-sea areas and are at least one order of magnitude lower than those reported for coastal areas subjected to enhanced anthropogenic inputs (Gogou et al., 2000; Parinos et al., 2013; Kaiser et al., 2014; Romero et al., 2015; and references therein). Two main pathways have

been identified for the introduction of petroleum hydrocarbons into the deep EMS, which are direct discharges from merchant shipping and oil transportation (UNEP, 2010) and atmospheric transport and deposition (Gogou et al., 1996; Castro-Jiménez et al., 2012; Parinos et al., 2013).

2.3.5.2. Regional variability and oceanographic control on the geochemical composition of deep Eastern Mediterranean Sea surface sediments

The PCA provides a robust overview of the variables and processes controlling the geochemical composition of the investigated deep-sea surface sediments (Fig. 2.23).

The significant positive loadings of ∑TerNA, ∑TerN-OH, ∑Mar, UCM and depth on PC1 are indicative of a considerable contribution from both natural (marine and terrestrial) and anthropogenic (degraded petroleum products) OM preserved in deep-sea surface sediments of the EMS. Moreover, the negative PC1 loadings of CPI_{NA} and $CPI_{N\text{-}OH}$ ratios vs. depth indicate that the terrestrial OM is relatively altered with increasing water column depth. Although the negative PC1 loading of CPI_{NA} ratio could be also indicative of an enhanced contribution from non degraded petroleum inputs, the patterns of aliphatic hydrocarbons for the investigated sediment samples indicate no important bias associated to non degraded petroleum products on CPI_{NA} ratio values (Parinos et al., 2013). Overall, PC1 represents the degradation processes and fate of the sedimentary OM in the study area.

The second PC separates samples with high carbonate contents, molar TN/OC ratios and enhanced contribution of clay-sized particles from those with high lithogenic contents. Therefore, samples with positive loadings on PC2 are enriched in fine marine carbonate particles, while those with negative loadings are enriched in lithogenic particles (see section 5.2.2).

Finally, PC3 separates samples with high contents of OC, TN and clays from those with high values of $\delta^{13}C$. Consequently, positive loadings on PC3 are associated to sediments with an enhanced contribution of OC-rich fine particles, thus pointing to hydrodynamic processes that control grain size sorting and remobilization/deposition of sedimentary material with different OC contents (see section 5.2.2).

2.3.5.2.1. Processes modulating the biogeochemical signal of the sedimentary organic matter

The low OC and TN contents in the surface sediments of the study area reflect the oligotrophic character of the EMS (e.g., Krom et al., 2003). In the studied sediments some processes may have further pushed TN to OC ratios towards low values (Fig. 2.24a). These include the preferential degradation of N-rich proteinaceous components of algal OM during early diagenesis (Meyers et al., 1996; Meyers, 1997; Hopmans et al., 2004) and the enrichment of OC relative to TN due to the input of petroleum residues (Friligos et al., 1998). Furthermore, a significant contribution of inorganic N, presumably as NH4+ adsorbed on clays (Müller, 1977; Meyers, 1997), is inferred from the positive intercept on the N axis at around 0.02% (Fig. 2.24a).

Although isotopic fractionation specifically associated with early diagenesis is negligible and the isotopic composition of sedimentary OM is fairly conservative (e.g., Di Leonardo et al., 2009 and references therein), $\delta^{13}C$ values can be potentially shifted by microbial rearrangements (Lehmann et al., 2002) and inputs of anthropogenic OM. $\delta^{13}C$ values for crude oil and petroleum products are in the order of -28.5‰ and -28.9‰, respectively (Rumolo et al., 2011 and references therein). In the study area, the positive PC1 loadings of depth and UCM indicate an enhanced contribution of degraded petroleum products with increasing water depth. This points to an enrichment of the sediments in degraded petroleum hydrocarbons in the deep Ionian Sea and western Cretan Straits' stations H03 and Red3.1 where such an isotopic shift is observed (Figs. 2.21e and 2.25), in addition to maximum concentrations of UCM along with relatively low molar TN/OC ratios (<0.11) (Figs. 2.21d and 2.22a and Table 2.6).

Lipid biomarkers provide further information on the natural sources of sedimentary OM. The significant positive correlation of ∑TerNA and ∑TerN-OH concentrations (not normalized to OC) to OC contents suggests a close association of terrestrial OM to OC, while the significant positive correlation of ∑TerNA and ∑TerN-OH to %clay suggests that the transport and accumulation of terrestrial OM is associated to fine particles (see section 5.2.2). The relatively uniform spatial distribution of CPI_{NA} and $CPI_{N\text{-}OH}$ ratio values (Fig. 2.26) together with the negative PC1 loadings of CPI_{NA} and CPIN-OH ratios vs. depth (Fig. 2.23), are overall indicative of the reworking of the terrestrial OM accumulated in deep EMS basins. Moreover, the elevated values of the [NA]/[N-OH] ratio in the study area (Fig. 2.26 and Table 2.7) are indicative of the enhanced degradation of ∑TerN-OH relatively to ∑TerNA. The above are rather consistent with the long-range atmospheric transport, and long residence time in the water column and into the sediments of the terrestrial OM, and the fact that ∑TerNA are more resistant to degradation than their alcohol counterparts (Gogou and Stephanou, 2004). Moreover, the relatively elevated retention time of terrestrial OC in the inner shelf of the Adriatic Sea before being conveyed to the Ionian Sea by dense shelf water cascading events, allows for its significant microbial degradation or marine dilution (Tesi et al., 2008).

While a significant positive correlation is observed for ∑Mar concentrations (not normalized to OC contents) and OC, indicating that the latter exerts an important control on the distribution of algal markers' concentrations in the study area, no significant correlation is observed between ∑Mar and grain size. These correlations together with the deviation trend observed for molar TN/OC ratios from the classical Redfield ratio (16/106) with increasing water depth, which is more evident for the deep Ionian Sea stations (Fig. 2.24a), probably reflect the preferential degradation processes during the transport and deposition of marine labile sedimentary OM, that probably also masks the association of marine OM to fine particles. The observations above, jointly with the presence of cholesterol ($_{27}\Delta^5$) and its significant positive correlation with the concentrations of marine algal markers, are altogether indicative of the re-working of algal OM by zooplankton and benthic invertebrates (Volkman et al., 1990; Gogou and Stephanou, 2004).

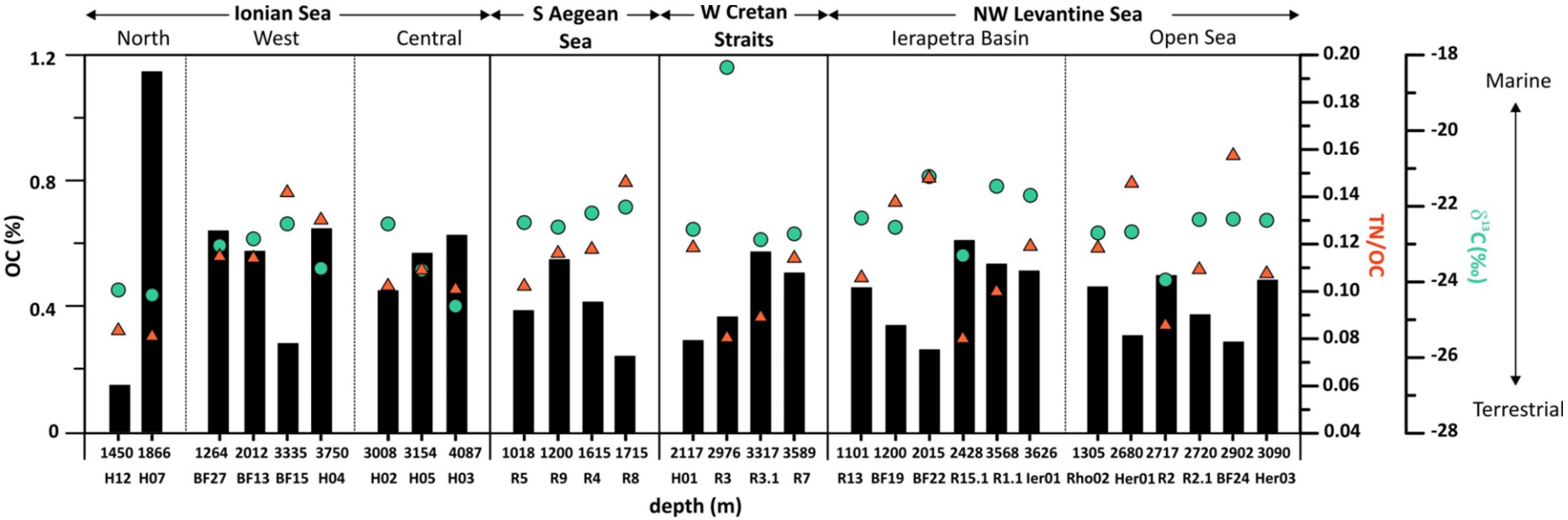

Figure 2.25. Distribution of OC content and bulk sediment tracers (TN/OC and $\delta^{13}C$) in surface sediments of the deep Eastern Mediterranean Sea. The histogram reflects a spatially variable mixture of marine and terrestrial sources for sedimentary OM. Orange triangles and green circles correspond to molar TN/OC ratios and $\delta^{13}C$ values, respectively.

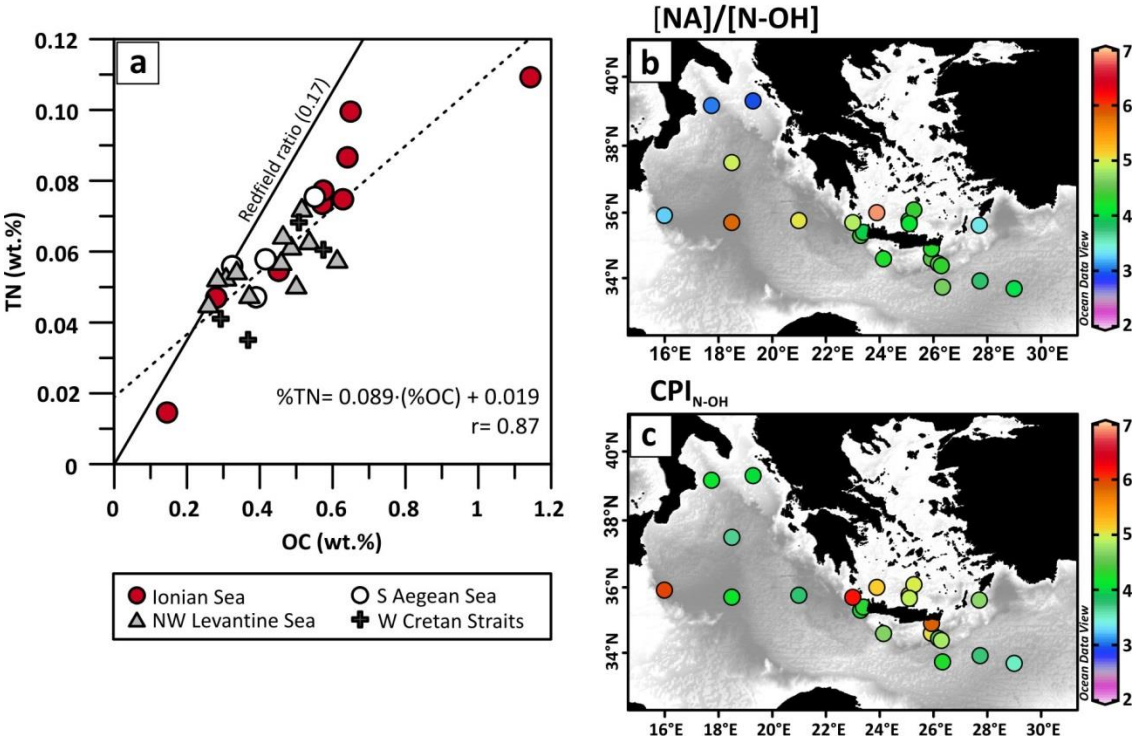

Figure 2.26. Spatial distribution of lipid biomarker indices (a) [NA]/[N-OH], (b) CPI_{NA} and (c) $CPI_{N\text{-}OH}$. Abbreviations of lipid biomarker indices are defined in the text.

2.3.5.2.2. Sediment transport and deposition processes

The second and third PCs of the PCA highlight the main processes that affect sediment dispersal and deposition in the study area. These relate to pelagic settling of marine skeletons from surface waters (corresponding to PC2), and hydrodynamic sorting of organic-rich fine sediment by bottom currents (corresponding to PC3).

Particulate matter exported from the upper layers of the water column in the EMS is primarily composed of biogenic particles and atmospheric dust, which while settling to the seabed are able to transfer OC, other nutrient elements, and OC-associated organic pollutants (e.g., Stavrakakis et al., 2000, 2013; Theodosi et al., 2013). In the deep EMS, the distribution of pelagic carbonates (second PC) seems to be mainly influenced by planktonic contributions. In the study area, the phytoplankton biomass and primary production are relatively higher in regions of cyclonic water mass circulation. The Rhodes cold-core gyre, situated in the southeast of the Rhodes Island (NW Levantine Sea), is the most prominent dynamic feature in the EMS and is the main source area of the LIW. In this cyclonic gyre, which is enhanced during winter period, dense water masses from deeper layers tend to upwell at its centre, feeding the upper layers with nutrient-rich waters (Salihoğlu et al., 1990). Therefore, this gyre plays an important role in the productivity of the Levantine Sea.

The third PC separated samples with high OC, TN and clay contents, which is indicative of a close OM-mineral association. This is in agreement with the high OC contents found in the fine-grained sediment samples from the deeper stations representing an essentially quiet environment (Figs.

2.20, 2.21 and 2.25). This is in contrast to the lower OC contents observed in coarser samples (d50 >14 μm) from shallower depths where currents up to 20 cm s^{-1} occur commonly (Kontoyiannis et al., 2005; Ursella et al., 2014). Fine-grained particles have high capacity for OM adsorption due to their large specific surface area, and thus enhanced OM contents relatively to coarse-grained particles (Mayer, 1994; Hedges and Keil, 1995). Physical processes such as hydrodynamic sorting remobilize and transport sedimentary material with different OC contents, with the OC-rich finest ones easily reaching the deep EMS. A similar situation has been reported in active sedimentary environments such as the submarine canyons in the Western Mediterranean Sea (Pedrosa-Pàmies et al., 2013), the northwestern Gulf of Mexico (Goñi et al., 1998) and the Peru Margin (Bergamaschi et al., 1997). However, none of these studies reported such OM-mineral associations at depths beyond 4000 m. This indicates that this organic-mineral interaction is maintained from the shallow to high depths, which constitute the final sedimentary sink. In short, the deep EMS behaves as a depocenter for OM-rich fine particles.

Moreover, in the EMS these bulk sediments show a poorer sorting than the lithogenic fraction (Fig. 2.20). This could be related to the presence of coarse biogenic carbonate particles in bulk samples or the effective hydrodynamic sorting linked to the prevailing depositional conditions in such deep low-energy environments (Friedman, 1969).

The poor sorting and positive skewness found in grain-size types I, II, IV and V of the bulk sediment samples (Fig. 2.20a) in the southern Aegean Sea and the northwestern Levantine Sea, is explained by the prevalence of pelagic biogenic sedimentation, as shown by the high positive score values observed on PC2 (Fig. 2.23b). Accordingly, high percentages of $CaCO_3$ have been measured in stations of the southern Aegean Sea, the northwestern Levantine Sea and western Cretan Straits, which correlate to %clay fraction of the bulk sediment samples and the concentrations of alkenones (Table 2.7). This links to the formation of clay-carbonate concretions that have been reported in particularly large amounts in the southern Aegean Sea (Emelyanov and Shimkus, 1986). Vertical mixing and upward transport of nutrients in the eddies and gyres, such as the Rhodes gyre, may trigger primary production and subsequently the sinking and dominance of pelagic biogenic particles over particles from other sources in the northwestern Levantine Sea (Siokou-Frangou et al., 1999). The $\%OC_{mar}$ and the $\sum$Mar distribution are indicative in that respect as they show a general eastward increasing trend with peak concentrations in deep basins of the northwestern Levantine Sea.

Surface sediments in the Ierapetra Basin (stations Red15, Red1.1 and Ier01) also show positive scores on PC3 (Fig. 2.23b), which point to an influence of hydrodynamic sorting processes. The relatively high OC content in these stations (Fig. 2.25), along with the elevated values of the associated natural and anthropogenic lipid concentrations (Table 2.7), suggests that the Hellenic Trench is a sink of OC associated to fine particles transferred by the active outflows of the Cretan Straits, besides the pelagic sedimentation related to the well-known semi-permanent Ierapetra anticyclone (Larnicol et al., 2002; Taupier-Letage, 2008).

Sediments with grain size types I-III of the bulk sediment samples (Fig. 2.20a) in the Ionian Sea show lower $CaCO_3$ contents due to the dilution by lithogenic components, with station H02 being the only exception. High positive score values on PC3 (Fig. 2.23b), and the significant positive correlation for OC and TN contents to %clay of the lithogenic fraction, further suggest a significant

influence of hydrodynamic sorting processes, which largely determine a differential distribution of OM in surface sediments according to grain size. In this area, the Otranto Strait may act as a preferential conduit by funnelling fine OC-rich particles from the Adriatic Sea towards the deep basins of the adjacent Ionian Sea, which may eventually reach the Levantine Sea (Bensi et al., 2013). The enhanced contributions of OC_{terr} (Table 2.6) and terrestrial biomarkers concentrations (Figs. 2.22b-c and Table 2.7) of the Ionian samples off the southern mouth of the Adriatic Sea, probably also reflect the preferential degradation of labile marine OM in deep Ionian Sea basins due to slower sedimentation rates and longer residence time of OM. Low OC content (Fig. 2.21c), poor sorting, very negatively skewed, high %sand of grain size type VI (Fig. 2.20a) at the shallower station H12 just south of Otranto Strait supports winnowing of fine OC-rich particles due to episodic events of high current speed exiting the Adriatic Sea (Bignami et al., 1991; Gacic et al., 1996; Poulos et al., 1999).

Finally, station Red3 from the upper slope of western Cretan Straits representing grain size type VII of the bulk sediment samples (Fig. 2.20a) shows the highest contents of sand (47.7%), which is poorly sorted. This is in agreement with the occurrence of the topographically restricted deep outflow of the western Cretan Straits. These straits are characterized by maximum outflow speeds during winter and minimum speeds during fall (Kontoyiannis et al., 2005). The turbulent, fluctuating outflow current should normally trigger sediment resuspension and induce selective transport, thus leaving coarse OC-poor particles in the upper slope of the western Cretan Straits (negative factor scores of PC2 and PC3) and carrying fine OC-rich particles to the lower slope. A similar pattern has been also observed in other submarine canyon settings of the Mediterranean Sea, such as the Cap de Creus Canyon (Sanchez-Vidal et al., 2008) and the Blanes Canyon (Pedrosa-Pàmies et al., 2013). The top $\delta^{13}C$ values found in the upper slope (Fig. 2.25 and Tables 2.6-2.7) indicates high contribution of marine OC, which however is not supported by the lipid biomarkers results. Winnowing of fine particles loaded with terrestrial OC, thus shifting the isotopic signal of the remaining coarse particles towards high and more marine values seems to be the most plausible explanation.

2.3.6. Conclusions

Surface sediments collected from deep basins of the oligotrophic EMS were investigated using a multi-proxy approach that involved elemental composition, grain size, stable isotopes and selected lipid biomarkers' analyses resulting in a robust database to determine sediment sources, the degradation and preservation state of OM, and processes that affect sediment dispersal and deposition. The PCA analysis helped to identify the main controlling factors of the observed geochemical variability in the investigated sediments. Such factors are sediment sources in terms of allochthonous vs. autochthonous, a highly variable physiography, the thermohaline structure, and the regional and local circulation, leading to hydrodynamic sorting and regulating particle settling/deposition and OM preservation state.

Surface sediments of the investigated part of the EMS mostly consist of airborne lithogenic particles and biogenic carbonate particles, the latter deriving from primary production into surface waters. Sedimentary OM appears in rather low contents (0.15 – 1.15% OC), with bulk and molecular organic tracers reflecting a mixed contribution from both natural (autochthonous and allochthonous) and anthropogenic sources. Samples from locations in the Ionian Sea and the

western Cretan Straits that are under the direct influence of the Adriatic dense waters outflow through the Otranto Strait and of currents exiting the southern Aegean Sea, respectively, are appreciably sorted. Current regime impacted not only grain size but also OC loadings within each subregion of the study area, with winnowing of fine OC-rich particles to the deepest EMS. In contrast, coarse OC-poor particles tend to occur in upper slope settings. While OC associated to fine particles was relatively non-degraded terrestrial OM, marine OM was found to be mostly degraded and reworked during transport processes and before reaching the deep seafloor.

The spatial variability in the yields of sedimentary OC and lipid biomarkers presented in this study highlights the heterogeneous nature of the particle load exported to the deep basins of the Eastern Mediterranean Sea. Such variability must be taken into account during the development of quantitative carbon budgets for this area.

2.3.7. Acknowledgments

This research has been supported by the EU-funded project PERSEUS (GA 287600), the EU-Greek co-funded project KRIPIS (MIS 451724; NSRF) and REDECO (CTM2008-04973-E/MAR), BIOFUN (CTM2007-28739-E) and MEDECOS (ΣΑΕ 013/8 -2010ΣΕ01380001) projects. Researchers from GRC Geociències Marines benefited from a Grups de Recerca Consolidats grant 2014 SGR 1068 by the Generalitat de Catalunya autonomous government. We sincerely thank chief scientist K.C. Emeis (R/V Meteor) and the officers and crews of R/V Meteor, R/V Aegaeo and R/V Sarmiento de Gamboa for their precious help during the cruises. Elemental and isotopic analyses have been performed at the Scientific-Technical Services of the University of Barcelona. R.P.-P. is supported by a predoctoral FPU grant and A.S.-V. by a Ramon y Cajal contract. Dr. Juergen Mobius is acknowledged for his constructive comments on an earlier version of the manuscript. We would like to thank the Editor and Dr. T. Tesi and three anonymous referees for their constructive comments that helped us significantly improve the quality of the manuscript during the revision process.

2.3.8. References

Amblàs, D., Canals, M., Lastras, G., Berné, S. and Loubrieu, B.: Imaging the Seascapes of the Mediterranean, Oceanography, 17(4), 144–155, doi:10.5670/oceanog.2004.11, 2004.

Bensi, M., Cardin, V., Rubino, A., Notarstefano, G. and Poulain, P. M.: Effects of winter convection on the deep layer of the Southern Adriatic Sea in 2012, J. Geophys. Res. Ocean., 118(11), 6064–6075, doi:10.1002/2013JC009432, 2013.

Bergamaschi, B. A., Tsamakis, E., Keil, R. G., Eglinton, T. I., Montluçon, D. B. and Hedges, J. I.: The effect of grain size and surface area on organic matter, lignin and carbohydrate concentration, and molecular compositions in Peru Margin sediments, Geochim. Cosmochim. Acta, 61(6), 1247–1260, doi:10.1016/S0016-7037(96)00394-8, 1997.

Bethoux, J. P.: Budgets of the Mediterranean Sea. Their dependence on the local climate and on the characteristics of the Atlantic waters, Oceanol. Acta, 2, 157–163, 1979.

Bethoux, J. P.: Oxygen consumption, new production, vertical advection and environmental evolution in the Mediterranean Sea, Deep Sea Res. Part A. Oceanogr. Res. Pap., 36(5), 769–781, doi:10.1016/0198-0149(89)90150-7, 1989.

Bianchi, A., Tholosan, O., Garcin, J., Polychronaki, T., Tselepides, A., Buscail, R. and Duineveld, G.: Microbial activities at the benthic boundary layer in the Aegean Sea, Prog. Oceanogr., 57(2), 219–236, doi:10.1016/S0079-6611(03)00034-X, 2003.

Blott, S. J. and Pye, K.: GRADISTAT: A grain size distribution and statistics package for the analysis of unconsolidated sediments, Earth Surf. Process. Landforms, 26(11), 1237–1248, doi:10.1002/esp.261, 2001.

Bosc, E., Bricaud, A. and Antoine, D.: Seasonal and interannual variability in algal biomass and primary production in the Mediterranean Sea, as derived from 4 years of SeaWiFS observations, Global Biogeochem. Cycles, 18(1), GB1005, doi:10.1029/2003GB002034, 2004.

Bouloubassi, I., Lipiatou, E., Saliot, A., Tolosa, I., Bayona, J. M. and Albaigés, J.: Carbon sources and cycle in the western Mediterranean-the use of molecular markers to determine the origin of organic matter, Deep Sea Res. Part II Top. Stud. Oceanogr., 44(3-4), 781–799, doi:10.1016/S0967-0645(96)00094-X, 1997.

Burdige, D. J.: Preservation of organic matter in marine sediments: controls, mechanisms, and an imbalance in sediment organic carbon budgets?, Chem. Rev., 107(2), 467–85, doi:10.1021/cr050347q, 2007.

Canals, M., Danovaro, R., Heussner, S., Lykousis, V., Puig, P., Trincardi, F., Calafat, A., Durrieu de Madron, X. and Palanques, A.: Cascades in Mediterranean Submarine Grand Canyons, Oceanography, 22(1), 26–43, doi:10.5670/oceanog.2009.03, 2009.

Carlier, A., Ritt, B., Rodrigues, C. F., Sarrazin, J., Olu, K., Grall, J. and Clavier, J.: Heterogeneous energetic pathways and carbon sources on deep eastern Mediterranean cold seep communities, Mar. Biol., 157(11), 2545–2565, doi:10.1007/s00227-010-1518-1, 2010.

Castro-Jiménez, J., Berrojalbiz, N., Wollgast, J. and Dachs, J.: Polycyclic aromatic hydrocarbons (PAHs) in the Mediterranean Sea: atmospheric occurrence, deposition and decoupling with settling fluxes in the water column., Environ. Pollut., 166, 40–7, doi:10.1016/j.envpol.2012.03.003, 2012.

Chester, R., Baxter, G. G., Behairy, A. K. A., Connor, K., Cross, D., Elderfield, H. and Padgham, R. C.: Soil-sized eolian dusts from the lower troposphere of the eastern Mediterranean Sea, Mar. Geol., 24(3), 201–217, doi:10.1016/0025-3227(77)90028-7, 1977.

Collatz, G. J., Berry, J. a. and Clark, J. S.: Effects of climate and atmospheric CO_2 partial pressure on the global distribution of C4 grasses: present, past, and future, Oecologia, 114(4), 441–454, doi:10.1007/s004420050468, 1998.

Collister, J. W., Rieley, G., Stern, B., Eglinton, G. and Fry, B.: Compound-specific $\delta^{13}C$ analyses of leaf lipids from plants with differing carbon dioxide metabolisms, Org. Geochem., 21(6-7), 619–627, doi:10.1016/0146-6380(94)90008-6, 1994.

Correggiari, A., Guerzoni, S., Lenaz, R., Quarantotto, G. and Rampazzo, G.: Dust deposition in the central Mediterranean (Tyrrhenian and Adriatic Seas): Relationships with marine sediments and riverine input, Terra Nov., 1(6), 549–558, doi:10.1111/j.1365-3121.1989.tb00431.x, 1989.

Cros, L.: Calcareous nannoplankton in surficial sediments of the Catalano-Balearic Sea (northeastern Mediterranean), in 5Th INA Conference in Salamanca Proceedings, pp. 47–59., 1995.

Danovaro, R., Fabiano, M. and Della Croce, N.: Labile organic matter and microbial biomasses in deep-sea sediments (Eastern Mediterranean Sea), Deep Sea Res. Part I Oceanogr. Res. Pap., 40(5), 953–965, doi:10.1016/0967-0637(93)90083-F, 1993.

Danovaro, R., Company, J. B., Corinaldesi, C., D'Onghia, G., Galil, B., Gambi, C., Gooday, A. J., Lampadariou, N., Luna, G. M., Morigi, C., Olu, K., Polymenakou, P. N., Ramirez-Llodra, E., Sabbatini, A., Sardà, F., Sibuet, M. and Tselepides, A.: Deep-sea biodiversity in the Mediterranean Sea: the known, the unknown, and the unknowable., PloS One, 5(8), e11832, doi:10.1371/journal.pone.0011832, 2010.

Durrieu de Madron, X., Abassi, A., Heussner, S., Monaco, A., Aloisi, J. C., Radakovitch, O., Giresse, P., Buscail, R. and Kerherve, P.: Particulate matter and organic carbon budgets for the Gulf of Lions (NW Mediterranean), Oceanol. Acta, 23(6), 717–730, doi:10.1016/S0399-1784(00)00119-5, 2000.

Eglinton, G. and Hamilton, R. J.: Leaf Epicuticular Waxes, Science (80-.)., 156(3780), 1322–1335, doi:10.1126/science.156.3780.1322, 1967.

Eglinton, T. I., Eglinton, G., Dupont, L., Sholkovitz, E. R., Montluçon, D. and Reddy, C. M.: Composition, age, and provenance of organic matter in NW African dust over the Atlantic Ocean, Geochemistry, Geophys. Geosystems, 3(8), 1–27, 2002.

Ehrmann, W., Schmiedl, G., Hamann, Y., Kuhnt, T., Hemleben, C. and Siebel, W.: Clay minerals in late glacial and Holocene sediments of the northern and southern Aegean Sea, Palaeogeogr. Palaeoclimatol. Palaeoecol., 249(1-2), 36–57, doi:10.1016/j.palaeo.2007.01.004, 2007.

Emelyanov, E. M. and Shimkus, K. M.: Geochemistry and Sedimentology of the Mediterranean Sea, D. Reidel Publishing Company, Dordrecht, Holland., 1986.

Folk, R. L. and Ward, W. C.: Brazos River bar: A study in the significance of grain size parameters, J. Sediment. Res., 27(1), 3–26, doi:10.1306/74D70646-2B21-11D7-8648000102C1865D, 1957.

Frenz, M., Baumann, K. H., Boeckel, B., Hoppner, R. and Henrich, R.: Quantification of foraminifer and coccolith carbonate in South Atlantic surface sediments by means of carbonate grain-size distributions, J. Sediment. Res., 75(3), 464–475, doi:10.2110/jsr.2005.036, 2005.

Friedman, G. M.: Trace elements as possible environmental indicators in carbonate sediments, Depos. Environ. Carbonate Rocks, 193–198, 1969.

Friligos, N., Moriki, A., Sklivagou, E., Krasakopoulou, E. and Hatzianestis, I.: Geochemical characteristics of the surficial sediments of the Aegean Sea, in 3rd MTP-MATER Workshop, vol. 35, pp. 28–209, Rhodos., 1998.

Garcia-Orellana, J., Pates, J. M., Masqué, P., Bruach, J. M. and Sanchez-Cabeza, J. A.: Distribution of artificial radionuclides in deep sediments of the Mediterranean Sea., Sci. Total Environ., 407(2), 887–98, doi:10.1016/j.scitotenv.2008.09.018, 2009.

Goericke, R. and Fry, B.: Variations of marine plankton $\delta^{13}C$ with latitude, temperature, and dissolved CO_2 in the world ocean, Global Biogeochem. Cycles, 8(1), 85–90, doi:10.1029/93GB03272, 1994.

Gogou, A. and Stephanou, E. G.: Marine organic geochemistry of the Eastern Mediterranean, Mar. Chem., 85(1-2), 1–25, doi:10.1016/j.marchem.2003.08.005, 2004.

Gogou, A., Stratigakis, N., Kanakidou, M. and Stephanou, E. G.: Organic aerosols in Eastern Mediterranean: components source reconciliation by using molecular markers and atmospheric back trajectories, Org. Geochem., 25(1-2), 79–96, doi:10.1016/S0146-6380(96)00105-2, 1996.

Gogou, A., Apostolaki, M. and Stephanou, E. G.: Determination of organic molecular markers in marine aerosols and sediments: one-step flash chromatography compound class fractionation and capillary gas chromatographic analysis, J. Chromatogr. A, 799(1-2), 215–231, doi:10.1016/S0021-9673(97)01106-0, 1998.

Gogou, A., Bouloubassi, I. and Stephanou, E. G.: Marine organic geochemistry of the Eastern Mediterranean: 1. Aliphatic and polyaromatic hydrocarbons in Cretan Sea surficial sediments, Mar. Chem., 68(4), 265–282, doi:10.1016/S0304-4203(99)00082-1, 2000.

Gogou, A., Bouloubassi, I., Lykousis, V., Arnaboldi, M., Gaitani, P. and Meyers, P. A.: Organic geochemical evidence of Late Glacial–Holocene climate instability in the North Aegean Sea, Palaeogeogr. Palaeoclimatol. Palaeoecol., 256(1-2), 1–20, doi:10.1016/j.palaeo.2007.08.002, 2007.

Gogou, A., Sanchez-Vidal, A., Durrieu de Madron, X., Stavrakakis, S., Calafat, A., Stabholz, M., Psarra, S., Canals, M., Heussner, S., Stavrakaki, I. and Papathanassiou, E.: Carbon flux to the deep in three open sites of the Southern European Seas (SES), J. Mar. Syst., 129, 224–233, doi:10.1016/j.jmarsys.2013.05.013, 2014a.

Gogou, A., Sanchez-Vidal, A., Durrieu de Madron, X., Stavrakakis, S., Calafat, A., Stabholz, M., Psarra, S., Canals, M., Heussner, S., Stavrakaki, I. and Papathanassiou, E.: Carbon flux to the deep in three open sites of the Southern European Seas (SES), J. Mar. Syst., 129, 224–233, doi:10.1016/j.jmarsys.2013.05.013, 2014b.

Goñi, M. A., Ruttenberg, K. C. and Eglinton, T. I.: A reassessment of the sources and importance of land-derived organic matter in surface sediments from the Gulf of Mexico, Geochim. Cosmochim. Acta, 62(18), 3055–3075, doi:10.1016/S0016-7037(98)00217-8, 1998.

Goñi, M. A., Teixeira, M. J. and Perkey, D. W.: Sources and distribution of organic matter in a river-dominated estuary (Winyah Bay, SC, USA), Estuar. Coast. Shelf Sci., 57(5-6), 1023–1048, doi:10.1016/S0272-7714(03)00008-8, 2003.

Goñi, M. A., Monacci, N., Gisewhite, R., Ogston, A., Crockett, J. and Nittrouer, C.: Distribution and sources of particulate organic matter in the water column and sediments of the Fly River Delta, Gulf of Papua (Papua New Guinea), Estuar. Coast. Shelf Sci., 69, 225–245, doi:10.1016/j.ecss.2006.04.012, 2006.

Goudeau, M.-L. S., Grauel, A.-L., Bernasconi, S. M. and de Lange, G. J.: Provenance of surface sediments along the southeastern Adriatic coast off Italy: An overview, Estuar. Coast. Shelf Sci., 134, 45–56, doi:10.1016/j.ecss.2013.09.009, 2013.

Gough, M. A. and Rowland, S. J.: Characterization of unresolved complex mixtures of hydrocarbons in petroleum, Nature, 344(6267), 648–650, doi:10.1038/344648a0, 1990.

Grice, K., Klein Breteler, W., Schouten, S., Grossi, V., Leeuw, J. W. and Damsté, J. S. S.: Effects of zooplankton herbivory on biomarker proxy records, Paleoceanography, 13(6), 686–693, doi:10.1029/98PA01871, 1998.

Grimalt, J. O. and Albaigés, J.: Characterization of the depositional environments of the Ebro Delta (western Mediterranean) by the study of sedimentary lipid markers, Mar. Geol., 95(3-4), 207–224, doi:10.1016/0025-3227(90)90117-3, 1990.

Guerzoni, S. and Molinaroli, E.: Input of Various Chemicals Transported by Saharan Dust and Depositing at the Sea Surface in the Mediterranean Sea, Enviromental Chem., 5, 237–268, doi:10.1007/b107149, 2005.

Guerzoni, S., Chester, R., Dulac, F., Herut, B., Loÿe-Pilot, M.-D., Measures, C., Migon, C., Molinaroli, E., Moulin, C., Rossini, P., Saydam, C., Soudine, A. and Ziveri, P.: The role of atmospheric deposition in the biogeochemistry of the Mediterranean Sea, Prog. Oceanogr., 44(1-3), 147–190, doi:10.1016/S0079-6611(99)00024-5, 1999.

Hamann, Y., Ehrmann, W., Schmiedl, G., Krüger, S., Stuut, J.-B. and Kuhnt, T.: Sedimentation processes in the Eastern Mediterranean Sea during the Late Glacial and Holocene revealed by end-member modelling of the terrigenous fraction in marine sediments, Mar. Geol., 248(1-2), 97–114, doi:10.1016/j.margeo.2007.10.009, 2008.

Harmelin-Vivien, M., Loizeau, V., Mellon, C. and Beker, B.: Comparison of C and N stable isotope ratios between surface particulate organic matter and microphytoplankton in the Gulf of Lions (NW Mediterranean), Cont. Shelf Res., 28(15), 1911–1919, doi:10.1016/j.csr.2008.03.002, 2008.

Hedges, J. I. and Keil, R. G.: Sedimentary organic matter preservation: an assessment and speculative synthesis, Mar. Chem., 49(2-3), 81–115, doi:10.1016/0304-4203(95)00008-F, 1995.

Hedges, J. I. and Oades, J. M.: Comparative organic geochemistries of soils and marine sediments, Org. Geochem., 27(7-8), 319–361, doi:10.1016/S0146-6380(97)00056-9, 1997.

Hedges, J. I., Keil, R. G. and Benner, R.: What happens to terrestrial organic matter in the ocean?, Org. Geochem., 27(5-6), 195–212, doi:10.1016/S0146-6380(97)00066-1, 1997.

Heussner, S., Calafat, A. and Palanques, A.: Quantitative and qualitative features of particle fluxes in the North-Balearic Basin, EUROMARGE-NB Final Report, Ed. By Canals, M., Casamor, JL, Cacho, I., Calafat, AM, Monaco, A., MAST II Program. EC, 2, 41–66, 1996.

Hopmans, E. C., Weijers, J. W. ., Schefuß, E., Herfort, L., Sinninghe Damsté, J. S. and Schouten, S.: A novel proxy for terrestrial organic matter in sediments based on branched and isoprenoid tetraether lipids, Earth Planet. Sci. Lett., 224(1-2), 107–116, doi:10.1016/j.epsl.2004.05.012, 2004.

Hu, J., Peng, P., Jia, G., Mai, B. and Zhang, G.: Distribution and sources of organic carbon, nitrogen and their isotopes in sediments of the subtropical Pearl River estuary and adjacent shelf, Southern China, Mar. Chem., 98(2-4), 274–285, doi:10.1016/j.marchem.2005.03.008, 2006.

IOC, IHO and BODC: Centenary edition of the GEBCO digital atlas, published on CD-ROM on behalf of the Intergovernmental Oceanographic Commission and the International Hydrographic Organization as part of the General Bathymetric Chart of the Oceans, Liverpool, UK., 2003.

Jickells, T. D.: Atmospheric inputs of metals and nutrients to the oceans: their magnitude and effects, Mar. Chem., 48(3-4), 199–214, doi:10.1016/0304-4203(95)92784-P, 1995.

Jickells, T. D., An, Z. S., Andersen, K. K., Baker, A. R., Bergametti, G., Brooks, N., Cao, J. J., Boyd, P. W., Duce, R. A., Hunter, K. A., Kawahata, H., Kubilay, N., laRoche, J., Liss, P. S., Mahowald, N., Prospero, J. M., Ridgwell, A. J., Tegen, I. and Torres, R.: Global iron connections between desert dust, ocean biogeochemistry, and climate., Science, 308(5718), 67–71, doi:10.1126/science.1105959, 2005.

Kaiser, J., Ruggieri, N., Hefter, J., Siegel, H., Mollenhauer, G., Arz, H. W. and Lamy, F.: Lipid biomarkers in surface sediments from the gulf of genoa, Ligurian sea (NW Mediterranean sea) and their potential for the reconstruction of palaeo-environments, Deep Sea Res. Part I Oceanogr. Res. Pap., 89, 68–83, doi:10.1016/j.dsr.2014.04.009, 2014.

Kelepertsis, A. E., Alexakis, D. E., Nastos, P. T. and Kanellopoulou, E. A.: The presence of volcanic ash in the western Greece and its association with the eruption of the Etna volcano, Italy. Consequences on the Environment., in 8th International Conference on Environmental Science and Technology, pp. 408–415, Lemnos Island, Greece., 2003.

Kemp, A. E. S., Pearce, R. B., Koizumi, I., Pike, J. and Rance, S. J.: The role of mat-forming diatoms in the formation of Mediterranean sapropels, Nature, 398(6722), 57–61, doi:10.1038/18001, 1999.

Kontoyiannis, H., Balopoulos, E., Gotsis-Skretas, O., Pavlidou, A., Assimakopoulou, G. and Papageorgiou, E.: The hydrology and biochemistry of the Cretan Straits (Antikithira and Kassos Straits) revisited in the period June 1997–May 1998, J. Mar. Syst., 53(1-4), 37–57, doi:10.1016/j.jmarsys.2004.06.007, 2005.

Krom, M. D., Groom, S. and Zohary, T.: The Eastern Mediterranean, The Biogeo., edited by G. B. Black, K. D. and Shimmield, Blackwell Publishing, Oxford., 2003.

Krom, M. D., Woodward, E. M. S., Herut, B., Kress, N., Carbo, P., Mantoura, R. F. C., Spyres, G., Thingstad, T. F., Wassmann, P., Wexels-Riser, C., Kitidis, V., Law, C. S. and Zodiatis, G.: Nutrient cycling in the south east Levantine basin of the eastern Mediterranean: Results from a phosphorus starved system, Deep Sea Res. Part II Top. Stud. Oceanogr., 52(22-23), 2879–2896, doi:10.1016/j.dsr2.2005.08.009, 2005.

Larnicol, G., Ayoub, N. and Le Traon, P. Y.: Major changes in Mediterranean Sea level variability from 7 years of TOPEX/Poseidon and ERS-1/2 data, J. Mar. Syst., 33-34, 63–89, doi:10.1016/S0924-7963(02)00053-2, 2002.

Lascaratos, A., Williams, R. G. and Tragou, E.: A mixed-layer study of the formation of Levantine intermediate water, J. Geophys. Res., 98(C8), 14739, doi:10.1029/93JC00912, 1993.

Lascaratos, A., Roether, W., Nittis, K. and Klein, B.: Recent changes in deep water formation and spreading in the eastern Mediterranean Sea: a review, Prog. Oceanogr., 44(1-3), 5–36, doi:10.1016/S0079-6611(99)00019-1, 1999.

Lehmann, M. F., Bernasconi, S. M., Barbieri, A. and McKenzie, J. A.: Preservation of organic matter and alteration of its carbon and nitrogen isotope composition during simulated and in situ early sedimentary diagenesis, Geochim. Cosmochim. Acta, 66(20), 3573–3584, doi:10.1016/S0016-7037(02)00968-7, 2002.

Di Leonardo, R., Vizzini, S., Bellanca, A. and Mazzola, A.: Sedimentary record of anthropogenic contaminants (trace metals and PAHs) and organic matter in a Mediterranean coastal area (Gulf of Palermo, Italy), J. Mar. Syst., 78(1), 136–145, doi:10.1016/j.jmarsys.2009.04.004, 2009.

Malanotte-Rizzoli, P. and Hecht, A.: Large-scale properties of the eastern modelling Mediterranean - A review, Oceanol. Acta, 11(4), 323–335, 1988.

Malanotte-Rizzoli, P., Manca, B. B., Alcala, M. R. D., Bergamasco, A., Bregant, D. and Georgopoulos, D.: A synthesis of the Ionian Sea hydrography, circulation and water mass pathways during POEM-Phase I, Prog. Oceanogr., 39(2), 153–204, doi:10.1016/S0079-6611(97)00013-X, 1997.

Manca, B. B., Kovaĉević, V., Gaĉić, M. and Viezzoli, D.: Dense water formation in the Southern Adriatic Sea and spreading into the Ionian Sea in the period 1997–1999, J. Mar. Syst., 33-34, 133–154, doi:10.1016/S0924-7963(02)00056-8, 2002.

Marlowe, I. T., Green, J. C., Neal, A. C., Brassell, S. C., Eglinton, G. and Course, P. A.: Long chain (n-C37–C39) alkenones in the Prymnesiophyceae. Distribution of alkenones and other lipids and their taxonomic significance, Br. Phycol. J., 19(3), 203–216, doi:10.1080/00071618400650221, 1984.

Masqué, P., Fabres, J., Canals, M., Sanchez-Cabeza, J. A., Sanchez-Vidal, A., Cacho, I., Calafat, A. and Bruach, J. M.: Accumulation rates of major constituents of hemipelagic sediments in the deep

Alboran Sea: a centennial perspective of sedimentary dynamics, Mar. Geol., 193(3-4), 207–233, doi:10.1016/S0025-3227(02)00593-5, 2003.

Mayer, L. M.: Relationships between mineral surfaces and organic carbon concentrations in soils and sediments, Chem. Geol., 114(3-4), 347–363, doi:10.1016/0009-2541(94)90063-9, 1994.

Meador, T. B., Gogou, A., Spyres, G., Herndl, G. J., Krasakopoulou, E., Psarra, S., Yokokawa, T., De Corte, D., Zervakis, V. and Repeta, D. J.: Biogeochemical relationships between ultrafiltered dissolved organic matter and picoplankton activity in the Eastern Mediterranean Sea, Deep Sea Res. Part II Top. Stud. Oceanogr., 57(16), 1460–1477, doi:10.1016/j.dsr2.2010.02.015, 2010.

Medimap Group: Morpho-bathymetry of the Mediterranean Sea, E: 1=2000000, CIESM/Ifremer Sp. Publ., Maps and Atlases, two maps (Western Mediterranean and Eastern Mediterranean), Montecarlo / Brest, Monaco / France., 2007.

Meyers, P. A.: Preservation of elemental and isotopic source identification of sedimentary organic matter, Chem. Geol., 114(3-4), 289–302, doi:10.1016/0009-2541(94)90059-0, 1994.

Meyers, P. a.: Organic geochemical proxies of paleoceanographic, paleolimnologic, and paleoclimatic processes, Org. Geochem., 27(5-6), 213–250, doi:10.1016/S0146-6380(97)00049-1, 1997.

Meyers, P. A. and Arnaboldi, M.: Paleoceanographic implications of nitrogen and organic carbon isotopic excursions in mid-Pleistocene sapropels from the Tyrrhenian and Levantine Basins, Mediterranean Sea, Palaeogeogr. Palaeoclimatol. Palaeoecol., 266(1-2), 112–118, doi:10.1016/j.palaeo.2008.03.018, 2008.

Meyers, P. A., Silliman, J. E. and Shaw, T. J.: Effects of turbidity flows on organic matter accumulation, sulfate reduction, and methane generation in deep-sea sediments on the Iberia Abyssal Plain, Org. Geochem., 25(1-2), 69–78, doi:10.1016/S0146-6380(96)00106-4, 1996.

Milliff, R. F. and Robinson, A. R.: Structure and Dynamics of the Rhodes Gyre System and Dynamical Interpolation for Estimates of the Mesoscale Variability, J. Phys. Oceanogr., 22(4), 317–337, doi:10.1175/1520-0485(1992)022<0317:SADOTR>2.0.CO;2, 1992.

Millot, C. and Taupier-Letage, I.: Additional evidence of LIW entrainment across the Algerian subbasin by mesoscale eddies and not by a permanent westward flow, Prog. Oceanogr., 66, 231–250, doi:10.1016/j.pocean.2004.03.002, 2005.

Mortlock, R. A. and Froelich, P. N.: A simple method for the rapid determination of biogenic opal in pelagic marine sediments, Deep Sea Res. Part A. Oceanogr. Res. Pap., 36(9), 1415–1426, doi:10.1016/0198-0149(89)90092-7, 1989.

Müller, P. J.: C/N ratios in Pacific deep-sea sediments: Effect of inorganic ammonium and organic nitrogen compounds sorbed by clays, Geochim. Cosmochim. Acta, 41(6), 765–776, doi:10.1016/0016-7037(77)90047-3, 1977.

Nieuwenhuize, J., Maas, Y. E. M. and Middelburg, J. J.: Rapid analysis of organic carbon and nitrogen in particulate materials, Mar. Chem., 45(3), 217–224, doi:10.1016/0304-4203(94)90005-1, 1994.

Ohkouchi, N., Kawamura, K., Kawahata, H. and Taira, A.: Latitudinal distributions of terrestrial biomarkers in the sediments from the Central Pacific, Geochim. Cosmochim. Acta, 61(9), 1911–1918, doi:10.1016/S0016-7037(97)00040-9, 1997.

Olgun, N., Duggen, S., Andronico, D., Kutterolf, S., Croot, P. L., Giammanco, S., Censi, P. and Randazzo, L.: Possible impacts of volcanic ash emissions of Mount Etna on the primary productivity in the oligotrophic Mediterranean Sea: Results from nutrient-release experiments in seawater, Mar. Chem., 152, 32–42, doi:10.1016/j.marchem.2013.04.004, 2013.

Orlic, M., Gacic, M. and Laviolette, P. E.: The currents and circulation of the Adriatic Sea, Oceanol. Acta, 15(2), 109–124, 1992.

Parinos, C., Gogou, A., Bouloubassi, I., Pedrosa-Pàmies, R., Hatzianestis, I., Sanchez-Vidal, A., Rousakis, G., Velaoras, D., Krokos, G. and Lykousis, V.: Occurrence, sources and transport pathways of natural and anthropogenic hydrocarbons in deep-sea sediments of the eastern Mediterranean Sea, Biogeosciences, 10(9), 6069–6089, doi:10.5194/bg-10-6069-2013, 2013.

Pedrosa-Pàmies, R., Sanchez-Vidal, A., Calafat, A., Canals, M. and Durán, R.: Impact of storm-induced remobilization on grain size distribution and organic carbon content in sediments from the Blanes Canyon area, NW Mediterranean Sea, Prog. Oceanogr., 118, 122–136, doi:10.1016/j.pocean.2013.07.023, 2013.

Perdue, E. M. and Koprivnjak, J.-F.: Using the C/N ratio to estimate terrigenous inputs of organic matter to aquatic environments, Estuar. Coast. Shelf Sci., 73(1-2), 65–72, doi:10.1016/j.ecss.2006.12.021, 2007.

Polymenakou, P. N., Tselepides, A., Stephanou, E. G. and Bertilsson, S.: Carbon speciation and composition of natural microbial communities in polluted and pristine sediments of the Eastern Mediterranean Sea, Mar. Pollut. Bull., 52(11), 1396–1405, doi:10.1016/j.marpolbul.2006.03.021, 2006.

Psarra, S., Tselepides, A. and Ignatiades, L.: Primary productivity in the oligotrophic Cretan Sea (NE Mediterranean): seasonal and interannual variability, Prog. Oceanogr., 46(2-4), 187–204, doi:10.1016/S0079-6611(00)00018-5, 2000.

Rabitti, S., Bianchi, F., Boldrin, A., Daros, L., Socal, G. and Totti, C.: Particulate matter and phytoplankton in the Ionian Sea, Oceanol. Acta, 17(3), 297–307, 1994.

Rampen, S. W., Willmott, V., Kim, J.-H., Uliana, E., Mollenhauer, G., Schefuß, E., Sinninghe Damsté, J. S. and Schouten, S.: Long chain 1,13- and 1,15-diols as a potential proxy for palaeotemperature reconstruction, Geochim. Cosmochim. Acta, 84, 204-216, 2012.

Ratmeyer, V., Balzer, W., Bergametti, G., Chiapello, I., Fischer, G. and Wyputta, U.: Seasonal impact of mineral dust on deep-ocean particle flux in the eastern subtropical Atlantic Ocean, Mar. Geol., 159(1-4), 241–252, doi:10.1016/S0025-3227(98)00197-2, 1999.

Redfield, A. C., Ketchum, B. H. and Richards, F. A.: The influence of organisms on the composition of sea-water, in The Sea, edited by M. N. Hill, pp. 26–77, Interscience, New York., 1963.

Robinson, A. R., Malanotte-Rizzoli, P., Hecht, A., Michelato, A., Roether, W., Theocharis, A., Ünlüata, Ü., Pinardi, N., Artegiani, A. and Bergamasco, A.: General circulation of the Eastern Mediterranean, Earth-Science Rev., 32(4), 285–309, 1992.

Robinson, A. R., Leslie, W. G., Theocharis, A. and Lascaratos, A.: Mediterranean Sea Circulation, in Encyclopedia of Ocean Sciences, pp. 1689–1706, Academic Press., 2001.

Roether, W. and Well, R.: Oxygen consumption in the Eastern Mediterranean, Deep Sea Res. Part I Oceanogr. Res. Pap., 48(6), 1535–1551, doi:10.1016/S0967-0637(00)00102-3, 2001.

Romero, I. C., Schwing, P. T., Brooks, G. R., Larson, R. A., Hastings, D. W., Ellis, G., Goddard, E. A. and Hollander, D. J.: Hydrocarbons in Deep-Sea Sediments following the 2010 Deepwater Horizon Blowout in the Northeast Gulf of Mexico, edited by W.-C. Chin, PloS One, 10(5), e0128371, doi:10.1371/journal.pone.0128371, 2015.

Roussiez, V., Ludwig, W., Monaco, A., Probst, J.-L., Bouloubassi, I., Buscail, R. and Saragoni, G.: Sources and sinks of sediment-bound contaminants in the Gulf of Lions (NW Mediterranean Sea): A multi-tracer approach, Cont. Shelf Res., 26(16), 1843–1857, doi:10.1016/j.csr.2006.04.010, 2006.

Rullkötter, J.: Organic matter: the driving force for early diagenesis, in Marine geochemistry, edited by H. D. Schulz and M. Zabel, pp. 125–168, Springer Berlin Heidelberg., 2006.

Rumolo, P., Barra, M., Gherardi, S., Marsella, E. and Sprovieri, M.: Stable isotopes and C/N ratios in marine sediments as a tool for discriminating anthropogenic impact., J. Environ. Monit., 13(12), 3399–408, doi:10.1039/c1em10568j, 2011.

Rutten, A., de Lange, G. ., Ziveri, P., Thomson, J., Van Santvoort, P. J. M., Colley, S. and Corselli, C.: Recent terrestrial and carbonate fluxes in the pelagic eastern Mediterranean; a comparison between sediment trap and surface sediment, Palaeogeogr. Palaeoclimatol. Palaeoecol., 158(3-4), 197–213, doi:10.1016/S0031-0182(00)00050-X, 2000.

Salihoğlu, İ., Saydam, C., Baştürk, Ö., Yilmaz, K., Göçmen, D., Hatipoğlu, E. and Yilmaz, A.: Transport and distribution of nutrients and chlorophyll-a by mesoscale eddies in the northeastern Mediterranean, Mar. Chem., 29, 375–390, doi:10.1016/0304-4203(90)90024-7, 1990.

Sanchez-Vidal, A., Pasqual, C., Kerhervé, P., Calafat, A., Heussner, S., Palanques, a., Durrieu de Madron, X., Canals, M. and Puig, P.: Impact of dense shelf water cascading on the transfer of organic matter to the deep western Mediterranean basin, Geophys. Res. Lett., 35(5), L05605, doi:10.1029/2007GL032825, 2008.

Van Santvoort, P. J. M., de Lange, G. J., Thomson, J., Cussen, H., Wilson, T. R. S., Krom, M. D. and Ströhle, K.: Active post-depositional oxidation of the most recent sapropel (S1) in sediments of the eastern Mediterranean Sea, Geochim. Cosmochim. Acta, 60(21), 4007–4024, doi:10.1016/S0016-7037(96)00253-0, 1996.

Van Santvoort, P. J. M., De Lange, G. J., Thomson, J., Colley, S., Meysman, F. J. R. and Slomp, C. P.: Oxidation and origin of organic matter in surficial eastern Mediterranean hemipelagic sediments, Aquat. Geochemistry, 8(3), 153–175, 2002.

Schlitzer, R.: Ocean Data View, http://odv.awi.de, 2011.

Schlitzer, R., Roether, W., Oster, H., Junghans, H.-G., Hausmann, M., Johannsen, H. and Michelato, A.: Chlorofluoromethane and oxygen in the Eastern Mediterranean, Deep Sea Res. Part A. Oceanogr. Res. Pap., 38(12), 1531–1551, doi:10.1016/0198-0149(91)90088-W, 1991.

Seiter, K., Hensen, C., Schröter, J. and Zabel, M.: Organic carbon content in surface sediments—defining regional provinces, Deep Sea Res. Part I Oceanogr. Res. Pap., 51(12), 2001–2026, doi:10.1016/j.dsr.2004.06.014, 2004.

Selvaraj, K., Lee, T. Y., Yang, J. Y. T., Canuel, E. A., Huang, J. C., Dai, M., Liu, J. T. and Kao, S. J.: Stable isotopic and biomarker evidence of terrigenous organic matter export to the deep sea during tropical storms, Mar. Geol., 364, 32–42, doi:10.1016/j.margeo.2015.03.005, 2015.

Siokou-Frangou, I., Gotsis-Skretas, O., Christou, E. D. and Pagou, K.: Plankton characteristics in the Aegean, Ionian and NW Levantine Seas, in The Eastern Mediterranean as a Laboratory Basin for the Assessment of Contrasting Ecosystems, edited by P. Malanotte-Rizzoli and V. N. Eremeev, pp. 465–473, Kluwer Academic Publisher, Dordrecht, Boston, London., 1999.

Skonieczny, C., Bory, A., Bout-Roumazeilles, V., Abouchami, W., Galer, S. J. G., Crosta, X., Diallo, A. and Ndiaye, T.: A three-year time series of mineral dust deposits on the West African margin: Sedimentological and geochemical signatures and implications for interpretation of marine paleo-dust records, Earth Planet. Sci. Lett., 364, 145–156, doi:10.1016/j.epsl.2012.12.039, 2013.

Statham, P. J. and Hart, V.: Dissolved iron in the Cretan Sea (eastern Mediterranean), Limnol. Oceanogr., 50(4), 1142–1148, doi:10.4319/lo.2005.50.4.1142, 2005.

Stavrakakis, S., Chronis, G., Tselepides, A., Heussner, S., Monaco, A. and Abassi, A.: Downward fluxes of settling particles in the deep Cretan Sea (NE Mediterranean), Prog. Oceanogr., 46(2-4), 217–240, doi:10.1016/S0079-6611(00)00020-3, 2000.

Stavrakakis, S., Gogou, A., Krasakopoulou, E., Karageorgis, A. P., Kontoyiannis, H., Rousakis, G., Velaoras, D., Perivoliotis, L., Kambouri, G., Stavrakaki, I. and Lykousis, V.: Downward fluxes of sinking particulate matter in the deep Ionian Sea (NESTOR site), eastern Mediterranean: seasonal and interannual variability, Biogeosciences, 10(11), 7235–7254, doi:10.5194/bg-10-7235-2013, 2013.

Struck, U., Emeis, K.-C., Voß, M., Krom, M. D. and Rau, G. H.: Biological productivity during sapropel S5 formation in the Eastern Mediterranean Sea: evidence from stable isotopes of nitrogen and carbon, Geochim. Cosmochim. Acta, 65(19), 3249–3266, doi:10.1016/S0016-7037(01)00668-8, 2001.

Taupier-Letage, I.: On the use of thermal images for circulation studies: applications to the Eastern Mediterranean basin, in Remote Sensing of the European Seas, edited by V. Barale and M. Gade, pp. 153–164, Springer, Netherlands., 2008.

Tesi, T., Miserocchi, S., Goñi, M. A., Langone, L., Boldrin, A. and Turchetto, M.: Organic matter origin and distribution in suspended particulate materials and surficial sediments from the western Adriatic Sea (Italy), Estuar. Coast. Shelf Sci., 73(3-4), 431–446, doi:10.1016/j.ecss.2007.02.008, 2007a.

Tesi, T., Miserocchi, S., Goñi, M. A. and Langone, L.: Source, transport and fate of terrestrial organic carbon on the western Mediterranean Sea, Gulf of Lions, France, Mar. Chem., 105(1-2), 101–117, doi:10.1016/j.marchem.2007.01.005, 2007b.

Tesi, T., Langone, L., Goñi, M. A., Turchetto, M., Miserocchi, S. and Boldrin, A.: Source and composition of organic matter in the Bari canyon (Italy): Dense water cascading versus particulate export from the upper ocean, Deep Sea Res. Part I Oceanogr. Res. Pap., 55(7), 813–831, doi:10.1016/j.dsr.2008.03.007, 2008.

Theocharis, A., Georgopoulos, D., Lascaratos, A. and Nittis, K.: Water masses and circulation in the central region of the Eastern Mediterranean: Eastern Ionian, South Aegean and Northwest Levantine, 1986–1987, Deep sea Res. Part II Top. Stud. Oceanogr., 40(6), 1121–1142, doi:Water masses and circulation in the central region of the Eastern Mediterranean: Eastern Ionian, South Aegean and Northwest Levantine, 1986–1987, 1993.

Theocharis, A., Balopoulos, E., Kioroglou, S., Kontoyiannis, H. and Iona, A.: A synthesis of the circulation and hydrography of the South Aegean Sea and the Straits of the Cretan Arc (March 1994–January 1995), Prog. Oceanogr., 44(4), 469–509, doi:10.1016/S0079-6611(99)00041-5, 1999.

Theodosi, C., Parinos, C., Gogou, A., Kokotos, A., Stavrakakis, S., Lykousis, V., Hatzianestis, J. and Mihalopoulos, N.: Downward fluxes of elemental carbon, metals and polycyclic aromatic hydrocarbons in settling particles from the deep Ionian Sea (NESTOR site), Eastern Mediterranean, Biogeosciences, 10(7), 4449–4464, doi:10.5194/bg-10-4449-2013, 2013.

Thingstad, T. F., Krom, M. D., Mantoura, R. F. C., Flaten, G. A. F., Groom, S., Herut, B., Kress, N., Law, C. S., Pasternak, A., Pitta, P., Psarra, S., Rassoulzadegan, F., Tanaka, T., Tselepides, A., Wassmann, P., Woodward, E. M. S., Riser, C. W., Zodiatis, G. and Zohary, T.: Nature of phosphorus limitation in the ultraoligotrophic eastern Mediterranean., Science, 309(5737), 1068–71, doi:10.1126/science.1112632, 2005.

Triantaphyllou, M. V.: Coccolithophore export production and response to seasonal surface water variability in the oligotrophic Cretan Sea (NE Mediterranean), Micropaleontology, 50(Suppl_1), 127–144, doi:10.2113/50.Suppl_1.127, 2004.

Tsapakis, M. and Stephanou, E. G.: Occurrence of gaseous and particulate polycyclic aromatic hydrocarbons in the urban atmosphere: study of sources and ambient temperature effect on the gas/particle concentration and distribution, Environ. Pollut., 133(1), 147–156, doi:10.1016/j.envpol.2004.05.012, 2005.

Turchetto, M., Boldrin, A., Langone, L., Miserocchi, S., Tesi, T. and Foglini, F.: Particle transport in the Bari Canyon (southern Adriatic Sea), Mar. Geol., 246(2-4), 231–247, doi:10.1016/j.margeo.2007.02.007, 2007.

UNEP/MAP/MEDPOL: Sub-regional assessment of the Status of Marine and Coastal Ecosystems and of Pressures to the Marine and Coastal Environment Eastern Mediterranean Sea UNEP(DEPI)/MED WG.350/Inf.4, pp. 37–38, Barcelona., 2010.

Ursella, L., Kovačević, V. and Gačić, M.: Tidal variability of the motion in the Strait of Otranto, Ocean Sci., 10(1), 49–67, doi:10.5194/os-10-49-2014, 2014.

Volkman, J. K.: A review of sterol markers for marine and terrigenous organic matter, Org. Geochem., 9(2), 83–99, doi:10.1016/0146-6380(86)90089-6, 1986.

Volkman, J. K.: Lipid markers for marine organic matter, in Marine Organic Matter: Biomarkers, Isotopes and DNA, edited by J. K. Volkman, pp. 27–70, Springer Verlag, Berlin., 2006.

Volkman, J. K., Kearney, P. and Jeffrey, S. W.: A new source of 4-methyl sterols and 5α (H)-stanols in sediments: prymnesiophyte microalgae of the genus Pavlova, Org. Geochem., 15(5), 489–497, doi:10.1016/0146-6380(90)90094-G, 1990.

Volkman, J. K., Barrett, S. M. and Blackburn, S. I.: Eustigmatophyte microalgae are potential sources of C29 sterols, C22-C28 n-alcohols and C28-C32 n-alkyl diols in freshwater environments, Org. Geochem., 30(5), 307–318, doi:10.1016/S0146-6380(99)00009-1, 1999.

Wang, Z., Fingas, M. and Page, D. S.: Oil spill identification, J. Chromatogr. A, 843(1-2), 369–411, doi:10.1016/S0021-9673(99)00120-X, 1999.

Weldeab, S., Emeis, K.-C., Hemleben, C. and Siebel, W.: Provenance of lithogenic surface sediments and pathways of riverine suspended matter in the Eastern Mediterranean Sea: evidence from 143Nd/144Nd and 87Sr/86Sr ratios, Chem. Geol., 186(1-2), 139–149, doi:10.1016/S0009-2541(01)00415-6, 2002.

Ziveri, P., Rutten, A., de Lange, G. ., Thomson, J. and Corselli, C.: Present-day coccolith fluxes recorded in central eastern Mediterranean sediment traps and surface sediments, Palaeogeogr. Palaeoclimatol. Palaeoecol., 158(3-4), 175–195, doi:10.1016/S0031-0182(00)00049-3, 2000.

Zoccolotti, L. and Salusti, E.: Observations of a vein of very dense marine water in the southern Adriatic Sea, Cont. Shelf Res., 7(6), 535–551, doi:10.1016/0278-4343(87)90020-3, 1987.

2.4. Enhanced carbon export to the abyssal depths driven by atmosphere dynamics

R. Pedrosa-Pàmies[a], A. Sanchez-Vidal[a*], M. Canals[a], N. Lampadariou[b], D. Velaoras[c], A. Gogou[c], C. Parinos[c], A. Calafat[a]

[a] GRC Geociències Marines, Departament de Dinàmica de la Terra i de l'Oceà, Facultat de Ciències de la Terra, Universitat de Barcelona, Barcelona, Spain.

[b] Hellenic Centre for Marine Research, Institute of Oceanography, Heraklion, Crete, Greece.

[c] Hellenic Centre for Marine Research, Institute of Oceanography, Anavyssos, Attiki, Greece

Submitted May 2016. Geophysical Research Letters.

Abstract

Long-term biogeochemical observations are critical to understand the natural ability of the oceans to fix CO_2 into organic carbon and export it to the deep as sinking particles. Here we present results from a three-year (2010-13) sediment trap deployment that allowed to detect interannual variations of carbon fluxes beyond 4000 m depth in the Eastern Mediterranean Sea. Anomalous atmospheric conditions triggering strong heat losses in winter-spring 2012 resulted in convective mixing, nutrient uplifting and a diatom-dominated bloom south-east of Crete. Phytoplankton growth, reinforced by the arrival of nutrients from airborne Etna volcano ash, was the highest in the last decade (satellite-derived Chl-a concentrations up to 1.9 mg m^{-3}). This situation caused carbon export to increase by 2 orders of magnitude (12.2 mg m^{-2} d^{-1}) with respect to typical values, which demonstrates how pulses of sinking fresh phytodetritus linked to rare atmospheric processes can episodically impact one of the most oligotrophic environments in the world ocean.

2.4.1. Introduction

One of the grand challenges in marine biogeochemistry is to improve our understanding on the regional, seasonal and multi-annual variability of ocean uptake of CO_2, and the biological and physical processes that regulate this process (Achterberg, 2014). Only a small fraction of the carbon fixed by marine plankton will be exported as sinking particles to the deep ocean and sequestered out of further contact with the atmosphere on timescales of thousands of years (see review in Henson et al., 2012). In this framework, quantification of sinking organic carbon (OC) becomes critical to tie shifts in ocean productivity with atmospheric CO_2 concentrations, and to better understand feedbacks between the carbon cycle and the climate system. This is of special importance in oligotrophic waters, which roughly cover 75% of the ocean's surface (Lewis et al., 1986) and contribute over 30% of the global marine carbon fixation (Longhurst et al., 1995; Marañón et al., 2003).

One of the most oligotrophic environments in the global ocean is the Eastern Mediterranean Sea (EMS) (Krom et al., 1991). Despite relatively high nutrient inputs from the atmosphere, the anti-estuarine circulation of the EMS, with nutrient-depleted Atlantic Water flowing in through the Strait of Sicily and nutrient-rich Levantine Intermediate Water (LIW) flowing out at intermediate depths, results in a net outflow of nutrients and ultra-oligotrophic conditions (e.g., Ribera d'Alcalà, 2003; Huertas et al., 2012). This leads to a phytoplanktonic community dominated by heavily grazed pico- and nano- phytoplankton (Yacobi et al., 1995; Zohary and Robarts, 1998; Christaki, 2001; Siokou-Frangou et al., 2010) and drives primary production rates below 200 mg C m^{-2} d^{-1} (Psarra et al., 2000; Moutin and Raimbault, 2002), which translates into very low amounts of OC reaching the EMS deep sea (Warnken, 2003; Koppelmann et al., 2004; Stavrakakis et al., 2013; Gogou et al., 2014).

Here we present the results of a three years (2010-13) continuous monitoring of sinking particles to the abyssal EMS (i.e. beyond 4000 m water depth). Peculiar atmospheric conditions in one of the years triggered a significant nutrient enrichment in surface waters and a shift of the phytoplanktonic community towards diatom-dominance, which significantly enhanced carbon export to the deep. Our data provide unequivocal evidence that atmosphere-driven fluctuations of the marine environment play an important role in carbon fixation, export and transfer to oligotrophic abyssal regions.

2.4.2. Data and methods

Data on air-sea heat fluxes were obtained from the Modern Era Retrospective-analysis for Research and Applications (MERRA), a NASA satellite dataset reanalysis using a new version of the Goddard Earth Observing System Data Assimilation System Version 5 (GEO-5). Net air-sea heat exchange (Qnet) represents the net sum of sensible heat flux from conduction (SHF), latent heat flux from evaporation (LHF), short-wave flux from incoming solar radiation and long-wave flux from back solar radiation. The non-radiative flux (i.e. the sum of sensible and latent heat flux) is often named turbulent heat flux while the other two components form the radiative flux. In our analysis we have used monthly averaged sensible and latent heat flux data.

Monthly Sea Surface Height (SSH) was calculated with a Mediterranean configuration of the NEMO ocean model provided by the Mediterranean Monitoring and Forecasting Centre (Med-MFC) (MOHC et al., 2014, and references therein). Monthly Sea Surface Temperature (SST) and Chlorophyll-a concentration (Chl-a) were obtained from Moderate Resolution Imaging Spectrometer (MODIS), in orbit on the Aqua platform, using 4-km resolution level 3-binned data. Both monthly SST and Chl-a data are processed and distributed by the NASA Goddard Earth Sciences (GES) Data, Information Services Center (DISC) and Ocean Biology Processing Group (OBPG). Due to the lack of in situ measurements, concentrations of dissolved molecular oxygen (O2) and nitrate (N) and phosphate (P) nutrients at the limit of the euphotic zone (200 m) were obtained from the Biogeochemical Flux Model (OPATM-BFM) outputs which are known to agree fairly well with data from cruises and fixed monitoring stations in the Mediterranean Sea (Lazzari et al., 2010, 2012, 2016). Si nutrient data were obtained from the PELAgic biogeochemistry for Global Ocean Simulations (PELAGOS025) which is a coupling between the NEMO ocean model and the Biogeochemical Flux Model (BFM, Vichi et al., 2013).

The concentrations of sulphur dioxide (SO_2) injected throughout the troposphere and into the stratosphere (total column amount) were obtained from the Nasa Goddard Earth Science Data and Information Services Center (GES DISC) from the OMI/Aura Level-3e SO_2 Data Product OMSO2e (Version 003) (Krotkov and Li, 2012). The SO_2 concentration is expressed in Dobson units (1 DU = 0.029 g m^{-2}, Spinei et al., 2010).

Sinking particles were collected at 4285 m water column depth with a PPS3 Technicap sequential sampling sediment trap (0.125 m^2 collecting area, 12 collecting cups) from June 2010 to May 2013 at the 4310 m deep Ierapetra Basin (Fig. 2.27a-b, red dot). The trap was moored 25 m above the bottom and the sampling interval was 1 month. After every 12 months recovery, samples were stored in dark at 4 ºC until they were processed in the laboratory. Swimmers were hand-picked under a microscope with fine tweezers, and samples were three times stirred with ultrapure water, centrifuged and the supernatant removed to eliminate salt and formaldehyde. Samples were then freeze-dried and weighted to determine total mass fluxes.

OC content and its stable isotope $\delta^{13}C$ were measured in 25% HCl treated samples on a Flash 1112 EA elemental analyser interfaced to a Delta C Finnigan MAT isotope ratio mass spectrometer. Uncertainties were lower than 0.1% and 0.05‰, respectively. Biogenic opal (SiO2 0.4H2O) content was analysed using a two-step 2.5 h extraction with a 0.5M Na2CO3 solution at 85 ºC, followed by the measurement of dissolved Si and Al contents in both leachates with a Perkin-Elmer Optima 3200RL Inductive Coupled Plasma Optical Emission Spectrometer (ICP-OES). The Si content of the first leachate was corrected by the Si/Al ratio of the second one in order to correct for the excess Si dissolved from aluminosilicates (Kamatani and Oku, 2000; Fabres et al., 2002; Ragueneau et al., 2005). Uncertainty of opal was lower than 0.4%.

Morphology and composition of sinking particles were investigated with a Scanning Electron Microscope (SEM- J7100 FE) equipped with Energy Dispersive Spectrometry (EDS), which allowed semi-quantitative analyses of major chemical components of particles.

2.4.3. Results

2.4.3.1. Air-sea exchanges and ocean response

Time series of monthly sensible and latent heat flux, SSH, dissolved O_2 content and 8-day averaged Chl-a concentration above the sediment trap are shown in Figure 2.28a-c, while time averaged maps of Q_{net}, SST, SSH and Chl-a for the three monitored years are presented in Figure 2.29a-d. While seasonal variability is clearly visible in the time series, extreme values within the 2010-13 study period correspond to winter-spring 2012, with enhanced air-sea turbulent heat losses (SHF and LHF up to 39, 128 W m^{-2}, respectively), low SSH (down to -0.50 cm) and peak of dissolved O_2 concentration at the lower limit of the euphotic zone (208 mmol O_2 m^{-3}) (Fig. 2.28a-b). In the same period, intense winter buoyancy losses were recorded east of the mooring location in the Rhodes Gyre (RG), with the highest Q_{net} and lowest SST in January-March 2012 (Fig. 2.29a-b). Chl-a concentration in the core of the RG in March 2012 is the highest (up to 1.90 mg Chl-a m^{-3}) (Fig. 2.29d) within the 2010-13 period and also within the entire MODIS-Aqua NASA GES DISC series available since June 2002, both in the Ierapetra Basin (Fig. 2.28c) and the RG (data not shown).

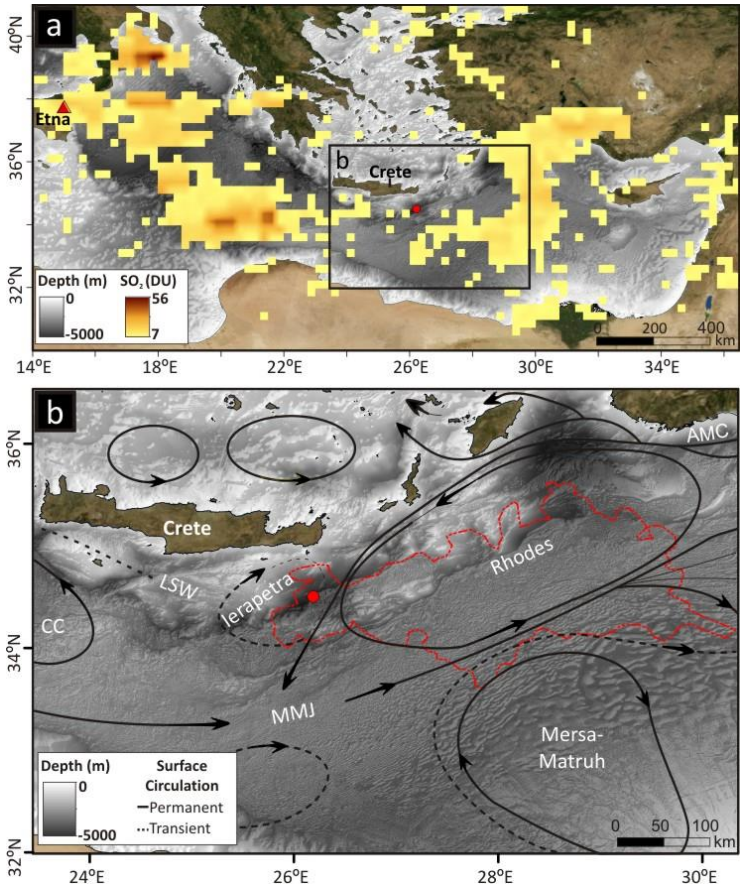

Figure 2.27. a) Cumulative total column SO_2 of March and April 2012. DU: Dobson unit (1 DU = 0.029 g m^{-2}, Spinei et al., 2010). B) Schematic representation of the upper thermocline circulation in the study area (Robinson and Golnaraghi, 1993). Circulation patterns and water masses: MMJ-Mid-Mediterranean Jet, AMC-Asia Minor Current, LSW-Levantine Surface Water, CC- Cretan Cyclone. The red dot shows the sediment trap location and the dashed red polygon is the contour of the Rhodes Gyre phytoplankton bloom of March 2012 as indicated by Chl-a concentrations above 0.2 mg m^{-3} (48291.3 km^2). Bathymetric data from EMODnet Bathymetry portal.

2.4.3.2. Particle fluxes

Beyond extremely low values (i.e. well below 1 mg m^{-2} d^{-1}) for OC and opal fluxes during most of the sampling period, a significant increase was recorded in April 2012 (Fig. 2.28e-f). By that time, OC and opal fluxes were ~14-fold (up to 12.2 mg $m^{-2}d^{-1}$) and ~128-fold (up to 58.7 mg $m^{-2}d^{-1}$) higher than those recorded in the same month in 2011 and 2013, respectively.

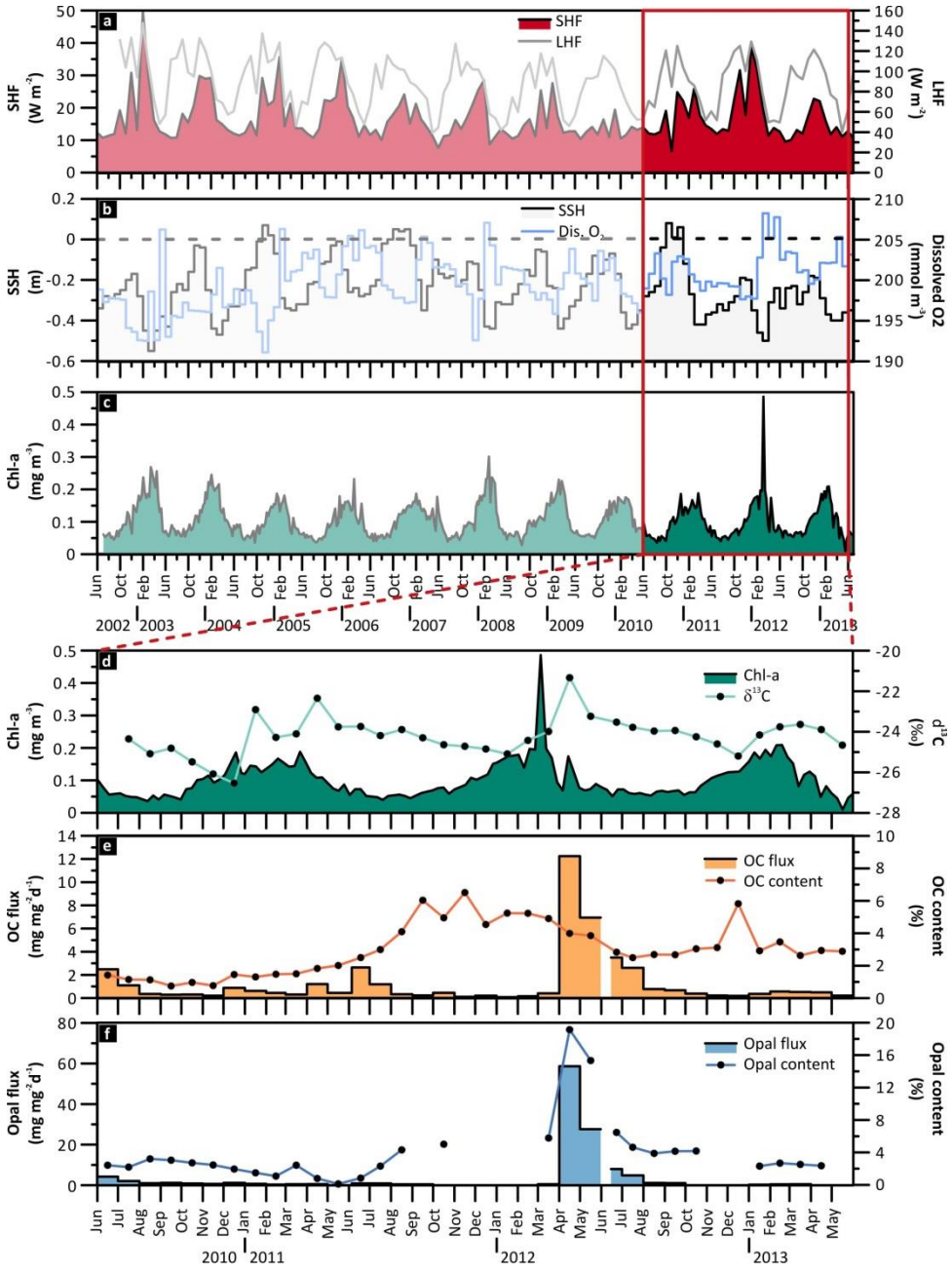

Figure 2.28. 10-year monthly time-series of a) sensible (red area) and latent (grey line) heat fluxes (positive values denote heat loss), b) sea surface height above mean sea level (black line) and dissolved O_2 concentration (blue line), c) Chl-a concentration (green area). Detail of the 3-year time series of d) 8-day average Chl-a concentration (green area) and monthly $\delta^{13}C$ (green line with black dots), e) monthly organic carbon flux (orange area) and content (orange line with black dots) and f) monthly opal flux (blue area) and content (blue line with black dots). Satellite data have been obtained from one grid cell above the location of the sediment trap: 34.3-34.6º N, 26.0-26.3º E.

Molar biogenic silicon to OC ratio (Si/OC) of the settling particles ranged from 0.08 to 0.86, with the highest value recorded in April 2012. Furthermore, the OC exported during this event shows the highest $\delta^{13}C$ values during the entire monitoring period, which were close to -20‰ (Fig. 2.28d). This indicates that most of the settling OC derived from marine algae (Goericke and Fry, 1994; Harmelin-Vivien et al., 2008).

Settling particles collected in April 2012 were embedded in a mucilaginous matrix. SEM observations showed that these particles contained highly diverse, well preserved, medium-size (from 5 to 300 μm) long-chain-forming centric (radially symmetric) diatoms such as *Chaetoceros spp.*, *Thalassioria spp.* And *Rhizosolenia spp.* (Fig. 2.30a). Among these fresh phytoplankton cells, micrometre-sized spherules (diameter ranging from 0.1 to 10 μm) were also observed (Figs. 2.30b and supplementary Fig. 2.31). The EDS analysis of these spherules showed the presence of Si, Al, Mg, Fe, S, K, Ca and Na as major elements (Fig. 2.30c). Their spheroidal shape and S-content (Lefèvre et al., 1986; Kelepertsis et al., 2003; Calabrese and D'Alessandro, 2015; Jeong et al., 2016), and the lack of significant arrival of desert dust events during winter 2011-12 as simulated by BSC-DREAM8b v2.0 (Basart et al., 2012), suggest that these particles were volcanic ash. Accordingly, Mount Etna in Sicily, 1080 km WNW of the study site and the Europe's tallest and most active volcano, released significant amounts of volcanic ash into the atmosphere in March 18-19 and April 1, 12 and 24, 2012. Cumulative total column SO_2 illustrate how Etna's volcanic ash plumes were wind carried hundreds of kilometres eastward over the EMS (Fig. 2.27a). Relative lateral advection of the falling ash spherules may have caused these particles to reach abyssal depths (Siegel et al., 2008).

2.4.4. Discussion

2.4.4.1. Atmospheric Forcing

Oceanographic research over the last decades has revealed that extreme weather events, such as typhoons and storms, can significantly enhance OC export to the deep sea floor in oligotrophic environments (Siegel et al., 1999; Siswanto et al., 2008; Hung et al., 2009; Lomas et al., 2010; Chen et al., 2013). One good example of how an abrupt shift in weather conditions can encompass a multitude of physical and biogeochemical variables is intense open ocean deep convection occurring in the NW Mediterranean Sea (MEDOC Group., 1970), which increase phytoplankton productivity and OC export to the deep sea floor (Stabholz et al., 2013; Auger et al., 2014). One of the strongest events recorded up to date was that occurring in winter 2011-12, when atmospheric conditions involving particularly strong cold and dry northerly winds triggered intense convection not only in the NW Mediterranean Sea but also in the southern Adriatic Sea (Bensi et al., 2013; Durrieu de Madron et al., 2013; Janeković et al., 2014).

Indeed, winter 2011-12 was particularly cold across all of Eurasia, and January and February were some of the coldest months in the last 50 years over the Greek region (Tolika et al., 2014). The prevalence of these low temperature conditions seems to be mainly associated with the occurrence of an intense NNW or NNE atmospheric flow, as a consequence of the phasing between a negative Artic Oscillation and a positive Eastern Mediterranean Pattern (Hatzaki et al., 2009). The resulting atmospheric blocking, caused by the extension of the Siberian High over the

Balkans and the situation over NW Europe, favoured the arrival of northerly cold and relatively dry air masses over the Balkans and the Eastern Mediterranean region (WMO, 2013), leading to strong heat losses over the EMS (Fig. 2.29a) and lowered SST (Fig. 2.29b). This situation caused a large vertical temperature gradient with the subsequent buoyancy loss and mixing between surface and intermediate-deep waters through intense vertical convective overturning processes in March 2012. A reinforced cyclonic RG with low SSH in its centre (Figs. 2.28b and 2.29c) illustrates the deepening of the mixed layer (Béranger et al., 2010) which corresponds to the main mechanism of Levantine Intermediate Water formation in winter-spring (Lascaratos et al., 1999).

2.4.4.2. Oceanographic and Biological Response

Intense convection in early 2012 (winter) caused the upwelling of relatively cold water masses that spread along isopycnal surfaces from the periphery of the RG to the southeast of Crete. As a result, the core of the RG acquired a shape like plume extending over the Ierapetra Basin (Fig. 2.29b). This favoured the build-up of phytoplanktonic biomass thanks to the injection of nutrients upwelled from below (Ediger and Yilmaz, 1996; Napolitano et al., 2000). The concentrations of essential nutrients such as N and P in the core of the RG were much higher (up to 2.72 μM and 0.13 μM, respectively (supplementary Table 2.8) than in adjacent areas (<1.00 μM and <0.04 μM, respectively) (data not shown), which supports convection as a main N and P supplier to the euphotic layer. In addition, N:P ratios in the RG (21:1), which were similar to those found in the 200-600 m deep LIW (Krom et al., 2010), significantly exceed the Redfield ratio (16:1) in agreement with the well-known P-limitation of the EMS (Thingstad et al., 2005; Krom et al., 2010).

Sinking particles in April 2012 comprised numerous diatoms frustules, which is consistent with a diatom-dominance bloom and silicic acid overconsumption during diatom growth. Despite no substantial variation in the modelled nutrient concentrations in surface waters during the three monitored bloom periods (supplementary Table 2.8), the diatom abundance was significantly higher in April 2012. Taking into account that Si can be limiting for diatom growth in the Mediterranean Sea when upwelled Si has been exhausted (Leblanc et al., 2003; Crombet et al., 2011), an additional input of Si would be needed to account for the Si-depleted conditions that sustained the high diatom production rates in April 2012. Releasing of Si, and also probably Fe, into seawater from volcanic ash ejected during Mount Etna eruptions in March-April 2012 is one plausible source, although the lack of direct nutrient measurements during the event prevents confirmation. A few studies have documented the release of nutrients bioavailable for phytoplankton growth in the Mediterranean Sea by Etna ash fallout, altering the nutrient budget and changing the composition of phytoplankton assemblages towards diatom-dominance (Censi et al., 2010; Olgun et al., 2013). Long-chained centric diatoms found in the sinking particles, which are known for their fast growth in response to nutrient enrichments (Kemp et al., 2000; Rigual-Hernandez et al., 2013), may have been benefited from Si released into the euphotic zone from Etna ash. While the fertilizing potential of newly erupted Mount Etna ash particles in the oligotrophic EMS had been mentioned previously, this is the first time that the synergistic effect of atmospheric forcing and volcanic ash deposition on phytoplankton blooming is observed in the EMS and probably beyond.

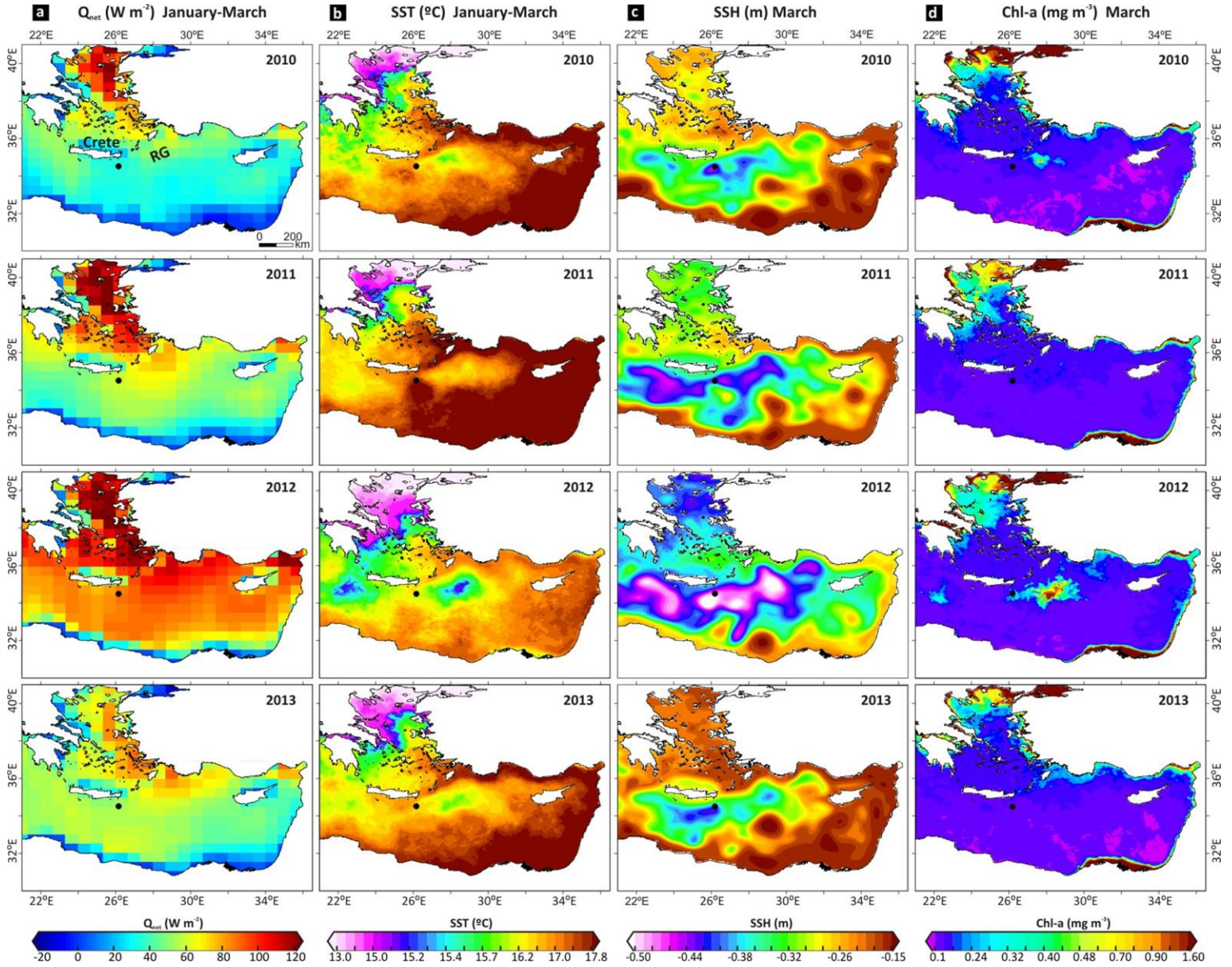

Figure 2.29. Time averaged (3-month) maps of a) net heat flux (with positive values denoting oceanic heat loss) and b) sea surface temperature in January to March, and time-averaged (1-month) maps of c) sea surface height and d) Chl-a concentration in March 2010, 2011, 2012 and 2013. RG: Rhodes Gyre.

The decline of the diatom bloom in April 2012 may have been triggered by nutrient limitation and aggregate formation followed by rapid sedimentation (Alldredge and Silver, 1988). Coagulation of diatoms is principally controlled by the species composition and by the abundance of extrapolymeric substances (Passow et al., 1994; Crocker and Passow, 1995). The mucilaginous matrix embedding sinking particles is, therefore, attributed to the production of transparent exopolymers from diatom exudates rich in acidic polysaccharides (Alldredge et al., 1993; Logan et al., 1995; Gogou and Repeta, 2010), which may enhance post-bloom flocculation and massive sinking when nutrients run out (Smetacek, 1985, 2000; Alldredge and Gotschalk, 1989). The consumption of silicic acid during diatom growth led to a marked increase of the molar Si/OC ratio (from <0.2 to up to 1) in the settling biogenic particles in April 2012, thereby enhancing Si burial. Our observations demonstrate that diatom particles sunk from the upper ocean layers reaching the deep Ierapetra Basin in less than a month transit time without altering much of their bulk morphology or assemblage. This is in agreement with the estimated sinking speeds of diatoms (175 m d^{-1}) reported by Takahashi (1986).

2.4.4.3. Impact on the Carbon Cycle

The presence of well-preserved diatom cells (Fig. 2.30a), the strong relationship between opal and OC export (r^2=0.93, p<0.001) and the high percentages of opal after March 2012 (up to 19.2%) provide evidence of the role of diatom blooms in driving downward OC flux from the surface to depths beyond 4000 m in the EMS (Fig. 2.28e). Our data show how during anomalous atmospheric conditions the area below RG, which has been considered as a nutrient 'oasis' in the EMS 'desert' (Mazzocchi et al., 1997; Siokou-Frangou et al., 2010), is impacted by the enhanced sedimentation of relatively well preserved diatom cells. These findings demonstrate (1) the coupling of atmospheric conditions including dust (ash) fall, sea surface dynamics and the abyssal ecosystem through the stimulation of primary production and an enhanced fast vertical flux of OC, and (2) that relatively fresh diatom cells can reach bathypelagic depths down to 4000 m in the EMS. Our findings support the view that this process likely is ubiquitous and prevalent across the global oligotrophic ocean (Agusti et al., 2015).

Assuming that sinking particles in April 2012 are representative of the OC load after the input of nutrients through convection and ash supply, we estimate that particulate OC exported through the whole RG area (Fig. 2.27b) during the single event of April 2012 accounted for at least 17,738 t OC (or 591 t OC d^{-1}), which is at least 10-25 times higher than OC exported in the same area during years with just weak winter convection. Such impressive figures, even though they may underestimate reality because maximum Chl-a concentrations were not recorded above the mooring location (Fig. 2.29d), show the importance that infrequent, atmosphere-driven events leading to major phytoplankton blooms in oligotrophic regions have in fuelling the biological carbon pump drawing down carbon to the ocean's interior. The total amount of OC sinking during 2012 (807.7 mg OC m^{-2} yr^{-1}) is similar to that found in other bathypelagic regions such as the central gyre of the North Pacific (Kawahata et al., 1998) or the temperate nutrient-rich North Atlantic Ocean (Honjo and Manganini, 1993).

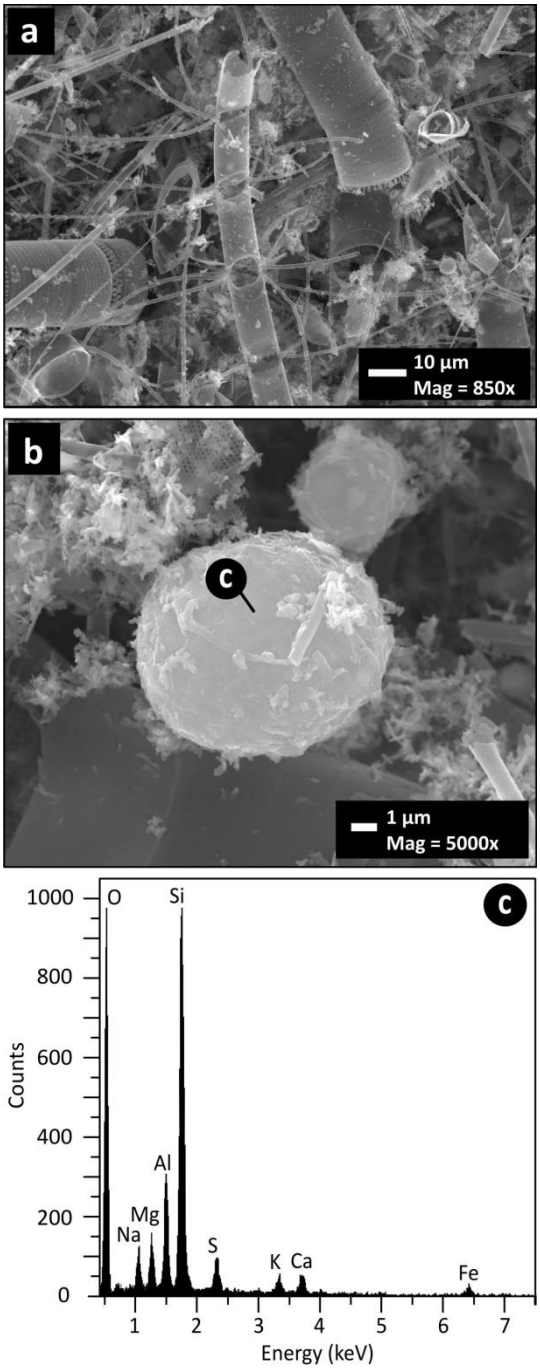

Figure 2.30. a) and b) Scanning electron micrographs of settling particles in April 2012. The first image, a, shows high diversity of non-degraded diatoms such as *Chaetoceros spp.* And *Thalassioria spp.*, and the second one, b, reveal the presence of microspherules. C) EDS spectra of a microspherule found in the settled particles of April 2012. Mag-Magnification.

According to some authors (e.g., Francois et al., 2002), fresh organic matter exported below the euphotic zone is effectively remineralized during its transit through mesopelagic and bathypelagic layers, as most of the sinking particulate OC is transformed into dissolved OC and mineralized by microbes in the upper 1000 m of the water column (Buesseler and Boyd, 2009). Instead, we found labile photosynthetic cells and mucilaginous organic matter reaching the abyssal EMS, therefore representing a major input of energy for bathyal microbial communities and the deep ecosystem at large. The arrival of a high fraction of labile material at bathypelagic depths may

have induced high bacterial production, which can contribute to carbon remineralization and thus oxygen consumption. This is further in agreement with the enhanced oxygen consumption found in EMS deep waters when compared to the open ocean (La Ferla et al., 2003; Meador et al., 2010), which maximize during moments of dense water formation (Santinelli et al., 2010). Our findings reinforce the hypothesis that the Rhodes Gyre area plays a significant role in the biogeochemical functioning of the oligotrophic EMS, acting occasionally as an 'oasis in a marine desert', in respect to the so-called 'Mediterranean paradox' hypothesis (Sournia, 1973).

2.4.5. Acknowledgments

This research has been supported by the REDECO (CTM2008-04973-E/MAR) and PERSEUS (GA 287600) projects. Researchers from GRC Geociències Marines benefited from a *Grups de Recerca Consolidats* grant (2014 SGR 1068) by *Generalitat de Catalunya* autonomous government. We sincerely thank the officers, crews of *R/V* Aegaeo, C. Pasqual, O. Veres and P. Lopez- Fernandez for their precious help during cruises, and A. Rumín-Caparrós and D. Zúñiga for their valuable comments. Elemental analyses and SEM have been performed at the Scientific and Technological Centres of the University of Barcelona. R.P.-P. is supported by a predoctoral FPU grant and A.S.-V. by a Ramon y Cajal contract. The data used in this study are listed in the figures and references. Particle flux data is stored in PANGAEA (doi: 10.1594/PANGAEA.860809). We would like to thank the editor Tatiana Ilyina and the two anonymous referees for their constructive comments that helped significantly to improve the quality of this paper.

2.4.6. Supplementary table and figure

	2010	2011	2012	2013
N (µM)	2.75	2.57	2.72	2.63
P (µM)	0.13	0.12	0.13	0.13
Si (µM)	2.98	3.12	3.71	4.21
Time-weighted total OC flux (mg OC m^{-2} yr^{-1})	143.4	237.8	807.7	291.1

Table 2.8. Mean nutrient concentrations (N, P and Si) of winter-early spring months (from January to March) in the core of the Rhodes Gyre at the limit of the euphotic zone (200 m), and the total annual time-weighted OC fluxes during the studied period (from 2010 to 2013).

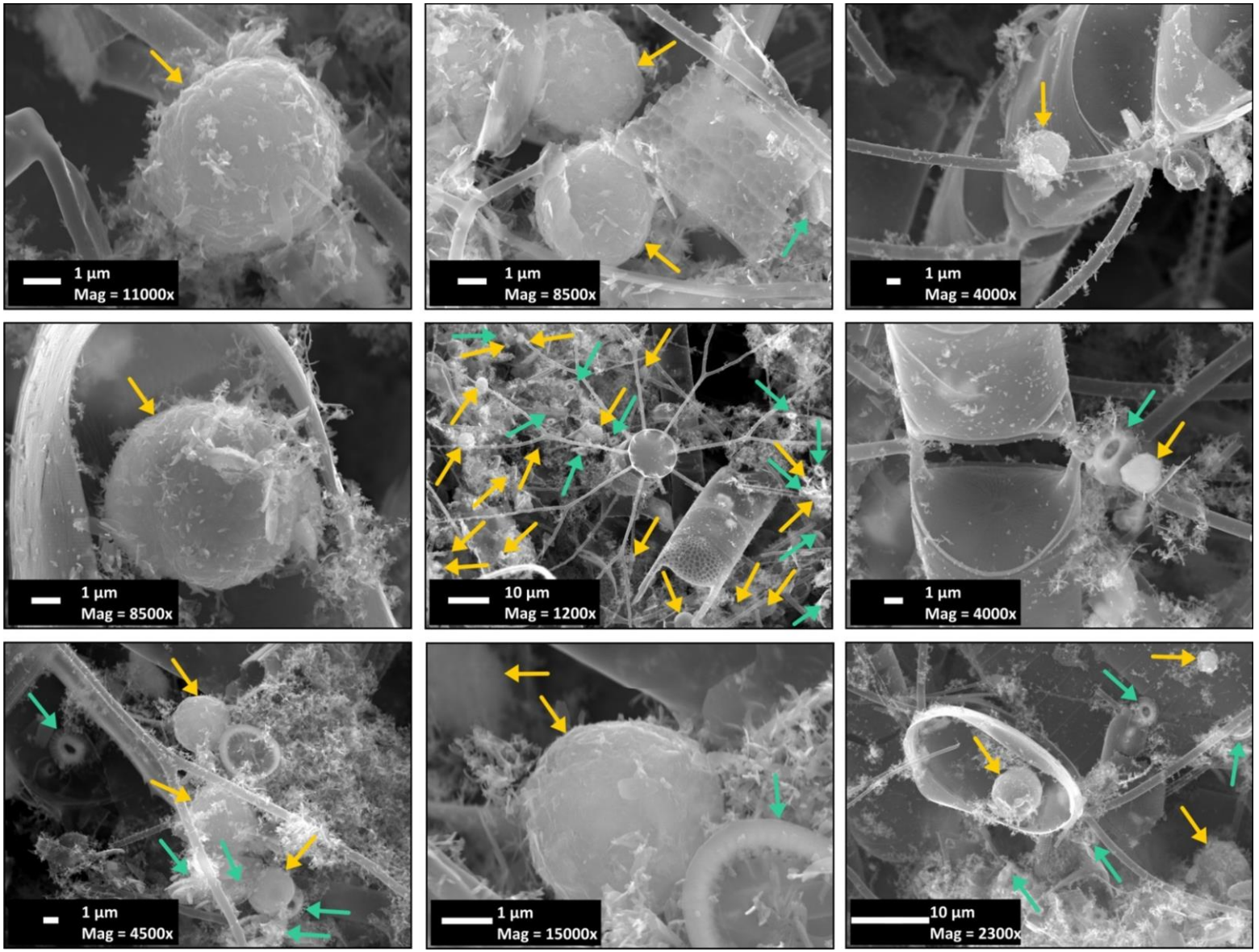

Figure 2.31. Scanning electron micrographs of settling particles in April 2012. Images reveal the abundant presence of microspherules among the well preserved diatoms. Yellow arrows show ash microspherules, and green arrows show coccolithophores. Both major components (airborne lithogenics including ash and dust, and calcium carbonate produced by pelagic organisms) accounted for 73% of the total mass flux. Mag-Magnification.

2.4.7. References

Achterberg, E. P.: Grand challenges in marine biogeochemistry, Front. Mar. Sci., 1(7), 1–5, doi:10.3389/fmars.2014.00007, 2014.

Agusti, S., González-Gordillo, J. I., Vaqué, D., Estrada, M., Cerezo, M. I., Salazar, G., Gasol, J. M. and Duarte, C. M.: Ubiquitous healthy diatoms in the deep sea confirm deep carbon injection by the biological pump., Nat. Commun., 6, 7608, doi:10.1038/ncomms8608, 2015.

Alldredge, A. L. and Gotschalk, C. C.: Direct observations of the mass flocculation of diatom blooms: characteristics, settling velocities and formation of diatom aggregates, Deep Sea Res. Part A. Oceanogr. Res. Pap., 36(2), 159–171, doi:10.1016/0198-0149(89)90131-3, 1989.

Alldredge, A. L. and Silver, M. W.: Characteristics, dynamics and significance of marine snow, Prog. Oceanogr., 20(1), 41–82, doi:10.1016/0079-6611(88)90053-5, 1988.

Alldredge, A. L., Passow, U. and Logan, B. E.: The abundance and significance of a class of large, transparent organic particles in the ocean, Deep Sea Res. Part I Oceanogr. Res. Pap., 40(6), 1131–1140, doi:10.1016/0967-0637(93)90129-Q, 1993.

Auger, P. A., Ulses, C., Estournel, C., Stemmann, L., Somot, S. and Diaz, F.: Interannual control of plankton communities by deep winter mixing and prey/predator interactions in the NW Mediterranean: Results from a 30-year 3D modelling study, Prog. Oceanogr., 124, 12–27, doi:10.1016/j.pocean.2014.04.004, 2014.

Basart, S., Pérez, C., Nickovic, S., Cuevas, E. and Baldasano, J. M.: Development and evaluation of the BSC-DREAM8b dust regional model over Northern Africa, the Mediterranean and the Middle East, Tellus B, 64, doi:10.3402/tellusb.v64i0.18539, 2012.

Bensi, M., Cardin, V., Rubino, A., Notarstefano, G. and Poulain, P. M.: Effects of winter convection on the deep layer of the Southern Adriatic Sea in 2012, J. Geophys. Res. Ocean., 118(11), 6064–6075, doi:10.1002/2013JC009432, 2013.

Béranger, K., Drillet, Y., Houssais, M.-N., Testor, P., Bourdallé-Badie, R., Alhammoud, B., Bozec, A., Mortier, L., Bouruet-Aubertot, P. and Crépon, M.: Impact of the spatial distribution of the atmospheric forcing on water mass formation in the Mediterranean Sea, J. Geophys. Res., 115(C12), C12041, doi:10.1029/2009JC005648, 2010.

Buesseler, K. O. and Boyd, P. W.: Shedding light on processes that control particle export and flux attenuation in the twilight zone of the open ocean, Limnol. Oceanogr., 54(4), 1210–1232, doi:10.4319/lo.2009.54.4.1210, 2009.

Calabrese, S. and D'Alessandro, W.: Characterization of the Etna volcanic emissions through an active biomonitoring technique (moss-bags): part 2–morphological and mineralogical features., Chemosphere, 119, 1456–64, doi:10.1016/j.chemosphere.2014.08.087, 2015.

Censi, P., Randazzo, L. A., Zuddas, P., Saiano, F., Aricò, P. and Andò, S.: Trace element behaviour in seawater during Etna's pyroclastic activity in 2001: Concurrent effects of nutrients and formation of alteration minerals, J. Volcanol. Geotherm. Res., 193(1-2), 106–116, doi:10.1016/j.jvolgeores.2010.03.010, 2010.

Chen, K.-S., Hung, C.-C., Gong, G.-C., Chou, W.-C., Chung, C.-C., Shih, Y.-Y. and Wang, C.-C.: Enhanced POC export in the oligotrophic northwest Pacific Ocean after extreme weather events, Geophys. Res. Lett., 40(21), 5728–5734, doi:10.1002/2013GL058300, 2013.

Christaki, U.: Nanoflagellate predation on auto- and heterotrophic picoplankton in the oligotrophic Mediterranean Sea, J. Plankton Res., 23(11), 1297–1310, doi:10.1093/plankt/23.11.1297, 2001.

Crocker, K. M. and Passow, U.: Differential aggregation of diatoms, Mar. Ecol. Prog. Ser., 117(1-3), 249–257, doi:10.3354/meps117249, 1995.

Crombet, Y., Leblanc, K., Quéguiner, B., Moutin, T., Rimmelin, P., Ras, J., Claustre, H., Leblond, N., Oriol, L. and Pujo-Pay, M.: Deep silicon maxima in the stratified oligotrophic Mediterranean Sea, Biogeosciences, 8(2), 459–475, doi:10.5194/bg-8-459-2011, 2011.

Durrieu de Madron, X., Houpert, L., Puig, P., Sanchez-Vidal, A., Testor, P., Bosse, A., Estournel, C., Somot, S., Bourrin, F., Bouin, M. N., Beauverger, M., Beguery, L., Calafat, A., Canals, M., Cassou, C., Coppola, L., Dausse, D., D'Ortenzio, F., Font, J., Heussner, S., Kunesch, S., Lefevre, D., Le Goff, H., Martín, J., Mortier, L., Palanques, A. and Raimbault, P.: Interaction of dense shelf water cascading and open-sea convection in the northwestern Mediterranean during winter 2012, Geophys. Res. Lett., 40(7), 1379–1385, doi:10.1002/grl.50331, 2013.

Ediger, D. and Yilmaz, A.: Characteristics of deep chlorphyll maximum in the Northeastern Mediterranean with respect to environmental conditions, J. Mar. Syst., 9(3-4), 291–303, doi:10.1016/S0924-7963(96)00044-9, 1996.

Fabres, J., Calafat, A., Sanchez-Vidal, A., Canals, M. and Heussner, S.: Composition and spatio-temporal variability of particle fluxes in the Western Alboran Gyre, Mediterranean Sea, J. Mar. Syst., 33, 431–456, doi:10.1016/S0924-7963(02)00070-2, 2002.

La Ferla, R., Azzaro, M., Civitarese, G. and Ribera d'Alcalà, M.: Distribution patterns of carbon oxidation in the eastern Mediterranean Sea: Evidence of changes in the remineralization processes, J. Geophys. Res., 108(C9), 8111, doi:10.1029/2002JC001602, 2003.

Francois, R., Honjo, S., Krishfield, R. and Manganini, S.: Factors controlling the flux of organic carbon to the bathypelagic zone of the ocean, Global Biogeochem. Cycles, 16(4), 34–1–34–20, doi:10.1029/2001GB001722, 2002.

Goericke, R. and Fry, B.: Variations of marine plankton δ13 C with latitude, temperature, and dissolved CO 2 in the world ocean, Global Biogeochem. Cycles, 8(1), 85–90, doi:10.1029/93GB03272, 1994.

Gogou, A. and Repeta, D. J.: Particulate-dissolved transformations as a sink for semi-labile dissolved organic matter: Chemical characterization of high molecular weight dissolved and surface-active organic matter in seawater and in diatom cultures, Mar. Chem., 121(1-4), 215–223, doi:10.1016/j.marchem.2010.05.001, 2010.

Gogou, A., Sanchez-Vidal, A., Durrieu de Madron, X., Stavrakakis, S., Calafat, A., Stabholz, M., Psarra, S., Canals, M., Heussner, S., Stavrakaki, I. and Papathanassiou, E.: Carbon flux to the deep in three open sites of the Southern European Seas (SES), J. Mar. Syst., 129, 224–233, doi:10.1016/j.jmarsys.2013.05.013, 2014.

Harmelin-Vivien, M., Loizeau, V., Mellon, C. and Beker, B.: Comparison of C and N stable isotope ratios between surface particulate organic matter and microphytoplankton in the Gulf of Lions (NW Mediterranean), Cont. Shelf Res., 28(15), 1911–1919, doi:10.1016/j.csr.2008.03.002, 2008.

Hatzaki, M., Flocas, H. A., Giannakopoulos, C. and Maheras, P.: The Impact of the Eastern Mediterranean Teleconnection Pattern on the Mediterranean Climate, J. Clim., 22(4), 977–992, doi:10.1175/2008JCLI2519.1, 2009.

Henson, S. A., Sanders, R. and Madsen, E.: Global patterns in efficiency of particulate organic carbon export and transfer to the deep ocean, Global Biogeochem. Cycles, 26(1), doi:10.1029/2011GB004099, 2012.

Honjo, S. and Manganini, S. J.: Annual biogenic particle fluxes to the interior of the North Atlantic Ocean; studied at 34°N 21°W and 48°N 21°W, Deep Sea Res. Part II Top. Stud. Oceanogr., 40(1-2), 587–607, doi:10.1016/0967-0645(93)90034-K, 1993.

Huertas, I. E., Ríos, A. F., García-Lafuente, J., Navarro, G., Makaoui, A., Sánchez-Román, A., Rodriguez-Galvez, S., Orbi, A., Ruíz, J. and Pérez, F. F.: Atlantic forcing of the Mediterranean oligotrophy, Global Biogeochem. Cycles, 26(2), doi:10.1029/2011GB004167, 2012.

Hung, C.-C., Gong, G.-C., Chung, W.-C., Kuo, W.-T. and Lin, F.-C.: Enhancement of particulate organic carbon export flux induced by atmospheric forcing in the subtropical oligotrophic northwest Pacific Ocean, Mar. Chem., 113(1-2), 19–24, doi:10.1016/j.marchem.2008.11.004, 2009.

Janeković, I., Mihanović, H., Vilibić, I. and Tudor, M.: Extreme cooling and dense water formation estimates in open and coastal regions of the Adriatic Sea during the winter of 2012, J. Geophys. Res. Ocean., 119(5), 3200–3218, doi:10.1002/2014JC009865, 2014.

Jeong, G. Y., Park, M. Y., Kandler, K., Nousiainen, T. and Kemppinen, O.: Mineralogical properties and internal structures of individual fine particles of Saharan dust, Atmos. Chem. Phys. Discuss., 1–28, doi:10.5194/acp-2016-308, 2016.

Kamatani, A. and Oku, O.: Measuring biogenic silica in marine sediments, Mar. Chem., 68(3), 219–229, doi:10.1016/S0304-4203(99)00079-1, 2000.

Kawahata, H., Suzuki, A. and Ohta, H.: Sinking particles between the equatorial and subarctic regions (0.DEG.N-46.DEG.N) in the central Pacific., Geochem. J., 32(2), 125–133, doi:10.2343/geochemj.32.125, 1998.

Kelepertsis, A. E., Alexakis, D. E., Nastos, P. T. and Kanellopoulou, E. A.: The presence of volcanic ash in the western Greece and its association with the eruption of the Etna volcano, Italy. Consequences on the Environment., in 8th International Conference on Environmental Science and Technology, pp. 408–415, Lemnos Island, Greece., 2003.

Kemp, A. E. S., Pike, J., Pearce, R. B. and Lange, C. B.: The "Fall dump" – a new perspective on the role of a "shade flora" in the annual cycle of diatom production and export flux, Deep Sea Res. Part II Top. Stud. Oceanogr., 47(9-11), 2129–2154, doi:10.1016/S0967-0645(00)00019-9, 2000.

Koppelmann, R., Weikert, H., Halsband-Lenk, C. and Jennerjahn, T.: Mesozooplankton community respiration and its relation to particle flux in the oligotrophic eastern Mediterranean, Global Biogeochem. Cycles, 18(1), doi:10.1029/2003GB002121, 2004.

Krom, M. D., Kress, N., Brenner, S. and Gordon, L. I.: Phosphorus limitation of primary productivity in the eastern Mediterranean Sea., Limnol. Oceanogr., 36(3), 424–432, doi:10.4319/lo.1991.36.3.0424, 1991.

Krom, M. D., Emeis, K.-C. and Van Cappellen, P.: Why is the Eastern Mediterranean phosphorus limited?, Prog. Oceanogr., 85(3-4), 236–244, doi:10.1016/j.pocean.2010.03.003, 2010.

Krotkov, N. A. and Li, C.: OMI/Aura Sulphur Dioxide (SO2) Total Column 1-orbit L2 Swath 13x24 km,version 003, Greenbelt, MD, USAGoddard Sp. Flight Cent. Distrib. Act. Arch. Cent. (GSFC DAAC), Accessed July 1, 2015, doi:10.5067/Aura/OMI/DATA2022, 2012.

Lascaratos, A., Roether, W., Nittis, K. and Klein, B.: Recent changes in deep water formation and spreading in the eastern Mediterranean Sea: a review, Prog. Oceanogr., 44(1-3), 5–36, doi:10.1016/S0079-6611(99)00019-1, 1999.

Lazzari, P., Teruzzi, A., Salon, S., Campagna, S., Calonaci, C., Colella, S., Tonani, M. and Crise, A.: Pre-operational short-term forecasts for Mediterranean Sea biogeochemistry, Ocean Sci., 6(1), 25–39, doi:10.5194/osd-6-1223-2009, 2010.

Lazzari, P., Solidoro, C., Ibello, V., Salon, S., Teruzzi, A., Béranger, K., Colella, S. and Crise, A.: Seasonal and inter-annual variability of plankton chlorophyll and primary production in the Mediterranean Sea: a modelling approach, Biogeosciences, 9(1), 217–233, doi:10.5194/bg-9-217-2012, 2012.

Lazzari, P., Solidoro, C., Salon, S. and Bolzon, G.: Spatial variability of phosphate and nitrate in the Mediterranean Sea: A 158odelling approach, Deep Sea Res. Part I Oceanogr. Res. Pap., 108, 39–52, doi:10.1016/j.dsr.2015.12.006, 2016.

Leblanc, K., Quéguiner, B., Garcia, N., Rimmelin, P. and Raimbault, P.: Silicon cycle in the NW Mediterranean Sea: seasonal study of a coastal oligotrophic site, Oceanol. Acta, 26(4), 339–355, doi:10.1016/S0399-1784(03)00035-5, 2003.

Lefèvre, R., Gaudichet, A. and Billon-Galland, M. A.: Silicate microspherules intercepted in the plume of Etna volcano, Nature, 322(6082), 817–820, doi:10.1038/322817a0, 1986.

Lewis, M. R., Hebert, D., Harrison, W. G., Platt, T. and Oakey, N. S.: Vertical nitrate fluxes in the oligotrophic ocean., Science, 234(4778), 870–3, doi:10.1126/science.234.4778.870, 1986.

Logan, B. E., Passow, U., Alldredge, A. L., Grossartt, H.-P. and Simont, M.: Rapid formation and sedimentation of large aggregates is predictable from coagulation rates (half-lives) of transparent exopolymer particles (TEP), Deep Sea Res. Part II Top. Stud. Oceanogr., 42(1), 203–214, doi:10.1016/0967-0645(95)00012-F, 1995.

Lomas, M. W., Steinberg, D. K., Dickey, T., Carlson, C. A., Nelson, N. B., Condon, R. H. and Bates, N. R.: Increased ocean carbon export in the Sargasso Sea linked to climate variability is countered by its enhanced mesopelagic attenuation, Biogeosciences, 7(1), 57–70, doi:10.5194/bg-7-57-2010, 2010.

Longhurst, A., Sathyendranath, S., Platt, T. and Caverhill, C.: An estimate of global primary production in the ocean from satellite radiometer data, J. Plankton Res., 17(6), 1245–1271, doi:10.1093/plankt/17.6.1245, 1995.

Marañón, E., Behrenfeld, M. J., González, N., Mouriño, B. and Zubkov, M. V: High variability of primary production in oligotrophic waters of the Atlantic Ocean: uncoupling from phytoplankton biomass and size structure, Mar. Ecol. Prog. Ser., 257, 1–11, 2003.

Mazzocchi, M., Christou, E., Fragopoulu, N. and Siokoufrangou, I.: Mesozooplankton distribution from Sicily to Cyprus (Eastern Mediterranean) .1. General aspects, Oceanol. Acta, 20(3), 521–535, 1997.

Meador, T. B., Gogou, A., Spyres, G., Herndl, G. J., Krasakopoulou, E., Psarra, S., Yokokawa, T., De Corte, D., Zervakis, V. and Repeta, D. J.: Biogeochemical relationships between ultrafiltered dissolved organic matter and picoplankton activity in the Eastern Mediterranean Sea, Deep Sea Res. Part II Top. Stud. Oceanogr., 57(16), 1460–1477, doi:10.1016/j.dsr2.2010.02.015, 2010.

MEDOC Group.: Observation of Formation of Deep Water in the Mediterranean Sea, 1969, Nature, 227(5262), 1037–1040, doi:10.1038/2271037a0, 1970.

MOHC, MPI-M, ECMWF and MéteoFrance: Technical Note on CMUG ECV Quality Assessment Report., D3.1, V2.1., 2014.

Moutin, T. and Raimbault, P.: Primary production, carbon export and nutrients availability in western and eastern Mediterranean Sea in early summer 1996 (MINOS cruise), J. Mar. Syst., 33-34, 273–288, doi:10.1016/S0924-7963(02)00062-3, 2002.

Napolitano, E., Oguz, T., Malanotte-Rizzoli, P., Yilmaz, A. and Sansone, E.: Simulations of biological production in the Rhodes and Ionian basins of the eastern Mediterranean, J. Mar. Syst., 24(3-4), 277–298, doi:10.1016/S0924-7963(99)00090-1, 2000.

Olgun, N., Duggen, S., Andronico, D., Kutterolf, S., Croot, P. L., Giammanco, S., Censi, P. and Randazzo, L.: Possible impacts of volcanic ash emissions of Mount Etna on the primary productivity in the oligotrophic Mediterranean Sea: Results from nutrient-release experiments in seawater, Mar. Chem., 152, 32–42, doi:10.1016/j.marchem.2013.04.004, 2013.

Passow, U., Alldredge, A. L. and Logan, B. E.: The role of particulate carbohydrate exudates in the flocculation of diatom blooms, Deep Sea Res. Part I Oceanogr. Res. Pap., 41(2), 335–357, doi:10.1016/0967-0637(94)90007-8, 1994.

Psarra, S., Tselepides, A. and Ignatiades, L.: Primary productivity in the oligotrophic Cretan Sea (NE Mediterranean): seasonal and interannual variability, Prog. Oceanogr., 46(2-4), 187–204, doi:10.1016/S0079-6611(00)00018-5, 2000.

Ragueneau, O., Savoye, N., Del Amo, Y., Cotten, J., Tardiveau, B. and Leynaert, A.: A new method for the measurement of biogenic silica in suspended matter of coastal waters: using Si:Al ratios to correct for the mineral interference, Cont. Shelf Res., 25(5-6), 697–710, doi:10.1016/j.csr.2004.09.017, 2005.

Ribera d'Alcalà, M.: Nutrient ratios and fluxes hint at overlooked processes in the Mediterranean Sea, J. Geophys. Res., 108(C9), 8106, doi:10.1029/2002JC001650, 2003.

Rigual-Hernandez, A. S., Barcena, M. A., Jordan, R. W., Sierro, F. J., Flores, J. A., Meier, K. J. S., Beaufort, L. and Heussner, S.: Diatom fluxes in the NW Mediterranean: evidence from a 12-year sediment trap record and surficial sediments, J. Plankton Res., 35(5), 1109–1125, doi:10.1093/plankt/fbt055, 2013.

Robinson, A. R. and Golnaraghi, M.: Circulation and dynamics of the Eastern Mediterranean Sea; quasi-synoptic data-driven simulations, Deep Sea Res. Part II Top. Stud. Oceanogr., 40(6), 1207–1246, doi:10.1016/0967-0645(93)90068-X, 1993.

Santinelli, C., Nannicini, L. and Seritti, A.: DOC dynamics in the meso and bathypelagic layers of the Mediterranean Sea, Deep Sea Res. Part II Top. Stud. Oceanogr., 57(16), 1446–1459, doi:10.1016/j.dsr2.2010.02.014, 2010.

Siegel, D. A., McGillicuddy, D. J. and Fields, E. A.: Mesoscale eddies, satellite altimetry, and new production in the Sargasso Sea, J. Geophys. Res., 104(C6), 13359, doi:10.1029/1999JC900051, 1999.

Siegel, D. A., Fields, E. and Buesseler, K. O.: A bottom-up view of the biological pump: Modeling source funnels above ocean sediment traps, Deep Sea Res. Part I Oceanogr. Res. Pap., 55(1), 108–127, doi:10.1016/j.dsr.2007.10.006, 2008.

Siokou-Frangou, I., Christaki, U., Mazzocchi, M. G., Montresor, M., Ribera d'Alcalá, M., Vaqué, D. and Zingone, A.: Plankton in the open Mediterranean Sea: a review, Biogeosciences, 7(5), 1543–1586, doi:10.5194/bg-7-1543-2010, 2010.

Siswanto, E., Ishizaka, J., Morimoto, A., Tanaka, K., Okamura, K., Kristijono, A. and Saino, T.: Ocean physical and biogeochemical responses to the passage of Typhoon Meari in the East China Sea observed from Argo float and multiplatform satellites, Geophys. Res. Lett., 35(15), L15604, doi:10.1029/2008GL035040, 2008.

Smetacek, V. S.: Role of sinking in diatom life-history cycles: ecological, evolutionary and geological significance, Mar. Biol., 84(3), 239–251, doi:10.1007/BF00392493, 1985.

Smetacek, V. S.: Oceanography: The giant diatom dump, Nature, 406(6796), 574–5, doi:10.1038/35020665, 2000.

Sournia, A.: La production primaire planctonique en Méditerranée. Essai de mise à jour, Bull. l'etude en commun la Méditerranée, 5, 1–128, 1973.

Spinei, E., Carn, S. A., Krotkov, N. A., Mount, G. H., Yang, K. and Krueger, A.: Validation of ozone monitoring instrument SO 2 measurements in the Okmok volcanic cloud over Pullman, WA, July 2008, J. Geophys. Res., 115, D00L08, doi:10.1029/2009JD013492, 2010.

Stabholz, M., Durrieu de Madron, X., Canals, M., Khripounoff, A., Taupier-Letage, I., Testor, P., Heussner, S., Kerhervé, P., Delsaut, N., Houpert, L., Lastras, G. and Dennielou, B.: Impact of open-ocean convection on particle fluxes and sediment dynamics in the deep margin of the Gulf of Lions, Biogeosciences, 10(2), 1097–1116, doi:10.5194/bg-10-1097-2013, 2013.

Stavrakakis, S., Gogou, A., Krasakopoulou, E., Karageorgis, A. P., Kontoyiannis, H., Rousakis, G., Velaoras, D., Perivoliotis, L., Kambouri, G., Stavrakaki, I. and Lykousis, V.: Downward fluxes of sinking particulate matter in the deep Ionian Sea (NESTOR site), eastern Mediterranean: seasonal and interannual variability, Biogeosciences, 10(11), 7235–7254, doi:10.5194/bg-10-7235-2013, 2013.

Takahashi, K.: Seasonal fluxes of pelagic diatoms in the subarctic Pacific, 1982–1983, Deep Sea Res. Part A. Oceanogr. Res. Pap., 33(9), 1225–1251, doi:10.1016/0198-0149(86)90022-1, 1986.

Thingstad, T. F., Krom, M. D., Mantoura, R. F. C., Flaten, G. A. F., Groom, S., Herut, B., Kress, N., Law, C. S., Pasternak, A., Pitta, P., Psarra, S., Rassoulzadegan, F., Tanaka, T., Tselepides, A., Wassmann, P., Woodward, E. M. S., Riser, C. W., Zodiatis, G. and Zohary, T.: Nature of phosphorus limitation in the ultraoligotrophic eastern Mediterranean., Science, 309(5737), 1068–71, doi:10.1126/science.1112632, 2005.

Tolika, K., Maheras, P., Pytharoulis, I. and Anagnostopoulou, C.: The anomalous low and high temperatures of 2012 over Greece – an explanation from a meteorological and climatological perspective, Nat. Hazards Earth Syst. Sci., 14(3), 501–507, doi:10.5194/nhess-14-501-2014, 2014.

Vichi, M., Cossarini, G., Gutierrez Mlot, E., Lazzari, P., Lovato, T., Mattia, G., Masina, S., McKiver, W., Pinardi, N., Solidoro, C. and Zavatarelli, M.: The Biogeochemical Flux Model (BFM): Equation Description and User Manual. BFM version 5 (BFM- V5). Release 1.0, BFM Report series N, 1. March 2013. CMCC, Bologna, Italy, 2013.

Warnken, C.: Biogeochemie von Schwebstoffen, Sinkstoffen und Sedimenten im Ierapetra-Tief (östliches Mittelmeer). Diploma thesis, Inst. Für Biogeochem. Und Meereschem, University of Hamburg, Hamburg, 2003.

WMO: World Meteorological Organization Regional Climate Centres –Assessment of the observed extreme conditions during late boreal winter 2011/2012, Geneva, Switzerland, 2013.

Yacobi, Y. Z., Zohary, T., Kress, N., Hecht, A., Robarts, R. D., Waiser, M., Wood, A. M. and Li, W. K. W.: Chlorophyll distribution throughout the southeastern Mediterranean in relation to the physical structure of the water mass, J. Mar. Syst., 6(3), 179–190, doi:10.1016/0924-7963(94)00028-A, 1995.

Zohary, T. and Robarts, R. D.: Experimental study of microbial P limitation in the eastern Mediterranean, Limnol. Oceanogr., 43(3), 387–395, doi:10.4319/lo.1998.43.3.0387, 1998.

2.5. Resum de resultats

Aquesta Tesi ha donat fruit a quatre articles científics dels quatre ambients sedimentaris estudiats: la plataforma interna de Barcelona, el canyó de Blanes i el talús adjacent, els talussos i conques profundes de la Mediterrània oriental, i la conca profunda de Ierapetra. A continuació es presenta un resum dels resultats obtinguts (vegeu una descripció més completa als subcapítols 2.1-2.4).

Tant a l'estudi de la plataforma interna de Barcelona (subcapítol 2.1), com al del canyó de Blanes i àrees adjacents (subcapítol 2.2), s'ha dut a terme una anàlisi geoquímica bàsica (composició elemental i relació isotòpica) i sedimentològica (mida de gra) dels sediments superficials recollits durant l'estiu-tardor 2012 i la tardor-hivern 2008-2009, respectivament. Els sediments superficials analitzats mostren una disminució exponencial significativa de la mida de gra de les partícules des de la plataforma fins a zones més profundes del marge continental (Figures 2.3, 2.4 i 2.11). Gràcies a la tècnica de separació del sediment per mida de gra desenvolupada en aquesta Tesi, s'ha pogut discernir l'origen i estat de preservació de la matèria orgànica a les diferents fraccions de sediment (sorra, 63 µm-2 mm; llim groller, 40-63 µm; llim fi, 4-40 µm; argila, <4 µm). Les concentracions més altes d'OC sempre s'han trobat a la fracció argila, assolint un màxim de fins a 8.68% (Taules 2.2 i 2.4). Mentre que les partícules grolleres (>63 µm) són pobres en OC i es troben a la plataforma continental i a la capçalera del canyó, les partícules fines (<4 µm) i relativament riques en OC es troben a profunditats majors. A més a més, el contingut en OC a la fracció fina disminueix en profunditat. El contingut d'OC, la ràtio TN/OC i la relació isotòpica $\delta^{13}C$, que avaluats conjuntament ens permeten diferenciar origen de l'OC, varien significativament en cada fracció de sediment, detectant-se contribucions relativament majors d'OC marí a la fracció argila dels sediments profunds (Figures 2.5 i 2.12). L'anàlisi dels principals forçaments externs (vent, onatge, precipitació, descarrega fluvial, concentració de Chl-a superficial i corrents prop del fons) ha permès identificar quins són els processos responsables de la classificació i deposició de les partícules minerals en funció de la seva mida de gra, així com de la redistribució de l'OC particulat, i com les condicions d'onatge i les descàrregues fluvials i d'emissaris són clau per a transferència i distribució del material particulat als marges continentals.

Els estudis del subcapítol 2.3 i 2.4 han estat essencials per conèixer la distribució, les fonts i la preservació de la matèria orgànica en els sediments del fons (subcapítol 2.3) i per entendre els processos que controlen la transferència vertical de material particulat cap al fons (subcapítol 2.4) en una de les regions més oligotròfiques del món, la Mediterrània oriental. Els resultats obtinguts de les anàlisis biogeoquímiques dels sediments recollits als talussos i conques profundes (1018 – 4087 m de profunditat) de la Mediterrània oriental reflecteixen el caràcter oligotròfic d'aquesta conca, amb concentracions de OC i nitrogen d'entre 0.15% a 1.15% i 0.06% i 0.11%, respectivament (Taula 2.7). Els valors obtinguts de les ràtios TN/OC, les relacions isotòpiques $\delta^{13}C$ i els biomarcadors lípidics analitzats (brassicasterol, dinosterol, C30diols&keto-ols, alquenones, *n*-alcans, *n*-alcanols, UCM) evidencien una contribució mixta de les fonts autòctones i al·lòctones a la matèria orgànica sedimentària. Així doncs, s'ha observat tant la presència de matèria orgànica marina relativament degradada, derivada d'algues fitoplanctòniques, com de terrestre, derivada de plantes vasculars, i antropogènica, derivada de productes degradats del petroli. Aquest estudi ha posat de manifest que les conques profundes de la Mediterrània oriental són depocentres de

material fi i ric amb OC com a conseqüència de processos d'agregació i classificació hidrodinàmica dels sediments.

Finalment, es van registrar fluxos d'OC i òpal a la conca profunda de Ierapetra, al sud-oest de l'illa de Creta (mar de Llevant) des de juny 2010 a maig 2013. La sedimentació d'OC i òpal a 4285 m de profunditat durant tot el període estudiat va ser extremadament baixa (inferior a 1 g m^{-2} d^{-1}) exceptuant al mes d'abril de 2012, quan aquests fluxos incrementaren en 2 ordres la seva magnitud (Figura 2.20). L'observació mitjançant microscòpia electrònica de rastreig de les partícules sedimentades recollides durant aquest esdeveniment ha evidenciat que aquestes contenien una elevada abundància i diversitat de diatomees ben preservades així com també esfèrules micromètriques corresponents a cendres volcàniques. En aquest estudi s'ha demostrat l'existència de forts vincles entre condicions atmosfèriques anòmales (fortes pèrdues de calor durant hiverns extrems i l'arribada de centres volcàniques), una producció primària elevada i l'exportació de matèria orgànica fresca cap a profunditats batipelàgiques en una de les zones més oligotròfiques del món.

Capítol 3

Discussió

En aquest capítol es presenta una discussió conjunta dels resultats obtinguts al capítol 2 d'aquesta Tesi amb la finalitat d'oferir una visió integradora de la distribució, mecanismes de transport i origen de la matèria orgànica a la mar Mediterrània.

3.1. Caracterització de la matèria orgànica

3.1.1. Distribució i fonts de la matèria orgànica al marge continental nord-català

La concentració d'OC als sediments superficials del marge nord-català varia entre 0.17 i 2.9%, valors comparables als descrits amb anterioritat a la Mediterrània occidental (Accornero et al., 2003; Cartes et al., 2002; Martín et al., 2008; Masqué et al., 2003; Zúñiga et al., 2007). Les elevades ràtios TN/OC i els baixos valors de $\delta^{13}C$ suggereixen que a la plataforma continental de Barcelona la major part de la matèria orgànica és d'origen terrestre (>85% del total d'OC dels sediments), molt probablement provinent tant de descàrregues fluvials del riu Besòs o Tordera com de descàrregues d'emissaris. Tot i així, allà on l'arribada de material continental és menor, la contribució de matèria orgànica d'origen marí (és a dir, provinents de la productivitat primària de les aigües superficials) pot arribar a representar un 70%. A zones més profundes, tant a l'eix del canyó de Blanes com al talús del marge continental, les contribucions de matèria orgànica marina són majors.

La quantitat i l'origen de l'OC contingut en cada fracció de mida de gra dels sediments varia significativament, sobretot entre les fraccions argila i sorra (Figura 3.1), fet que evidencia la necessitat de dur a terme anàlisis biogeoquímiques a les diferents fraccions de sediment per tal de poder estudiar com la classificació hidrodinàmica de les partícules afecta a la distribució, quantitat i preservació de l'OC als sediments. A tots els ambients sedimentaris estudiats, la concentració més alta d'OC (fins a 8.68%) sempre es troba a la fracció argila (<4 μm) (Figura 3.1a-c). Aquest resultat es suma a la creixent evidència que la matèria orgànica s'associa principalment a les partícules d'argila degut a la seva elevada superfície específica i, per tant, elevada capacitat d'adsorció, agregació i protecció de les partícules orgàniques (Keil et al., 1998; Mayer, 1994a, 1994b). També s'ha detectat que la concentració d'OC a la fracció argila dels sediments disminueix des de la plataforma interna (8.68% OC a 10 m) fins a peu de talús (0.81 % a 1200 m) (Figura 3.2a). Paral·lelament, s'ha enregistrat un increment de la relació isotòpica $\delta^{13}C$ a la fracció argila en profunditat, amb valors baixos (<-25.2‰) que suggereixen un origen terrestre de la matèria orgànica a la plataforma interna de Barcelona, i amb valors elevats (~-22.5‰) i per tant suggerint un origen marí als sediments profunds del canyó de Blanes i talús adjacent (Figura 3.2 b). Això és degut a que a la plataforma interna, a la interfície entre l'aigua dolça de les descàrregues fluvials i la de mar, s'hi duen a terme processos de floculació causant la sedimentació de partícules minerals i partícules orgàniques fines majoritàriament d'origen terrestre que encara no han patit forts processos de remineralització (Lick et al., 1993). Per contra, les partícules mida argila, que abans de ser dipositades romanen en suspensió durant llargues distàncies a la columna d'aigua, poden patir processos d'oxidació (Arnarson i Keil, 2007), i incorporar material d'origen marí (Bergamaschi et al., 1997; Blair i Aller, 2012).

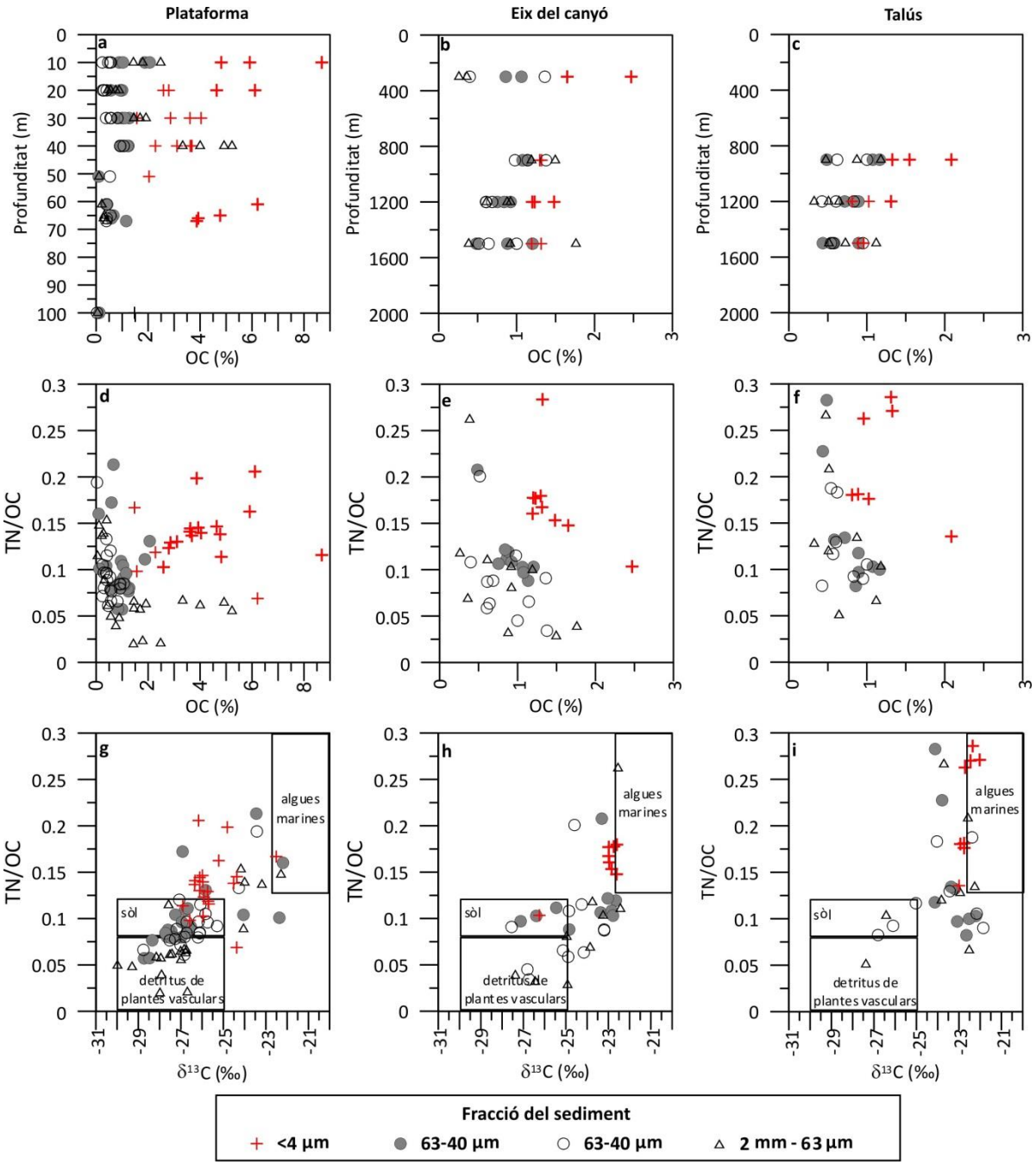

Figura 3.1. Relació entre la profunditat i la concentració d'OC (a-c), la ràtio TN/OC i la concentració d'OC (d-f) i la ràtio TN/OC i la relació isotòpica $\delta^{13}C$ (g-i) a cada fracció de gra dels sediments analitzats als diferents ambients sedimentaris del marge continental nord-català: plataforma continental de Barcelona, eix del canyó de Blanes i talús adjacent.

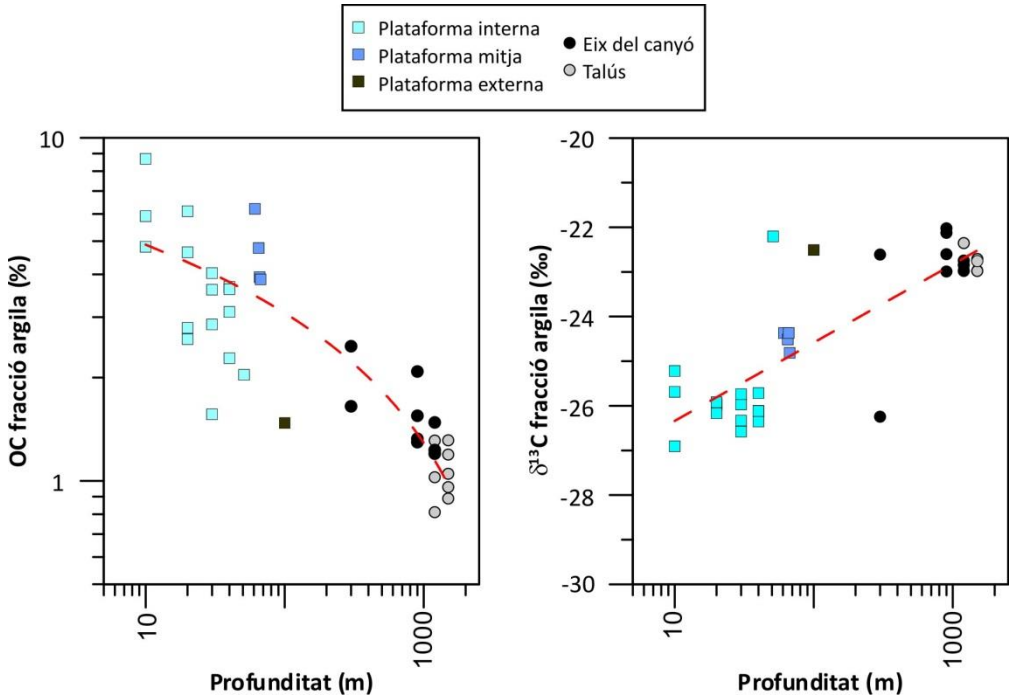

Figura 3.2. Concentració d'OC (a) i $\delta^{13}C$ (b) de la fracció argila als sediments de la plataforma interna (10-50 m de profunditat), mitja (60-70 m de profunditat) i externa (100 m) de Barcelona, i de l'eix del canyó de Blanes (300, 900, 1200 i 1500 m) i el seu talús adjacent (900, 1200 i 1500 m). Les dades s'ajunten a una funció potencial a) OC=-79ln(profunditat)+6.66 (r=0.79) i b) $\delta^{13}C$=0.76ln(profunditat)-28.1 (r=0.84).

Contràriament a la fracció argila, la fracció sorra en general presenta baixes concentracions d'OC (<1.5%), i un ampli rang de variació de $\delta^{13}C$ (de -30‰ a -22.3‰). Tot i així, a la plataforma continental interna la concentració d'OC de la fracció sorra incrementa en profunditat (fins a 5.23%) (Figura 3.1a) en zones on l'efecte de l'onatge minva (40 m), com a conseqüència de la deposició de partícules orgàniques lleugeres com són els fragments de restes vegetals. En aquest ambient sedimentari, l'augment de la ràtio TN/OC a la fracció sorra en profunditat és possible que es degui a la incorporació bacteriana de nitrogen de l'aigua en el material vegetal llenyós quan aquest es degrada (Nuwer i Keil, 2005).

3.1.2. Distribució, fonts i preservació de la matèria orgànica a la Mediterrània oriental

Els sediments dels talussos i conques profundes de la Mediterrània oriental (1018-4087 m de profunditat) estan caracteritzats per una composició granulomètrica llim-argilosa, amb valors de d50 de 3.5 a 56.6 µm. Mentre que les concentracions més altes d'argila es troben a la conca de Ierapetra, les concentracions més altes de llim i sorres es localitzen a la mar Jònica i als estrets de Creta, respectivament. Els resultats obtinguts evidencien que els principals processos que controlen la composició granulomètrica i biogeoquímica dels sediments superficials de la Mediterrània oriental són els processos de 1) degradació de la matèria orgànica, 2) transport vertical (sedimentació pelàgica) i 3) transport lateral (classificació dels sediments per corrents de fons).

La concentració d'OC als sediments varia de 0.15 a 1.15%, amb un valor mitjà de 0.47%. Tant els continguts més baixos com els més alts es localitzen a la mar Jònica, al sud de l'estret d'Otranto i al golf de Taranto, respectivament. Els continguts d'OC són relativament inferiors als trobats a la conca occidental, reflectint el gradient oligotròfic creixent d'oest a est a la mar Mediterrània (Krom et al., 2003). Igual que al marge nord-català, a la Mediterrània oriental profunda s'ha detectat una correlació significativa entre els continguts d'OC i la fracció argila. Això indica que la interacció entre les partícules orgàniques i les minerals fines es manté des de zones someres fins a profunditats batipelàgiques.

Les baixes ràtios de TN/OC (<0.11), la creixent abundància d'UCM en profunditat, la manca de correlació entre la matèria orgànica marina (∑Mar) i les partícules fines (<4 μm) i la presència de colesterol als sediments, el qual està positivament correlacionat amb les concentracions dels biomarcadors algals, indiquen que els sediments superficials de la conca oriental profunda 1) han patit processos de degradació i retreballament per part del zooplàncton i organismes bentònics, perdent els components proteics rics amb nitrogen derivats de les algues marines (Meyers, 1997), i 2) han introduït residus del petroli rics amb OC (Friligos et al., 1998). La matèria orgànica terrestre acumulada als sediments, la qual es troba associada principalment amb les partícules argila, pateix una degradació creixent amb profunditat, amb una degradació preferencial dels components làbils (∑TerN-OH) respecte els refractaris (∑TerNA).

A la Mediterrània oriental profunda la distribució dels carbonats es correlaciona positivament amb la concentració d'argiles i d'alquenones en aquelles àrees influenciades per la sedimentació pelàgica de productes derivats de la productivitat primària. Així doncs, és a la mar de Llevant, a regions amb circulació ciclònica, com és el cas del gir de Rodes, i al sud de la mar Egea (mar de Creta), on es troben les contribucions d'OC marí més elevades, representant fins al 87.7% de l'OC total dels sediments. A la conca profunda de Ierapetra, influenciada principalment per processos de sedimentació pelàgica vinculats al gir anticiclònic semipermanent de Ierapetra i al gir de Rodes (veure secció 3.2.2), abunda el material fi amb continguts relativament elevats d'OC i lípids associats, tant naturals com antropogènics.

Al contrari, els sediments superficials de la mar Jònica és caracteritzen per tenir contribucions relativament elevades d'OC d'origen terrestre (fins al 64% de l'OC total). En aquesta mar l'estret d'Otranto actua com a conducte preferencial d'entrada de partícules riques amb OC d'origen terrestre provinents de la mar Adriàtica, una mar on la formació d'aigua densa i ocurrència de cascades d'aigua densa redistribueix i exporta cap a la mar Jònica material d'origen fluvial (Tesi et al., 2008; Turchetto et al., 2007). Tot i l'elevat contingut d'OC terrestre preservat a la mar Jònica, els valors són inferiors als que trobem al marge nord-català a profunditats similars (>70% de l'OC total), molt probablement a causa de la llarga distància respecte l'àrea font d'entrada del material terrestre. Als estrets de Creta, l'increment de partícules fines i contingut en OC en profunditat ve explicat per la presència de corrents intensos durant l'hivern (Kontoyiannis et al., 2005), els quals generen una distribució diferencial de la matèria orgànica en funció de la mida de gra dels sediments. Aquest mateix patró de circulació i transport de sediments selectiu també s'ha observat al marge continental nord-català (veure secció 3.2.1).

3.2. Mecanismes de transferència de carboni orgànic

La identificació dels factors que controlen l'exportació de partícules biogèniques cap a l'oceà profund és, des de fa més de 30 anys, un dels grans reptes de la biogeoquímica marina per tal de comprendre el cicle de carboni (Boyd i Trull, 2007). L'ocurrència d'esdeveniments atmosfèrics extrems durant el període estudiat ha permès investigar l'impacte d'aquests en el transport i exportació de l'OC, tant a sediments de plataforma i talús, com en els fluxos de partícules a mar obert.

3.2.1. Temporals costaners

L'estudi de la mida de gra dels sediments superficials del marge nord-català ha permès determinar quins són els processos responsables de la distribució dels sediments i de la matèria orgànica. La mida de gra disminueix significativament en profunditat (de 10 a 1500 m). La reducció en profunditat de la velocitat del corrent prop del fons, sigui aquella deguda a onatge o a altres esdeveniments energètics, en sembla la principal causa. Així doncs, augments de velocitat causats per l'onatge produeixen un rentat dels sediments més fins a la plataforma continental (principalment de 10 a 20 m), i mentre que a la plataforma s'hi troben sediments sorrencs (d50 >100 μm) a peu de talús la composició passa a ser argilo-llimosa (d50 <10 μm).

Els sediments superficials mostren una clara i significant variabilitat temporal, tant de la seva composició granulomètrica com de les concentracions i origen de l'OC contingut a les diferents fraccions del sediment. S'ha detectat que els principals factors ambientals que modulen aquesta variabilitat temporal són les tempestes i les aportacions fluvials i/o d'emissaris. En aquest context, la fracció argila, rica amb OC, juntament amb les partícules de mida sorra orgàniques, són les partícules més susceptibles de ser resuspeses i transportades durant llargues distàncies, contribuint així a l'arribada d'OC a zones profundes.

A la plataforma continental interna (de 10 - 40 m de profunditat) s'ha detectat que l'onatge, tant en condicions de temporals extrems com de relativa calma, és qui modula la dispersió i redistribució dels sediments superficials. La velocitat orbital de l'onatge decreix en profunditat, de 1.7 m s^{-1} a 10 m fins a 0.4 m·s^{-1} a 40 m. D'aquesta manera, el material terrestre provinent de les descàrregues fluvials i d'emissaris pateix una classificació intensa regida per la força de l'onatge. Tant les partícules mida argila riques amb OC com les restes vegetals lleugeres no inicien la seva deposició fins a profunditats de 30-40 m.

Durant tempestes extremes s'ha observat que l'onatge i corrents de fons generats són eficients en termes de remobilització, resuspensió i transferència de les fraccions més fines i riques amb OC talús avall, canalitzades preferentment a través dels canyons submarins (Figura 3.3). Durant el període d'estudi, l'esdeveniment més extrem registrat va ser la tempesta costanera del desembre de 2008, amb un període de retorn de 100 anys. Aquesta pertorbació meteorològica, caracteritzada per ratxes de vents de l'est de fins a 20 m s^{-1}, va generar alçades d'ona significativa de 4.7 m amb períodes de 8.8 s i alçades d'ona màximes de fins a 8 m davant de la ciutat de Blanes. Durant aquesta tempesta hi van haver fortes precipitacions que provocaren l'augment de

les descàrregues fluvials a tota la zona del marge continental nord-català. El riu Tordera, pròxim a la capçalera del canyó de Blanes, descarregà durant la tempesta una quantitat total de 9635.6 kt d'aigua i 0.6 kt de sediment principalment llimós (Sanchez-Vidal et al., 2013). Paral·lelament al fort onatge, durant la tempesta es van registrar corrents de fons de fins a 0.70 m s^{-1} a la capçalera del canyó de Blanes (300 m), i d'aproximadament 0.3 m s^{-1} al llarg de l'eix del canyó fins a 1500 m. Els corrents registrats al talús adjacent al canyó de Blanes indiquen que l'augment dels corrents va ser menor (fins a 0.20 m s^{-1}).

L'erosió i remobilització del sediment a la plataforma continental i capçalera del canyó per l'acció de l'onatge i corrents associats sobre el fons marí, per una banda, i la descàrrega fluvial del riu Tordera, per l'altra, produïren dos plomalls tèrbols: un en superfície (impulsat pel vent i els corrents), i un enganxat al fons (impulsat pel contrast de densitat amb l'aigua circumdant, l'efecte de la gravetat, corrents de plataforma, la corrent del nord i la deriva litoral). Aquests corrents foren capaços de transportar grans volums de sorra i restes carbonatades (>300 μm) fins a la capçalera del canyó de Blanes, així com resuspendre i transportar partícules de fins a 100 μm cap a profunditats superiors. La remobilització de grans quantitats de la fracció més fina del sediment (<4 μm), que és a la vegada la més rica amb OC va implicar la transferència de grans quantitats d'OC cap a profunditats superiors de 1500 m. Els sediments descarregats pel riu Tordera durant aquest esdeveniment foren principalment llims (Sanchez-Vidal et al., 2013), i van assolir, com a mínim, la plataforma continental mitja, tal i com evidencia l'elevat contingut d'OC terrestre a les fraccions llims d'aquest ambient sedimentari (fins al 87% respecte el total).

Els resultats obtinguts indiquen que els esdeveniments atmosfèrics extrems al marge continental nord-català tenen una clara repercussió en la dinàmica sedimentària i redistribució de l'OC, no només a les zones someres sinó també a les zones profundes. La transferència de grans volums d'OC durant tempestes extremes com la del desembre de 2008 (5563 t OC, Sanchez-Vidal et al., 2012) podria tenir un fort impacte en els ecosistemes profunds i els recursos vius marins, com ja s'ha documentat amb anterioritat durant l'ocurrència d'altres esdeveniments extrems com el DSWC (Canals et al., 2006; Company et al., 2008),

3.2.2. Convecció a mar obert

Els fluxos de partícules obtinguts a la conca profunda de Ierapetra entre els anys 2010 i 2013 mostren una elevada variabilitat temporal, amb valors que oscil·laren entre 1.46 mg m^{-2} d^{-1} i 306.66 mg m^{-2} d^{-1}, i amb una mitjana de 46.0 mg m^{-2} d^{-1}. Durant el període d'estudi els corrents registrats a 4287 m de profunditat van ser molt febles, amb una velocitat mitjana d'1.6 cm s^{-1}. El corrent més intens es va registrar al març de 2012, amb una velocitat de 9.8 cm s^{-1} cenyida a la topografia (direcció sud – oest) (Figura 3.2). Aquests corrents tant baixos indiquen que l'arribada de partícules va ser probablement regida per la sedimentació pelàgica. La matèria particulada exportada verticalment des de les aigües superficials a la conca profunda de Ierapetra està composta principalment per material litogènic (5.0 - 90.0%), seguit del carbonat de calci (10.0 - 85.0%), òpal (0.12 - 19.1%) i OC (0.8 - 6.5%).

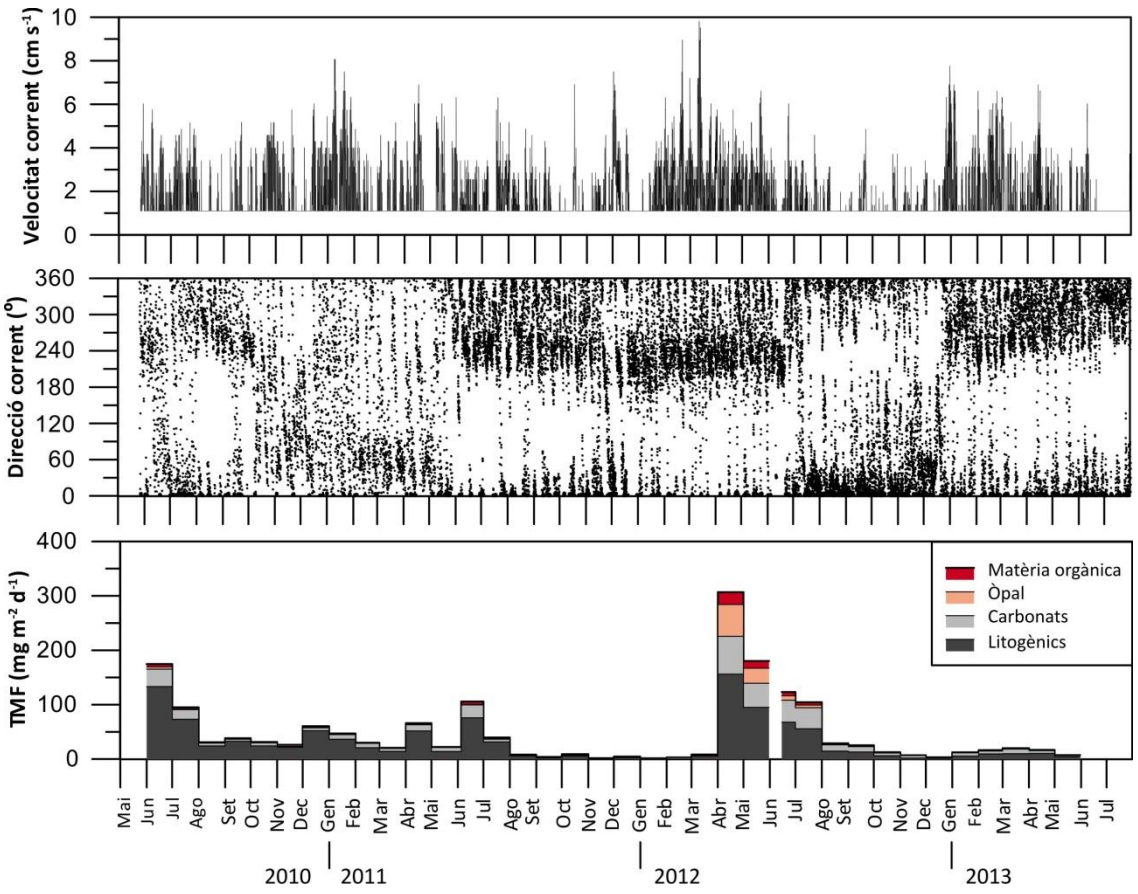

Figura 3.3. a) Velocitat i b) direcció del corrent i c) fluxos de massa total a la conca profunda de Ierapetra des de juny 2010 a maig 2013.

Els fluxos d'OC i òpal a 4285 m durant la major part del període d'estudi van ser extremadament baixos, amb valors per sota d'1 mg m^{-2} d^{-1}. No obstant això, a l'abril de 2012, l'exportació d'OC i òpal incrementà 14 i 128 vegades, respectivament, en relació als mesos d'abril de 2011 i de 2013. Les partícules sedimentades l'abril de 2012 presentaren una matriu mucilaginosa, atribuïda a exopolímers transparents d'exsudats de les diatomees (Alldredge et al., 1993), i una composició isotòpica que assenyala una clara contribució d'OC marí (δ^{13}C -21.3‰) (Harmelin-Vivien et al., 2008). Això indica que una floració de diatomees fou la principal causa de l'elevada exportació de matèria orgànica a elevades profunditats. L'observació d'una elevada abundància i diversitat de diatomees mitjançant microscòpia electrònica de rastreig corrobora la hipòtesi, i a més a més, el baix estat de degradació de les mateixes confirma que la velocitat de caiguda podria haver estat considerable. La velocitat de sedimentació de 143 m d^{-1} per les partícules recol·lectades durant l'abril 2012 s'aproxima molt a la velocitat de sedimentació estimada per les diatomees en estudis previs (175 m d^{-1}) (Takahashi, 1986). A més, també s'observen esfèrules micromètriques que, tant la seva forma, com la seva composició, indiquen que són cendres volcàniques (Calabrese i D'Alessandro, 2015; Lefèvre et al., 1986).

Les anàlisis qualitatives i quantitatives de les imatges satèl·lit de SHF, LHF, SST, SSH, concentració de nutrients (N i P), O_2 dissolt i Chl-a ha permès establir la relació entre les condicions oceanogràfiques a les aigües superficials i els processos d'exportació de material particulat a profunditats batipelàgiques. El període d'estudi va coincidir amb un hivern molt fred i amb una primavera amb activitat volcànica intensa. L'hivern 2011-12 es caracteritzà per ser un dels més

freds dels últims 50 anys a la regió d'Euràsia. L'arribada de vent de nord fred i sec va provocar fortes pèrdues de calor a tota la Mediterrània oriental, especialment en zones amb intensa circulació ciclònica, com és el gir de Rodes. Aquesta situació va causar, al març de 2012, una pèrdua de flotabilitat de les aigües superficials, iniciant processos de convecció (Figura 3.3). Al gir de Rodes, la convecció intensa va provocar l'ascens de masses d'aigua freda i rica amb nutrients, afavorint el creixement fitoplanctònic, i especialment el de diatomees. Evidenciat per les imatges satèl·lit de concentració de Chl-a, la floració fitoplanctònica observada al març de 2012 va ser la més gran registrada des de l'any 2002, tant al centre del gir com a les aigües circumdants corresponents a la conca de Ierapetra. Aquesta excepcional floració va ser reforçada, molt probablement, per l'arribada de nutrients (principalment Si) provinents de la deposició de cendres volcàniques de les erupcions del volcà Etna durant la primavera 2012. Aquest enriquiment de Si a les aigües superficials va afavorir la proliferació de diatomees (Censi et al., 2010; Olgun et al., 2013), les quals tenen una elevada capacitat d'agregació i per tant augmenten la velocitat de sedimentació dels agregats orgànics quan s'esgoten els nutrients (Smetacek, 1985, 2000).

La presència de diatomees ben preservades a les partícules sedimentades a l'abril 2012, així com també la forta relació entre el OC i l'òpal exportat (r^2= 0.93, p<0.001) i els alts continguts d'òpal en aquestes partícules (19.2%), evidencia que els blooms de diatomees són clau per a la transferència ràpida d'OC cap a profunditats superiors a 4000 m a la Mediterrània oriental. L'arribada de material làbil a profunditats batipelàgiques representa una aportació important de material nutritiu per a les comunitats microbianes batials, les quals poden contribuir a la remineralització del carboni i, conseqüentment, a la reducció d'oxigen a les aigües profundes. La exportació total, estimada, d'OC pel gir de Rodes durant l'abril 2012 (591 t OC d^{-1}) reforça la hipòtesis de que el gir de Rodes juga un paper rellevant en la bomba biològica i en el funcionament biogeoquímic de l'oligotròfica Mediterrània oriental, actuant ocasionalment com un "oasis" dins del que es pot considerar un "desert marí"(Sournia, 1973).

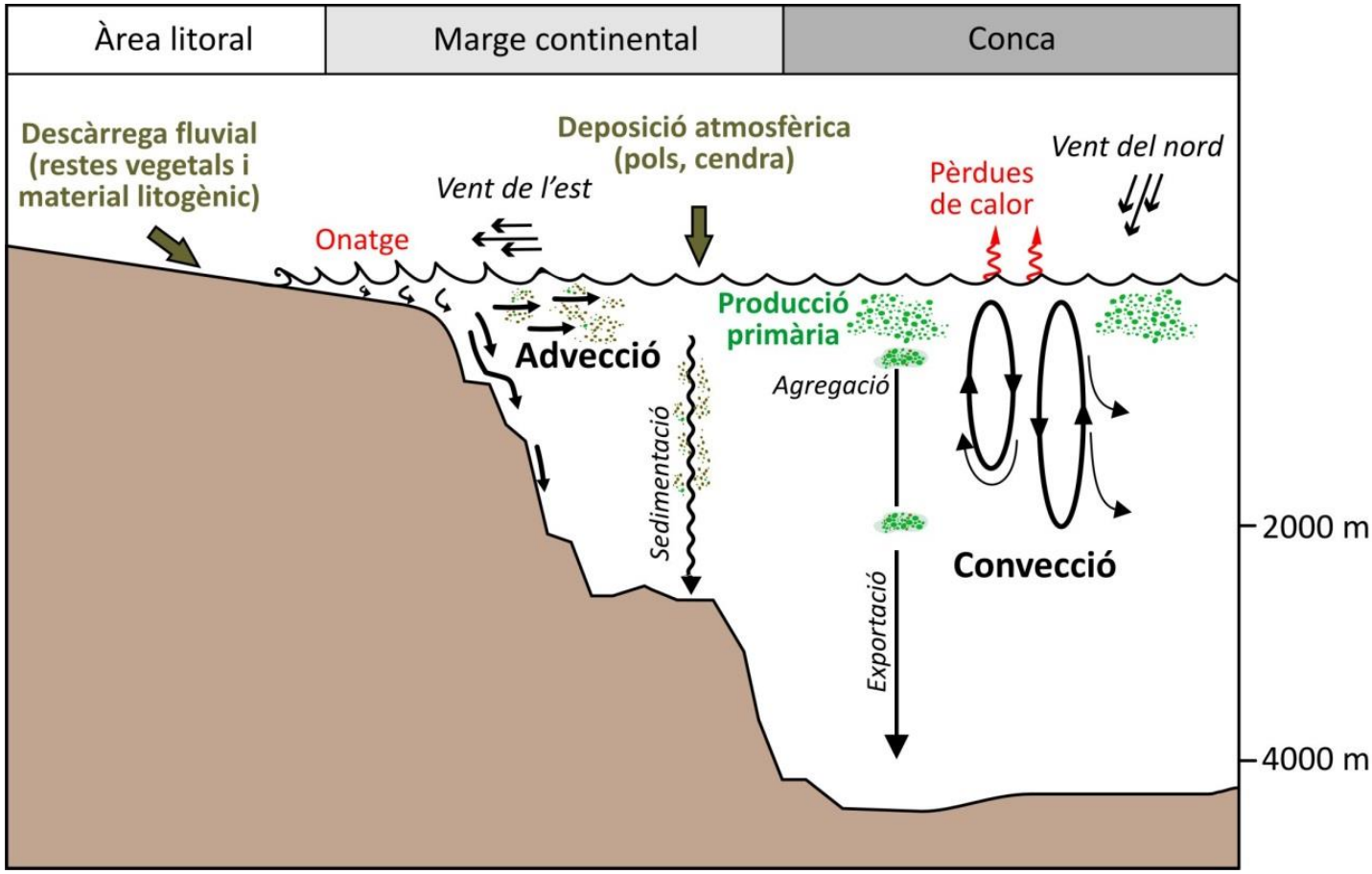

Figura 3.3. Representació esquemàtica de l'impacte dels temporals costaners i convecció a mar obert en el transport de partícules. En aquest diagrama no s'hi ha senyalitzat l'impacte de la formació d'aigua densa de plataforma (DSWC, de l'anglès *Dense Shelf Water Cascading*), que es produeix quan hi ha fortes pèrdues de calor a la plataforma continental, les aigües guanyen densitat i s'enfonsen, i es produeix una exportació massiva de sediments similar o fins i tot superior al que ocorre durant les tempestes costaneres.

Conclusions

Capítol 4

En aquesta Tesi s'ha realitzat un estudi combinat de les característiques biogeoquímiques de sediments superficials de plataforma continental, talussos i conques profundes de la mar Mediterrània i dels fluxos de partícules a una conca profunda de la Mediterrània oriental. Això, juntament amb l'estudi detallat de les condicions meteorològiques, hidrològiques i oceanogràfiques de cada ambient, ha permès millorar el coneixement sobre els processos responsables del transport de sediments i OC, i identificar com els forçaments externs propicien aquest transport. Cal destacar que el període d'adquisició de dades d'aquesta Tesi ha coincidit amb dos processos oceanogràfics d'alt nivell energètic, la tempesta costanera al marge nord-català de desembre 2008, i un hivern 2011-12 especialment fred a tota la conca Mediterrània, fets que han facilitat l'estudi de la vinculació d'aquests esdeveniments amb processos de transferència de material fins a profunditats batipelàgiques.

L'estudi dels sediments superficials tant a nivell granulomètric com biogeoquímic, amb especial atenció al contingut i estat de preservació de la matèria orgànica, ha permès determinar quina és la distribució d'OC en cada fracció de mida de gra del sediment. La fracció argila és la que conté majors continguts d'OC a tots els ambients sedimentaris. La concentració d'OC a les argiles, així com també la contribució d'OC terrestre en aquesta fracció, disminueix en profunditat a causa de processos de remineralització i incorporació de material d'origen marí, respectivament. Als marges continentals, els sediment sorrencs i llimosos rics amb OC terrestre estan associats principalment a partícules terrígenes provinents de descàrregues fluvials.

S'ha detectat una forta relació entre els condicionants atmosfèrics (que desencadenen les tempestes amb onatge, les descarregues fluvials, la convecció a mar obert, i les deposicions atmosfèriques) amb l'origen i la quantitat de material que es transporta al llarg del marge continental i/o s'exporta fins a profunditats abissals.

Al marge continental nord-català el corrent prop del fons generat pel fort onatge és un dels principals factors que controlen la sedimentació de partícules. Els corrents generats durant temporals costaners transporten grans volums de material particulat fi i ric amb OC des de la plataforma cap a la conca profunda on seran dipositats, essent els canyons submarins els conductes preferencials de transport. El transport de la fracció argila és, doncs, un component rellevant en el cicle del carboni

De la mateixa manera, un dels principals factors que controlen els fluxos de partícules i l'exportació d'OC a profunditats batipelàgiques a la Mediterrània oriental és l'aport de nutrients resultant de la convecció a mar obert i la deposició atmosfèrica. L'acoblament de vents freds i secs del nord amb una erupció volcànica poden causar un augment significatiu de la producció primària i l'exportació de fitodetritus fresc més enllà de 4000 m de profunditat. A més a més, s'ha observat que les conques profundes de la Mediterrània oriental actuen com a depocentre de partícules fines riques amb matèria orgànica i contaminants associats, com són per exemple els residus del petroli.

Així doncs, les aportacions de matèria orgànica marina i terrestre als marges continentals i a les conques profundes de la Mediterrània estan controlades per forçaments d'origen atmosfèric. Mentre que l'entrada de matèria orgànica marina fàcilment degradable està controlada per increments de la producció primària de caire periòdic i esporàdic (blooms primaverals i induïts per processos de barreja de la columna d'aigua i deposició atmosfèrica), l'arribada de material

terrestre ve modulada principalment per la intensitat de les descàrregues fluvials i d'emissaris als marges continentals i per la deposició atmosfèrica a les conques profundes.

Implicacions

Els resultats d'aquesta Tesi posen en evidència que:

Analitzar biogeoquímicament les diferents fraccions de mida de gra dels sediments aporta informació cabdal per entendre els mecanismes de transport i emmagatzematge de l'OC.

Millorar el coneixement sobre els processos responsables del transport de sediments i carboni orgànic, i identificar com els forçaments externs que propicien aquest transport, és essencial per conèixer el rol de la dinàmica sedimentària en el cicle del carboni.

Dur a terme monitoratges a llarg termini dels fluxos de partícules a l'oceà és essencial per entendre la capacitat natural que tenen els oceans per fixar CO_2 i exportar-lo en forma de carboni orgànic particulat.

Possibles línies de futur

Els treballs realitzats han fet sorgir noves incògnites, algunes de les quals podrien ser investigades mitjançant l'aprofundiment de dades ja disponibles, i d'altres requeririen un nou disseny experimental i una nova obtenció de mostres. A continuació es presenten una sèrie de possibles tasques que es podrien desenvolupar:

Realitzar un estudi detallat dels biomarcadors lipídics que hi ha a cada fracció de sediment per tal d'avaluar més detalladament l'origen i estat de preservació de la matèria orgànica en cada fracció. Aquesta informació seria de gran utilitat per estudiar els processos de degradació durant la transferència de les partícules cap a zones més profundes.

Monitoritzar els fluxos de partícules durant un període de temps més llarg amb l'objectiu de continuar investigant quins són els forçaments que afecten a l'exportació de carboni i amb quina freqüència succeeixen a la conca profunda de Ierapetra. A més, seria molt interessant posar en aquesta línia instrumentada 2 o 3 trampes a diferents nivells de profunditat de la columna d'aigua per tal d'estudiar la remineralització de l'OC al llarg de la columna d'aigua.

Estudiar les comunitats microbianes de les mostres de les trampes de sediment per a poder establir millor el rol d'aquests en l'exportació i la remineralització de les partícules fins a profunditat batipelàgiques.

Dur a terme periòdicament anàlisis de nutrients (N, P, Si i Fe) tant a les aigües superficials com a les aigües profundes de la Mediterrània oriental per poder establir exactament quin paper juga cada un d'ells a la bomba biològica.

Integrar els resultats obtinguts dels fluxos d'OC de Ierapetra amb els d'altres estudis realitzats durant el mateix any 2011-12 a la mar Mediterrània (i especialment al golf de Lleó i a la mar Adriàtica) per tal de dur a terme una avaluació de l'impacte d'un hivern rigorosament fred en l'exportació d'OC a tota la conca.

Capítol 5

Bibliografia

Accornero, A., Picon, P., Bovée, F. de, Charrière, B. i Buscail, R.: Organic carbon budget at the sediment–water interface on the Gulf of Lions continental margin, Cont. Shelf Res., 23(1), 79-92, doi:10.1016/S0278-4343(02)00168-1, 2003.

Agusti, S., González-Gordillo, J. I., Vaqué, D., Estrada, M., Cerezo, M. I., Salazar, G., Gasol, J. M. i Duarte, C. M.: Ubiquitous healthy diatoms in the deep sea confirm deep carbon injection by the biological pump., Nat. Commun., 6, 7608, doi:10.1038/ncomms8608, 2015.

Alldredge, A. L., Passow, U. i Logan, B. E.: The abundance and significance of a class of large, transparent organic particles in the ocean, Deep Sea Res. Part I Oceanogr. Res. Pap., 40(6), 1131-1140, doi:10.1016/0967-0637(93)90129-Q, 1993.

Amblàs, D.: Morfodinàmica sedimentària de marges continentals passius silicoclàstics/ Sedimentary morphodynamics of siliciclastic passive continental margins, Universitat de Barcelona, 2012.

Amblàs, D., Canals, M., Lastras, G., Berné, S. i Loubrieu, B.: Imaging the Seascapes of the Mediterranean, Oceanography, 17(4), 144-155, doi:10.5670/oceanog.2004.11, 2004.

Amblàs, D., Canals, M., Urgeles, R., Lastras, G., Liquete, C., Hughes-Clarke, J. E., Casamor, J. L. i Calafat, A.: Morphogenetic mesoscale analysis of the northeastern Iberian margin, NW Mediterranean Basin, Mar. Geol., 234(1-4), 3-20, doi:10.1016/j.margeo.2006.09.009, 2006.

Anderson, L. A.: On the hydrogen and oxygen content of marine phytoplankton, Deep Sea Res. Part I Oceanogr. Res. Pap., 42(9), 1675-1680, doi:10.1016/0967-0637(95)00072-E, 1995.

Antia, A. N.: Solubilization of particles in sediment traps: revising the stoichiometry of mixed layer export, Biogeosciences, 2(2), 189-204, doi:10.5194/bg-2-189-2005, 2005.

Arístegui, J., Duarte, C. M., Agustí, S., Doval, M., Alvarez-Salgado, X. A., Hansell, D. A., Carlson, C. A., Ducklow, H. W., Michaels, A. F., Giorgio, P. A. del, Duarte, C. M., Doval, M. D., Hansell, D. A., Peltzer, E. T., Hayward, N. A., Hansell, D. A., Carlson, C. A., Álvarez-Salgado, X. A., Pérez, F. F., Ríos, A. F., Doval, M. D., Hansell, D. A., Carlson, C. A., Jahnke, R. A. i Scholten, J. C.: Dissolved organic carbon support of respiration in the dark ocean., Science, 298(5600), 1967, doi:10.1126/science.1076746, 2002.

Arístegui, J., Gasol, J. M., Duarte, C. M. i Herndld, G. J.: Microbial oceanography of the dark ocean's pelagic realm, Limnol. Oceanogr., 54(5), 1501-1529, doi:10.4319/lo.2009.54.5.1501, 2009.

Arnarson, T. S. i Keil, R. G.: Changes in organic matter–mineral interactions for marine sediments with varying oxygen exposure times, Geochim. Cosmochim. Acta, 71(14), 3545-3556, doi:10.1016/j.gca.2007.04.027, 2007.

Basart, S., Pérez, C., Nickovic, S., Cuevas, E. i Baldasano, J. M.: Development and evaluation of the BSC-DREAM8b dust regional model over Northern Africa, the Mediterranean and the Middle East, Tellus B, 64, doi:10.3402/tellusb.v64i0.18539, 2012.

Bergamaschi, B. A., Tsamakis, E., Keil, R. G., Eglinton, T. I., Montluçon, D. B. i Hedges, J. I.: The effect of grain size and surface area on organic matter, lignin and carbohydrate concentration, and molecular compositions in Peru Margin sediments, Geochim. Cosmochim. Acta, 61(6), 1247-1260, doi:10.1016/S0016-7037(96)00394-8, 1997.

Bergamasco, A. i Malanotte-Rizzoli, P.: The circulation of the Mediterranean Sea: a historical review of experimental investigations, Adv. Oceanogr. Limnol., 1(1), 11-28, doi:10.1080/19475721.2010.491656, 2010.

Beuvier, J., Sevault, F., Herrmann, M., Kontoyiannis, H., Ludwig, W., Rixen, M., Stanev, E., Béranger, K. i Somot, S.: Modeling the Mediterranean Sea interannual variability during 1961–2000: Focus on the Eastern Mediterranean Transient, J. Geophys. Res., 115(C8), C08017, doi:10.1029/2009JC005950, 2010.

Bibby, T. S., Gorbunov, M. Y., Wyman, K. W. i Falkowski, P. G.: Photosynthetic community responses to upwelling in mesoscale eddies in the subtropical North Atlantic and Pacific Oceans, Deep Sea Res. Part II Top. Stud. Oceanogr., 55(10), 1310-1320, doi:10.1016/j.dsr2.2008.01.014, 2008.

Blair, N. E. i Aller, R. C.: The fate of terrestrial organic carbon in the marine environment, Ann. Rev. Mar. Sci., 4(1), 401-423, doi:10.1146/annurev-marine-120709-142717, 2012.

Bloesch, J. i Burns, N. M.: A critical review of sedimentation trap technique, Schweizerische Zeitschrift für Hydrol., 42(1), 15-55, 1980.

Bonnin, J., Heussner, S., Calafat, A., Fabres, J., Palanques, A., Durrieu de Madron, X., Canals, M., Puig, P., Avril, J. i Delsaut, N.: Comparison of horizontal and downward particle fluxes across canyons of the Gulf of Lions (NW Mediterranean): Meteorological and hydrodynamical forcing, Cont. Shelf Res., 28(15), 1957-1970, doi:10.1016/j.csr.2008.06.004, 2008.

Boudreau, B. P.: Diagenetic Models and Their Implementation. Modeling Transport and Reactions in Aquatic Sediments, Springer, Halifax, Canada., 1997.

Boyd, P. W. i Trull, T. W.: Understanding the export of biogenic particles in oceanic waters: Is there consensus?, Prog. Oceanogr., 72(4), 276-312, doi:10.1016/j.pocean.2006.10.007, 2007.

Buesseler, K. O., Antia, A. N., Chen, M., Fowler, S. W., Gardner, W. D., Gustafsson, O., Harada, K., Michaels, A. F., Van Der Loeff, M. R. i Sarin, M.: An assessment of the use of sediment traps for estimating upper ocean particle fluxes, J. Mar. Res., 65(3), 345-416, 2007.

Burd, A. B. i Jackson, G. A.: Particle Aggregation, Ann. Rev. Mar. Sci., 1(1), 65-90, doi:10.1146/annurev.marine.010908.163904, 2009.

Burdige, D. J.: Geochemistry of marine sediments, Princeton University Press, Princeton, New Jersey., 2006.

Calabrese, S. i D'Alessandro, W.: Characterization of the Etna volcanic emissions through an active biomonitoring technique (moss-bags): part 2--morphological and mineralogical features., Chemosphere, 119, 1456-64, doi:10.1016/j.chemosphere.2014.08.087, 2015.

Canals, M., Casamor, J. L., Lastras, G., Monaco, A., Acosta, J., Berne, S., Loubrieu, B., Weaver, P. P. E., Grehan, A. i Dennielou, B.: The role of canyons on strata formation, Oceanography, 17(4), 80-91, doi:http://dx.doi.org/10.5670/oceanog.2004.06, 2004.

Canals, M., Puig, P., de Madron, X. D., Heussner, S., Palanques, A. i Fabres, J.: Flushing submarine canyons., Nature, 444, 354-357, doi:10.1038/nature05271, 2006.

Cartes, J. E., Grémare, A., Maynou, F., Villora-Moreno, S. i Dinet, A.: Bathymetric changes in the distributions of particulate organic matter and associated fauna along a deep-sea transect down the catalan sea slope (Northwestern Mediterranean), Prog. Oceanogr., 53(1), 29-56, doi:10.1016/S0079-6611(02)00023-X, 2002.

Censi, P., Randazzo, L. A., Zuddas, P., Saiano, F., Aricò, P. i Andò, S.: Trace element behaviour in seawater during Etna's pyroclastic activity in 2001: Concurrent effects of nutrients and formation of alteration minerals, J. Volcanol. Geotherm. Res., 193(1-2), 106-116, doi:10.1016/j.jvolgeores.2010.03.010, 2010.

Ciais, P., Sabine, C., Bala, G., Bopp, L., Brovkin, V., Canadell, J., Chhabra, A., DeFries, R., Galloway, J. i Heimann, M.: Carbon and other biogeochemical cycles, en Climate Change 2013: The Physical Science Basis. Contribution of Working Group I to the Fifth Assessment Report of the Intergovernmental Panel on Climate Change, p. 465-570, Cambridge University Press., 2014.

Collister, J. W., Rieley, G., Stern, B., Eglinton, G. i Fry, B.: Compound-specific $\delta^{13}C$ analyses of leaf lipids from plants with differing carbon dioxide metabolisms, Org. Geochem., 21(6-7), 619-627, doi:10.1016/0146-6380(94)90008-6, 1994.

Company, J. B., Puig, P., Sardà, F., Palanques, A., Latasa, M. i Scharek, R.: Climate influence on deep sea populations., PLoS One, 3(1), e1431, doi:10.1371/journal.pone.0001431, 2008.

D'Ortenzio, F. i Ribera d'Alcalà, M.: On the trophic regimes of the Mediterranean Sea: a satellite analysis, Biogeosciences, 6(2), 139-148, doi:10.5194/bg-6-139-2009, 2009.

Danovaro, R., Company, J. B., Corinaldesi, C., D'Onghia, G., Galil, B., Gambi, C., Gooday, A. J., Lampadariou, N., Luna, G. M., Morigi, C., Olu, K., Polymenakou, P. N., Ramirez-Llodra, E., Sabbatini, A., Sardà, F., Sibuet, M. i Tselepides, A.: Deep-sea biodiversity in the Mediterranean Sea: the known, the unknown, and the unknowable., PLoS One, 5(8), e11832, doi:10.1371/journal.pone.0011832, 2010.

Dell'Anno, A., Mei, M. L., Pusceddu, A. i Danovaro, R.: Assessing the trophic state and eutrophication of coastal marine systems: a new approach based on the biochemical composition of sediment organic matter, Mar. Pollut. Bull., 44(7), 611-622, doi:10.1016/S0025-326X(01)00302-2, 2002.

Deuser, W. G.: Seasonal and interannual variations in deep-water particle fluxes in the Sargasso Sea and their relation to surface hydrography, Deep Sea Res. Part A. Oceanogr. Res. Pap., 33(2), 225-246, doi:10.1016/0198-0149(86)90120-2, 1986.

Deuser, W. G., Muller-Karger, F. E. i Hemleben, C.: Temporal variations of particle fluxes in the deep subtropical and tropical North Atlantic: Eulerian versus Lagrangian effects, J. Geophys. Res., 93(C6), 6857, doi:10.1029/JC093iC06p06857, 1988.

Díaz, J. i Maldonado, A.: Transgressive sand bodies on the Maresme continental shelf, western Mediterranean Sea, Mar. Geol., 91(1-2), 53-72, doi:10.1016/0025-3227(90)90132-4, 1990.

Doblin, M. A., Petrou, K., Sinutok, S., Seymour, J. R., Messer, L. F., Brown, M. V., Norman, L., Everett, J. D., McInnes, A. S., Ralph, P. J., Thompson, P. A. i Hassler, C. S.: Nutrient uplift in a cyclonic eddy increases diversity, primary productivity and iron demand of microbial communities relative to a western boundary current, PeerJ, 4, e1973, doi:10.7717/peerj.1973, 2016.

Durán, R., Canals, M., Sanz, J. L., Lastras, G., Amblàs, D. i Micallef, A.: Morphology and sediment dynamics of the northern Catalan continental shelf, northwestern Mediterranean Sea, Geomorphology, 204, 1-20, doi:10.1016/j.geomorph.2012.10.004, 2014.

Durrieu de Madron, X., Houpert, L., Puig, P., Sanchez-Vidal, A., Testor, P., Bosse, A., Estournel, C., Somot, S., Bourrin, F., Bouin, M. N., Beauverger, M., Beguery, L., Calafat, A., Canals, M., Cassou, C., Coppola, L., Dausse, D., D'Ortenzio, F., Font, J., Heussner, S., Kunesch, S., Lefevre, D., Le Goff, H., Martín, J., Mortier, L., Palanques, A. i Raimbault, P.: Interaction of dense shelf water cascading and open-sea convection in the northwestern Mediterranean during winter 2012, Geophys. Res. Lett., 40(7), 1379-1385, doi:10.1002/grl.50331, 2013.

Eglinton, G. i Hamilton, R. J.: Leaf Epicuticular Waxes, Science (80-.)., 156(3780), 1322-1335, doi:10.1126/science.156.3780.1322, 1967.

Eglinton, T. I. i Eglinton, G.: Molecular proxies for paleoclimatology, Earth Planet. Sci. Lett., 275(1-2), 1-16, doi:10.1016/j.epsl.2008.07.012, 2008.

Fabres, J., Calafat, A., Sanchez-Vidal, A., Canals, M. i Heussner, S.: Composition and spatio-temporal variability of particle fluxes in the Western Alboran Gyre, Mediterranean Sea, J. Mar. Syst., 33, 431-456, doi:10.1016/S0924-7963(02)00070-2, 2002.

Flexas, M. M., Durrieu de Madron, X., Garcia, M. A., Canals, M. i Arnau, P.: Flow variability in the Gulf of Lions during the MATER HFF experiment (March–May 1997), J. Mar. Syst., 33-34(May 1997), 197-214, doi:10.1016/S0924-7963(02)00059-3, 2002.

Font, J., Garcialadona, E. i Gorriz, E. G.: The seasonality of mesoscale motion in the northern current of the western Mediterranean-several years of evidence, Oceanol. Acta, 18(2), 207-219, 1995.

Friligos, N., Moriki, A., Sklivagou, E., Krasakopoulou, E. i Hatzianestis, I.: Geochemical characteristics of the surficial sediments of the Aegean Sea, en 3rd MTP-MATER Workshop, vol. 35, p. 28-209, Rhodos., 1998.

Garcia-Castellanos, D., Estrada, F., Jiménez-Munt, I., Gorini, C., Fernández, M., Vergés, J. i De Vicente, R.: Catastrophic flood of the Mediterranean after the Messinian salinity crisis, Nature, 462(7274), 778-781, doi:10.1038/nature08555, 2009.

Gardner, W. D.: Baltimore Canyon as a modern conduit of sediment to the deep sea, Deep Sea Res. Part A. Oceanogr. Res. Pap., 36(3), 323-358, doi:10.1016/0198-0149(89)90041-1, 1989.

Gardner, W. D., Biscaye, P. E. i Richardson, M. J.: A sediment trap experiment in the Vema Channel to evaluate the effect of horizontal particle fluxes on measured vertical fluxes, J. Mar. Res., 55(5), 995-1028, 1997.

Gearing, J. ., Gearing, P. ., Rudnick, D. ., Requejo, A. . i Hutchins, M. .: Isotopic variability of organic carbon in a phytoplankton-based, temperate estuary, Geochim. Cosmochim. Acta, 48(5), 1089-1098, doi:10.1016/0016-7037(84)90199-6, 1984.

Goericke, R. i Fry, B.: Variations of marine plankton δ13 C with latitude, temperature, and dissolved CO_2 in the world ocean, Global Biogeochem. Cycles, 8(1), 85-90, doi:10.1029/93GB03272, 1994.

Gogou, A., Apostolaki, M. i Stephanou, E. G.: Determination of organic molecular markers in marine aerosols and sediments: one-step flash chromatography compound class fractionation and capillary gas chromatographic analysis, J. Chromatogr. A, 799(1-2), 215-231, doi:10.1016/S0021-9673(97)01106-0, 1998.

Gogou, A., Sanchez-Vidal, A., Durrieu de Madron, X., Stavrakakis, S., Calafat, A., Stabholz, M., Psarra, S., Canals, M., Heussner, S., Stavrakaki, I. i Papathanassiou, E.: Carbon flux to the deep in three open sites of the Southern European Seas (SES), J. Mar. Syst., 129, 224-233, doi:10.1016/j.jmarsys.2013.05.013, 2014.

Goldberg, E. D.: Marine geochemistry. Chemical scavengers of the sea, J. Geol., 62, 249-265, 1954.

Goñi, M. A., Monacci, N., Gisewhite, R., Ogston, A., Crockett, J. i Nittrouer, C.: Distribution and sources of particulate organic matter in the water column and sediments of the Fly River Delta, Gulf of Papua (Papua New Guinea), Estuar. Coast. Shelf Sci., 69, 225-245, doi:10.1016/j.ecss.2006.04.012, 2006.

Grice, K., Klein Breteler, W., Schouten, S., Grossi, V., Leeuw, J. W. i Damsté, J. S. S.: Effects of zooplankton herbivory on biomarker proxy records, Paleoceanography, 13(6), 686-693, doi:10.1029/98PA01871, 1998.

Guerzoni, S., Chester, R., Dulac, F., Herut, B., Loÿe-Pilot, M.-D., Measures, C., Migon, C., Molinaroli, E., Moulin, C., Rossini, P., Saydam, C., Soudine, A. i Ziveri, P.: The role of atmospheric deposition in the biogeochemistry of the Mediterranean Sea, Prog. Oceanogr., 44(1-3), 147-190, doi:10.1016/S0079-6611(99)00024-5, 1999.

Guieu, C., Chester, R., Nimmo, M., Martin, J.-M., Guerzoni, S., Nicolas, E., Mateu, J. i Keyse, S.: Atmospheric input of dissolved and particulate metals to the northwestern Mediterranean, Deep Sea Res. Part II Top. Stud. Oceanogr., 44(3-4), 655-674, doi:10.1016/S0967-0645(97)88508-6, 1997.

Guieu, C., Dulac, F., Ridame, C. i Pondaven, P.: Introduction to project DUNE, a DUst experiment in a low Nutrient, low chlorophyll Ecosystem, Biogeosciences, 11(2), 425-442, doi:10.5194/bg-11-425-2014, 2014.

Harmelin-Vivien, M., Loizeau, V., Mellon, C. i Beker, B.: Comparison of C and N stable isotope ratios between surface particulate organic matter and microphytoplankton in the Gulf of Lions (NW Mediterranean), Cont. Shelf Res., 28(15), 1911-1919, doi:10.1016/j.csr.2008.03.002, 2008.

Hedges, J. I. i Keil, R. G.: Sedimentary organic matter preservation: an assessment and speculative synthesis, Mar. Chem., 49(2-3), 81-115, doi:10.1016/0304-4203(95)00008-F, 1995.

Hedges, J. I. i Oades, J. M.: Comparative organic geochemistries of soils and marine sediments, Org. Geochem., 27(7-8), 319-361, doi:10.1016/S0146-6380(97)00056-9, 1997.

Hedges, J. I., Keil, R. G. i Benner, R.: What happens to terrestrial organic matter in the ocean?, Org. Geochem., 27(5-6), 195-212, doi:10.1016/S0146-6380(97)00066-1, 1997.

Heim, A.: Der Schlammabsatz am Grunde des Vierwaldstättersees, Vierteljahresschrift Naturforschenden Gesellschaft in Zurich, A5, 164-182, 1900.

Heussner, S., Ratti, C. i Carbonne, J.: The PPS 3 time-series sediment trap and the trap sample processing techniques used during the ECOMARGE experiment, Cont. Shelf Res., 10(9-11), 943-958, doi:10.1016/0278-4343(90)90069-X, 1990.

Heussner, S., Calafat, A. i Palanques, A.: Quantitative and qualitative features of particle fluxes in the North-Balearic Basin, EUROMARGE-NB Final Report, Ed. by Canals, M., Casamor, JL, Cacho, I., Calafat, AM, Monaco, A., MAST II Program. EC, 2, 41-66, 1996.

Heussner, S., Durrieu de Madron, X., Radakovitch, O., Beaufort, L., E. Biscaye, P., Carbonne, J., Etcheber, H. i Monaco, A.: Spatial and temporal patterns of downward particle fluxes on the continental slope of the Bay of Biscay (northeastern Atlantic), Deep Sea Res. Part II Top. Stud. Oceanogr., 46(10), 2101-2146, doi:10.1016/S0967-0645(99)00057-0, 1999.

Honjo, S.: Fluxes of particles to the Interior of the open oceans, en Particle flux in the ocean, vol. 57, editat per V. Ittekkot, P. Schäfer, S. Honjo, i P. J. Depetris, p. 91-154, John Wiley and Sons Ltd., New York. [en línia] Available from: http://ci.nii.ac.jp/naid/10003566451/en/, 1996.

Iglesias-Rodríguez, M. D., Brown, C. W., Doney, S. C., Kleypas, J., Kolber, D., Kolber, Z., Hayes, P. K. i Falkowski, P. G.: Representing key phytoplankton functional groups in ocean carbon cycle models: Coccolithophorids, Global Biogeochem. Cycles, 16(4), 47-1-47-20, doi:10.1029/2001GB001454, 2002.

Ivanov, V. V., Shapiro, G. I., Huthnance, J. M., Aleynik, D. L. i Golovin, P. N.: Cascades of dense water around the world ocean, Prog. Oceanogr., 60(1), 47-98, doi:10.1016/j.pocean.2003.12.002, 2004.

Jickells, T. i Moore, C. M.: The Importance of Atmospheric Deposition for Ocean Productivity, Annu. Rev. Ecol. Evol. Syst., 46(1), 481-501, doi:10.1146/annurev-ecolsys-112414-054118, 2015.

Jickells, T. D., An, Z. S., Andersen, K. K., Baker, a R., Bergametti, G., Brooks, N., Cao, J. J., Boyd, P. W., Duce, R. a, Hunter, K. a, Kawahata, H., Kubilay, N., LaRoche, J., Liss, P. S., Mahowald, N., Prospero, J. M., Ridgwell, A.J., Tegen, I. i Torres, R.: Global iron connections between desert dust, ocean biogeochemistry, and climate, Science (80)., 308(5718), 67-71, doi:10.1126/science.1105959, 2005.

Kamatani, A. i Oku, O.: Measuring biogenic silica in marine sediments, Mar. Chem., 68(3), 219-229, doi:10.1016/S0304-4203(99)00079-1, 2000.

Karl, D. M., Christian, J. R., Dore, J. E., Hebel, D. V., Letelier, R. M., Tupas, L. M. i Winn, C. D.: Seasonal and interannual variability in primary production and particle flux at Station ALOHA, Deep Sea Res. Part II Top. Stud. Oceanogr., 43(2-3), 539-568, doi:10.1016/0967-0645(96)00002-1, 1996.

Karl, D. M., Bates, N. R., Emerson, S., Harrison, P. J., Jeandel, C., Llinâs, O., Liu, K.-K., Marty, J.-C., Michaels, A. F., Miquel, J. C., Neuer, S., Nojiri, Y. i Wong, C. S.: Temporal Studies of Biogeochemical Processes Determined from Ocean Time-Series Observations During the JGOFS Era, en Ocean Biogeochemistry, p. 239-267, Springer Berlin Heidelberg, Berlin, Heidelberg., 2003.

Kastner, M.: Oceanic minerals: their origin, nature of their environment, and significance., Proc. Natl. Acad. Sci. U. S. A., 96(7), 3380-7, doi:10.1073/pnas.96.7.3380, 1999.

Keil, R. G., Tsamakis, E., Giddings, J. C. i Hedges, J. I.: Biochemical distributions (amino acids, neutral sugars , and lignin phenols) among size-classes of modern marine sediments from the Washington coast, 62(8), 1347-1364, doi:10.1016/S0016-7037(98)00080-5, 1998.

Kontoyiannis, H., Balopoulos, E., Gotsis-Skretas, O., Pavlidou, A., Assimakopoulou, G. i Papageorgiou, E.: The hydrology and biochemistry of the Cretan Straits (Antikithira and Kassos Straits) revisited in the period June 1997–May 1998, J. Mar. Syst., 53(1-4), 37-57, doi:10.1016/j.jmarsys.2004.06.007, 2005.

Krom, M. D., Kress, N., Brenner, S. i Gordon, L. I.: Phosphorus limitation of primary productivity in the eastern Mediterranean Sea., Limnol. Oceanogr., 36(3), 424-432, doi:10.4319/lo.1991.36.3.0424, 1991.

Krom, M. D., Groom, S. i Zohary, T.: The Eastern Mediterranean, The Biogeo., editat per G. B. Black, K. D. and Shimmield, Blackwell Publishing, Oxford., 2003.

Krom, M. D., Herut, B. i Mantoura, R. F. C.: Nutrient budget for the Eastern Mediterranean: Implications for phosphorus limitation, Limnol. Oceanogr., 49(5), 1582-1592, doi:10.4319/lo.2004.49.5.1582, 2004.

Krom, M. D., Woodward, E. M. S., Herut, B., Kress, N., Carbo, P., Mantoura, R. F. C., Spyres, G., Thingstad, T. F., Wassmann, P., Wexels-Riser, C., Kitidis, V., Law, C. S. i Zodiatis, G.: Nutrient cycling in the south east Levantine basin of the eastern Mediterranean: Results from a phosphorus starved system, Deep Sea Res. Part II Top. Stud. Oceanogr., 52(22-23), 2879-2896, doi:10.1016/j.dsr2.2005.08.009, 2005.

Krotkov, N. A. i Li, C.: OMI/Aura Sulphur Dioxide (SO2) Total Column 1-orbit L2 Swath 13x24 km,version 003, Greenbelt, MD, USAGoddard Sp. Flight Cent. Distrib. Act. Arch. Cent. (GSFC DAAC), Accessed July 1, 2015, doi:10.5067/Aura/OMI/DATA2022, 2012.

Larnicol, G., Ayoub, N. i Le Traon, P. Y.: Major changes in Mediterranean Sea level variability from 7 years of TOPEX/Poseidon and ERS-1/2 data, J. Mar. Syst., 33-34, 63-89, doi:10.1016/S0924-7963(02)00053-2, 2002.

Lastras, G., Canals, M., Amblàs, D., Lavoie, C., Church, I., De Mol, B., Duran, R., Calafat, A., Hughes-Clarke, J. E., Smith, C. J. i Heussner, S.: Understanding sediment dynamics of two large submarine valleys from seafloor data: Blanes and La Fonera canyons, northwestern Mediterranean Sea, Mar. Geol., 280(1-4), 20-39, doi:10.1016/j.margeo.2010.11.005, 2011.

Laws, E. A., Falkowski, P. G., Smith, W. O., Ducklow, H. i McCarthy, J. J.: Temperature effects on export production in the open ocean, Global Biogeochem. Cycles, 14(4), 1231-1246, doi:10.1029/1999GB001229, 2000.

Lazzari, P., Teruzzi, A., Salon, S., Campagna, S., Calonaci, C., Colella, S., Tonani, M. i Crise, A.: Pre-operational short-term forecasts for Mediterranean Sea biogeochemistry, Ocean Sci., 6(1), 25-39, doi:10.5194/osd-6-1223-2009, 2010.

Lazzari, P., Solidoro, C., Ibello, V., Salon, S., Teruzzi, A., Béranger, K., Colella, S. i Crise, A.: Seasonal and inter-annual variability of plankton chlorophyll and primary production in the Mediterranean Sea: a modelling approach, Biogeosciences, 9(1), 217-233, doi:10.5194/bg-9-217-2012, 2012.

Lazzari, P., Solidoro, C., Salon, S. i Bolzon, G.: Spatial variability of phosphate and nitrate in the Mediterranean Sea: A modeling approach, Deep Sea Res. Part I Oceanogr. Res. Pap., 108, 39-52, doi:10.1016/j.dsr.2015.12.006, 2016.

Lefèvre, R., Gaudichet, A. i Billon-Galland, M. A.: Silicate microspherules intercepted in the plume of Etna volcano, Nature, 322(6082), 817-820, doi:10.1038/322817a0, 1986.

De Leo, F. C., Smith, C. R., Rowden, A. a, Bowden, D. a i Clark, M. R.: Submarine canyons: hotspots of benthic biomass and productivity in the deep sea., Proc. Biol. Sci., 277(1695), 2783-92, doi:10.1098/rspb.2010.0462, 2010.

Lick, W., Huang, H. i Jepsen, R.: Flocculation of fine-grained sediments due to differential settling, J. Geophys. Res., 98(C6), 10279, doi:10.1029/93JC00519, 1993.

Liquete, C., Canals, M., De Mol, B., De Batist, M. i Trincardi, F.: Quaternary stratal architecture of the Barcelona prodeltaic continental shelf (NW Mediterranean), Mar. Geol., 250(3), 234-250, doi:10.1016/j.margeo.2008.01.014, 2008.

Lisitzin, A. P.: Oceanic sedimentation: lithology and geochemistry, editat per A. P. Lisitzin, American Geophysical Union, 1996.

Liu, K.-K., Atkinson, L., Quiñones, R. A. i Talaue-McManus, L.: Biogeochemistry of Continental Margins in a Global Context, p. 3-24, Springer Berlin Heidelberg., 2010.

Lopez-Fernandez, P., Calafat, A., Sanchez-Vidal, A., Mar Flexas, M. i Cateura, J.: Multiple drivers of particle fluxes in the Blanes submarine canyon and southern open slope: Results of a year round experiment, Prog. Oceanogr., 118, 95-107, doi:10.1016/j.pocean.2013.07.029, 2013.

Ludwig, W., Dumont, E., Meybeck, M. i Heussner, S.: River discharges of water and nutrients to the Mediterranean and Black Sea: Major drivers for ecosystem changes during past and future decades?, Prog. Oceanogr., 80(3-4), 199-217, doi:10.1016/j.pocean.2009.02.001, 2009.

Malanotte-Rizzoli, P.: Currents systems in the Mediterranean Sea, en Encyclopedia of Ocean Sciences, editat per J. Steele, S. Thorpe, i K. Turekian, p. 605-612, Academic Press, 2001.

Manca, B. B., Kovaĉević, V., Gaĉić, M. i Viezzoli, D.: Dense water formation in the Southern Adriatic Sea and spreading into the Ionian Sea in the period 1997–1999, J. Mar. Syst., 33-34, 133-154, doi:10.1016/S0924-7963(02)00056-8, 2002.

Markaki, Z., Oikonomou, K., Kocak, M., Kouvarakis, G., Chaniotaki, A., Kubilay, N. i Mihalopoulos, N.: Atmospheric deposition of inorganic phosphorus in the Levantine Basin, eastern Mediterranean: Spatial and temporal variability and its role in seawater productivity, Limnol. Oceanogr., 48(4), 1557-1568, doi:10.4319/lo.2003.48.4.1557, 2003.

Martín, J., Puig, P., Palanques, A., Masqué, P. i García-Orellana, J.: Effect of commercial trawling on the deep sedimentation in a Mediterranean submarine canyon, Mar. Geol., 252(3), 150-155, doi:10.1016/j.margeo.2008.03.012, 2008.

Marty, J. i Chiav, J.: Seasonal and interannual variations in phytoplankton production at DYFAMED time-series station , northwestern Mediterranean Sea, , 49, 2017-2030, 2002.

Masqué, P., Fabres, J., Canals, M., Sanchez-Cabeza, J. A., Sanchez-Vidal, A., Cacho, I., Calafat, A. i Bruach, J. M.: Accumulation rates of major constituents of hemipelagic sediments in the deep Alboran Sea: a centennial perspective of sedimentary dynamics, Mar. Geol., 193(3-4), 207-233, doi:10.1016/S0025-3227(02)00593-5, 2003.

Mayer, L. M.: Relationships between mineral surfaces and organic carbon concentrations in soils and sediments, Chem. Geol., 114(3-4), 347-363, doi:10.1016/0009-2541(94)90063-9, 1994a.

Mayer, L. M.: Surface area control of organic carbon accumulation in continental shelf sediments, Geochim. Cosmochim. Acta, 58(4), 1271-1284, 1994b.

McGillicuddy, D. J., Anderson, L. A., Bates, N. R., Bibby, T., Buesseler, K. O., Carlson, C. A., Davis, C. S., Ewart, C., Falkowski, P. G., Goldthwait, S. A., Hansell, D. A., Jenkins, W. J., Johnson, R., Kosnyrev, V. K., Ledwell, J. R., Li, Q. P., Siegel, D. A. i Steinberg, D. K.: Eddy/wind interactions stimulate extraordinary mid-ocean plankton blooms., Science, 316(5827), 1021-6, doi:10.1126/science.1136256, 2007.

Medimap Group: Morpho-bathymetry of the Mediterranean Sea, E: 1=2000000, CIESM/Ifremer Sp. Publ., Maps and Atlases, two maps (Western Mediterranean and Eastern Mediterranean), Montecarlo / Brest, Monaco / France., 2007.

Mermex group: Marine ecosystems' responses to climatic and anthropogenic forcings in the Mediterranean, Prog. Oceanogr., 91(2), 97-166, doi:10.1016/j.pocean.2011.02.003, 2011.

Meyers, P. A.: Preservation of elemental and isotopic source identification of sedimentary organic matter, Chem. Geol., 114(3-4), 289-302, doi:10.1016/0009-2541(94)90059-0, 1994.

Meyers, P. A.: Organic geochemical proxies of paleoceanographic, paleolimnologic, and paleoclimatic processes, Org. Geochem., 27(5-6), 213-250, doi:10.1016/S0146-6380(97)00049-1, 1997.

Meyers, P. A., Silliman, J. E. i Shaw, T. J.: Effects of turbidity flows on organic matter accumulation, sulfate reduction, and methane generation in deep-sea sediments on the Iberia Abyssal Plain, Org. Geochem., 25(1-2), 69-78, doi:10.1016/S0146-6380(96)00106-4, 1996.

Mihanović, H., Vilibić, I., Carniel, S., Tudor, M., Russo, A., Bergamasco, A., Bubić, N., Ljubešić, Z., Viličić, D., Boldrin, A., Malačič, V., Celio, M., Comici, C. i Raicich, F.: Exceptional dense water formation on the Adriatic shelf in the winter of 2012, Ocean Sci., 9(3), 561-572, doi:10.5194/os-9-561-2013, 2013.

Milliman, J. D.: Production and accumulation of calcium carbonate in the ocean: Budget of a nonsteady state, Global Biogeochem. Cycles, 7(4), 927-957, doi:10.1029/93GB02524, 1993.

Milliman, J. D. i Syvitski, J. P. M.: Geomorphic/Tectonic Control of Sediment Discharge to the Ocean: The Importance of Small Mountainous Rivers, J. Geol., 100(5), 525-544, doi:10.1086/629606, 1992.

Millot, C.: Circulation in the Western Mediterranean Sea, J. Mar. Syst., 20(1-4), 423-442, doi:10.1016/S0924-7963(98)00078-5, 1999.

Millot, C.: Another description of the Mediterranean Sea outflow, Prog. Oceanogr., 82(2), 101-124, doi:10.1016/j.pocean.2009.04.016, 2009.

Millot, C. i Taupier-Letage, I.: Additional evidence of LIW entrainment across the Algerian subbasin by mesoscale eddies and not by a permanent westward flow, Prog. Oceanogr., 66(2), 231-250, doi:10.1016/j.pocean.2004.03.002, 2005.

Mortlock, R. A. i Froelich, P. N.: A simple method for the rapid determination of biogenic opal in pelagic marine sediments, Deep Sea Res. Part A. Oceanogr. Res. Pap., 36(9), 1415-1426, doi:10.1016/0198-0149(89)90092-7, 1989.

Moutin, T. i Raimbault, P.: Primary production, carbon export and nutrients availability in western and eastern Mediterranean Sea in early summer 1996 (MINOS cruise), J. Mar. Syst., 33-34, 273-288, doi:10.1016/S0924-7963(02)00062-3, 2002.

Napolitano, E., Oguz, T., Malanotte-Rizzoli, P., Yilmaz, A. i Sansone, E.: Simulations of biological production in the Rhodes and Ionian basins of the eastern Mediterranean, J. Mar. Syst., 24(3-4), 277-298, doi:10.1016/S0924-7963(99)00090-1, 2000.

Nelson, D. M., Tréguer, P., Brzezinski, M. A., Leynaert, A. i Quéguiner, B.: Production and dissolution of biogenic silica in the ocean: Revised global estimates, comparison with regional data and relationship to biogenic sedimentation, Global Biogeochem. Cycles, 9(3), 359-372, doi:10.1029/95GB01070, 1995.

Neumeier, U., Ferrarin, C., Amos, C. L., Umgiesser, G. i Li, M. Z.: Sedtrans05: An improved sediment-transport model for continental shelves and coastal waters with a new algorithm for cohesive sediments, Comput. Geosci., 34(10), 1223-1242, doi:10.1016/j.cageo.2008.02.007, 2008.

Nieuwenhuize, J., Maas, Y. E. M. i Middelburg, J. J.: Rapid analysis of organic carbon and nitrogen in particulate materials, Mar. Chem., 45(3), 217-224, doi:10.1016/0304-4203(94)90005-1, 1994.

Nuwer, J. M. i Keil, R. G.: Sedimentary organic matter geochemistry of Clayoquot Sound, Vancouver Island, British Columbia, Limnol. Oceanogr., 50(4), 1119-1128, doi:10.4319/lo.2005.50.4.1119, 2005.

Ohkouchi, N., Kawamura, K., Kawahata, H. i Taira, A.: Latitudinal distributions of terrestrial biomarkers in the sediments from the Central Pacific, Geochim. Cosmochim. Acta, 61(9), 1911-1918, doi:10.1016/S0016-7037(97)00040-9, 1997.

Olgun, N., Duggen, S., Andronico, D., Kutterolf, S., Croot, P. L., Giammanco, S., Censi, P. i Randazzo, L.: Possible impacts of volcanic ash emissions of Mount Etna on the primary productivity in the oligotrophic Mediterranean Sea: Results from nutrient-release experiments in seawater, Mar. Chem., 152, 32-42, doi:10.1016/j.marchem.2013.04.004, 2013.

Ovchinnikov, M.: The formation of intermediate water in the Mediterranean, Oceanology, 24(2), 168-173, 1984.

Palanques, A., García-Ladona, E., Gomis, D., Martín, J., Marcos, M., Pascual, A., Puig, P., Gili, J.-M., Emelianov, M., Monserrat, S., Guillén, J., Tintoré, J., Segura, M., Jordi, A., Ruiz, S., Basterretxea, G., Font, J., Blasco, D. i Pagès, F.: General patterns of circulation, sediment fluxes and ecology of the Palamós (La Fonera) submarine canyon, northwestern Mediterranean, Prog. Oceanogr., 66(2-4), 89-119, doi:10.1016/j.pocean.2004.07.016, 2005.

Paulmier, A., Kriest, I. i Oschlies, A.: Stoichiometries of remineralisation and denitrification in global biogeochemical ocean models, Biogeosciences, 6(5), 923-935, doi:10.5194/bg-6-923-2009, 2009.

Perdue, E. M. i Koprivnjak, J.-F.: Using the C/N ratio to estimate terrigenous inputs of organic matter to aquatic environments, Estuar. Coast. Shelf Sci., 73(1-2), 65-72, doi:10.1016/j.ecss.2006.12.021, 2007.

Pérez, C., Nickovic, S., Baldasano, J. M., Sicard, M., Rocadenbosch, F. i Cachorro, V. E.: A long Saharan dust event over the western Mediterranean: Lidar, Sun photometer observations, and regional dust modeling, J. Geophys. Res., 111(D15), D15214, doi:10.1029/2005JD006579, 2006a.

Pérez, C., Nickovic, S., Pejanovic, G., Baldasano, J. M. i Özsoy, E.: Interactive dust-radiation modeling: A step to improve weather forecasts, J. Geophys. Res., 111(D16), D16206, doi:10.1029/2005JD006717, 2006b.

Petihakis, G., Triantafyllou, G., Tsiaras, K., Korres, G., Pollani, A. i Hoteit, I.: Eastern Mediterranean biogeochemical flux model - Simulations of the pelagic ecosystem, Ocean Sci., 5(1), 29-46, doi:10.5194/os-5-29-2009, 2009.

Pinardi, N. i Masetti, E.: Variability of the large scale general circulation of the Mediterranean Sea from observations and modelling: a review, Palaeogeogr. Palaeoclimatol. Palaeoecol., 158(3-4), 153-173, doi:10.1016/S0031-0182(00)00048-1, 2000.

Prospero, J. M.: The atmospheric transport of particles to the ocean, en Particle Fux in the Ocean, vol. 57, editat per V. Ittekkot, P. Shäfer, S. Honjo, i P. J. Depetris, p. 19-52, John Wiley & Sons Ltd., 1996.

Psarra, S., Tselepides, A. i Ignatiades, L.: Primary productivity in the oligotrophic Cretan Sea (NE Mediterranean): seasonal and interannual variability, Prog. Oceanogr., 46(2-4), 187-204, doi:10.1016/S0079-6611(00)00018-5, 2000.

Pujo-Pay, M., Conan, P., Oriol, L., Cornet-Barthaux, V., Falco, C., Ghiglione, J.-F., Goyet, C., Moutin, T. i Prieur, L.: Integrated survey of elemental stoichiometry (C, N, P) from the western to eastern Mediterranean Sea, Biogeosciences, 8(4), 883-899, doi:10.5194/bg-8-883-2011, 2011.

Ragueneau, O., Tréguer, P., Leynaert, A., Anderson, R. ., Brzezinski, M. ., DeMaster, D. ., Dugdale, R. ., Dymond, J., Fischer, G., François, R., Heinze, C., Maier-Reimer, E., Martin-Jézéquel, V., Nelson, D. . i Quéguiner, B.: A review of the Si cycle in the modern ocean: recent progress and missing gaps in the application of biogenic opal as a paleoproductivity proxy, Glob. Planet. Change, 26(4), 317-365, doi:10.1016/S0921-8181(00)00052-7, 2000.

Ragueneau, O., Savoye, N., Del Amo, Y., Cotten, J., Tardiveau, B. i Leynaert, A.: A new method for the measurement of biogenic silica in suspended matter of coastal waters: using Si:Al ratios to correct for the mineral interference, Cont. Shelf Res., 25(5-6), 697-710, doi:10.1016/j.csr.2004.09.017, 2005.

Redfield, A. C.: On the proportions of organic derivatives in sea water and their relation to the composition of plankton, en James Johnstone Memorial Volume, p. 177-192, University Press of Liverpool, Liverpool., 1934.

Redfield, A. C., Ketchum, B. H. i Richards, F. A.: The influence of organisms on the composition of sea-water, en The Sea, editat per M. N. Hill, p. 26-77, Interscience, New York., 1963.

Ribera d'Alcalà, M.: Nutrient ratios and fluxes hint at overlooked processes in the Mediterranean Sea, J. Geophys. Res., 108(C9), 8106, doi:10.1029/2002JC001650, 2003.

Robinson, A. R., Leslie, W. G., Theocharis, A. i Lascaratos, A.: Mediterranean Sea Circulation, en Encyclopedia of Ocean Sciences, p. 1689-1706, Academic Press., 2001.

Rodellas, V., Garcia-Orellana, J., Masqué, P., Feldman, M. i Weinstein, Y.: Submarine groundwater discharge as a major source of nutrients to the Mediterranean Sea., Proc. Natl. Acad. Sci. U. S. A., 112(13), 3926-30, doi:10.1073/pnas.1419049112, 2015.

Rovira, A. i Batalla, R. J.: Temporal distribution of suspended sediment transport in a Mediterranean basin: The Lower Tordera (NE SPAIN), Geomorphology, 79(1), 58-71, doi:10.1016/j.geomorph.2005.09.016, 2006.

Rumolo, P., Cartes, J. E., Fanelli, E., Papiol, V., Sprovieri, M., Mirto, S., Gherardi, S. i Bonanno, A.: Seasonal variations in the source of sea bottom organic matter off Catalonia coasts (western Mediterranean): links with hydrography and biological response, J. Oceanogr., 71(4), 325-343, doi:10.1007/s10872-015-0291-7, 2015.

Sanchez-Vidal, A., Canals, M., Calafat, A., Lastras, G., Pedrosa-Pàmies, R., Menéndez, M., Medina, R., Company, J. B., Hereu, B., Romero, J. i Alcoverro, T.: Impacts on the Deep-Sea Ecosystem by a Severe Coastal Storm, PLoS One, 7(1), e30395, doi:10.1371/journal.pone.0030395, 2012.

Sanchez-Vidal, A., Higueras, M., Martí, E., Liquete, C., Calafat, A. i Kerhervé, P.: Riverine transport of terrestrial organic matter to the North Catalan margin, NW Mediterranean Sea, Prog. Oceanogr., 118, 71-80, doi:10.1016/j.pocean.2013.07.020, 2013.

Schroeder, K., Ribotti, A., Borghini, M., Sorgente, R., Perilli, A. i Gasparini, G. P.: An extensive western Mediterranean deep water renewal between 2004 and 2006, Geophys. Res. Lett., 35(18), L18605, doi:10.1029/2008GL035146, 2008.

Schroeder, K., Garcìa-Lafuente, J., Josey, S. A., Artale, V., Nardelli, B. B., Carrillo, A., Gačić, M., Gasparini, G. Pietro, Herrmann, M., Ludwig, W., Millot, C., Özsoy, E., Pisacane, G., Sánchez-Garrido, J. C., Sannino, G., Santoleri, R., Somot, S., Struglia, M., Stanev, E., Taupier-Letage, I., Tsimplis, M. N., Vargas-Yáñez, M., Zervakis, V. i Zodiatis, G.: Circulation of the Mediterranean Sea and its Variability, en The Climate of the Mediterranean Region, editat per P. Lionello, p. 187-256, Elsevier Insights, Amsterdam,., 2012.

Segschneider, J., Beitsch, A., Timmreck, C., Brovkin, V., Ilyina, T., Jungclaus, J., Lorenz, S. J., Six, K. D. i Zanchettin, D.: Impact of an extremely large magnitude volcanic eruption on the global climate and carbon cycle estimated from ensemble Earth System Model simulations, Biogeosciences, 10(2), 669-687, doi:10.5194/bg-10-669-2013, 2013.

Shepard, F. P. i Dill, R. F.: Submarine canyons and other sea valleys, Rand McNally., 1966.

Siegenthaler, U. i Sarmiento, J. L.: Atmospheric carbon dioxide and the ocean, Nature, 365(6442), 119-125, doi:10.1038/365119a0, 1993.

Siokou-Frangou, I., Christaki, U., Mazzocchi, M. G., Montresor, M., Ribera d'Alcalá, M., Vaqué, D. i Zingone, A.: Plankton in the open Mediterranean Sea: a review, Biogeosciences, 7(5), 1543-1586, doi:10.5194/bg-7-1543-2010, 2010.

Smetacek, V. S.: Role of sinking in diatom life-history cycles: ecological, evolutionary and geological significance, Mar. Biol., 84(3), 239-251, doi:10.1007/BF00392493, 1985.

Smetacek, V. S.: Oceanography: The giant diatom dump, Nature, 406(6796), 574-5, doi:10.1038/35020665, 2000.

Sournia, A.: La production primaire planctonique en Méditerranée. Essai de mise à jour, Bull. l'etude en commun la Méditerranée, 5, 1-128, 1973.

Spinei, E., Carn, S. A., Krotkov, N. A., Mount, G. H., Yang, K. i Krueger, A.: Validation of ozone monitoring instrument SO 2 measurements in the Okmok volcanic cloud over Pullman, WA, July 2008, J. Geophys. Res., 115, D00L08, doi:10.1029/2009JD013492, 2010.

Stabholz, M., Durrieu de Madron, X., Canals, M., Khripounoff, A., Taupier-Letage, I., Testor, P., Heussner, S., Kerhervé, P., Delsaut, N., Houpert, L., Lastras, G. i Dennielou, B.: Impact of open-ocean convection on particle fluxes and sediment dynamics in the deep margin of the Gulf of Lions, Biogeosciences, 10(2), 1097-1116, doi:10.5194/bg-10-1097-2013, 2013.

Statham, P. J. i Hart, V.: Dissolved iron in the Cretan Sea (eastern Mediterranean), Limnol. Oceanogr., 50(4), 1142-1148, doi:10.4319/lo.2005.50.4.1142, 2005.

Takahashi, K.: Seasonal fluxes of pelagic diatoms in the subarctic Pacific, 1982–1983, Deep Sea Res. Part A. Oceanogr. Res. Pap., 33(9), 1225-1251, doi:10.1016/0198-0149(86)90022-1, 1986.

Tanaka, T. Y. i Chiba, M.: A numerical study of the contributions of dust source regions to the global dust budget, Glob. Planet. Change, 52(1), 88-104, doi:10.1016/j.gloplacha.2006.02.002, 2006.

Tassone, A., Fuente, J. A. M. de la, Pérez, L. C., Roca, E. i Artigas, M. C.: Evolución del sector septentrional del margen continental catalán durante el Cenozoico, Acta geológica hispánica, 29(2), 3-38, 1994.

Tesi, T., Langone, L., Goñi, M. A., Turchetto, M., Miserocchi, S. i Boldrin, A.: Source and composition of organic matter in the Bari canyon (Italy): Dense water cascading versus particulate export from the upper ocean, Deep Sea Res. Part I Oceanogr. Res. Pap., 55(7), 813-831, doi:10.1016/j.dsr.2008.03.007, 2008.

Theocharis, A. i Kontoyiannis, H.: Interannual Variability of the Circulation and Hydrography in the Eastern Mediterranean (1986-1995), en The Eastern Mediterranean as a Laboratory Basin for the Assessment of Contrasting Ecosystems, p. 453-464, Springer Netherlands, Dordrecht., 1999.

Thingstad, T. F., Krom, M. D., Mantoura, R. F. C., Flaten, G. A. F., Groom, S., Herut, B., Kress, N., Law, C. S., Pasternak, A., Pitta, P., Psarra, S., Rassoulzadegan, F., Tanaka, T., Tselepides, A., Wassmann, P., Woodward, E. M. S., Riser, C. W., Zodiatis, G. i Zohary, T.: Nature of phosphorus limitation in the ultraoligotrophic eastern Mediterranean., Science, 309(5737), 1068-71, doi:10.1126/science.1112632, 2005.

Tréguer, P. J. i De La Rocha, C. L.: The World Ocean Silica Cycle, Ann. Rev. Mar. Sci., 5(1), 477-501, doi:10.1146/annurev-marine-121211-172346, 2013.

Tubau, X.: Anàlisi de sistemes de canyons submarins en marges continentals amb característiques contrastades , i el seu paper en el transport i acumulació de deixalles marines, Universitat de Barcelona, 2015.

Tuominen, L., Kairesalo, T. i Hartikainen, H.: Comparison of methods for inhibiting bacterial activity in sediment., Appl. Environ. Microbiol., 60(9), 3454-7, 1994.

Turchetto, M., Boldrin, A., Langone, L., Miserocchi, S., Tesi, T. i Foglini, F.: Particle transport in the Bari Canyon (southern Adriatic Sea), Mar. Geol., 246(2-4), 231-247, doi:10.1016/j.margeo.2007.02.007, 2007.

Ulses, C., Estournel, C., Durrieu de Madron, X. i Palanques, A.: Suspended sediment transport in the Gulf of Lions (NW Mediterranean): Impact of extreme storms and floods, Cont. Shelf Res., 28(15), 2048-2070, doi:10.1016/j.csr.2008.01.015, 2008.

Vetter, E. W., Smith, C. R. i De Leo, F. C.: Hawaiian hotspots: enhanced megafaunal abundance and diversity in submarine canyons on the oceanic islands of Hawaii, Mar. Ecol., 31(1), 183-199, doi:10.1111/j.1439-0485.2009.00351.x, 2010.

Vichi, M., Cossarini, G., Gutierrez Mlot, E., Lazzari, P., Lovato, T., Mattia, G., Masina, S., McKiver, W., Pinardi, N., Solidoro, C. i Zavatarelli, M.: The Biogeochemical Flux Model (BFM): Equation Description and User Manual. BFM version 5 (BFM- V5). Release 1.0, BFM Report series N, 1. March 2013. CMCC, Bolonia, Itàlia., 2013.

Volkman, J. K.: A review of sterol markers for marine and terrigenous organic matter, Org. Geochem., 9(2), 83-99, doi:10.1016/0146-6380(86)90089-6, 1986.

Volkman, J. K.: Lipid Markers for Marine Organic Matter, en Marine Organic Matter: Biomarkers, Isotopes and DNA, vol. 2, editat per J. K. Volkman, p. 27-70, Springer-Verlag, Berlin., 2006.

Walling, D. E.: The Impact of Global Change on Erosion and Sediment Transport by Rivers: Current Progress and Future Challenges, United Nations Educational, Scientific and Cultural Organization, Paris, França., 2009.

Walling, D. E. i Fang, D.: Recent trends in the suspended sediment loads of the world's rivers, Glob. Planet. Change, 39(1), 111-126, doi:10.1016/S0921-8181(03)00020-1, 2003.

Wambeke, F. Van, Heussner, S., Diaz, F., Raimbault, P. i Conan, P.: Small-scale variability in the coupling / uncoupling of bacteria , phytoplankton and organic carbon f luxes along the continental margin of the Gulf of Lions, Northwestern Mediterranean Sea, , 34, 411-429, doi:10.1016/S0924-7963(02)00069-6, 2002.

Wang, Z., Fingas, M. i Page, D. S.: Oil spill identification, J. Chromatogr. A, 843(1-2), 369-411, doi:10.1016/S0021-9673(99)00120-X, 1999.

Watson, A. J. i Orr, J. C.: Carbon Dioxide Fluxes in the Global Ocean, en Ocean Biogeochemistry, p. 123-143, Springer Berlin Heidelberg, Berlin, Heidelberg., 2003.

Weaver, C. E.: Marine Transport and Deposition, en Clay, Muds, and Shales, vol. 44, editat per C. E. Weaver, p. 279-343, Elsevier., 1990.

Wüst, G.: On the vertical circulation of the Mediterranean Sea, J. Geophys. Res., 66(10), 3261-3271, doi:10.1029/JZ066i010p03261, 1961.

Yogev, T., Rahav, E., Bar-Zeev, E., Man-Aharonovich, D., Stambler, N., Kress, N., Béjà, O., Mulholland, M. R., Herut, B. i Berman-Frank, I.: Is dinitrogen fixation significant in the Levantine Basin, East Mediterranean Sea?, Environ. Microbiol., 13(4), 854-71, doi:10.1111/j.1462-2920.2010.02402.x, 2011.

Zúñiga, D., García-Orellana, J., Calafat, A., Price, N. B., Adatte, T., Sanchez-Vidal, A., Canals, M., Sanchez-Cabeza, J. A., Masqué, P. i Fabres, J.: Late Holocene fine-grained sediments of the Balearic Abyssal Plain, Western Mediterranean Sea, Mar. Geol., 237(1), 25-36, doi:10.1016/j.margeo.2006.10.034, 2007.

Zúñiga, D., Flexas, M. M., Sanchez-Vidal, A., Coenjaerts, J., Calafat, A., Jordà, G., García-Orellana, J., Puigdefàbregas, J., Canals, M., Espino, M., Sardà, F. i Company, J. B.: Particle fluxes dynamics in Blanes submarine canyon (Northwestern Mediterranean), Prog. Oceanogr., 82(4), 239-251, doi:10.1016/j.pocean.2009.07.002, 2009.

Annex

Taules

Estació	Tipus de mostra	Mostrejador	Mesos de mostreig	Anys de mostreig	Ambient sedimentari	Mediterrània	Profunditat (m)	Latitud decimal (N)	Longitud decimal (E)	Projecte	Vaixell oceanogràfic
Mediterrània occidental											
Canyó de Blanes											
P1	Sediment	Multicorer	Maig	2009	Plataforma mitja	Nord-Occidental	51	41,67	2,85	Prometeo	Garcia del Cid
P2	Sediment	Multicorer	Maig	2009	Plataforma mitja	Nord-Occidental	61	41,65	2,80	Prometeo	Garcia del Cid
P3	Sediment	Multicorer	Maig	2009	Plataforma mitja	Nord-Occidental	67	41,64	2,79	Prometeo	Garcia del Cid
P4	Sediment	Multicorer	Maig	2009	Plataforma mitja	Nord-Occidental	66	41,63	2,78	Prometeo	Garcia del Cid
P5	Sediment	Multicorer	Maig	2009	Plataforma mitja	Nord-Occidental	65	41,62	2,75	Prometeo	Garcia del Cid
P6	Sediment	Multicorer	Maig	2009	Plataforma externa	Nord-Occidental	87	41,56	2,76	Prometeo	Garcia del Cid
BC300	Sediment	Multicorer	Novembre/Maig	2008/2009	Eix del canyó	Nord-Occidental	281	41,66	2,90	Prometeo	Garcia del Cid
BC900	Sediment	Multicorer	Novembre/Maig	2008/2009	Eix del canyó	Nord-Occidental	893	41,57	2,84	Prometeo	Garcia del Cid
BC1200	Sediment	Multicorer	Novembre/Febrer, Maig	2008/2009	Eix del canyó	Nord-Occidental	1193	41,53	2,85	Prometeo	Garcia del Cid
BC1500	Sediment	Multicorer	Novembre/Febrer, Maig	2008/2009	Eix del canyó	Nord-Occidental	1485	41,66	2,85	Prometeo	Garcia del Cid
OS900	Sediment	Multicorer	Novembre/Febrer, Maig	2008/2009	Talús adjacent	Nord-Occidental	902	41,27	2,82	Prometeo	Garcia del Cid
OS1200	Sediment	Multicorer	Novembre/Febrer, Maig	2008/2009	Talús adjacent	Nord-Occidental	1188	41,22	2,82	Prometeo	Garcia del Cid
OS1500	Sediment	Multicorer	Novembre/Febrer, Maig	2008/2009	Talús adjacent	Nord-Occidental	1476	41,15	2,89	Prometeo	Garcia del Cid
Plataforma continental de Barcelona											
1,1	Sediment	Draga	Agost, Setembre, Octubre i Novembre	2012	Plataforma interna	Nord-Occidental	10	41,38	2,19	Pudem	Itxasbide
1,2	Sediment	Draga	Agost, Setembre, Octubre i Novembre	2012	Plataforma interna	Nord-Occidental	20	41,38	2,20	Pudem	Itxasbide
2,3	Sediment	Draga	Agost, Setembre, Octubre i Novembre	2012	Plataforma interna	Nord-Occidental	30	41,37	2,21	Pudem	Itxasbide
1,4	Sediment	Draga	Agost, Setembre, Octubre i Novembre	2012	Plataforma interna	Nord-Occidental	40	41,37	2,21	Pudem	Itxasbide

Taula 1. Localització, data i profunditat de les mostres obtingudes en el decurs de la Tesi de la Mediterrània occidental.

Estació	Tipus de mostra	Mostrejador	Mesos de mostreig	Anys de mostreig	Ambient sedimentari	Mediterrània	Profunditat (m)	Latitud decimal (N)	Longitud decimal (E)	Projecte	Vaixell oceanogràfic
Mediterrània oriental											
Mar Jònica											
H12	Sediment	Multicorer	Gener	2007	Vall d'Otranto	Oriental	1450	39,30	19,30	Meteor M71/3	Meteor
H07	Sediment	Multicorer	Gener	2007	Vall de Taranto	Oriental	1866	39,17	17,75	Meteor M71/3	Meteor
BF27	Sediment	Multicorer	Juny	2009	Talús de Calàbria	Oriental	1264	38,22	16,63	Biofun	Sarmiento de Gamboa
BF13	Sediment	Multicorer	Juny	2009	Arc de Calàbria	Oriental	2012	37,66	16,56	Biofun	Sarmiento de Gamboa
BF15	Sediment	Multicorer	Juny	2009	Conca Jònica	Oriental	3335	36,20	16,35	Biofun	Sarmiento de Gamboa
H04	Sediment	Multicorer	Gener	2007	Conca Jònica	Oriental	3750	35,92	16,00	Meteor M71/3	Meteor
H02	Sediment	Multicorer	Gener	2007	Conca Jònica	Oriental	3008	35,75	21,00	Meteor M71/3	Meteor
H05	Sediment	Multicorer	Gener	2007	Conca Jònica	Oriental	3154	37,50	18,50	Meteor M71/3	Meteor
H03	Sediment	Multicorer	Gener	2007	Conca Jònica	Oriental	4087	35,70	18,50	Meteor M71/3	Meteor
Mar Egea (Mar de Creta)											
RED5	Sediment	Multicorer	Maig	2010	Fosses del mar de Creta	Oriental	1018	35,68	25,10	Redeco	Aegeo
RED9	Sediment	Multicorer	Maig	2011	Fosses del mar de Creta	Oriental	1200	36,00	23,89	Redeco	Aegeo
RED4	Sediment	Multicorer	Maig	2010	Fosses del mar de Creta	Oriental	1615	35,76	25,10	Redeco	Aegeo
RED8	Sediment	Multicorer	Maig	2011	Fosses del mar de Creta	Oriental	1715	36,07	25,28	Redeco	Aegeo
Estrets de Creta (Oest)											
H01	Sediment	Multicorer	Gener	2007	Estret de Kythira	Oriental	2117	35,70	23,00	Meteor M71/3	Meteor
RED3	Sediment	Multicorer	Maig	2010	Estre d'Antikythira	Oriental	2976	35,40	23,40	Redeco	Aegeo
RED3.1	Sediment	Multicorer	Maig	2010	Estre d'Antikythira	Oriental	3317	35,30	23,32	Redeco	Aegeo
RED7	Sediment	Multicorer	Maig	2011	Estret de Ptolemy	Oriental	3589	34,60	24,15	Redeco	Aegeo
Mar de Llevant											
Conca de Ierapetra											
Trap	Partícules sedimentàries	Línia instrumentada	Anual	2010-2013	Ierapetra	Oriental	4325	34,50	26,19	Redeco	Aegeo
RED13	Sediment	Multicorer	Juny	2012	Dorsal de Creta-Rhodes	Oriental	1101	34,95	25,93	Redeco	Aegeo
BF19	Sediment	Multicorer	Juny	2009	Fossa abissal Hellènica	Oriental	1200	34,51	25,76	Biofun	Sarmiento de Gamboa
BF22	Sediment	Multicorer	Juny	2009	Fossa abissal Hellènica	Oriental	2015	34,48	25,87	Biofun	Sarmiento de Gamboa
RED15.1	Sediment	Multicorer	Juny	2012	Fossa abissal Hellènica	Oriental	2428	34,61	25,92	Redeco	Aegeo
RED1.1	Sediment	Multicorer	Juny	2012	Fossa abissal Hellènica	Oriental	3568	34,40	26,25	Redeco	Aegeo
IER01	Sediment	Multicorer	Gener	2007	Fossa abissal Hellènica	Oriental	3626	34,44	26,19	Meteor M71/3	Meteor
Mar obert											
RHO02	Sediment	Multicorer	Gener	2007	Estret de Rodes	Oriental	1305	35,62	27,70	Meteor M71/3	Meteor
HER01	Sediment	Multicorer	Gener	2007	Dorsal la Mediterrània oriental	Oriental	2680	33,92	27,74	Meteor M71/3	Meteor
RED2	Sediment	Multicorer	Maig	2010	Dorsal la Mediterrània oriental	Oriental	2717	33,74	26,15	Redeco	Aegeo
RED2.1	Sediment	Multicorer	Maig	2010	Dorsal la Mediterrània oriental	Oriental	2720	33,71	26,34	Redeco	Aegeo
BF24	Sediment	Multicorer	Juny	2009	Fossa abissal de Pliny	Oriental	2902	34,15	25,57	Biofun	Sarmiento de Gamboa
HER03	Sediment	Multicorer	Gener	2007	Conca Herodotus	Oriental	3090	33,67	29,00	Meteor M71/3	Meteor

Taula 2. Localització, data i profunditat de les mostres obtingudes en el decurs de la Tesi de la Mediterrània oriental